

Investigation of the function, pharmacology and oligomerisation of GPR40, GPR41 and GPR43

A thesis presented for the degree of Doctor of Philosophy

Leigh Ann Stoddart

Division of Biochemistry and Molecular Biology

Institute of Biomedical and Life Science

University of Glasgow

April 2007



**UNIVERSITY
of
GLASGOW**

Abstract

GPR40, GPR41 and GPR43 are a small family of GPCRs. Fatty acids were identified as the ligands for these receptors in 2003. High levels of circulating fatty acids have been linked to a variety of diseases, including type 2 diabetes mellitus, cancer, and high levels of fatty acids are produced by anaerobic bacteria at the site of infection. High levels of GPR40 have been detected in the β cells of the pancreas and all three receptors have been shown to be expressed in immune cells. Due to the recent identification of the ligand for these receptors, their pharmacology, function and oligomerisation was investigated during this study.

A [35 S]GTP γ S binding assay was developed to monitor the activation of GPR41 using a GPR41-G α_{i3} Cys 351 Ile fusion protein. Using the fusion protein improved the signal to background ratio and allowed the potency of a variety of short chain fatty acids to be determined. A GPR40-G α_q fusion protein was also generated, but basal levels of [35 S]GTP γ S binding in G α_q immunoprecipitates was high and did not increase significantly upon the addition of long chain fatty acids. Treatment of membranes expressing GPR40-G α_q with fatty acid free BSA reduced the basal [35 S]GTP γ S binding in a concentration dependent manner and allowed the responsiveness of GPR40 to fatty acids to be uncovered. This also allowed the potency of a variety of thiazolidinediones and small molecule agonists to be determined. It was found that troglitazone was the most potent thiazolidinedione tested. Rosiglitazone also acted as an agonist of GPR40, albeit with lower potency than troglitazone, whereas ciglitazone and pioglitazone displayed little potency. Using clones of Flp-In TReX HEK293 cells where GPR40-eYFP was cloned into the Flp-In locus, the expression of GPR40-eYFP could be controlled by the addition of doxycycline. Using this cell line confirmed that GPR40 mediated the rise in $[Ca^{2+}]_i$ induced by the addition of troglitazone. The expression of GPR40 was detected in the rat β cell line, INS-1E. Addition of lauric acid or troglitazone to these cells induced a large, transient rise of $[Ca^{2+}]_i$. Membranes prepared from INS-1E cells also displayed high basal [35 S]GTP γ S binding, which could be reduced by fatty acid free BSA. The combination of fatty acid free BSA and lauric acid or troglitazone increased [35 S]GTP γ S binding. The high levels of [35 S]GTP γ S binding observed in membranes expressing GPR40 may reflect the binding of an endogenous ligand to GPR40.

Homology models of all three receptors based on the crystal structure of rhodopsin indicated that a conserved Arg residue in TM 5 may co-ordinate the carboxylate group of

the fatty acid. To confirm this observation a series of mutant receptors were generated, with the Arg residue in TM5 mutated to alanine. Neutralisation of the charge in TM5 in GPR41 and GPR43 resulted in receptors that were unable to respond to short chain fatty acids. Further mutants of GPR43 were generated in which the Arg in TM5 was replaced by Lys, Leu or Ser. None of these mutants were able to mediate a rise in $[Ca^{2+}]_i$ in response to short chain fatty acids. The equivalent mutation in GPR40 did not abolish the receptors ability to respond to long chain fatty acids. There are two further conserved basic residues in TM regions of the receptors; an Arg/Lys in TM2 and a His in TM4. These residues were also mutated to alanine. In GPR41 and GPR43, both mutants had similar function to the wild type receptors. Both GPR40 mutants were also able to respond to a variety of fatty acids measured by their ability to mediate a rise in $[Ca^{2+}]_i$ in a FLIPR based assay system. A series of further GPR40 mutants were generated where two of the three basic TM residues were mutated. The most striking observation was found with the mutant in which the His in TM4 and Arg in TM5 mutated to alanine, this mutant was unable to mediate a rise in $[Ca^{2+}]_i$ in response to a variety of saturated fatty acids. This may indicate that upon loss of charge in TM5 the His in TM4 compensates and vice versa. None of the small molecule agonists or thiazolidinediones were able to activate the TM4 or TM5 mutants. This indicated that the synthetic agonists of GPR40 require a more conserved binding pocket which may be due to their more rigid structure.

The ability of GPR40 and GPR43 to form homo-oligomers was also investigated. It was found that GPR40 and GPR43 formed homo-oligomers as monitored by co-immunoprecipitation, FRET in single, living cells and by time resolved FRET.

Contents

1	Introduction	16
1.1	General introduction	16
1.2	G protein coupled receptors	16
1.2.1	Structure of GPCRs	16
1.2.2	GPCR family subtypes	18
1.2.3	G proteins	20
1.2.4	Signal transduction and ligand binding	25
1.2.5	Receptor theory and constitutive activation	28
1.2.6	GPCR regulation	29
1.3	Orphan GPCRs	30
1.4	GPR40 family of fatty acid receptors	32
1.4.1	Identification of genes encoding for the receptors	32
1.4.2	Identification of GPR40 as a receptor for fatty acids	32
1.4.3	Identification of GPR41 and GPR43 as receptors for short chain fatty acids	40
1.4.4	Two further GPCRs that are activated by free fatty acids	46
1.5	GPCR oligomerisation	49
1.5.1	Methods to monitor GPCR oligomerisation	49
1.5.2	Functional significance of GPCR oligomerisation	52
1.6	Project aims	54
2	Material and Methods	58
2.1	Materials	58
2.1.1	General reagents, enzymes and kits	58
2.1.2	Tissue culture plasticware and reagents	59
2.1.3	Radiochemicals	60
2.1.4	Antisera	60
2.2	Buffers	61
2.2.1	General buffers	61
2.2.2	Molecular biology solutions	61
2.3	Molecular biology protocols	62
2.3.1	Preparation of LB plates	62
2.3.2	Preparation of competent bacterial cells	62
2.3.3	Transformation of competent bacterial cells	63
2.3.4	Preparation of plasmid DNA	63
2.3.5	Quantification of DNA	64
2.3.6	Digestion of DNA with restriction endonucleases	64
2.3.7	DNA gel electrophoresis	64
2.3.8	DNA purification from agarose gels	65
2.3.9	Alkaline phosphatase treatment of plasmid vectors	65
2.3.10	Ligation of DNA	65
2.3.11	Polymerase chain reaction	65
2.3.12	DNA sequencing	67
2.4	Generation of GPR40 constructs	67
2.4.1	C-terminally epitope tagged constructs	67
2.4.2	Fluorescent fusions	68
2.4.3	Receptor-G protein fusion	68
2.4.4	Single point basic mutations	69
2.4.5	Double basic mutations	69
2.4.6	TM3 mutations	70
2.5	Generation of GPR41 constructs	71

2.5.1	C-terminally epitope tagged constructs	71
2.5.2	Fluorescent fusions	71
2.5.3	Receptor-G protein fusion	72
2.5.4	Basic mutants	72
2.6	Generation of GPR43 constructs	73
2.6.1	N-terminally epitope tagged	73
2.6.2	C-terminally epitope tagged	74
2.6.3	Fluorescent fusions	74
2.6.4	Basic mutations	75
2.6.5	TM3 mutations	76
2.7	Cell culture	77
2.7.1	Cell maintenance	77
2.7.2	Passage of cells	78
2.7.3	Transient transfection	79
2.7.4	Generation of Flp-In T-Rex HEK293 inducible cell line	79
2.7.5	Cell harvesting	79
2.8	Biochemical assays and other methods of analysis	79
2.8.1	Preparation of cell membranes	79
2.8.2	BCA protein quantification	80
2.8.3	Co-immunoprecipitation	80
2.8.4	Sodium dodecylsulphate polyacrylamide gel electrophoresis	81
2.8.5	Western blotting	81
2.8.6	Time resolved FRET	82
2.8.7	FRET imaging in single living cells	83
2.8.8	[³⁵ S]GTPγS binding assays	84
2.8.9	Single cell calcium assay	84
2.8.10	FLIPR based calcium assay	85
2.8.11	RT-PCR	85
3	Development of functional assays to monitor activation of GPR40, GPR41 and GPR43	87
3.1	Introduction	87
3.2	Functional assays to monitor activation of GPR41	89
3.3	Function of N- and C-terminally modified forms of GPR43 and C-terminally modified forms of GPR40	90
3.4	BSA allows the pharmacology of GPR40 to be uncovered	93
3.5	Detection of GPR40, GPR41 and GPR43 in a β-cell line and the function of GPR40 in these cells	95
3.6	Discussion	96
4	Characterisation of GPR40 synthetic agonists and antagonist	130
4.1	Introduction	130
4.2	Agonist activity of thiazolidinediones at GPR40	131
4.3	Potency of small molecule agonists of GPR40	132
4.4	Characterisation of GW1100 as an antagonist at GPR40	133
4.5	Ability of synthetic agonists to activate endogenously expressed GPR40	135
4.6	Discussion	135
5	Mutagenesis to identify residues important in fatty acid binding and fatty acid chain length selectivity	158
5.1	Introduction	158
5.2	Mutation of conserved transmembrane basic residues in GPR43	160
5.3	Mutation of conserved transmembrane basic residues in GPR41	162
5.4	Mutation of conserved basic transmembrane residues in GPR40	163
5.5	Mutation of the region implicated in fatty acid chain length selectivity in GPR40 and GPR43	167

5.6	Discussion	169
6	Detection of GPR40 and GPR43 homo-oligomers using a variety of techniques	214
6.1	Introduction	214
6.2	Co-immunoprecipitation allows detection of GPR40 and GPR43 homo-oligomers	215
6.3	Investigation of homo-oligomerisation of GPR40 and GPR43 using FRET imaging in living cells	216
6.4	Demonstration of homo-oligomerisation of GPR40 and GPR43 using Tr-FRET	217
6.5	Discussion	217
7	Final Discussion	229
8	References	237
9	Additional Material	267

List of Figures

Figure 1.1 Diversity of GPCR signalling	55
Figure 1.2 Chemical structures of synthetic agonists and an antagonist used in my studies	56
Figure 1.3 Structure of thiazolidinediones	57
Figure 3.1 Comparison of levels of [³⁵ S]GTPγS binding using a GPR41-Gα ₁₃ Cys ³⁵¹ Ile fusion protein to that when GPR41 is co-transfected with Gα ₁₃	102
Figure 3.2 Potency of various short chain fatty acids at GPR41-Gα ₁₃ Cys ³⁵¹ Ile measured by [³⁵ S]GTPγS binding.....	103
Figure 3.3 Co-transfection of GPR41 with either Gα ₁₆ or a Gα _q /Gα _{i1} chimera (Gα _{qG66Di5}) allows the response to agonist to be observed by monitoring [Ca ²⁺] _i	105
Figure 3.4 GPR43 can mediate mobilisation of [Ca ²⁺] _i in Gα _{q/11} knock out cells when co-transfected with Gα _q	106
Figure 3.5 Detrimental effect of N-terminally tagging GPR43	107
Figure 3.6 A variety of C-terminal tags do not affect the ability of GPR43 to mediate a rise in [Ca ²⁺] _i in response to acetate	108
Figure 3.7 Stimulation of GPR43 specifically with various short chain fatty acids causes a transient rise in [Ca ²⁺] _i in HEK293T cells.....	109
Figure 3.8 Short chain fatty acids can activate GPR43 in a concentration-dependent manner in a FLIPR based [Ca ²⁺] _i mobilization assay	110
Figure 3.9 GPR40 can mediate mobilisation of [Ca ²⁺] _i in response to caproic acid in Gα _{q/11} knock out cells when co-transfected with Gα _q	112
Figure 3.10 A variety of C-terminal modifications do not affect the ability of GPR40 to mediate a rise of [Ca ²⁺] _i in response to caproic acid.....	113
Figure 3.11 GPR40-eCFP responds to different fatty acids but kinetics of Ca ²⁺ mobilisation depends on the identity of the fatty acid used	114
Figure 3.12 Increasing concentrations of fatty acid free BSA reduces the magnitude of [Ca ²⁺] _i release generated by GPR40 and GPR43 in response to fatty acids.....	116
Figure 3.13 GPR40 appears to display high constitutive activity in [³⁵ S]GTPγS binding studies.....	117
Figure 3.14 Increasing concentrations of fatty acid free BSA reduces the ‘basal’ [³⁵ S]GTPγS binding of GPR40-Gα _q	118
Figure 3.15 The Gα _{q/11} specific inhibitor YM254890 reduces the basal [³⁵ S]GTPγS loading of GPR40-Gα _q	119
Figure 3.16 Varying concentrations of fatty acid free BSA alter the potency of palmitic acid at GPR40-Gα _q	120
Figure 3.17 The addition of fatty acid free BSA allows the potency of fatty acids at GPR40-Gα _q to be determined.....	122
Figure 3.18 Fatty acid free BSA has no effect on the basal [³⁵ S]GTPγS loading of GPR41-Gα ₁₃ Cys ³⁵¹ Ile and only reduces stimulated levels at high concentrations.....	124
Figure 3.19 Varying concentrations of fatty acid free BSA have little effect on the potency of propionate at GPR41-Gα ₁₃ Cys ³⁵¹ Ile.....	125

Figure 3.20 Expression of GPR40, GPR41 and GPR43 in INS-1E cells	127
Figure 3.21 Elevation of $[Ca^{2+}]_i$ by lauric acid in INS-1E cells	128
Figure 3.22 Endogenously expressed GPR40 also displays high levels of basal $[^{35}S]GTP\gamma S$	129
Figure 4.1 Troglitazone can produce a rise in $[Ca^{2+}]_i$ via GPR40	141
Figure 4.2 Other thiazolidinediones can act as agonists at GPR40 in a single cell calcium assay	142
Figure 4.3 Thiazolidinediones activate GPR40 in a concentration-dependent manner in a $[^{35}S]GTP\gamma S$ binding assay with varying degrees of potency but only in the presence of fatty acid free BSA.....	143
Figure 4.4 GSK250089A can apparently only act as an agonist of GPR40- $G\alpha_q$ in the presence of fatty acid free BSA	148
Figure 4.5 Potency of synthetic small molecules agonists at GPR40 measured in the $[^{35}S]GTP\gamma S$ binding assay	149
Figure 4.6 GW1100 is an antagonist of GPR40- $G\alpha_q$	151
Figure 4.7 'Basal' $[^{35}S]GTP\gamma S$ binding at GPR40- $G\alpha_q$ is substantially reduced by GW1100 in the presence and absence of fatty acid free BSA in a concentration dependent manner	152
Figure 4.8 Agonist activity of GSK250089A can be detected in the presence of GW1100	153
Figure 4.9 GW1100 can inhibit troglitazone-mediated activation of GPR40	154
Figure 4.10 Ability of troglitazone and GSK250089A to elicit mobilization of $[Ca^{2+}]_i$ in INS-1E cells and increase $[^{35}S]GTP\gamma S$ binding in INS-1E cell membranes.....	155
Figure 5.1 Amino acid sequence alignment of GPR40, GPR41 and GPR43.....	177
Figure 5.2 GPR40 homology model with a small molecule agonist docked in the proposed binding site	179
Figure 5.3 GPR41 and GPR43 homology models.....	181
Figure 5.4 GPR40 and GPR43 homology models showing position of TM3 triplet implicated in fatty acid chain length selectivity	183
Figure 5.5 Effect of mutation of three conserved basic residues in GPR43 on the ability to mediate a rise in $[Ca^{2+}]_i$ in response to short chain fatty acids.....	184
Figure 5.6 Arginine is required at position 180 in GPR43 to allow the receptor to respond to short chain fatty acids.....	185
Figure 5.7 GPR43 Lys ⁶⁵ Ala has lost the ability to mediate a rise in $[Ca^{2+}]_i$ when challenged with butyrate but retains the ability to respond to acetate or propionate	186
Figure 5.8 GPR43 His ¹⁴⁰ Ala has gained the ability to generate a rise in $[Ca^{2+}]_i$ in response to caproic acid and caprylic acid.....	188
Figure 5.9 Localisation of GPR43 mutants visualised using eYFP fluorescence	190
Figure 5.10 Ability of GPR41 basic mutants to mediate a rise in $[Ca^{2+}]_i$ when challenged with propionate or butyrate.....	191
Figure 5.11 Ability of GPR41 mutants to mediate a concentration-dependent increase in $[^{35}S]GTP\gamma S$ binding in response to propionate.....	192
Figure 5.12 Localisation of GPR41 mutants visualised using eYFP fluorescence	194

Figure 5.13 Activation of wild type and single point mutant GPR40 receptors by lauric acid in single cell $[Ca^{2+}]_i$ assays	195
Figure 5.14 The addition of fatty acid free BSA can reduce the basal $[^{35}S]GTP\gamma S$ loading of GPR40 mutant- $G\alpha_q$ fusion proteins	198
Figure 5.15 Comparison of $[^{35}S]GTP\gamma S$ concentration response curves to different ligands generated by wild type GPR40- $G\alpha_q$, GPR40 Lys ⁶² Ala- $G\alpha_q$ and GPR40 Arg ¹⁸³ Ala- $G\alpha_q$	200
Figure 5.16 Localisation of GPR40 single mutants visualised by eYFP fluorescence.....	202
Figure 5.17 Lauric acid mediated rise in $[Ca^{2+}]_i$ via GPR40 double mutants	203
Figure 5.18 Cellular localisation of GPR40 double mutants visualised using eYFP fluorescence	206
Figure 5.19 Responses to various chain length fatty acids by GPR40 GGG ⁹³⁻⁹⁵ STW	208
Figure 5.20 GPR40 GGG ⁹³⁻⁹⁵ STW can mediate a rise in $[Ca^{2+}]_i$ when challenged with acetate.....	209
Figure 5.21 Cellular localisation of GPR40 GGG ⁹³⁻⁹⁵ STW visualised using eYFP fluorescence	211
Figure 5.22 Amino acid positions differing between GPR41 and GPR42.....	212
Figure 5.23 GPR40 homology model showing positions of Tyr ⁹¹ and Phe ¹⁹¹ in relation to proposed binding site of small molecule agonists	213
Figure 6.1 Co-immunoprecipitation of differentially epitope-tagged forms of the human GPR40 receptor.....	221
Figure 6.2 Co-immunoprecipitation of differentially epitope-tagged forms of the human GPR43 receptor.....	222
Figure 6.3 FRET imaging of GPR40 homo-oligomerisation in single cells	224
Figure 6.4 FRET imaging of GPR43 homo-oligomerisation in single cells	226
Figure 6.5 GPR40 homo-oligomer detected using Tr-FRET	227
Figure 6.6 GPR43 homo-oligomer detected using Tr-FRET	228
Figure 7.1 Amino acid sequence alignment of human and rat GPR40.....	235
Figure 7.2 Position of residues that differ between human and rat GPR40	236

List of Tables

Table 2.1 Primary and secondary antibody dilutions for western blotting	81
Table 2.2 FRET bleedthrough coefficients	83
Table 3.1 Potency of short chain fatty acids at GPR41 measured in the [³⁵ S]GTPγS binding assay	104
Table 3.2 Potency of various short chain fatty acids at GPR43 measured by a FLIPR based [Ca ²⁺] _i mobilization assay.....	111
Table 3.3 Potency of various fatty acids at GPR40 measured by a FLIPR-based [Ca ²⁺] _i mobilisation assay	115
Table 3.4 Potency of palmitic acid in the presence of varying concentrations of fatty acid free BSA	121
Table 3.5 Potency of various fatty acids at GPR40-Gα _q measured by a [³⁵ S]GTPγS binding assay in the presence of 10μM fatty acid free BSA.....	123
Table 3.6 Potency of propionate at GPR41-Gα _{i3} Cys ³⁵¹ Ile in the presence of varying concentrations of fatty acid free BSA	126
Table 4.1 Potency of thiazolidinediones at GPR40-Gα _q measured by in the [³⁵ S]GTPγS binding assay	145
Table 4.2 Potency of thiazolidinediones at GPR40 measured in a FLIPR based [Ca ²⁺] _i mobilisation assay	146
Table 4.3 Potency of synthetic small molecules at GPR40 measured in a FLIPR based [Ca ²⁺] _i assay	147
Table 4.4 Potency of synthetic small molecules at GPR40 measured in a [³⁵ S]GTPγS binding assay	150
Table 4.5 Comparison of potency of various thiazolidinediones at GPR40 and PPARγ..	156
Table 4.6 Potency of various small molecule ligands determined in three different assay systems	157
Table 5.1 Potency of various short chain fatty acids at GPR43 mutants	187
Table 5.2 Potency of propionate at GPR41 mutants measured by [³⁵ S]GTPγS binding studies.....	193
Table 5.3 Potency of fatty acids agonists at GPR40 single mutants.....	196
Table 5.4 Potency of thiazolidinediones and small molecule agonists at GPR40 single mutants	197
Table 5.5 Potency of palmitic acid, troglitazone and GSK250089A at GPR40 Lys ⁶² Ala-Gα _q and GPR40 Arg ¹⁸³ Ala-Gα _q measured in a [³⁵ S]GTPγS binding assay	201
Table 5.6 Potency of fatty acids agonists at GPR40 double mutants	204
Table 5.7 Potency of thiazolidinediones and small molecule agonists at GPR40 double mutants	205
Table 5.8 Potency of a range of fatty acids at TM3 mutants of GPR40 and GPR43	210

Acknowledgements

First and foremost I would like to thank Professor Graeme Milligan for help, guidance and reassurance throughout the course of this project. I would also like to thank Dr Andrew Brown at GlaxoSmithKline for his help and input into this project.

To all the past and present members of Lab 253 a big thank you must be extended. In particular I would like to thank Shirley Appelbe for her help with co-immunoprecipitation and Tr-FRET and Laura Jenkins for her endless patience with the calcium experiments. Carl Haslem, Kirk Lawless and Mark Wigglesworth at GlaxoSmithKline also deserve a special thank you with all their help during my time in Harlow. A thank you also goes to the modellers at GlaxoSmithKline, Eric Biggam and Steve Garland, whose help with the receptor models was invaluable to decipher the results for the mutagenesis studies.

I would like to thank all my friends within the lab, especially Shirley, Laura, Geraldine and Zoe, for all their help and support throughout the last three years. To all my friends out with the lab, thank you for allowing me to bore you with science when I needed to and for just being there when I didn't. To all my family – thank you for everything. And last but not least Damien, thank you for being my rock throughout everything.

Finally, I would like to dedicate my thesis to the memory of those that I've lost during the course of my PhD.

Author's declaration

The investigations presented in this thesis were conducted by its author. No part of the work has previously been presented in fulfilment of the regulations for any degree or diploma, either at this University or at any other institution.

Abbreviations

2BrP	2-bromo palmitate
[³⁵ S]GTPγS	guanosine 5'-O-(3-[³⁵ S]thio)triphosphate
APC	allophycocyanin
BRET	bioluminescence energy transfer
BSA	bovine serum albumin
Ca ²⁺	calcium
[Ca ²⁺] _i	intracellular calcium concentration
cAMP	cyclic adenosine 3',5'-monophosphate
cGMP	cyclic guanosine 3',5'-monophosphate
CNS	central nervous system
CPT1	carnitine palmitoyltransferase
CTX	cholera toxin
dNTP	deoxynucleoside triphosphate
DOP	δ opioid receptor
eCFP	enhanced cyan fluorescent protein
ER	endoplasmic reticulum
eYFP	enhanced yellow fluorescent protein
FLIPR	fluorometric imaging plate reader
FRET	fluorescence resonance energy transfer
G protein	guanine nucleotide binding protein
GABA	γ-aminobutyric acid
GDP	guanosine 5'-diphosphate
GFP	green fluorescent protein
GLP-1	glucagon-like peptide-1
GTP	guanosine 5'-triphosphate
GPCR	G protein-coupled receptor

GRK	G protein receptor kinase
GSIS	glucose-stimulated insulin secretion
GTP γ S	guanosine 5'-O-(3-thio)triphosphate
HEK	human embryonic kidney
IBD	irritable bowel disease
IL-12	interleukin-12
IP ₃	inositol 1,4,5 trisphosphate
KOP	κ opioid receptor
LB medium	Luria-Bertani medium
LC-CoA	long chain acyl-CoA
LPS	lipopolysaccharide
MOP	μ opioid receptor
NIDDM	non-insulin-dependent diabetes mellitus
PCR	polymerase chain reaction
PDX-1	pancreatic duodenal homeobox-1
PKA	protein kinase A
PKC	protein kinase C
PLC	phospholipase C
PPAR	peroxisome proliferator activated receptor
PPRE	peroxisome proliferator responsive element
PTX	pertussis toxin
RET	resonance energy transfer
rGPR41	rat GPR41
RGS	regulator of G protein signalling
RLuc	<i>Renilla</i> luciferase
SDS	sodium dodecyl sulphate
SDS-PAGE	sodium dodecyl sulphate polyacrylamide gel electrophoresis
siRNA	small interfering RNA

TM transmembrane
Tr-FRET time resolved FRET

1 Introduction

1.1 General introduction

To allow communication between cells, tissues and organs, receptors are found on the cell surface that specifically recognise a huge variety of signals ranging from light to proteins. Cell surface receptors are divided into different classes depending on their amino acid sequence and their homology to other receptors. The largest family is called the G protein coupled receptor (GPCR) family and in human is encoded by over 800 genes (Hill, 2006). GPCRs serve to transduce a signal from outside to inside a cell. They achieve this by activating proteins within the cell which can trigger multiple signal transduction pathways. GPCR dysfunction has been shown to be associated with a variety of human diseases ranging from allergic rhinitis to schizophrenia. Around 30% of drugs in clinical use are targeted against GPCRs, although these drugs only act on approximately 30 receptors (Wise et al., 2004). This makes the GPCR superfamily an attractive target for the development of new pharmaceutical medicines and for gaining a greater understanding of many disease processes (Hill, 2006).

1.2 G protein coupled receptors

1.2.1 Structure of GPCRs

GPCRs can be identified by their seven transmembrane (TM) spanning α -helices. These helices lead to a distinctive hydrophobicity pattern in the amino acid sequence, which makes the identification of putative GPCRs fairly easy. Seven TM spanning helices results in the N- and C- terminus of the protein being at different sides of the membrane, and for GPCRs the N-terminus is extracellular and consequently the C-terminus is intracellular. The TM helices are joined by three intracellular and three extracellular loops. GPCRs vary enormously in their length, with the shortest receptors consisting of around 300 amino acids (e.g. GPR40) and the longest of around 1000 amino acids (e.g. GABA receptors). Differences in the length of the N- and C- terminal domains and the intracellular and extracellular loops contribute to this wide range of sequence length.

The first crystal structure of a GPCR was presented by Palczewski et al (2000), which showed the ground state structure of the light activated receptor, bovine rhodopsin, at 2.8Å

resolution. This structure provided a wealth of information about the structural organisation of the receptor and gave clues to the mechanisms involved during receptor activation and the relay of the signal inside the cell. The structure revealed a highly organised arrangement of the TM regions, which was in agreement with lower resolution data generated using electron microscopy, with the seven TM regions being arranged in a counter clockwise orientation with the core of the receptor being primarily comprised of TMs 2, 3, 5, 6 and 7 with TMs 1 and 4 being peripherally sequestered and more exposed to the lipid bilayer (Unger et al., 1997; Palczewski et al., 2000).

The TM domains in rhodopsin vary in length from 19 to 34 residues and the crystal structure of bovine rhodopsin confirmed that they can be both kinked and/or tilted. TM1 and 2 were found to be tilted from the plane of the membrane by 25° . TM1 contains a 12° bend within it, which is caused by a proline residue and TM2 deviates 30° from the ideal helix due to two glycine residues at the top of the helix. TM3 is the longest helix and is the most tilted from the plane of the membrane, showing a 33° tilt. This TM region also contains two internal bends, one due to a proline within the sequence and the other occurs at a serine, which does not usually cause a bend in a helix and appears to be related to the packing of the helices. The C-terminal end of TM3, which occurs near the intracellular face of the receptor, contains the highly conserved D(E)RY (Asp/Glu-Arg-Tyr) motif found in nearly all rhodopsin-like receptors (see section 1.2.2), and has been linked to the stabilisation of the inactive receptor and to the activation of the receptor (see section 1.2.4.2). TM regions 4 and 6 both run almost perpendicular to the membrane but the presence of two proline residues in TM4 and one in TM6 cause both of the helices to be kinked. The proline residue in TM6 is one of the most conserved residues in GPCRs. TM5 tilts at 26° and contains two internal kinks that occur at phenylalanine and histidine residues. TM7 possesses the highly conserved NPXXY motif, which is thought to be involved in forming structural domains that facilitate interactions with TM6, which are important in holding the receptor in the inactive state. The crystal structure also highlighted the presence of another short helix in the cytoplasmic surface, which is termed helix 8. It is an extension of TM7 and two cysteine residues at the end of the helix are modified by the attachment of palmitic acid moieties which insert into the membrane.

The extracellular domains of rhodopsin, as shown by the crystal structure, form a compact lid and parts of this fold inwards to enclose the covalently bound retinal molecule. The extracellular loops also contain two cysteine residues which are highly conserved in the GPCR family. They are thought to form a disulphide bond which stabilises the receptor structure. Within the N-terminal region and the extracellular loops of nearly all GPCRs

can be found one or more N-linked glycosylation sites (Asn-X-Ser/Thr), where X can be any amino acid except proline or asparagine (Kristainsen et al., 2004). For several GPCRs, the prevention of glycosylation results in reduced cell surface expression but has limited effect on ligand binding or the function of the receptors that are successfully delivered to the cell surface (Davidson et al., 1995; Ray et al., 1998). This indicates that this region of a GPCR is important in the correct trafficking of the receptor to the plasma membrane.

The intracellular loops were poorly defined in the crystal structure of bovine rhodopsin which indicates that they have a high degree of flexibility (Palczewski et al., 2000). Other studies have indicated that they play an important role in G protein coupling (see section 1.2.4.3). The third intracellular loop contains serine and threonine residues that provide recognition sites for protein kinases that are involved in receptor desensitisation and internalisation (see section 1.2.6).

1.2.2 GPCR family subtypes

GPCRs function to transduce signals, in the form of ligands, into intracellular responses. GPCRs can be activated by a wide variety of ligand types, including light, ions, amino acids, nucleotides, peptides, biogenic amides, lipids and proteins. Activation of a receptor, by ligand binding, can trigger a variety of responses within a cell. Classically, these signals are generated through activation of heterotrimeric G proteins but there are a growing number of other proteins that can interact with GPCRs such as β -arrestins and neurochondrin. The GPCR superfamily can be subdivided into three major subfamilies (Families A-C) and three small subfamilies (D-F) based on sequence homology and the pharmacological nature of the ligand.

Family A is the largest class in the GPCR family and is the most studied. Members of this family contain residues that are highly conserved although their overall homology is low. The conserved residues are mainly found in the TM regions and include the D(E)RY motif in TM3 and the NPXXY motif in TM7 as mentioned in section 1.2.1. Other residues commonly found in TM regions of family A GPCRs, include an asparagine in TM1, an aspartic acid in TM2, a tryptophan in TM4 and a proline in TM6. As mentioned in section 1.2.1, extracellular loops 1 and 2 often contain cysteine residues that are connected by a disulphide bond. The arginine residue of the D(E)RY motif is the only residue that is conserved in all family A receptors (Probst et al., 1992).

Family A receptors can be divided into three subgroups on the basis of their mechanisms for ligand binding. Family A α includes rhodopsin and the biogenic amine receptors, such as the adrenergic and dopamine receptors, and bind their ligands within a core formed by their TM helices. Members of subfamily A β use their N-terminal region and extracellular loops as well as the TM helices to make up their ligand binding domain. The ligands for this subfamily are usually peptides and the subfamily includes the receptors for chemokines, opioids and somatostatin. The receptors that make up subfamily A γ usually contain a longer N-terminal region which has been found to be very important in ligand binding, although some residues in the extracellular loops have also been implicated. Receptors within this subfamily include those for glycoprotein hormones such as lutenising hormone.

Family B receptors are characterised by the presence of a large extracellular domain which is involved in ligand binding. This family does not contain any of the conserved residues that are found in family A receptors. They do contain conserved prolines in TM regions although these differ from those conserved in family A. They also do not contain the D(E)RY motif. The N-terminal region of these receptors contains several cysteine residues which form a network of disulphide bridges. Family B is a smaller family and only contains about 20 different receptors. The receptors in this family include those for calcitonin, vasoactive intestinal polypeptide, glucagon and glucagon like peptide.

The receptors that make up family C all contain an extremely long N-terminus, which is usually 500-600 amino acids long. They contain little sequence homology across the family but do contain cysteine residues in extracellular loops 2 and 3 which may form a disulphide bond. The ligand binding domain of these receptors is proposed to be formed exclusively by the N-terminal region (Conn and Pin, 1997). The crystal structure of the ligand binding domain of the metabolic glutamate receptor has been elucidated. It forms a homodimer through both disulphide bonds and hydrophobic interactions (Kunishima et al., 2000; Tsuchiya et al., 2002).

The three additional families of GPCRs derive from genes that code for the pheromone receptors that bind to the G $\alpha_{i/o}$ family of G proteins (Dulac and Axel, 1995), the frizzled/smoothened receptors (Foord et al., 2002) and a family of cAMP-receptors found in *Dictyostelium discoideum* (Herald et al., 1992). The frizzled/smoothened receptors are involved in embryonic development and in mammals there are 10 frizzled and 1 smoothened receptors which are structurally similar to family B GPCRs (Foord et al., 2002).

The crystal structure for bovine rhodopsin is the only detailed structural information that exists for mammalian GPCRs and it is thought that all family A receptors will share a high degree of structural homology to rhodopsin even though their sequences are divergent. As mentioned above, family B receptors do not have any of the conserved residues found in family A receptors but a similar overall morphology to family A receptor has been proposed. The TM regions are likely to be kinked and tilted to different degrees than in family A receptors and due to the lack of a palmitoylation site within the C-terminal region they are unlikely to have an intracellular helix 8. There is little structural information on the TM regions of other families of GPCRs so their arrangement is unknown.

1.2.3 G proteins

The structural changes within a GPCR that occur upon ligand binding allow the receptor to interact more effectively with guanine nucleotide binding proteins (G proteins). G proteins consist of three different polypeptides, giving a heterotrimeric protein made up of an α , β , and γ subunit. In the inactive state guanosine 5' diphosphate (GDP) is bound to the α subunit. The GPCR acts as a guanine nucleotide exchange factor which promotes the release of GDP from the α subunit and its replacement with guanosine 5' triphosphate (GTP). GTP is present in the cell at higher concentrations than GDP. The exchange of GDP for GTP results in the dissociation of the α subunit from the β and γ subunits, which are tightly associated. Both the α and $\beta\gamma$ subunits are then able to interact with and regulate effector systems, in effect transducing the signal from the receptor to the cell. The α subunit has intrinsic GTPase activity, which catalyses the hydrolysis of the terminal phosphate of the GTP; this returns the α subunit into an inactive state with GDP bound and promotes the re-association of the $\beta\gamma$ subunits. Early biochemical studies on G proteins found that rates of hydrolysis of GTP to GDP in purified α subunits were too slow to explain the rapid turnover seen in physiological systems. This led to the discovery of RGS, or regulators of G protein signalling, proteins which act as GTP-ase activating proteins. They have been shown to interact with G α subunits and promote the hydrolysis of GTP which therefore inactivates the G protein within a shorter time scale (De Vries et al., 1999).

1.2.3.1 G protein α subunit

There are 16 different genes for G protein α subunits which through alternative splicing results in at least 28 distinct α subunits. The α subunits can be classified into four subfamilies; $G\alpha_s$, $G\alpha_{i/o}$, $G\alpha_{q/11}$ and $G\alpha_{12/13}$ (Milligan and Kostenis, 2006).

The $G\alpha_s$ family consists of $G\alpha_{s(s)}$, $G\alpha_{s(L)}$, $G\alpha_{s(XL)}$, which are alternatively spliced products of the $G\alpha_s$ gene, and $G\alpha_{olf}$. $G\alpha_s$ is known as the stimulatory G protein as its activation stimulates production of cyclic AMP (cAMP) through activation of adenylyl cyclase. The $G\alpha_s$ family have also been shown to activate maxi K^+ channels, Src tyrosine kinases and the tubulin GTPase (Popova et al., 1994). Expression of the $G\alpha_s$ splice variants is ubiquitous and there is some evidence that they are alternatively expressed under various conditions (Novotny and Svoboda, 1998). $G\alpha_{olf}$ is only found mainly in olfactory neurons and certain CNS ganglia (Drinnan et al., 1991; Herve et al., 1993).

The $G\alpha_{i/o}$ family includes $G\alpha_{o1}$, $G\alpha_{o2}$, $G\alpha_{i1-3}$, $G\alpha_z$, $G\alpha_{t1/2}$ and $G\alpha_{gust}$. Many of the members of this family act to inhibit the production of cAMP by adenylyl cyclase and were originally identified as the inhibitory G proteins (Bokoch et al., 1984). Other functions of this family include activation of K^+ channels, inhibition of Ca^{2+} channels, activation of Rap1GAPII-dependent ERK/MAP kinase (Mochizuki et al., 1999) and activation of Src tyrosine kinases (Milligan and Kostenis, 2006). $G\alpha_{t1/2}$ stimulate cGMP phosphodiesterases (Granovsky et al., 2001). $G\alpha_{i1-3}$ are widely expressed, although preferential expression is found in neuronal systems. $G\alpha_{o1/2}$ are specifically expressed in neurons and neuroendocrine cells. $G\alpha_{t1}$ and $G\alpha_{t2}$ have a highly restricted distribution and are only found in retinal rod and cone outer segments respectively (Lerea et al., 1986), although expression has also been reported in taste buds (McLaughlin et al., 1994). $G\alpha_{gust}$ also has limited expression and is found in sweet and bitter taste buds and chemoreceptor cells in the airways and it is responsible for sensing bitter taste via activation of phosphodiesterases (Margolskee, 2002).

The $G\alpha_{q/11}$ family is composed of $G\alpha_q$, $G\alpha_{11}$, $G\alpha_{14}$, $G\alpha_{15}$ and $G\alpha_{16}$. All members of this family activate phospholipase C β (PLC β) isoforms. Active PLC β hydrolyses phosphatidyl inositol 4,5 bisphosphate into sn 1,2 diacylglycerol and inositol 1,4,5 trisphosphate (IP $_3$). PLC β can also be activated by $\beta\gamma$ subunits but this occurs mainly in haemopoietic cells. IP $_3$ binds to specific IP $_3$ gated Ca^{2+} release channels (IP $_3$ receptors) that are found on the smooth endoplasmic reticulum. These channels are show high specificity for inositol

1,4,5 trisphosphate. IP₃ receptors are regulated by positive feedback as released Ca²⁺ binds to IP₃ receptors to further increase Ca²⁺ release. Released Ca²⁺ can activate ryanodine receptors which are also Ca²⁺ channels. This Ca²⁺ activated Ca²⁺ release give a rapid all or nothing Ca²⁺ signalling response. This rise in intracellular [Ca²⁺] ([Ca²⁺]_i) is transient. Ca²⁺ levels are returned to normal via multiple mechanisms which include Ca²⁺ ATPases that are found on the plasma membrane and endoplasmic reticulum and Na⁺Ca²⁺ antiporters.

Gα_{q/11} are widely expressed, whereas Gα₁₄, Gα₁₅ and Gα₁₆ are expressed in haematopoietic cells. Gα₁₄, Gα₁₅ and Gα₁₆ are naturally promiscuous Gα subunits. Most GPCRs couple to a family of α subunits whereas promiscuous G proteins couple to a wide range of GPCRs that do not couple to Gα_q or Gα₁₁. This allows them to be used to link a variety of predominately Gα_s and Gα_{i/o} coupled receptors to the PLCβ pathway (Kostenis et al., 2005).

Gα₁₂ and Gα₁₃ form a separate G protein α subunit family. They are both widely expressed and are associated with communications involved between heterotrimeric G proteins and the cellular responses mediated by monomeric GTP-binding proteins, including morphology and cell proliferation (Riobo and Manning, 2005). They mediate this crosstalk by activating a range of signalling proteins including phospholipase D and PLCε (Wing et al., 2003).

The crystal structure of a variety of G protein α subunits has been elucidated, either on their own or complexed with βγ, effector or regulatory proteins (Noel et al., 1993; Coleman et al., 1994; Wall et al., 1995; Tesmer et al., 1997; Chen et al., 2005). As expected with proteins that share at least 50% homology across the family, they all have highly similar structures. The α subunit is composed of two main domains; the first domain is responsible for binding and hydrolyzing GTP to GDP while the second comprises of a unique helical domain that buries the GTP in the core of the protein (Noel et al., 1993; Coleman et al., 1994). The GTPase domain of the α subunit is composed of 5 α helices surrounding a 6-stranded β sheet (Coleman et al., 1994). The α subunits are not transmembrane proteins but undergo modifications to allow them to attach to the membrane. The widely expressed members of the Gα_{i/o} family undergo N-myristoylation, which co-translationally attaches myristic acid (C14:0) to the N-terminal glycine following removal of the initiating methionine. All G protein α subunits, apart from Gα_{t1/2}, contain a cysteine near the N-terminus which is within the target site for post-translational addition of palmitic acid (C16:0) via a reversible thio-ester linkage (Wedegaertner et al., 1995). It

has been shown that these modifications are important for plasma membrane targeting and for the association of the α subunit with the $\beta\gamma$ subunits (Linder et al., 1991; Milligan et al., 1995).

Endo-toxins produced by *Vibrio cholerae* and *Bordetella pertussis* use G protein α subunits as their target. Both toxins are mono-ADP-ribosyltransferases; cholera toxin (CTX) is a N-linked transferase whereas pertussis toxin (PTX) is a C-linked transferase. The CTX target is an arginine residue within the GTPase domain of the α subunit of $G\alpha_s$ family, and modification of this residue prevents the α subunit from hydrolysing GTP to GDP and therefore results in a constitutively active protein. The PTX target is a cysteine residue four residues from the end of $G\alpha_{i/o}$ family α subunits. The incorporation of the ADP-ribose onto the α subunit prevents it from interacting with the receptor and therefore can no longer be activated (Hepler and Gilman, 1992). $G\alpha_{i/o}$ α subunits can be modified to prevent ADP-ribosylation by mutation of the target cysteine to any other residue (Bahia et al., 1998). CTX and PTX have proved to be very useful in defining the roles of $G\alpha_{i/o}$ and $G\alpha_q$. A specific inhibitor of $G\alpha_{q/11}$ has recently been described by Takasaki et al., (2004), which was isolated from the culture broth of *Chromobacterium* sp. and named YM254890. It is thought that it prevents the exchange of GDP for GTP on the α subunit and its specificity makes it an important and useful tool for studying $G\alpha_{q/11}$ mediated events.

The action of PTX on $G\alpha_{i/o}$ α subunits has led to the finding that the C-terminal tail of the α subunit is important for receptor recognition (Kostenis et al., 2005). This resulted in the creation of chimeric G proteins α subunits in which the terminal 5 amino acids have been replaced with the corresponding sequence of another α subunit. These chimeric G proteins allow the switching of the pathway that a receptor activates. The most common chimeric G proteins have a $G\alpha_q$ backbone and the last 5 residues of another α subunit such as $G\alpha_s$ or $G\alpha_{i1}$ and they are widely used in the screening for ligands at orphan GPCRs (see section 1.3). It is now appreciated that there are additional regions within the α subunit that are involved in GPCR interaction, including the N-terminal domain (Kostenis et al., 2005).

1.2.3.2 G protein $\beta\gamma$ subunits

There are five different β and 12 different γ subunits that have been identified. Most cell types express multiple β and γ subtypes, although β_3 and γ_8 are only found in retinal cone cells and β_1 and γ_1 are only found in retinal rod cells. β_5 is found in neurons in neuroendocrine organs and $\beta_{5(L)}$ is only found in the retina (Milligan and Kostenis, 2006).

The large number of β and γ subunits give rise to numerous possible combinations but it is likely that the subtle expression patterns of the subunits limit the likelihood of pairings. For example, it has been shown that β_2 cannot form a functional dimer with γ_1 (Spring et al., 1994). Most pairs can interact with similar affinity to α subunits. An exception is the $\beta_1\gamma_1$ pair as it forms better interactions with α_{t1} than the other $\beta\gamma$ pairs (Hamm, 1998).

The G protein β subunits have a β propeller structure based on a seven WD (tryptophan-aspartate)-40 repeats (Lambright et al., 1994; Wall et al., 1995; Sondek et al., 1996). The γ subunit interacts with the β subunit via N-terminal coiled-coil interactions and through a series of extensive contacts along the base of β subunit. The association between β and γ subunits is very strong and dissociation can usually only be achieved through protein denaturation. The exception to this rule is found in the β_5 subunit which has been shown to dissociate from the γ subunit, which allows it to interact with a number of RGS proteins that contain a γ -subunit-like domain (Levay et al., 1999). The $\beta\gamma$ dimer interacts with the α subunit via a hydrophobic pocket present when the α subunit has GDP bound. The conformational changes that occur in the α subunit upon GTP binding results in a loss of the hydrophobic pocket and therefore dissociation of $\beta\gamma$ (Lambright et al., 1996).

Lipid modifications are also found on the γ subunits. For most of the γ subunits it is a geranylgeranyl (C20) modification, apart from γ_1 which is farnesylated (C15). The modifications occur at the extreme C-terminus of the subunit through a stable thioether bond on the cysteine found in the 'CAAX' box motif. The three terminal residues are subsequently cleaved resulting in the cysteine becoming the new C-terminus. There are no lipid modifications found on the β subunits (Wedegaertner et al., 1995).

It was originally thought that the presence of $\beta\gamma$ was to suppress the activity of the α subunit when not in the GTP bound form and to tether it to the membrane before lipid modifications on the α subunits were identified (Milligan and Kostenis, 2006). It is now appreciated that $\beta\gamma$ have their own role within the cell and can bind to and activate a range of effector proteins. Target proteins for $\beta\gamma$ include PLC β isoforms, adenylyl cyclases, G protein receptor kinases (GRK), K⁺ channels and Ca²⁺ channels. Not all $\beta\gamma$ dimer pairs function equivalently and some have more affinity for certain effectors than others. For example, $\beta_1\gamma_2$ has been shown to stimulate one of the adenylyl cyclase isoforms, adenylyl cyclase II, but $\beta_5\gamma_1$ inhibits the activity of the same enzyme (Bayewitch et al., 1998). The conformation of the $\beta\gamma$ subunits does not undergo major structural changes upon activation

and it has now been proposed that the α subunits act to suppress the activity of the $\beta\gamma$ subunits (Cabrera-Vera et al., 2003).

1.2.4 Signal transduction and ligand binding

1.2.4.1 Ligand binding

The means by which a GPCR binds its ligand differs for the different families of receptors. Even within family A there are major differences in the areas important in ligand binding. As mentioned previously, detailed structural information exists only for rhodopsin. The ligand for rhodopsin, 11-*cis*-retinal, is covalently attached to the receptor through the formation of a Schiff base with lysine²⁹⁶ in TM7 within a binding crevice formed by the TM helices. 11-*cis*-retinal acts as an inverse agonist (see section 1.2.5) which keeps the receptor inactive in the absence of light, and exposure to light results in isomerisation of 11-*cis*-retinal to all-*trans*-retinal, which acts as the agonist to activate the receptor (Sakmar, 1998). Interactions between 11-*cis*-retinal and the receptor also occur between the C9 of retinal and glycine¹²¹ in TM3 and with aromatic residues in the outer portion of TM6 (Han et al., 1997; Nakayama et al., 1991).

Apart from rhodopsin, the best studied receptor-ligand interactions are those of the biogenic amine receptors. The ligands for these receptors also bind within a crevice formed by the TM regions and the main ligand-receptor interactions occur within TMs 3, 5 and 6. It has been found that the positively charged amine of catecholamines forms a salt bridge with an aspartic acid residue within TM3. The aspartic acid residue is conserved within the biogenic amine receptors. The importance of this residue has been demonstrated by mutagenesis studies on the β_2 adrenergic receptor (Strader et al., 1991), α_{1A} adrenergic receptor (Hwa et al., 1995), histamine H2 receptor (Gantz et al., 1992) and the muscarinic acetylcholine receptors (Spalding et al., 1994). In the β_2 adrenergic receptor, important interactions also occur between the catechol ring of adrenaline and two serine residues that occur one α helical turn apart in TM5. Further studies on this receptor have identified two residues in TM6, phenylalanine²⁹⁰ and asparagine²⁹³ which are thought to stabilise the catechol ring and hydrogen bond with the β -hydroxyl of adrenaline respectively (Tota et al., 1990; Wieland et al., 1996). Receptors that interact with eicosanoids, such as leukotrienes and prostanoids, have a similar mechanism for binding their ligands. The important residues in the binding crevice are from TMs 3, 6 and 7.

There is also a conserved arginine at the top of TM7, near the extracellular surface, that is proposed to coordinate the carboxyl head group of these ligands (Funk et al., 1993).

The members of GPCR family A whose ligands are peptides have a slightly different mechanism for ligand binding. These receptors include the angiotensin receptors, chemokine receptors and the opioid receptors. For these receptors, the ligands make important interactions with the N-terminus of the receptor and extracellular loops 1 and 2. Residues within the TM domains have also been shown to be important but these often lie at the top of the α helices (Gether, 2000). Family A GPCRs that are activated by nucleosides, such as the adenosine receptors, have ligand binding domains that are largely made up by the TM regions but the second extracellular loop also contributes (Ji et al., 1998). The protease activated receptors have a unique mechanism for activation. Their N-terminus contains a recognition sequence for proteases such as thrombin, and when this is cleaved the shortened N-terminus acts as a tethered agonist for the receptor through interactions with the extracellular loops (Nanevicz et al., 1996), much like those observed for the peptide GPCRs.

As mentioned above, family B GPCRs commonly contain a longer N-terminus than family A receptors. This long N-terminus has been shown to be very important in binding of ligands to the receptor. In a similar way to the family A receptors that are activated by peptides, the extracellular loops also play a role but none of the residues within the TM domains have been shown to be important in agonist binding (Gether, 2000). The family C receptors contain a very long N-terminus and this region forms the whole of the ligand binding domain. The crystal structure of the extracellular domain of the metabotropic glutamate mGluR1 receptor has been resolved, which demonstrated that the ligand binding domain forms a disulphide-linked dimer. The dimer formation of this domain has been likened to a Venus flytrap which opens and closes in response to agonist binding (Kunishima et al., 2000).

1.2.4.2 Signal transduction

To allow transduction of the signal from an agonist into a cell via a GPCR the receptor must be able to activate intracellular effectors. This is achieved by the receptor undergoing a series of conformational changes upon ligand binding that allow the effectors to bind and be activated. The changes that occur have been best studied for rhodopsin due to the covalent attachment of the 11-*cis*-retinal, which acts as an antagonist to keep the receptor in an inactive state whilst the absorption of a photon of light isomerises the 11-*cis*-retinal to

all-*trans*-retinal which induces several conformational changes within the receptor (Meng et al., 2001; Teller et al., 2001).

In the inactive state, a GPCR has various molecular constraints within the TM regions which prevent it from spontaneously activating. Many of these constraints involve interactions between residues that are found to be highly conserved within family A GPCRs (Urizar et al., 2005). The release of these constraints induces positional changes of certain TM helices. One of the regions that is heavily implicated as being very important in receptor activation is the DRY motif found at the bottom of TM3. The arginine in this triplet is conserved throughout family A GPCRs and is thought to form ionic interactions with a partly conserved aspartic acid/glutamic acid residue in the cytoplasmic end of TM6. The crystal structure of rhodopsin supports this idea as it shows a network of interactions between the glutamic acid and arginine of the ERY in TM3 and the glutamic acid of TM6 which is proposed to sustain the cytoplasmic ends of these two helices immobilized (Palczewski et al., 2000). This interaction has also been proposed for a variety of other family A GPCRs, including the β_2 adrenergic receptor (Ballesteros et al., 2001). Disruption of the ionic interactions between the arginine in TM3 and the glutamic acid in TM6 in rhodopsin is accompanied by the uptake of two protons (Arnis et al., 1994) which results in a change of environment for the residues and the movement of TM3 and TM6. The importance of the disruption of the ionic bond has been demonstrated by the introduction of mutations which neutralise the charge of the Asp/Glu. This results in a constitutively active receptor. This has been observed for many GPCRs, including rhodopsin (Cohen et al., 1993), β_2 adrenergic receptor (Rasmussen et al., 1999), α_{1A} adrenergic receptor (Scheer et al., 1996) and M_1 muscarinic receptor (Lu et al., 1997). The movement of these TM regions is thought to be a critical step in the creation of an active GPCR (Gether, 2000). Analysis of the crystal structure of rhodopsin shows that TM6 exists in a highly bent configuration due to a conserved proline within the α helix; it is thought that the movement of TM6 occurs around this hinge region in the absence of the interactions between TM6 and TM3.

1.2.4.3 Regions of GPCRs involved in interaction with G protein

A variety of different approaches have been used to decipher the regions within a GPCR that are involved in interacting and activating the G protein. These include site directed mutagenesis (Wess et al., 1990; Blin et al., 1995), the engineering of chimeric receptors to attempt to switch the G protein signalling to an alternative pathway (Hwa et al., 1996) and the use of synthetic peptides to mimic the regions within the receptor that are thought to

activate the G protein (Higashijima et al., 1990). These studies, and others, have shown that the second and third intracellular loops and the membrane proximal part of the carboxy terminus each play important roles in G protein coupling and activation (Gether, 2000). Each intracellular loop plays different roles; intracellular loop 3 appears to be the region important in G protein coupling specificity and intracellular loop 2 has been shown to be important for efficient G protein activation (Bluml et al., 1994; Burstein et al., 1995). The arginine in the DRY triplet had been proposed to interact directly with the G protein (Wess, 1998) but recent studies have shown that the arginine does not interact with the G protein and its function is to stabilise the inactive and activated conformations of the receptor (Flanagan, 2005). As mentioned above, the carboxy terminus of the G protein α subunit is one of the regions involved in interaction with the receptor. It has been proposed that the movement of TM3 and TM6 during receptor activation may allow insertion of the C-terminus of the α subunit into a cavity formed by the TM helices and this interaction induces the release of GDP (Gether, 2000).

1.2.5 Receptor theory and constitutive activation

The covalent attachment of 11-*cis*-retinal to rhodopsin holds the receptor in an inactive state and isomerisation of 11-*cis*-retinal to all-*trans*-retinal causes the receptor to undergo conformational changes that result in the receptor being in a conformation that allows activation of downstream effectors. Rhodopsin is unique within the GPCR superfamily as 11-*cis*-retinal prevents activation of the receptor in the absence of light as spontaneous isomerisation is a rare event, but measurable spontaneous activation of virtually all GPCRs can be recorded in the absence of agonist and this is termed constitutive activity (Milligan, 2003).

Models to explain the activation of GPCRs have been proposed and modified as our knowledge of receptor activation has expanded (Rang, 2006). The most widely accepted model for GPCR activation is the extended ternary complex model, which is an extension of a 2-state model. A 2-state model states that a receptor exists in equilibrium between an inactive conformation (R) and an active conformation (R*). In the absence of agonist the majority of the receptor population exists in the R state but as the energy barrier between the R and R* is sufficiently low it allows a small portion of the receptors to spontaneously switch to the R* state in which down stream effectors can be activated. The presence of an agonist serves to alter the equilibrium between R and R* and agonists are hypothesised to have higher affinity for the R* state, thus, in the presence of an agonist a larger portion of

the population will now be in the active state to generate a signal within the cell. The extended ternary complex model takes into account the interactions between the receptor and the G protein in addition to the interactions between the receptor and the agonist. Using these models and functional observations, the basic division of compounds into agonists and antagonists is no longer sufficient. Compounds that act as agonists can be described as full agonists, which produce a maximal effect in a given assay system under specific conditions, or partial agonists which produce a detectable but submaximal effect under the same conditions. Traditionally, an antagonist was defined as a compound that blocked the effect of agonists but monitoring the effects of these compounds on constitutive activity it was found that many were able to block some of the constitutive activity of a receptor by holding the receptor in the R state (Costa and Herz, 1989). This resulted in antagonists that block constitutive activity being defined as inverse agonists as they have higher affinity for R. As with agonists, inverse agonists can be termed full inverse agonists or partial inverse agonists. A neutral antagonist has equal affinity for R and R*, thus producing no change in the equilibrium but blocks the effects of both agonists and inverse agonists. Recent developments have found that the same receptor can activate several different signal transduction pathways depending on the agonist. It is likely that different agonists stabilise different active conformations of the receptor and this can result in agonist directed-trafficking of the signal (Perez and Karnik, 2005).

The degree of constitutive activity of a receptor can be altered by mutations. As mentioned previously, neutralisation of the charge of the aspartic acid/glutamic acid of the DRY motif at the bottom of TM3 often results in an increase of constitutive activity (Ballesteros et al., 2001; Montanelli et al., 2004). This residue is thought to interact with a residue in TM6 and mutation of this region also results in elevated levels of constitutive activity (Pauwels and Wurch, 1998; Seifert and Wenzel-Seifert, 2002), which supports the theory that this region is important in the movement of the TM helices associated with activation of the receptor. Naturally occurring mutations in this region are associated with several inherited and acquired diseases, mainly in the endocrine system, and result in constitutively active GPCRs (Parnot et al., 2002).

1.2.6 GPCR regulation

Following activation of a GPCR, a series of events occur to desensitise the receptor to prevent chronic receptor over stimulation. In the seconds following receptor activation, the receptor is phosphorylated at serine and threonine residues found within the C terminus and third intracellular loop. GPCRs can be phosphorylated by kinases that are activated by

the second messengers produced by GPCR activation, such as protein kinase A (PKA) and protein kinase C (PKC) and by G protein receptor kinases (GRKs) (Krupnick and Benovic, 1998). GRKs only phosphorylate agonist activated GPCRs whereas agonist activation is not required for second messenger phosphorylation (Ferguson, 2001). Phosphorylation of a GPCR serves to increase the affinity of the receptor for cytosolic cofactors termed arrestins. Arrestins preferentially bind to receptors phosphorylated by GRKs over those phosphorylated by second messenger dependent kinases (Lohse et al., 1990; Lohse et al., 1992). Arrestin binding sterically hinders G protein coupling, serving to uncouple the receptor from the G protein. Arrestins also function as endocytic adaptor proteins which can target a receptor for internalisation via clathrin-coated vesicles. Internalisation removes the receptor from the cell surface into intracellular membrane vesicles and once internalised a receptor can either be recycled back to the cell surface or targeted to lysosomes for degradation. Recycling involves the receptor becoming resensitised through dissociation from both the arrestin and the ligand and dephosphorylation by protein phosphatases. Receptors that are targeted for degradation can result in a reduction in the total number of receptors within a cell, which can also be achieved at the transcriptional level (Luttrell and Lefkowitz, 2002).

1.3 Orphan GPCRs

In humans, about 360 genes for GPCRs are thought to encode non-sensory receptors. Of these receptors the natural ligand has been identified for approximately 210, which leaves 150 receptors with no known ligand or function: these are termed orphan GPCRs (Wise et al., 2004). Many orphan GPCRs share low levels of homology with other receptors whose ligands have been identified, and subsequently cannot be classed within known specific sub-families. It has been found that many orphan GPCRs share greater levels of homology with each other and form new sub-families. These subfamilies are distributed throughout the GPCR superfamily tree, which implies they may be activated by a range of novel ligands and have a diverse range of function (Wilson et al., 1998). It is estimated that although about 50% of all drugs with known mechanisms exert their biological effects by targeting GPCRs, these drugs target only 30 of the known GPCRs. The potential of finding new drug targets and consequently new pharmaceutically active compounds has been a lure for many pharmaceutical companies to attempt to identify the activating ligands of orphan GPCRs.

There are two general strategies used for the identification of ligands for orphan GPCRs; reverse pharmacology and orphan receptor strategy. Reverse pharmacology uses compound libraries comprising of a variety of known endogenous ligands for other GPCRs, putative GPCR agonists and purified tissue extracts, and screens these compounds against a GPCR of unknown function. This approach is often used by pharmaceutical companies due to its high throughput capability. The more classic approach starts with the identification of a biologically active substance, usually a tissue extract which leads to the discovery of the receptor it activates. This is often termed the orphan receptor strategy. In contrast to reverse pharmacology, this technique is often used by smaller, mainly academic, laboratories.

To identify activation of a GPCR by a putative ligand, a functional assay must be utilised. More than half of all identifications of ligands at orphan GPCRs have been accomplished using techniques that monitor changes in intracellular Ca^{2+} [Ca^{2+}]_i levels. Changes in [Ca^{2+}]_i are a result of activation of the $\text{G}\alpha_{q/11}$ proteins. As only a proportion of GPCRs couple to $\text{G}\alpha_{q/11}$, the introduction of chimeric or promiscuous G proteins are required as these redirect signalling of a wide range of GPCRs into the Ca^{2+} pathway. As mentioned previously, an area of G proteins shown to be important in their interaction with GPCRs the extreme C-terminus. The replacement of the five carboxy terminal amino acids of $\text{G}\alpha_q$ with the corresponding residues of another G protein results in a chimeric G protein which is able to couple to a non $\text{G}\alpha_{q/11}$ receptor but activate the $\text{G}\alpha_{q/11}$ pathway. Mixtures of chimeric and promiscuous G proteins, often termed a 'G protein cocktail', are co-expressed with an orphan receptor. However, there are several reports that question the overall applicability of the G protein cocktail strategy to all GPCRs. A variety of other assay systems have been used in deorphanisation programmes, including reporter gene assays, assays monitoring the production of cAMP, yeast based assays and electrophysiological assays using oocytes. There are advantages and disadvantages to each assay system, factors such as costs and its conversion to a high throughput platform are key to many pharmaceutical companies, whereas for academic laboratories sensitivity is often more important.

1.4 GPR40 family of fatty acid receptors

1.4.1 Identification of genes encoding for the receptors

GPR40, GPR41, GPR42 and GPR43 were identified by Sawzdargo et al., (1997) as a tandemly encoded group of intronless genes located at chromosome 19q13.1. They were identified during a search for novel galanin receptors using sets of degenerate primers based on conserved sequences in human and rat galanin receptors. They contain seven TM domains characteristic of GPCRs, along with other features common to the GPCR family and without knowledge of their activating ligands were classed as orphan GPCRs (Sawzdargo et al., 1997). cDNA homologous to human GPR41 was cloned from rat lung (Bonini et al., 1997) and mouse GPR43 was cloned from leukaemia inhibitory factor stimulated M1 myeloid leukaemia cells (Senga et al., 2003). GPR40-43 represent a family of receptors and they are more closely related to each other than to other GPCRs. GPR41 and GPR42 share about 98% homology and differ by only six amino acids (corresponding to seven nucleotide differences). Only one receptor corresponding to GPR41/GPR42 can be identified in rodents (Brown et al., 2003) and GPR42 is now thought to be open reading frame pseudogene (Brown et al., 2005). The other three receptors share 34-42% similarity, with GPR41 and GPR43 being the most similar. The next most closely related receptors are the protease activated receptors, although GPR40-43 lack the long N-terminal extracellular domain which is cleaved to activate the protease activated receptors.

1.4.2 Identification of GPR40 as a receptor for fatty acids

GPR40 remained an orphan GPCR until 2003 when three papers were independently published that identified a range of medium and long chain saturated and unsaturated fatty acids as ligands for this receptor (Briscoe et al., 2003; Itoh et al., 2003; Kotarsky et al., 2003). Briscoe et al., (2003) identified an unsaturated long chain fatty acid, elaidic acid, as the only compound from a large library to act as an agonist at GPR40 in an assay system measuring the release of intracellular Ca^{2+} . They went on to demonstrate that over 40 different fatty acids were able to activate GPR40 in the micro-molar range and of these fatty acids, eicosatrienoic acid was the most potent with an pEC_{50} of 5.71 ± 0.11 (Briscoe et al., 2003). Itoh et al., (2003) used a similar method to also identify long chain fatty acids as agonists at GPR40 with similar potency as described by Briscoe et al. The lack of specificity of the receptor for different fatty acids may indicate that selectivity of the activating fatty acid is determined by local tissue specific environments. They also showed

that methyl linoleate, a non-carboxyl containing compound related to linoleic acid, was unable to activate the receptor hence indicating that a carboxyl group was required for agonist function (Itoh et al., 2003). Kotarsky et al., (2003) identified fatty acids as agonists of GPR40 by measuring the activation of a reporter gene. Using this method they found fatty acids to be less potent than as detailed by Briscoe et al., (2003) and Itoh et al., (2003). In this study they also described non-fatty acid agonists of GPR40. These were the insulin sensitising thiazolidinediones, rosiglitazone and MCC-555, and an experimental anti-obesity compound, MEDICA16.

1.4.2.1 Tissue distribution of GPR40

All three initial reports on GPR40 found high levels of mRNA in the pancreas (Briscoe et al., 2003; Itoh et al., 2003; Kotarsky et al., 2003). Briscoe et al., (2003) found by quantitative RT-PCR ubiquitous expression in all regions of the brain, with highest expression in the substantia nigra and medulla oblongata. This was not supported by the tissue distribution study carried out by Kotarsky et al., (2003) using northern blot analysis on human samples. In addition, Itoh et al., (2003) were unable to detect GPR40 mRNA in rat brain. Kotarsky et al., (2003) detected expression of GPR40 in the human liver, heart and skeletal muscle but this was not seen in human or rat tissue by Briscoe et al., (2003) or by Itoh et al., (2003). GPR40 expression has also been reported in human immune cells, with the highest levels of mRNA detected in monocytes (Briscoe et al., 2003). Functional GPR40 has also been detected in the human breast cancer cell lines, MCF-7 (Yonezawa et al., 2004) and MDA-MB-231 (Hardy et al., 2005). Further analysis of the expression of GPR40 in the pancreas found mRNA levels enriched in islets and in particular in the insulin producing β -cells (Briscoe et al., 2003, Itoh et al., 2003). GPR40 expression has also been detailed in various pancreatic cell lines, including MIN6, β -TC-3, HIT-T15 and INS-1E (Briscoe et al., 2003; Itoh et al., 2003; Kotarsky et al., 2003; Sharipo et al., 2005). Tomita et al., (2005) demonstrated expression of GPR40 in human islets and in islet cell tumours. Expression has also been detected in rat islets (Feng et al., 2005; Salehi et al., 2005).

1.4.2.2 GPR40 modes of signal transduction

The initial studies on GPR40 suggested that the receptor coupled to the Ca^{2+} mobilising G proteins, $G\alpha_q$ and $G\alpha_{11}$. The study by Briscoe et al., (2003) did not use chimeric or promiscuous G proteins and found that in a reporter cell line which indicates responsiveness to $G\alpha_{i/o}$ and $G\alpha_{q/11}$ pathways, a signal could be generated via GPR40 and

treatment with PTX did not affect the signal suggesting that the signal was generated via $G\alpha_{q/11}$ activation (Briscoe et al., 2003). Itoh et al., (2003) and Kotarsky et al., (2003) both concluded that GPR40 is predominately coupled to $G\alpha_{q/11}$ but they also suggested that the receptor could also weakly couple to $G\alpha_{i/o}$. Studies on cells endogenously expressing GPR40 support the $G\alpha_{q/11}$ coupling of the receptor (Hardy et al., 2005; Fujiwara et al., 2005). In particular, Shapiro et al., (2005) used the $G\alpha_{q/11}$ specific inhibitor, YM254890 (Takasaki et al., 2004) on the β -cell line, INS-1E, and this significantly reduced palmitic acid-induced mobilisation of $[Ca^{2+}]_i$. However, in the breast cancer cell line, MCF-7, treatment with PTX blocked the long chain fatty acid induced elevation of $[Ca^{2+}]_i$ (Yonezawa et al., 2004).

1.4.2.3 Dual role of FAs in β cells

Insulin secretion is stimulated by an increase in blood glucose. Glucose is taken up into the β cells through the non insulin dependent glucose transporter, GLUT 2 and metabolised to acetyl CoA. The resulting change in ATP/ADP ratio causes the closure of ATP sensitive K^+ channels, which in turn depolarises the plasma membrane. This depolarisation opens voltage dependent Ca^{2+} channels. The Ca^{2+} influx triggers insulin granule exocytosis. This Ca^{2+} influx is considered to be the major trigger for glucose-stimulated insulin secretion (GSIS) (Ashcroft et al., 1990; Prentki et al., 1996).

Fatty acids play an important role in normal β cell function. An increase in free fatty acid concentrations augments GSIS (Seyffert and Madison, 1967; Stein et al., 1997). The absence of circulating fatty acids causes loss of GSIS, which is reversible by replacement with exogenous fatty acids, and suggests that fatty acids are required for basal insulin secretion (Stein et al., 1996). In contrast to the augmentation of GSIS by short term elevated plasma fatty acids levels, chronically raised levels of fatty acids has been shown to impair insulin secretion (Prentki et al., 2002) and induce β cell apoptosis (Lee et al., 1994; El Assaad et al., 2003). There is a strong link between obesity, non-insulin dependent diabetes mellitus (NIDDM), and circulating plasma levels of fatty acids.

The mechanism by which fatty acids act as signalling molecules within β cells is complex. Fatty acids can cross the plasma membrane and be converted into long chain acyl-CoA (LC-CoA) in the cytosol. During glucose metabolism, malonyl Co-A is produced which inhibits carnitine palmitoyltransferase (CPT-1) on the mitochondrial membrane. This prevents the oxidation of fatty acids and produces a build of LC-CoA in the cytosol

(DeFronzo, 1997). The LC-CoA then acts as an effector molecule to enhance insulin release (Prentki and Corkey, 1996). Other mechanisms have been suggested such as triglyceride/free fatty acid cycling via lipolysis (Nolan et al., 2006).

1.4.2.4 Could the effects of FAs on β cells be explained through action on GPR40

The endogenous expression of GPR40 in a range of transformed pancreatic β -cell lines and in pancreatic β -cells has initiated a series of studies into the function of the receptor in these cells. Initial studies in MIN6 cells whereby GPR40 was silenced using siRNA demonstrated that fatty acids were then unable to amplify insulin release (Itoh et al., 2003). This was also shown by Salehi et al. (2005). Treatment of INS-1E cells with siRNA corresponding to GPR40 resulted in a significant reduction in insulin secretion in the presence of fatty acids and a rise in $[Ca^{2+}]_i$ in response to palmitic acid could no longer be detected (Shapiro et al., 2005; Schnell et al., 2006). The mechanism of GPR40-mediated insulin secretion from rat β -cells appears to involve a reduction in current through voltage gated K^+ channels and an increase in PKA activity (Feng et al., 2006).

An important finding by Salehi et al., (2005) was the possible antagonist effects of 2-bromo palmitate (2BrP) on GPR40. They showed that 2BrP inhibited linoleic acid mediated phosphatidyl inositol hydrolysis in human embryonic kidney, HEK293, cells transiently expressing mouse GPR40 and in MIN6 cells. 2BrP also showed partial agonist properties, by causing a slight activation of PI hydrolysis, although no attempt at quantification was undertaken (Salehi et al., 2005). 2BrP is classically described as an inhibitor of CPT-1 and therefore of mitochondrial long chain fatty acid oxidation. This supports the malonyl-CoA hypothesis of insulin release and has been shown to stimulate insulin secretion (Prentki et al., 1992). The interaction of this compound with GPR40 complicates its support to the malonyl-CoA hypothesis.

The most compelling evidence implicating GPR40 in the development of NIDDM comes from work carried out by Steneberg et al., (2005) using mouse models of GPR40. They developed GPR40 knockout mice and found that islets isolated from these mice were unable to increase insulin secretion in response to treatment with palmitic acid. Mice expressing GPR40, when fed a high fat diet, become obese and this leads to high plasma fatty acid levels, insulin resistance, hyperinulinemia and glucose intolerance, in short all the factors associated with NIDDM. By contrast, the GPR40 knockout mice, although they became obese, they did not develop glucose intolerance and became less insulin resistant.

To investigate the contribution of GPR40 overstimulation in the development of NIDDM, GPR40 was over expressed under the control of the *Ipfl/PDX-1* promoter in transgenic mice. In contrast to the knockout mice, those overexpressing GPR40 were glucose intolerant and hypoinsulinemic on a normal diet (Stenberg et al., 2005). This development of diabetes is comparable to the chronic effects of fatty acids on β cells (Haber et al., 2003).

The mechanisms of action of fatty acids in normal β cell function and in the development NIDDM are not fully understood. The studies on GPR40 in recombinant cell systems, β cell lines, isolated islets and in transgenic mice point towards this receptor being involved. It has been proposed that GPR40 interacts with the systems involving fatty acid metabolism within the β cells (Nolan et al., 2006).

Dissection of the role of GPR40 in pancreatic β -cells is hampered by the lack of high affinity, specific agonists and antagonists. The incentive of possible pharmacological intervention at this receptor for the treatment of NIDDM has lead to the recent publication of a range of GPR40 agonists based on a 3-(4-{[N-alkyl]amino}phenyl)propanoic acid template (Garrido et al., 2006). Using a reporter gene assay they found compounds with potencies in the nanomolar range. They also showed that a carboxylic moiety was not essential for agonist action at the receptor, with no effect on potency and a slight reduction in efficacy. The structure of six of these compounds is shown in Figure 1.2 (a-g). Further studies were carried out on one of the compounds, GW9508X (Compound (a) in Figure 1.2, and called GW839508X herein) (Briscoe et al., 2006). They observed similar potency of the compound to that observed in the reporter gene assay when measuring the release of $[Ca^{2+}]_i$ in HEK293 cells transiently expressing GPR40. GW839508X was also able to increase GSIS in MIN6 cells in a concentration dependent manner, although not to the same levels as linoleic acid. In addition to the characterisation of the agonist, they also described a GPR40 specific antagonist, GW1100 (Figure 1.2 (f)). This compound inhibited the enhancement of GSIS by GW839508X in MIN6 cells but only partially inhibited the GSIS achieved by linoleic acid.

Two polymorphisms in the open reading frame of human GPR40 have been reported, Arg²¹¹His (Hamid et al., 2005; Ogawa et al., 2005) and a rare Asp¹⁷⁵Asn polymorphism (Hamid et al., 2005). Hamid et al., (2005) found that the allelic frequency of the Arg²¹¹His polymorphism was similar in normal patients and patients with NIDDM. In a recombinant cell system, they found no difference in the potency of eicosatriynoic acid for GPR40

Arg²¹¹His or GPR40 Asp¹⁷⁵Asn but the Asp¹⁷⁵Asn receptor showed a reduction in maximal efficacy. However, studies on Japanese men have indicated that the Arg²¹¹His polymorphism is linked to insulin secretory capacity (Ogawa et al., 2005). They also found that serum insulin levels were higher in His/His homozygotes compared to Arg/Arg homozygotes. The full effects of these polymorphisms have yet to be studied in detail.

1.4.2.5 Possible role of GPR40 in other tissues

There is a large amount of literature on the effects of long chain fatty acids on a variety of tissues. Some of these effects may be mediated by action on GPR40. The expression and function of GPR40 in areas other than pancreatic β cells and the known effects on fatty acids on these tissues are detailed below.

In addition to the role of free fatty acids in the potentiation of GSIS, recent observations indicate that free fatty acids also potentiate glucagon release from the α cells (Bollheimer et al., 2004; Olofsson et al., 2004; Hong et al., 2005). Flodgren et al., (2007) were able to detect GPR40 mRNA in a hamster glucagonoma cell line, In-R1-G9 and found that the receptor co-localised with glucagon in the periphery of mouse islets. Treatment of both In-R1-G9 cells and isolated mouse islets with linoleic acid increased glucose stimulated glucagon release in a concentration dependent manner. Knockdown of GPR40 expression significantly reduced the ability of linoleic acid to increase glucagon exocytosis and pre-treatment of the cells with linoleic acid to remove existing receptor from the cell surface rendered additional fatty acid unable to increase glucagon secretion (Flodgren et al., 2007). Using in-situ hybridization, Briscoe et al., (2003) and Itoh et al., (2003) were both unable to detect GPR40 in the periphery of rat islet and GPR40 mRNA could not be detected in human glucagonoma tissue (Tomita et al., 2005). The reasons for these discrepancies are unclear but it may be due to the comparatively small number of α cells within the islets (Flodgren et al., 2007). The previous studies on mouse islets found that a release of $[Ca^{2+}]_i$ was induced upon addition of palmitic acid and the increase in $[Ca^{2+}]_i$ was required for fatty acid stimulated glucagon release (Olofsson et al., 2004). The study on GPR40 by Flodgren et al., (2007) did not monitor fatty acid mediated release of $[Ca^{2+}]_i$, but as GPR40-mediated $[Ca^{2+}]_i$ release has been observed in β cells (Shapiro et al., 2005) it is possible that the release of $[Ca^{2+}]_i$ in α cells may also be mediated through GPR40.

Expression of GPR40 on immune cells has only been demonstrated by Briscoe et al., (2003). They detected GPR40 mRNA specifically in human monocytes, although the expression of GPR40 was significantly lower than that of the related receptor, GPR43,

which is activated by short chain fatty acids (see section 1.5.3.3). Fatty acids are known to exert diverse effects on the immune system and various immune cell subtypes (Hwang, 2000). In obese patients, who have increased levels of plasma free fatty acids, an increased secretion of proinflammatory cytokines and infiltration of monocytes and macrophages has been reported (Dandona et al., 2004) although the exact mechanisms behind this are unclear and the contribution of GPR40 activation has not been examined.

As detailed above, expression of GPR40 has been detected in breast cancer cell lines in two separate studies (Yonezawa et al., 2004; Hardy et al., 2005). Previous epidemiological studies have indicated that women in countries with a high-fat diet have a significantly higher risk of developing breast cancer than those in countries with a low fat diet (Cohen et al., 1993; Rose, 1997). The increased risk of a high fat diet has been confirmed in a number of studies using animal models and cultured breast cancer cells (reviewed in Cohen et al., 1993). Recent studies on the breast cancer cell line, MDA-MB-231 have shown that oleic acid stimulated cell proliferation but palmitic acid induced apoptosis (Hardy et al., 2000; Hardy et al., 2003). Yonezawa et al., (2004) demonstrated that oleic acid and linoleic acid, both unsaturated fatty acids, were able to mediate a rapid, transient rise of $[Ca^{2+}]_i$ in the human breast cancer cell line, MCF-7, but palmitic acid and stearic acid, both saturated fatty acids, were unable to cause a rise in $[Ca^{2+}]_i$. They found that the effect of oleic acid and linoleic acid was PTX sensitive (Yonezawa et al., 2004). Hardy et al., (2005) found similar results with MDA-MB-231 cells. To dissect the role of GPR40 in these cells, they reduced the levels of GPR40 by siRNA treatment and found that the proliferatory effects of GPR40 were reduced (Hardy et al., 2005). The role of GPR40 in other types of cancer is yet to be assessed.

1.4.2.6 PPAR γ and thiazolidinediones

Kotarsky et al., (2003) found that the thiazolidinedione, rosiglitazone, can act as an agonist of GPR40. The thiazolidinediones are classically described as agonists of peroxisome proliferator activated receptor γ (PPAR γ). PPAR γ belongs to a family of ligand activated transcription factors called peroxisome proliferator activated receptors (PPARs), of which there are three major subtypes; α , β/δ and γ . They display distinct expression patterns; PPAR α is present in the liver, kidney and heart, PPAR δ is ubiquitously expressed and PPAR γ is predominately expressed in adipocytes, with lower levels found in skeletal muscle and liver tissue (Kliewer et al., 1994; Fajas et al., 1997). All three PPAR receptor subtypes are also found in pancreatic islet cells. PPAR γ is activated by high concentrations

of fatty acids and by prostaglandin J2 derivatives (Kliwer et al., 1995) as well as a range of thiazolidinediones.

The thiazolidinediones are orally-available insulin sensitising agents that act to reverse insulin resistance in target tissues, which therefore makes them a treatment for NIDDM. They act by promoting fatty acid storage in adipocytes, which lowers the levels of plasma fatty acids, and they affect the expression of adipocyte secreted hormones that are important in glucose homeostasis (Rangwala et al., 2004). Lehmann et al., (1995) demonstrated that thiazolidinediones could act in the nanomolar range as agonists at PPAR γ . The effectiveness of these compounds at reducing insulin resistance has led to a large range of compounds being developed, tested and licensed for use in the treatment of NIDDM. Troglitazone was the first thiazolidinedione to be used clinically, although a rare but serious side effect of liver toxicity resulted in it being removed from the market (Graham et al., 2003). Two further thiazolidinediones have been licensed clinically, rosiglitazone and pioglitazone and to date, do not cause as serious side effects (Tolman et al., 2003). The structures of the four thiazolidinediones used in this study are shown in Figure 1.3.

There has been a growing amount of literature published over the last few years that indicates that not all of the effect of the thiazolidinediones can be explained through action on PPAR γ . It is now well appreciated that thiazolidinediones have anti-proliferative effects on a variety of human cancer lines and the role of PPAR γ in cell cycle regulation and the mechanism by which they inhibit growth is unclear (Weng et al., 2006). A study on embryonic stem cells lacking expression of PPAR γ (PPAR $\gamma^{-/-}$) demonstrated that the anti-proliferative effects of troglitazone and ciglitazone were the same as in PPAR $\gamma^{+/+}$ cells (Palakurthi et al., 2001). They also demonstrated that both thiazolidinediones were able to mediate a rapid, transient rise in $[Ca^{2+}]_i$ in both PPAR $\gamma^{+/+}$ and PPAR $\gamma^{-/-}$ cells (Palakurthi et al., 2001). As mentioned above, the highest level of expression of PPAR γ is found in adipose tissue (Fajas et al., 1998) although the target tissue for thiazolidinedione is unknown and candidates include adipose tissue, skeletal muscle, liver tissue and the β cell (Evans et al., 2004). Although, the validity of adipose tissue as the target tissue has been brought into question by studies on mice that have been engineered to lack virtually all white and brown fat (Burant et al., 1997). In these mice it was found that troglitazone retained its insulin sensitising properties and reduced circulating levels of free fatty acids, which indicates a mode of action independent of adipose tissue (Burant et al., 1997). As transcription factors, PPARs act to regulate expression of specific genes that contain PPAR

DNA binding elements (PPRE) within the promoter regions (Tugwood et al., 1992). It has been found that thiazolidinediones rapidly induce phosphorylation of MAPK family members, effects which are too rapid to be due to new protein synthesis (Gardner et al., 2005). Shiau et al., (2005) developed a set of thiazolidinedione analogs, in which a double bond was introduced before the thiazolidine-2,4-dione ring, to give Δ^2 thiazolidinediones. The introduction of the double bond abrogated their PPAR γ activity as measured by a PPAR γ transcription factor ELISA and a reporter gene assay (Shiau et al., 2005). Δ^2 -troglitazone and Δ^2 -ciglitazone were shown to retain the ability to induce apoptosis in prostate cancer cells (Shiaue et al., 2005) and down regulate cyclin D1 in breast cancer cells (Huang et al., 2005).

1.4.3 Identification of GPR41 and GPR43 as receptors for short chain fatty acids

At a similar time to the publication of long chain fatty acids as agonists of GPR40, short chain fatty acids were described as the potential endogenous agonists for GPR41 (Brown et al., 2003; Le Poul et al., 2003) and GPR43 (Brown et al., 2003; Le Poul et al., 2003; Nilsson et al., 2003). Brown et al., (2003) used a series of recombinant cell systems to confirm that GPR43 was activated by the carboxylic acid, acetate, and went on to show that the receptor was activated by a range of short chain fatty acids with similar potency in a $[Ca^{2+}]_i$ mobilisation and $[^{35}S]GTP\gamma S$ binding assay. This was also confirmed by Le Poul et al., (2003) in a Ca^{2+} based assay system and cAMP assay and by Nilsson et al., (2003) in both a reporter gene assay and a Ca^{2+} based assay system. The rank order of potency was generally consistent between these different studies, with acetate (C2), propionate (C3) being equipotent followed by butyrate (C4), then valerate (C5), and formate (C1) (Brown et al., 2003; Le Poul et al., 2003; Nilsson et al., 2003). Due to the high sequence homology between GPR43 and GPR41, Brown et al., (2003) and Le Poul et al., (2003) also found that short chain fatty acids were agonists of GPR41. The potencies for short chain fatty acids at GPR41 were in a similar range to GPR43, although a different structure-activity relationship was identified. Propionate, valerate and butyrate were equipotent at GPR41, with acetate and hexanoate showing a measurably lower potency (Brown et al., 2003; Le Poul et al., 2003). Short chain fatty acids activate GPR41 and GPR43 with relatively low potency, generally in the mid micromolar range. The low potency of these ligands has led to suggestions that they may not be the endogenous agonists for the receptors (Milligan et al., 2006).

1.4.3.1 GPR42 is likely to be a pseudo gene

As mentioned previously, GPR41 and GPR42 share high sequence homology and differ by only six amino acid residues. Brown et al., (2003) found that GPR42 was unable to respond to short chain fatty acids. As only one ortholog of human GPR41 and GPR42 was found in rodent and bovine lineages, they undertook a mutagenesis study to replace the differing residues in GPR41 with the corresponding residues in GPR42. They found that mutation of Arg¹⁷⁴ in GPR41 to Trp resulted in the receptor being unable to respond to short chain fatty acids. The equivalent mutation in GPR42 (Trp¹⁷⁴Arg) was able to confer short chain fatty acid activity to the receptor. In addition to the lack of function of GPR42, no expression of the receptor could be detected in a range of normal human tissues (Brown et al., 2003). Due to its inability to respond to short chain fatty acids and no expression being detected, GPR42 is now considered to be a pseudo-gene (Brown et al., 2005).

1.4.3.2 Signalling and G protein coupling

GPR41 and GPR43 have distinct G protein coupling specificities. GPR41 couples efficiently to the PTX sensitive G protein, G α_{o1} and agonist function can be measured in [³⁵S]GTP γ S binding assays (Brown et al., 2003; Le Poul et al., 2003). Le Poul et al., (2003) found that it was necessary to co-express GPR41 with the promiscuous G protein, G α_{16} to measure the release of [Ca²⁺]_i. It has also been shown that mouse GPR41 can reduce forskolin-induced cAMP production in CHO-K1 cells (Xiong et al., 2004). GPR43 has been shown to couple to both PTX sensitive and insensitive G proteins (Brown et al., 2003; Le Poul et al., 2003, Nilsson et al., 2003). Although Nilsson et al., (2003) concluded that the receptor coupled mainly through PTX sensitive G proteins as they observed a 70% reduction in the signal generated by GPR43 in a [Ca²⁺]_i mobilisation assay upon PTX treatment. Neither GPR41 nor GPR43 has been tested for their ability to interact with a full panel of mammalian G protein. GPR43 has been tested for its ability to interact with a wide panel of chimeric yeast-mammalian G protein α subunits and it was found to interact with G α_{12} , G α_{13} , G α_{14} , G α_{41} and G α_{43} (Brown et al., 2003). It therefore appears that GPR43 is a more promiscuous receptor than GPR41.

1.4.3.3 Expression pattern

The initial studies on GPR41 detected high levels of mRNA in a range of normal human tissues with highest levels of expression found in adipose tissue (Brown et al., 2003). High levels of expression were also seen in the pancreas, spleen, lymph nodes, bone marrow and

peripheral blood mononuclear cells (Brown et al., 2003; Le Poul et al., 2003). GPR41 mRNA was detected in 3T3-L1 and 3T2-F442A adipose cell lines, and levels increased upon differentiation, although absolute levels remained low (Brown et al., 2003). The expression of GPR41 in adipose cells was confirmed by Xiong et al., (2004). They were able to identify mRNA corresponding to GPR41 in human adipose tissue, mouse white adipose tissue and in differentiated cells from the mouse adipogenic cell line, Ob-Luc. The expression of GPR41 in adipose cells was brought into question by Hong et al., (2005). They were unable to detect GPR41 expression in human adipose tissue, cultured pre-adipocytes or adipocytes, or in 3T3-L1 cells. The discrepancy of GPR41 expression in these studies is unknown, as Hong et al., (2005) used the same probes for detecting the receptor as Xiong et al., (2004).

GPR43 has a more specific expression pattern than GPR41. Levels of GPR43 mRNA can be detected in a variety of tissues but highest expression can be found in immune cells such as neutrophils, monocytes, peripheral blood mononuclear cells, B-lymphocytes and polymorphonuclear cells. Considerable levels of GPR43 were detected in bone marrow and spleen but this is thought to reflect the expression of the receptor on immune cells (Brown et al., 2003; Le Poul et al., 2003; Nilsson et al., 2003). The expression of GPR43 on immune cells is not surprising as mouse GPR43 was first identified from leucocytes (Senga et al., 2003). GPR43 has also been detected in neutrophils and eosinophils by hybridisation to high-density oligonucleotide arrays (Nakajima et al., 2004). Nilsson et al., (2003) also found expression of the receptor in skeletal muscle and heart. GPR43 has also been reported in adipose tissue (Hong et al., 2005), the breast cancer cell line, MCF-7 (Yonezawa et al., 2006) and rat distal ileum and colon (Karaki et al., 2006).

Two recent patents by Arena Pharmaceuticals indicated that both GPR41 and GPR43 may also be expressed in pancreatic islet cells and both receptors subject to up-regulation in *db/db* diabetic mice.

1.4.3.4 Role of short chain fatty acids in the immune response – could this response be mediated by GPR41 and GPR43

The initial studies on GPR43 and GPR41 all indicated that GPR43 was expressed at high levels and GPR41 to a lesser extent in a variety of immune cells (Brown et al., 2003; Le Poul et al., 2003; Nilsson et al., 2003). Le Poul et al., (2003) demonstrated that treatment of polymorphonuclear cells with acetate or propionate induces a rise in $[Ca^{2+}]_i$ and chemotaxis. This confirms various other studies in which short chain fatty acids mediate

the activation of leukocytes by Ca^{2+} mobilisation (Naccache et al., 1998; Nakao et al., 1992; Cavaglieri et al., 2003) and implicates GPR43 in the well known effects of short chain fatty acids on monocyte chemotaxis and movement towards sites of bacterial infection. High concentrations of short chain fatty acids have been reported in connection with severe anaerobic infections, which have the potential to activate GPR43 and mediate the recruitment of leukocytes to the site of infection.

Normal blood concentrations of short chain fatty acids are 100-150 μM acetate, 4-5 μM propionate and 1-3 μM butyrate (Cummings et al., 1987) but increased levels of fatty acids are associated with some disease states. The genetic condition propionic acidemia results in the accumulation of propionate in the blood due to mutations in propionyl-CoA carboxylase. The disease is characterised by a low blood pH due to the build up of propionate and the impairment of immune function leading to frequent infections (Feliz et al., 2003). It has been suggested that the immunosuppressive factor in propionic acidemia is propionate.

Alcohol consumption has been shown to increase circulating acetate concentrations by 250% (Siler et al., 1999) and levels of acetate may reach those required to activate GPR43. In patients with alcoholic hepatitis and cirrhosis it is common to find polymorphonuclear neutrophils at the site of disease (Bautista, 2002). Alcohol is metabolised to acetate by the liver which may explain the recruitment of polymorphonuclear neutrophils. Acute and chronic alcohol intake increases the susceptibility to bacterial and viral infections (Corberand et al., 1989; Bautista, 2002). The defective inflammatory response may be due to the desensitisation of the immune response through activation by excess acetate. To date no studies have been undertaken to examine the contribution activation of GPR43 makes towards the immune response.

1.4.3.5 Role of GPR41 and GPR43 in adipocytes

As detailed above, there is some debate about the expression of GPR41 in adipocytes. Brown et al., (2003), Le Poul et al., (2003) and Xiong et al., (2004) were all able to detect GPR41 mRNA in adipose tissue. Xiong et al., (2004) undertook studies to determine the function of GPR41 in adipocytes. Using the Ob-Luc cell line, in which one allele of the leptin gene is knocked in with a luciferase cassette which allows the expression of the leptin gene to be monitored via luciferase bioluminescence, they demonstrated that the addition of short chain fatty acids to these cells increased luciferase activity in a concentration dependent manner. They found a similar rank order of potency as observed

by Brown et al., (2003) and Le Poul et al., (2003), with acetate being significantly less potent than propionate or butyrate. To examine the contribution of GPR41 to the production of leptin, as they also detected GPR43 in these cells, they used siRNA treatment to knockdown the expression of GPR41. The knockdown of GPR41 almost completely abolished the ability of propionate to induce luciferase expression, and consequently leptin production. PTX treatment of Ob-Luc cells rendered short chain fatty acids unable to stimulate leptin production. The production of leptin has been linked to another $G\alpha_{i/o}$ coupled receptor, the adenosine A_1 receptor (Rice et al., 2000). They therefore concluded that activation of GPR41 in adipocytes is coupled to the production of leptin. Leptin is known as a potent suppressor of appetite through its action on the CNS (Cohen et al., 2001). The effects of propionate on appetite have been observed previously. Sodium propionate supplemented diets or infusion have been shown to reduce food intake in chickens and sheep through an unknown mechanism (Farningham and Whyte, 1993; Pinchasov and Elmaliyah. 1995). Xiong et al., (2003) also found that mice fed on a diet containing 3% sodium propionate ate less than control animals fed with an equimolar amount of sodium chloride.

In contrast to the findings by Xiong et al., (2003), Hong et al., (2005) came to a different conclusion as to the important short chain fatty acid receptors in adipocytes. They were unable to detect GPR41 mRNA in any cell line or tissue tested and decided to study the role of GPR43 in the differentiation of adipocytes. Using 3T3-L1 adipocytes, they demonstrated that treatment of the cells with acetate or propionate increased GPR43 expression and oil red O staining, which indicates the accumulation of lipids within the cells. Knockdown of GPR43 expression by siRNA treatment and subsequent treatment with short chain fatty acid resulted in a reduction in oil red O staining compared to wild type cells, which indicated that GPR43 is involved in the differentiation of adipocytes. Treatment of 3T3-L1 cells with acetate or propionate also inhibited isoproterenol stimulated lipolysis in a concentration dependent manner and this was abolished when GPR43 expression was reduced by siRNA treatment (Hong et al., 2005). This indicates that activation GPR43 plays a role in the inhibition of lipolysis. The role of GPR41 and GPR43 in adipose tissue and leptin production needs to be further examined. If GPR41 mediates leptin production in adipose tissue, it may prove to be a new target in the treatment of obesity and diabetes.

1.4.3.6 Role of short chain fatty acids in the colon

Large amounts of bacteria are present in a healthy colon which serves to digest polysaccharides, oligosaccharide and proteins in the gut. A by-product of this fermentation is the production of high concentrations of short chain fatty acids. In human colon, the total concentration of short chain fatty acids reaches between 60 and 130mmol L⁻¹, of which acetate is the most common and butyrate and propionate found in approximately similar concentration, with a molar ratio of 60:20:20 respectively (Cummings et al., 1987). They are produced by anaerobic bacterial fermentation of undigested dietary carbohydrates and fibre polysaccharides and been proposed to play a key role in the maintenance of colonic homeostasis (Wong et al., 2006). The development of irritable bowel disease (IBD) has been linked to a reduction of colonic short chain fatty acid production (Galvez et al., 2005), as levels of short chain fatty acids are decreased in the lumens of patients with ulcerative colitis (Vernia et al., 1988) and butyrate enemas have been reported to alleviate the symptoms of ulcerative colitis (Steihart et al., 1994; Patz et al., 1996), although their effectiveness has been questioned (Breuer et al., 1997). Butyrate is also linked to the inhibition of proliferation of a variety of cancer cell lines and it may have preventative effects in the development of colon cancer (Wong et al., 2006). The exact mechanism by which butyrate affects proliferation is unknown but it has been shown to be an inhibitor of histone deacetylase.

GPR43 mRNA has been detected in rat distal ileum and colon (Karaki et al., 2006). A recent study by Dass et al., (2007) attempted to uncover the role of GPR43 in intestinal motility. They also found that GPR43 mRNA was present in the rat gut, with highest levels detected in the colon and they investigated the contribution of GPR43 to the effects of the fatty acids in the gut. Electrical field stimulation evokes relaxation of rat distal colon and removal of the stimulation causes the colon to contract. The post stimulation contraction could be inhibited in a concentration-dependent manner by formate, butyrate, acetate, propionate and valerate. They found that butyrate, acetate and propionate were the most potent followed by valerate then formate. Using guinea-pig ileum, it was found that the fatty acids stimulated peristaltic motility, with a similar rank order of potency. Similar effects of fatty acids were observed in mouse gut, with short chain fatty acid inhibiting the post electrical field stimulation contraction of the colon. The rank order of potency of the fatty acids corresponds to that seen at GPR43 in HEK293 cells and to investigate the contribution of GPR43 to this effect they used GPR43 knockout mice. In the GPR43^{-/-} mice they found the same rank-order of inhibitory effects evoked by short chain fatty acids (Dass et al., 2007). To date, there have been no reports of GPR41 being expressed in the

gut, so it is unlikely to be up-regulated in the knockout mice and the rank order of potency of the short chain fatty acids at GPR41 is different in recombinant systems than that seen in this study. The data generated using the knockout mice suggests that GPR43 does not mediate the effects short chain fatty acids have on intestinal motility.

An area in which GPR41 and GPR43 are still proposed to be involved in is the development of IBD. IBD is characterised by chronic and spontaneously relapsing inflammation of the gut. The precise etiology of disease progression is still unknown and is proposed to involve a number of factors including environmental, genetic, microbial and immunological factors (Fiocchi et al., 1998). It has been proposed that the exacerbated inflammatory response towards the intestine results from an inappropriate reaction towards a luminal agent (Farrell et al., 2002). The intestinal epithelium acts as a barrier between the gut and the rest of the body but during the development of IBD the luminal wall can be compromised and this leads to the further up regulation of the immune response towards the gut. Neutrophils are proposed to play a key role in the development of IBD and other inflammatory processes in the gut. They are recruited to the colon and undergo activation to produce reactive oxygen intermediates and chemokines (Le Poul et al., 2003). The release of the short chain fatty acids from the gut into the blood stream may act as an erroneous signal to the immune system via activation of GPR43. If the activation of GPR43 is shown to play a role in the development of IBD it could lead to the development of new therapeutics in the treatment of this disease.

1.4.4 Two further GPCRs that are activated by free fatty acids

Recently, two further orphan GPCRs have been shown to be activated by free fatty acids; GPR84 and GPR120 (Hirasawa et al., 2005; Wang et al., 2006). GPR84 responds to medium chain fatty acids, C9 to C14, and GPR120 is activated by saturated, C14 to C18, and unsaturated, C16 to C22, long chain fatty acids.

1.4.4.1 GPR84

Previous studies on GPR84 identified the receptor as being expressed in neutrophils, eosinophils and phorbol ester activated peripheral blood mononuclear cells (Yousefi et al., 2001). Diindolylmethane was found to be a surrogate ligand for the receptor (Takeda et al., 2003) but a natural ligand was not identified until 2006 by Wang et al., (2006). Using a reverse pharmacology approach in combination with an assay to measure the release of $[Ca^{2+}]_i$, medium chain fatty acids were shown to activate GPR84. They found that

saturated fatty acids containing between 9 and 14 carbons were able to activate the receptor in a concentration-dependent manner in two different assay systems, one measuring the inhibition of forskolin stimulated cAMP production and the other measuring the activation of the G protein through binding of the non-hydrolysable analogue of GTP, [³⁵S]GTPγS. Of the fatty acids that were able to activate the receptor, capric acid (C10), undecanoic acid (C11) and lauric acids (C12) were shown to be the most potent (Wang et al., 2006). The potencies of medium chain fatty acids at GPR84 are comparable to that seen at GPR40, with fatty acids activating GPR84 in the micro-molar range. Unlike GPR40, GPR84 shows more selectivity in regards to fatty acid chain length and is likely to couple predominately through the Gα_{i/o} family of G proteins whereas GPR40 is a predominately Gα_{q/11} coupled receptor (Briscoe et al., 2003; Wang et al., 2006). Wang et al., (2006) found that GPR84 was primarily expressed in monocytes and neutrophils. Stimulation of a human monotypic leukaemia cell line, THP-1, and a mouse monocytes/macrophage cell line, RAW264.7, with lipopolysaccharide (LPS) resulted in an upregulation of GPR84 mRNA, which suggests that GPR84 may play a pivotal role in monocyte and macrophage activation. The treatment of LPS stimulated cells with capric acid, undecanoic acid, lauric acid and diindolylmethane increased the secretion of interleukin-12 p40 subunit (IL-12 p40) in a concentration dependent manner. IL-12 plays an important role in promoting cell mediated immunity to eradicate pathogens by inducing and maintaining T helper 1 responses and inhibiting T helper 2 responses (Hsieh et al., 1993). Venkataraman and Kuo (2005) studied the role of GPR84 in the immune system by generating a GPR84 knockout mouse. They found that GPR84^{-/-} mice specifically produced higher levels of IL-4 upon stimulation but no other phenotype could be detected (Venkataraman and Kuo, 2005). As mentioned in Section 1.4.2.5, medium and long chain fatty acids are known to exert diverse effects on the immune system (Hwang, 2000; Wanten, 2000). The expression pattern of GPR84 and its ability to be activated by medium chain fatty acids may provide a link between the activation of immune cells by fatty acids and the development of autoimmune diseases.

1.4.4.2 GPR120

GPR120 was deorphanised using a unique strategy in which the receptor was fused to a fluorescent protein and the levels of internalised receptor were monitored in response to a library of compounds. Using this technique they found that long chain fatty acids evoked specific internalisation of GPR120 and the ability of fatty acids to activate the receptor in a concentration-dependent manner was confirmed in a Ca²⁺ release assay. Most of fatty acids shown to activate GPR120 are also able to activate GPR40. For most of the fatty

acids both receptors show similar potencies, apart from α -linolenic acid and γ -linolenic acid which both are 10 times more potent at GPR120 than GPR40 (Briscoe et al., 2003; Hirasawa et al., 2005). The main area of GPR120 expression is the intestinal tract and lung in both mice and humans (Hirasawa et al., 2005). Expression of GPR120 is also found in the intestinal endocrine cell line STC-1 (Hirasawa et al., 2005; Katsuma et al., 2005). The activation of GPR120 by free fatty acids in STC-1 cells has been reported to inhibit cellular apoptosis initiated by serum deprivation (Katsuma et al., 2005). Using STC-1 cells, Hirasawa et al., (2005) demonstrated that the secretion of glucagon-like peptide-1 (GLP-1) was mediated through activation of GPR120 by fatty acids. STC-1 cells also express GPR40, so to identify which receptor was being activated by the fatty acids they reduced the expression of each receptor by siRNA treatment. Cells transfected with GPR40 siRNA showed no change in their ability to secrete GLP-1, whereas a significant reduction in GLP-1 secretion was observed in cells transfected with GPR120 siRNA. Increased plasma insulin and GLP-1 levels were also shown in the portal vein and the inferior vena cava in mice in response to α -linolenic acid but not to stearic acid or octanoic acid, which were unable to activate GPR120 *in vitro* (Hirasawa et al., 2005). Iakoubov et al., (2006) found that the atypical protein kinase C, PKC ξ , was required for oleic acid induced GLP-1 secretion via GPR120 in the murine GLUTag L cell line. GLP-1 is a well characterised natural modulator of glucose dependent insulin secretion and its receptor is found on pancreatic β cells and is therefore a target in the treatment of diabetes (Rotella et al., 2005). The GLP-1 receptor is a family B GPCR but it has proved to be a difficult target for clinical intervention as exogenous GLP-1 has a short half life (D'Alessio et al., 2005) and small molecule agonists for the GLP-1 receptor have only recently been described (Knudsen et al., 2007). Therefore targeting GPR120 rather than the GLP-1 receptor may prove to be an alternative strategy in the treatment of diabetes.

As detailed in section 1.4.2.4, there have recently been two papers describing GPR40 specific small molecule agonists (Garrido et al., 2006; Briscoe et al., 2006) and a GPR40 specific antagonist (Briscoe et al., 2006). The similarities between GPR40 and GPR120 in their activation by long chain fatty acids also means that the small molecule agonist described in detail by Briscoe et al., (2006), GW839508X, is an agonist of GPR120 although with less potency than at GPR40 (pEC_{50} for GPR40 = 7.32 ± 0.03 and for GPR120 = 5.46 ± 0.09). The small molecule antagonist, GW1100, was unable to block a GPR120 mediated rise in $[Ca^{2+}]_i$, indicating that it is a specific GPR40 antagonist. To date, the effect of these compounds on GPR84 has not been reported.

1.5 GPCR oligomerisation

Traditional models of GPCR ligand binding and signal transduction always portrayed GPCRs as monomeric signalling units. The finding that the functional γ -aminobutyric acid receptor (GABA_B receptor) was an obligate heterodimer of two distinct GPCR subunits GABA_BR1 and GABA_BR2 (Jones et al., 1998; Kaupmann et al., 1998; White et al., 1998; Sullivan et al., 2000) triggered immense interest into the possibility that GPCRs were not monomeric signalling units and were able to interact with each other.

There are a variety of techniques that can be used to demonstrate protein-protein interactions between GPCRs and some are covered below in section 1.5.2. Many of these techniques are not able to distinguish between a simple dimer and a higher order oligomeric structure. Therefore, I will refer to oligomerisation rather than dimerisation.

1.5.1 Methods to monitor GPCR oligomerisation

1.5.1.1 Co-immunoprecipitation

The starting point of many studies into the oligomerisation of GPCRs is their ability to be co-immunoprecipitated. Co-immunoprecipitation refers to the ability of one epitope tagged GPCR to be immunoprecipitated with another differentially tagged receptor and to be detected by western blotting. The commercial availability of a variety of specific antibodies for epitope tags has made this technique widespread (Milligan and Bouvier, 2005). Co-immunoprecipitation data has been subject to much scrutiny and has raised questions regarding the possibility of results being an artefact of the experimental procedure. During preparation of samples, the receptors have to be solubilised from the membrane upon which these membrane proteins may aggregate. To address this detergent extracts of membranes each expressing only one of the tagged receptors are combined prior to immunoprecipitation. These samples generally do not result in co-immunoprecipitation and therefore exclude the possibility of non-specific aggregation (Jordan and Devi, 1999).

1.5.1.2 Resonance energy transfer (RET) techniques

Techniques based on the energy transfer between a donor molecule and acceptor molecules have been extensively used to monitor the formation and existence of GPCR oligomers in living cells. Energy is transferred in a non-radiative manner as a result of a dipole-dipole

coupling mechanism and is referred to as resonance energy transfer (RET). The energy transfer is based on the Förster theory which demonstrates that energy transfer is highly dependent on the proximity of the donor and acceptor moieties (Förster, 1948). The donor and acceptor have to be within 100Å of each other to generate a significant energy transfer and this short distance is indicative of direct protein-protein interactions (Wu and Brand, 1994). The donor molecule can be a fluorescent or luminescent protein. Direct excitation of a fluorescent protein results in energy transfer to an acceptor fluorescent protein and is referred to as fluorescence resonance energy transfer (FRET). Whereas when the donor protein is a luminescent protein, the oxidation of a substrate results in energy transfer to a fluorescent protein and this technique is called bioluminescence resonance energy transfer (BRET). In both techniques, the energy is re-emitted by the acceptor protein at a wavelength that is characteristic of the acceptor moiety. The energy transfer is dependent on the overlap of the donor and acceptor excitation spectra, although significant overlap results in a reduction in the resolution of the RET signal generated. Additional factors that affect the energy transfer include the quantum yield of the donor and acceptor excitation spectra and the orientation of the donor and acceptor moieties. The bioluminescent or fluorescent proteins can be N- or C-terminally fused to the receptors of interest to allow expression in heterologous systems to investigate their interaction.

1.5.1.3 Bioluminescence energy transfer (BRET)

BRET utilises the bio-luminescent protein luciferase from the sea pansy, *Renilla reniformis* (Rluc) and a fluorescent acceptor protein. The technique is based on the natural phenomenon of bioluminescence found in marine animals such as *Renilla reniformis* and the jellyfish, *Aequora victoria*. Energy transfer results for the oxidation of the Rluc substrate coelenterazine and the transfer of energy from Rluc to the acceptor protein, green fluorescent protein (GFP) (Xu et al., 1999).

Originally, BRET systems used Rluc as the donor and a red shifted mutant of GFP, termed enhanced yellow fluorescent protein (eYFP). The spectral properties of Rluc overlap significantly with that of eYFP resulting in a poor signal to noise ratio (Xu et al., 1999). To address this issue, a modified version of this assay has been developed and termed BRET². It utilises a modified form of coelenterazine called DeepBlueC (PerkinElmer), which when oxidised by Rluc produces a different spectra which is transferred to a modified form of GFP termed GFP². The use of DeepBlueC and GFP² allows much higher spectral resolution between donor and acceptor and vastly improves the signal to noise ratio. This technique has been extensively used to detect protein-protein interactions and

in particular has been used to investigate the properties of receptor oligomerisation and the interaction of GPCRs with intracellular protein such as arrestins. By expressing different amounts of energy donor and energy acceptor-linked GPCRs, saturation curves can be generated that resemble ligand binding curves (Mercier et al., 2002). This can provide useful measurements of the relative interaction affinities of the GPCRs to form oligomers (Mercier et al., 2002; Ramsay et al., 2004; Wilson et al., 2005).

1.5.1.4 Fluorescence resonance energy transfer (FRET)

FRET utilises the ability of fluorescent donor and acceptor proteins that have overlapping donor emission and acceptor excitation spectra. Energy transfer occurs upon the excitation of the donor protein by an external light source. As mentioned above, mutations in GFP can alter its spectral properties and provide energy transfer pairs. The most widely used pairing is enhanced cyan fluorescent protein (eCFP) as the energy donor and eYFP as the acceptor. Several other combinations of different variants of GFP can also be used (Milligan and Bouvier, 2005). There are several variations of the FRET technique but one of the advantages is it can be used to monitor protein-protein interactions within living cells. To monitor protein-protein interactions within living cells, the proteins of interest have to be fused to the fluorescent proteins and expressed in heterologous systems. Imaging of the FRET within the cells requires three measurements to be recorded; sensitised fluorescence and donor and acceptor fluorescence. Recent advances have allowed FRET to be used to examine the existence of higher order GPCR oligomerisation. It utilises three component FRET systems based on serial energy transfer from cyan to yellow to red fluorescent proteins (He et al., 2004), and has been used to confirm the presence of higher order oligomers of the α_{1b} adrenergic receptor (Lopez-Gimenez et al., 2007).

A variation of FRET, called time resolved FRET (Tr-FRET) can be used to specifically detect the presence of interacting proteins at the surface of cell. This technique utilises antibodies directed at epitope tags, which can be introduced onto the N-terminus of a GPCR. The antibodies are labelled with donor and acceptor moieties suitable for FRET. The donor moiety is commonly europium chelate which has long-lived fluorescence (Bazin et al., 2002). Excitation of the europium results in the excitation of endogenous fluorophores, but this fluorescence is short lived. A time delay of over 50 μ s between excitation and measurement of FRET allows the fluorescence from the endogenous fluorophores to decay and results in improved signal-to-noise ratios. The acceptor moieties commonly used include allophycocyanin and Alexa Fluor 647 (Pfleger and Eidne,

2005). Attaching the epitope tags to the N-terminus of a GPCR ensures that the antibodies directed at the epitopes only have access to cell surface expressed GPCRs, and has been used in studies to detect GPCR oligomers at the cell surface (McVey et al., 2001; Canals et al., 2004).

1.5.1.5 Functional reconstitution

A further technique that has been used to investigate GPCR oligomerisation is termed functional reconstitution. In this technique two non-functional but different GPCR mutants, which are unable to signal when singly expressed, are coexpressed and if ligand binding or functionality can be restored it strongly suggests protein-protein interactions. This has been demonstrated for the angiotensin AT₁ receptor (Monnot et al., 1996), the α_{1b} adrenergic receptor (Carrillo et al., 2003) and the opioid receptors (Pascal and Milligan, 2005)

1.5.2 Functional significance of GPCR oligomerisation

Using the techniques described in section 1.5.2 and other complementary techniques, a large range of Family A GPCRs have been shown to homo-oligomerise and to hetero-oligomerise with both closely related receptors and to ones that they share little homology (Milligan, 2006). The functional significance of hetero-oligomerisation is poorly understood but roles have been proposed in protein folding, correct membrane delivery and interactions with G proteins.

There is a growing amount of evidence to suggest that GPCR oligomer formation occurs during protein synthesis and is important for correct cell surface delivery of the receptor (Bulenger et al., 2005). This has been demonstrated by the introduction of endoplasmic reticulum retention (ER) motifs which result in the modified receptor being retained in the ER along with a co-expressed, unmodified receptor. This has been demonstrated for the β_2 adrenergic receptor (Salahpour et al., 2004) and for the CXCR1 and CXCR2 chemokine receptors (Wilson et al., 2005). In the case of the GABA_BR1 and GABA_BR2 receptors, the GABA_BR1 receptor contains an ER retention sequence within its carboxy terminus and is not delivered to the cell surface when expressed alone. The GABA_BR2 can mask the ER retention sequence to enable the complex to be delivered to the cell surface (Sullivan et al., 2000).

An important proposed role for oligomerisation of GPCRs is in binding of G proteins. Models of rhodopsin and its associated G protein transducin have demonstrated that a dimer of rhodopsin provides an ideal footprint for a single heterotrimeric G protein to bind. The monomeric cytoplasmic surface of rhodopsin is too small to accommodate interactions with the α and $\beta\gamma$ subunits simultaneously (Fotiadis et al., 2004; Fotiadis et al., 2006). Biophysical studies using the BLT1 leukotriene B4 receptor also found that the basic signalling unit was composed of two receptors and the three subunits of the G protein (Baneres et al., 2003).

The effect of hetero-oligomerisation on ligand pharmacology and function has been investigated in a growing number of studies (Bulenger et al., 2005; Milligan, 2006). Studying the effect of hetero-oligomerisation is complicated by the probable presence of homo-oligomers, as only if the hetero-oligomer has a much higher affinity to form will there be just hetero-oligomers at the cell surface. There have been some examples of hetero-oligomerisation having an effect on the function of GPCRs. Two opioid receptor subtypes, MOP and DOP, when expressed singly each couple to PTX sensitive G protein but on co-expression they can generate signals that are insensitive to PTX treatment (George et al., 2000). These signals have been shown to be generated by activation of G_z , which reflects a switch in the G protein coupling of these receptors (Fan et al., 2006). This may reflect the hetero-oligomer being able to generate a unique interface that allows a different G protein to bind. The ability of a hetero-oligomer to activate different G proteins has also been demonstrated for the D1 and D2 dopamine receptors (Lee et al., 2004). Difference in the potency of ligands has also been demonstrated upon the co-expression of two receptors. For example, the co-expression of the orexin-1 receptor and the cannabinoid CB1 receptor enhances the potency of orexin-A 100 fold and this effect could be blocked by CB1 receptor antagonists (Hilairret et al., 2003). These effects could have wide reaching effects on the development of new clinically relevant compounds (Milligan, 2006). The physiological existence of hetero-oligomers has only been demonstrated for a handful of receptors. A selective agonist for the DOP-KOP opioid receptor hetero-oligomer displays similar effects *in vivo* as *in vitro* which supports the existence of opioid receptor hetero-oligomers in physiological systems (Waldhoer et al., 2005).

Rhodopsin is the only GPCR for which high resolution structural information is available. The initial crystal structure of rhodopsin did not contain any information regarding the quaternary structure of the receptor. This is due to the requirement to extract the receptors from the membranes by detergent treatment before the crystallisation process. The high

expression of rhodopsin in rod outer segments allowed investigations into the organisation of the receptor in its native state. This has been carried out on mouse outer rod segments by atomic force microscopy (Fotiadis et al., 2003; Liang et al., 2003). These studies clearly demonstrate the arrangement of the receptors in para-cystalline arrays with densely packed, double rows of the receptor. Data from studies on 2-dimensional crystals of squid rhodopsin also demonstrates a higher order of the receptors (Davies et al., 2001). Computational models based on the observations from these studies have been generated to determine the key contacts between the receptor monomers (Fotiadis et al., 2004; Fotiadis et al., 2006). From these models, TM4 and 5 have been implicated to play key role in the formation of receptor oligomers, and this has been supported by mutagenesis studies (Kota et al., 2006). Studies on other Family A GPCRs, such as the dopamine D2 receptor (Guo et al., 2003; Guo et al., 2005) and the α_{1b} adrenergic receptor (Carrillo et al., 2004) have also demonstrated that TM region 4 is important for oligomer formation. Although it appears that TM4 is important for oligomer formation, other regions have been implicated and there may not be a consensus across Family A receptor (Milligan, 2006).

1.6 Project aims

The aim of this study was to gain a greater understanding of the pharmacology and function of GPR40, GPR41 and GPR43. Due to their status as newly de-orphaned GPCRs, robust assays to monitor their activation were developed. The development of a [35 S]GTP γ S binding assay to monitor the activation of GPR40 allowed the pharmacology of synthetic small molecule agonists, antagonists and thiazolidinediones to be investigated. Using predictions from models of GPR40, GPR41 and GPR43, which were based on the crystal structure of rhodopsin, mutagenesis studies were undertaken to investigate residues that were implicated in binding fatty acids and the fatty acid chain length specificity of GPR40 and GPR43. The formation of GPR40 and GPR43 homo-oligomers was also investigated using several techniques including co-immunoprecipitation, Tr-FRET and FRET.

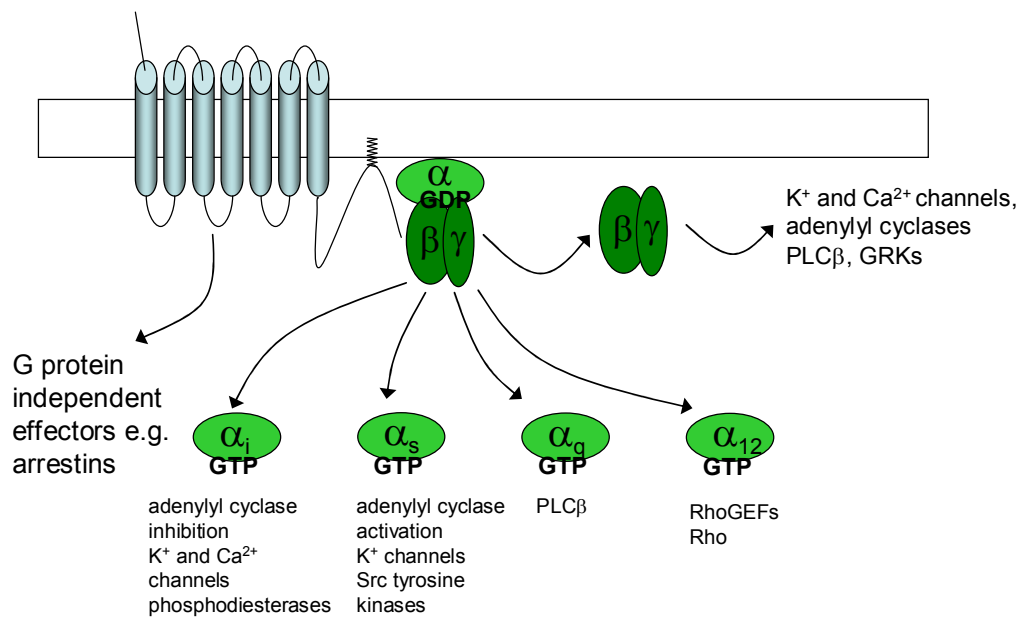


Figure 1.1 Diversity of GPCR signalling

Activation of GPCRs can mediate a variety of cellular responses via G protein and G protein independent mechanisms.

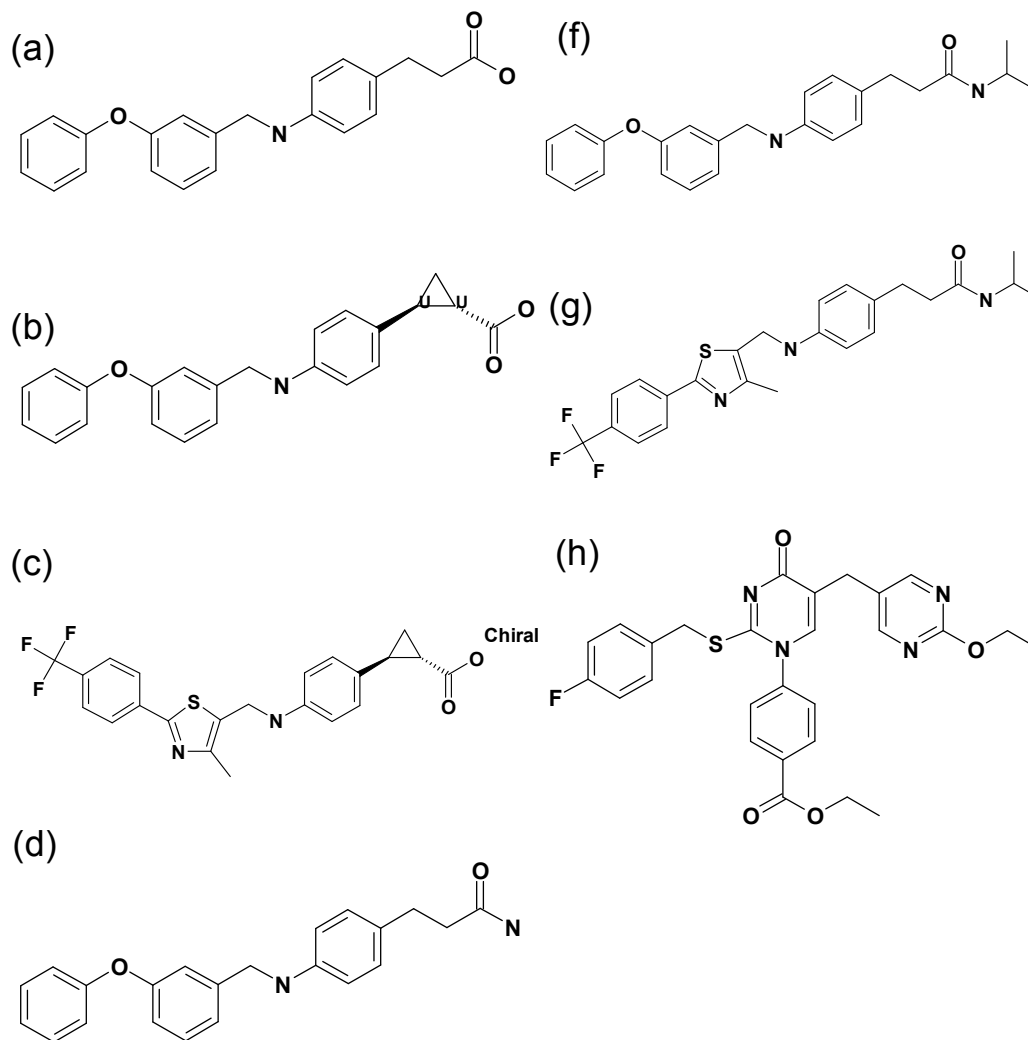


Figure 1.2 Chemical structures of synthetic agonists and an antagonist used in my studies

(a-g) Chemical structures of GPR40 synthetic agonists as detailed in Garrido et al., (2006). The above structures are termed: (a) GW839508X (2A), (b) GSK248257A (14A), (c) GSK250089A (14B), (d) GSK223112A (16A), (e) GSK272235A (18A), (f) GSK269778A (18B). Numbers in parenthesis refer to the compound numbers in Garrido et al., (2006). Compound (f) is the GPR40 antagonist GW1100 as described in Briscoe et al., (2006).

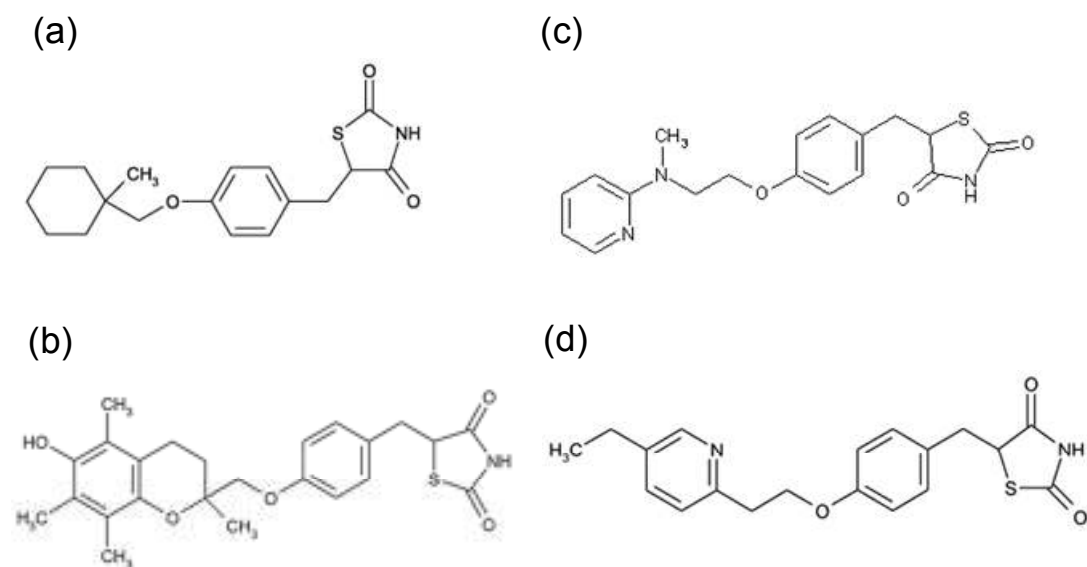


Figure 1.3 Structure of thiazolidinediones

Chemical structures of (a) ciglitazone, (b) troglitazone, (c) rosiglitazone and (d) pioglitazone.

2 Material and Methods

2.1 Materials

2.1.1 *General reagents, enzymes and kits*

Amersham Pharmacia Biotech UK Ltd., Little Chalfont, Buckinghamshire, UK

Full range RainbowTM molecular weight markers, 1st strand DNA synthesis kit, protein G

Axxora (UK) Ltd., Nottingham, UK

Ciglitazone, pioglitazone, rosiglitazone, troglitazone

BDH, Lutterworth, Leicestershire, UK

22mm coverslips, microscope slides

Chemicon Europe Ltd., Chandlers Ford, UK

ReBlot Plus solution

Fisher Scientific UK Ltd, Loughborough, Leicestershire, UK

NaCl, KCl, KH₂PO₄, Na₂HPO₄, Tris, Hepes, EDTA, SDS, CaCl₂, D-glucose, DTT, urea, glacial acetic acid, sucrose, bactotryptone, yeast extract, C₂H₃O₂K, MnCl₂, glycerol, MOPS, bactoagar, ethylene glycol, methanol, isopropanol, ethanol

Flowgen Bioscience Ltd., Nottingham, UK

Agarose

Invitrogen Ltd., Paisley, UK

NuPage Novex pre-cast 8-12% Bis-Tris gels, NuPage MOPS SDS running buffer, deoxyribonuclease

Konica Europe, Hohenbrunn, Germany

X-ray film

Merck Chemicals Ltd., Nottingham, UK

Nonident P-40, pansorbin

Molecular Devices, Sunnyvale, CA

Brilliant Black, Fluo 4

New England Biolabs, MA, USA

Restriction enzymes

Pierce, Perbio Science UK Ltd., Tattenhall, Cheshire, UK

Supersignal West Pico chemiluminescent substrate

Promega UK Ltd., Southampton, UK

Miniprep kit, Pfu DNA polymerase, restriction enzymes, T4 DNA ligase

Qiagen, Crawley, West Sussex, UK

Qiafilter maxiprep kit, QiaQuick gel extraction kit, QiaQuick PCR purification kit, RNeasy kit

Roche Applied Science, Lewes, East Sussex, UK

DNA molecular weight marker X, shrimp alkaline phosphatase, fatty acid free BSA, BSA, complete EDTA-free protease inhibitor tablet, dNTPs

Sigma-Aldrich Company Ltd., Poole, Dorset, UK

Probenecid, Triton X-100, Na-deoxycholate, MgCl₂, bromophenol blue, BCA solution A, CuSO₄, RbCl₂, ampicillin, M2-anti Flag antibody, Tween-20, ascorbic acid, GTP γ S, NaF, GDP, Fura-2, all fatty acids

Stratagene, Amsterdam, The Netherlands

QuikChange site directed mutagenesis kit

Thermo Fisher Scientific, Ulm, Germany

All oligonucleotides used for PCR reactions

2.1.2 Tissue culture plasticware and reagents

American Tissue Culture Collection, Rockville, USA

HEK293T cells

BD Bioscience, Cowley, UK

75cm² Falcon tissue culture flasks

Costar, Cambridge, MA, USA

5ml, 10ml and 25ml pipettes, 75cm² vented tissue culture flasks, 6 well plates, 10cm² dishes

Invitrogen, Paisley, UK

MEM with Earle's Salt and L-Glutamine, MEM non-essential amino acids, foetal bovine serum, lipofectamine, geneticin G418, new born calf serum, RPMI, 2-mercaptoethanol, lipofectamine, HEPES, Flp-In T-REx HEK293 cells

Greiner Bio-One, Kremsmünster, Austria

Poly-D-lysine coated 384-well black-wall, clear-bottom microtiter plates

Nalgene Nunc International, Rochester, NY

175 cm² tissue culture flasks

Roche Applied Science, Lewes, East Sussex, UK

Hygromycin B

Sigma-Aldrich Company Ltd., Poole, Dorset, UK

DMEM, L-glutamine, sodium pyruvate, 0.25% trypsin-EDTA, poly-D-lysine, doxycycline

2.1.3 Radiochemicals**Perkin-Elmer Life and Analytical Sciences, Beaconsfield, Buckinghamshire, UK**

[³⁵S]GTP γ S

2.1.4 Antisera**Amersham Pharmacia Biotech UK Ltd., Little Chalfont, Buckinghamshire, UK**

Donkey anti-mouse IgG-HRP conjugate, donkey anti-rabbit IgG-HRP conjugate

Cell Signaling Technologies, Danvers, MA, USA

Polyclonal anti-c-Myc antibody

Perkin-Elmer Life and Analytical Sciences, Beaconsfield, Buckinghamshire, UK

Anti-Flag-APC antibody, anti-c-Myc-Eu³⁺ antibody

Sigma-Aldrich Company Ltd., Poole, Dorset, UK

Anti-Flag M2 antibody

All G protein antibodies were produced in-house

2.2 Buffers

2.2.1 General buffers

Phosphate buffered saline (PBS) (10x)

137mM NaCl, 2.7mM KCl, 1.5mM KH₂PO₄, 10.2mM Na₂HPO₄, pH 7.4

Diluted 1 in 10 prior to use and stored at 4°C.

Tris-EDTA (TE) buffer

10mM Tris, 0.1mM EDTA, pH 7.4, stored at 4°C.

RIPA buffer (2x)

100mM HEPES (pH7.4), 300mM NaCl, 2% (v/v) Triton X-100, 1% (w/v) Na-deoxycholate, 0.2% (w/v) SDS, stored at 4°C.

Physiological saline solution

130mM NaCl, 5mM KCl, 1mM CaCl₂, 1mM MgCl₂, 20mM HEPES, 10mM D-glucose, pH 7.4.

Laemelli buffer (2x)

0.4M DTT, 0.17M SDS, 50mM Tris, 5M urea, 0.01% (w/v) bromophenol blue. Stored in aliquots at -20°C.

2.2.2 Molecular biology solutions

TAE buffer (50x)

40mM Tris, 1mM EDTA, 5.71% (v/v) glacial acetic acid. Diluted 1 in 50 prior to use.

DNA loading buffer (5x)

0.25% (w/v) bromophenol blue, 40% sucrose (w/v) in H₂O.

LB media (Luria-Bertani medium)

1% (w/v) bacto-tryptone, 0.5% (w/v) yeast extract, 1% NaCl (w/v), pH 7.4. Sterilised by autoclaving at 126°C.

Competent bacteria buffers

Competent bacteria buffer 1:

0.03M C₂H₃O₂K, 0.1M RbCl₂, 0.01M CaCl₂, 0.05M MnCl₂, 15% (v/v) glycerol, pH 5.8 with acetic acid. Filter sterilised through a 0.2µm filter and stored at 4°C.

Competent bacteria buffer 2:

10mM MOPS pH 6.5, 0.075M CaCl₂, 0.01M RbCl₂, 15% glycerol (v/v), pH 6.5 with concentrated HCl. Filter sterilised through a 0.2µm filter and stored at 4°C.

2.3 Molecular biology protocols***2.3.1 Preparation of LB plates***

LB was prepared as detailed in section 2.2.2 and to this 1.5% (w/v) bacto-agar was added. This was autoclaved and allowed to cool to 50°C prior to the addition of ampicillin (50µg/ml). The medium was mixed to ensure equal distribution of antibiotic and approximately 25ml poured per 10cm² petri dish. The plates were left to set at room temperature before being stored at 4°C.

2.3.2 Preparation of competent bacterial cells

DH5α cells were streaked onto an agar plate in the absence of antibiotics and incubated overnight at 37°C. A single colony was inoculated into a 5ml culture of LB broth and grown in a shaking incubator for 16 hours. This culture was used to inoculate 100 ml of LB broth that was grown with aeration at 37°C until the optical density at 550nm reached 0.48. The culture was chilled on ice for 10 minutes then centrifuged at 3220 x g for 10 minutes at 4°C. All traces of LB broth were removed and the pellet resuspended in 20ml of competent bacteria buffer 1. The suspension was incubated on ice for 5 minutes prior to centrifugation at 3220 x g for 10 minutes at 4°C. Following removal of supernatant, cell pellets were resuspended in 2ml of competent bacteria buffer 2. After incubation on ice for 15 minutes the competent bacteria were aliquoted and stored at -80°C until required.

2.3.3 Transformation of competent bacterial cells

An aliquot of competent bacteria was allowed to thaw on ice. To 50µl of competent bacteria between 1 and 10ng of DNA was added and incubated on ice for 15 minutes. The cells were subjected to a heat shock at 42°C for 90 seconds and returned to ice for 2 minutes. To the cells, 450µl of LB broth was added and incubated at 37°C for 45 minutes in a shaking incubator. 100µl of the reaction was spread onto a LB plate containing the appropriate antibiotic and incubated inverted overnight at 37°C.

2.3.4 Preparation of plasmid DNA

2.3.4.1 Mini-preps

Miniprep purification was carried out using Promega miniprep kits as per manufactures instructions. Briefly, cells were pelleted by centrifugation at 16,000 x g for 5 minutes and re-suspended by pipetting in 100µl of re-suspension buffer (50mM Tris-HCl, 10mM EDTA, pH 8.0 containing 100µg/ml RNase A). Cells were treated with 100µl of lysis buffer (200mM NaOH, 1% (w/v) SDS), mixed and incubated for 5 minutes. Lysis was terminated by the addition of 100µl of neutralisation buffer (3mM potassium acetate, pH 5.5). The cell lysates were centrifuged for 10 minutes at 16,000 x g and the supernatant loaded onto miniprep columns. The columns were centrifuged for 1 minute at 16,000 x g and washed twice with 750µl wash buffer (1.0mM NaCl, 50mM Tris-HCl, pH 7.0, 15% (v/v) isopropanol). After washing, bound DNA was eluted into a clean 1.5ml eppendorf tubes with 100µl sterile H₂O

2.3.4.2 Maxi-preps

The Qiagen Qiafilter kit was used to produce larger scale DNA samples. Purification of DNA was carried out as per manufactures instructions. Briefly, a 100ml culture of transformed bacteria was pelleted by centrifugation for 30 minutes at 3220 x g at 4°C. All traces of media were removed and the pellet resuspended in 10ml of chilled buffer P1 (50mM Tris-HCL pH 8.0, 10mM EDTA, 100µg/µl Rnase A). Cell lysis was achieved by the addition of 10ml buffer P2 (200mM NaOH, 1% (w/v) SDS) and incubated for 10 minutes at room temperature. 10ml of buffer P3 (3.0M potassium acetate pH 5.5) was added to neutralise the reaction and the solution was immediately applied to a QIAfilter cartridge and left for 10 minutes at room temperature to settle. Meanwhile, a Qiagen tip 500 was equilibrated by the addition of buffer QBT (750mM NaCl, 50mM MOPS pH 7.0,

15% (v/v) isopropanol). After 10 minutes, the lysed cells were added onto the equilibrated tip and allowed to filter through. The column was washed with 60ml of buffer QC (1.0M NaCl, 50mM MOPS pH 7.0, 15% (v/v) isopropanol). The DNA was eluted by the addition of 15ml of buffer QF (1.25M NaCl, 50mM Tris-HCl pH 8.5, 15% (v/v) isopropanol) to the tip. The DNA was precipitated by the addition of 10.5ml isopropanol and pelleted by centrifugation at 12,000 x g for 30 minutes at 4°C. The DNA pellet was washed with 5ml of room temperature 70% (v/v) ethanol and then centrifuged for 15 minutes at 12,000 x g at 4°C. The supernatant was carefully removed and the pellet allowed to air dry prior to resuspension in 1ml of sterile water.

2.3.5 Quantification of DNA

Quantification of DNA samples was performed by examining the absorbance of a 1:100 dilution of the sample at 260nm. An A_{260} value of 1 unit was taken to correspond to 50µg/ml of double stranded DNA. The A_{280} value of sample was also measured to assess the purity of the DNA solution. A DNA solution with A_{260}/A_{280} ratio of between 1.7 and 2.0 was considered pure enough for use.

2.3.6 Digestion of DNA with restriction endonucleases

Digests were prepared using the appropriate restriction enzyme (1-2 units), buffer as specified by the manufacturer, and 1µg of DNA, in a final volume of 20µl. Reactions were incubated at 37°C for a minimum of 2 hours.

2.3.7 DNA gel electrophoresis

Digested DNA samples or PCR reactions were examined using gel electrophoresis. Samples were diluted in 5x DNA loading buffer. A 1% (w/v) agarose gel was prepared by mixing agarose with 1 x TAE and 2.5mg/ml ethidium bromide. The gels were set in a horizontal gel tank and once set immersed in 1 x TAE. Samples were loaded and the gels ran at 75mA for 20-30 minutes. The DNA fragments were visualised using ultraviolet light. The size of each fragment was assessed by comparison with DNA molecular markers X.

2.3.8 DNA purification from agarose gels

The required DNA fragments were excised from the gel and purified using the QiaQuick gel extraction kit as per the manufacturer's instructions. DNA was eluted from the purification column using 30µl sterile water.

2.3.9 Alkaline phosphatase treatment of plasmid vectors

The 5' phosphate group of digested plasmid vector was removed to minimise re-ligation of the vector to itself. 200ng of digested vector was incubated with 2 units of shrimp alkaline phosphatase for 30 minutes at 37°C. The treated plasmid was isolated first by resolving on an agarose gel by electrophoresis and then extracted as previously described in section 2.3.8.

2.3.10 Ligation of DNA

Digested PCR fragments were ligated into plasmid vector using T4 DNA ligase. A ratio of 1:3 and 1:6 vector:PCR product was used in a volume of 10µl containing 1 unit of ligase and the supplied buffer. The reaction was incubated at room temperature for 4 hours. The ligation reactions were transformed as detailed in section 2.3.3.

2.3.11 Polymerase chain reaction

2.3.11.1 Standard PCR

PCR reactions were carried out to amplify specific sections of DNA. Pfu DNA polymerase was used due to its high fidelity and its ability to withstand higher temperatures. This PCR method was used to introduce tags and to introduce new restriction sites to construct fusion proteins. All reactions were performed using sterile materials. The PCR reactions contained;

Pfu polymerase buffer (10x)	5µl
DMSO (optional)	5µl
Deoxynucleotide tri-phosphates (dNTPs) (0.2mM of each dATP, dCTP, dGTP, dTTP)	5µl
Primer sense: 25pmol/µl	1µl
Primers antisense: 25pmol/µl	1µl

DNA template: 50ng/μl	1μl
Pfu enzyme: 1 unit	1μl
dH ₂ O to a final volume of	50μl

Reactions were carried out on an Eppendorf gradient Thermocycler. PCR cycles used were as follows and the annealing temperatures were dependent on the T_m of primers used;

1.	Preheating	95°C	5min
2.	Denaturation	95°C	1min
3.	Annealing	50-60°C	1min
4.	Extension	72°C	3min
5.	Repeat from step 2.	29x	
6.	End	72°C	10min
7.	Hold	4°C	

2.3.11.2 QuikChange mutagenesis PCR

The QuikChange site-directed mutagenesis method was used to make point mutations (either single or multiple residues). Manufactures instructions were followed when designing primers and carrying out the PCR reactions.

PCR reactions were compiled with the following components: 50ng DNA template, 15pM of both forward and reverse primers, 1μl of dNTP mix (0.2μM of each dATP, dCTP, dGTP and dTTP) and 1μl (2.5U) Pfu DNA polymerase, total volume of 50μl with reaction buffer. Samples were cycled 30 times in an Eppendorf Thermocycler system under the following conditions

Cycle 1:	95°C for 30 seconds
Cycles 2-30:	95°C for 30 seconds, 50°C for 1 minute 68°C for 1 minute per kbp of plasmid length

The product was treated with 1μl (10U) *DpnI* restriction enzyme and incubated for 60 minutes at 37°C. Control reactions contained 50ng DNA, 1μl of dNTP mix and 1μl Pfu, total volume of 30μl with reaction buffer. This allows the digestion of parental methylated

dsDNA. The digested mutated DNA and control were then transformed into DH5 α cells following the protocol described in section 2.3.3.

2.3.12 DNA sequencing

DNA sequencing was performed by The Sequencing Service (School of Life Sciences, University of Dundee, Scotland) using Applied Biosystems Big-Dye Ver 3.1 chemistry on an Applied Biosystems model 3730 automated capillary DNA sequencer.

2.4 Generation of GPR40 constructs

2.4.1 C-terminally epitope tagged constructs

GPR40-Flag

Primers to remove the stop codon of GPR40 and to introduce the Flag epitope sequence were used to generate C-terminally tagged GPR40-Flag;

sense 5' – CCGGGTACCATGGACCTGCCCCGCAGCTCTCCTTC – 3',

anti-sense 5' –

CTAGTCTAGACTA***AGACTTATCATCGTCGTCCTTGTAGTCCTTCTGGGACTTGCC***
CCCTTGCGT – 3'. The region encoding the Flag epitope tag is shown in bold italics.

The *Kpn*I and *Xba*I sites present in the sense and anti-sense primers respectively are underlined and the amplified fragment was digested and ligated into pcDNA3.

GPR40-c-Myc

Primers to remove the stop codon of GPR40 and to introduce the c-Myc epitope sequence were used to generate C-terminally tagged GPR40-c-Myc;

sense 5' – CCGGGTACCATGGACCTGCCCCGCAGCTCTCCTTC – 3',

anti-sense 5' –

CTAGTCTAGACTA***CAGATCTTCTTCAGAAATAAGTTTTGTTCTTCTGGGACTT***
GCCCCCTTGCGT – 3'. The region encoding the c-Myc epitope tag is shown in bold

italics. The *Kpn*I and *Xba*I sites present in the sense and anti-sense primers respectively are underlined and the amplified fragment was digested and ligated into pcDNA3.

2.4.2 Fluorescent fusions

GPR40-eCFP

Primers were designed to amplify GPR40 and to remove the stop codon; sense 5' – CCCCCAAGCTTCCACCATGGACCTGCCCCCGCAGCTC – 3', anti-sense 5' – AAAAGATATCCTTCTGGGACTTGCCCCCTTGC – 3'. The *Hind*III and *Eco*RV sites present in the sense and anti-sense primers respectively are underlined. The amplified fragment was digested and ligated into pcDNA3 in frame with eCFP ligated between *Not*I and *Xho*I.

GPR40-eYFP

Primers were designed to amplify GPR40 and to remove the stop codon; sense 5' – CCCCCAAGCTTCCACCATGGACCTGCCCCCGCAGCTC – 3', anti-sense 5' – AAAAGATATCCTTCTGGGACTTGCCCCCTTGC – 3'. The *Hind*III and *Eco*RV sites present in the sense and anti-sense primers respectively are underlined. The amplified fragment was digested and ligated into pcDNA3, in frame, with eYFP ligated between *Not*I and *Xho*I.

GPR40-eYFP was subcloned by digestion with *Hind*III and *Xho*I and ligation into the pcDNA5/FRT/TO vector.

2.4.3 Receptor-G protein fusion

GPR40-G α_q

Primers were designed to amplify GPR40 and to remove the stop codon; sense 5' – CCCCCAAGCTTCCACCATGGACCTGCCCCCGCAGCTC – 3', anti-sense 5' – AAAAGATATCCTTCTGGGACTTGCCCCCTTGC – 3'. The *Hind*III and *Eco*RV sites present in the sense and anti-sense primers respectively are underlined. Primers to amplify G α_q were also designed; sense 5' – AAAAGATATCACTCTGGAGTCCATCATGGCGTGC – 3', anti-sense 5' – TTTTTCCTTGCGGCCGCTTAGACCAGATTGTACTCCTTCAG – 3'. The *Eco*RV and *Not*I sites present in the sense and anti-sense primers respectively are underlined. The amplified fragments of GPR40 and G α_q were digested with the appropriate enzymes and ligated, in frame, into pcDNA3.

2.4.4 Single point basic mutations

GPR40 Lys⁶²Ala

Using the Stratagene QuikChange method, primers were designed to mutate Lys⁶² in GPR40 to Ala, with the mutated bases shown in bold italics;

Sense 5' – CTCTGCCCCTG**GCGGCGGTGGAGGCG** – 3'

Anti-sense 5' – CGCCTCCACCGCC**GCCAGGGGCAGAG**– 3'.

The primers were used to introduce the mutation into GPR40-eYFP or GPR40-Gα_q in pcDNA3 and the template was digested with *DpnI* to leave mutated plasmid. Sequencing was carried out to confirm the introduction of the mutation.

GPR40 His¹³⁷Ala

Using the Stratagene QuikChange method, primers were designed to mutate His¹³⁷ in GPR40 to Ala, with the mutated bases shown in bold italics;

Sense 5' – GCCCTCGTCCTGTGT**GCCCTGGGTCTGGTCTTTGGG** – 3'

Anti-sense 5 – CCCAAAGACCAGACCCAGG**GCACACAGGACGAGGCC** – 3'.

The primers were used to introduce the mutation into GPR40-eYFP in pcDNA3 and the template was digested with *DpnI* to leave mutated plasmid. Sequencing was carried out to confirm the introduction of the mutation.

GPR40 Arg¹⁸³Ala

Using the Stratagene QuikChange method, primers were designed to mutate Arg¹⁸³ in GPR40 to Ala, with the mutated bases shown in bold italics;

Sense 5' – GCCGCCCCGGCC**GCCTTCAGCCTCTCTCTCC** – 3'

Anti-sense 5' – GGAGAGAGAGGCTGAAG**GCGGCCGGGCCGGC** – 3'.

The primers were used to introduce the mutation into GPR40-eYFP or GPR40-Gα_q in pcDNA3 and the template digested with *DpnI* to leave mutated plasmid. Sequencing was carried out to confirm the introduction of the mutation.

2.4.5 Double basic mutations

GPR40 Lys⁶²Ala, His¹³⁷Ala

Using the Stratagene QuikChange method, primers were designed to mutate His¹³⁷ to Ala in GPR40 already containing a Lys⁶²Ala mutation, with the mutated bases shown in bold italics;

Sense 5' – GCCCTCGTCCTGTGT**GCCCTGGGTCTGGTCTTTGGG** – 3'

Anti-sense 5 – CCCAAAGACCAGACCCAGG**GC**CACACAGGACGAGGCC – 3’.

The primers were used to introduce the mutation into GPR40 Lys⁶²Ala-eYFP in pcDNA3 and the template was digested with *DpnI* to leave mutated plasmid. Sequencing was carried out to confirm the introduction of the mutation.

GPR40 Lys⁶²Ala, Arg¹⁸³Ala

Using the Stratagene QuikChange method, primers were designed to mutate Arg¹⁸³ to Ala in GPR40 already containing a Lys⁶²Ala mutation, with the mutated bases shown in bold italics; Sense 5’ – GCCGGCCCGGCC**GC**CTTCAGCCTCTCTCTCC – 3’

Anti-sense 5’ – GGAGAGAGAGGCTGAAG**GC**GGCCGGGCCGGC – 3’.

The primers were used to introduce the mutation into GPR40 Lys⁶²Ala-eYFP in pcDNA3 and the template was digested with *DpnI* to leave mutated plasmid. Sequencing was carried out to confirm the introduction of the mutation.

GPR40 His¹³⁷Ala, Arg¹⁸³Ala

Using the Stratagene QuikChange method, primers were designed to mutate Arg¹⁸³ to Ala in GPR40 already containing a His¹³⁷Ala mutation, with the mutated bases shown in italics; Sense 5’ – GCCGGCCCGGCC**GC**CTTCAGCCTCTCTCTCC – 3’

Anti-sense 5’ – GGAGAGAGAGGCTGAAG**GC**GGCCGGGCCGGC – 3’.

The primers were used to introduce the mutation into GPR40 His¹³⁷Ala-eYFP in pcDNA3 and the template was digested with *DpnI* to leave mutated plasmid. Sequencing was carried out to confirm the introduction of the mutation.

2.4.6 TM3 mutations

GPR40 GGG⁹³⁻⁹⁵STW

Using the Stratagene QuikChange method, primers were designed to mutate GGG⁹³⁻⁹⁵ in GPR40 to STW, with the mutated bases shown in bold italics;

Sense 5’ – CTTCCCACTCTATGCC**AGCACGTG**GTTCTGGCCGCCC – 3’

Anti-sense 5’ – GGGCGGCCAGGA**ACCACGTG**CTGGCATAGAGTGGGAAG – 3’.

The primers were used to introduce the mutation into GPR40-eYFP in pcDNA3 and the template was digested with *DpnI* to leave mutated plasmid. Sequencing was carried out to confirm the introduction of the mutation.

2.5 Generation of GPR41 constructs

2.5.1 C-terminally epitope tagged constructs

GPR41-Flag

Primers to remove the stop codon of GPR41 and to introduce the Flag epitope sequence were used to generate C-terminally tagged GPR41-Flag;

sense 5' – CCGGGTACCATGGATACAGGCCCGACCAGTCCTACTTC – 3',

anti-sense 5' –

CTAGTCTAGACTA***A***ACTTATCATCGTCGTCCTT***G***TAGTCGCTTTCAGCACAGGCCACCTGGCCACCAGTTCC – 3'. The region encoding the Flag epitope tag is shown

in bold italics. The *KpnI* and *XbaI* sites present in the sense and anti-sense primers respectively are underlined and the amplified fragment was digested and ligated into pcDNA3.

GPR41-c-Myc

Primers to remove the stop codon of GPR41 and to introduce the c-Myc epitope sequence were used to generate C-terminally tagged GPR41-c-Myc;

sense 5' – CCGGGTACCATGGATACAGGCCCGACCAGTCCTACTTC – 3',

anti-sense 5' –

CTAGTCTAGACTA***C***AGATCTTCTTCAGAAATAAGTTTT***G***TTTCGCTTTCAGCACAGGCCACCTGGCC – 3'. The region encoding the c-Myc epitope tag is shown in bold

italics. The *KpnI* and *XbaI* sites present in the sense and anti-sense primers respectively are underlined and the amplified fragment was digested and ligated into pcDNA3.

2.5.2 Fluorescent fusions

GPR41-eCFP

Primers were designed to amplify GPR41 and to remove the stop codon;

sense 5' – TACGGGGTACCCACCATGGATACAGGCCCGACCAG – 3', anti-sense

5' – TTTTCCTTTTGCGGCCGCTTTCAGCACAGGCCACCTG – 3'. The *KpnI* and

NotI sites present in the sense and anti-sense primers respectively are underlined. The amplified fragment was digested and ligated into pcDNA3 in frame with eCFP ligated between *NotI* and *XhoI*.

GPR41-eYFP

Primers were designed to amplify GPR41 and to remove the stop codon;

sense 5' – TACGGGGTTACCCACCATGGATACAGGCCCGACCAG – 3', anti-sense
5' – TTTTCCTTTTGCGGCCGCTGCTTTCAGCACAGGCCACCTG – 3'. The *KpnI* and
NotI sites present in the sense and anti-sense primers respectively are underlined. The
amplified fragment was digested and ligated into pcDNA3 in frame with eYFP ligated
between *NotI* and *XhoI*.

2.5.3 Receptor-G protein fusion

GPR41-G α_{i3} Cys³⁵¹Ile

Primers were designed to amplify GPR41 and to remove the stop codon;

sense 5' – TACGGGGTTACCCACCATGGATACAGGCCCGACCAG – 3', anti-sense
5' – TTTTCCTTTTGCGGCCGCTGCTTTCAGCACAGGCCACCTG – 3'. The *KpnI* and
NotI sites present in the sense and anti-sense primers respectively are underlined. Primers
to amplify G α_{i3} were also designed;

sense 5' – AAAAGGAAAAGGCGGCCGCGGCTGCACGTTGAGCGCCGAGGAC – 3',
anti-sense 5' – CCCCGCTCGAGTCAGTAAAGCCCGATTTCCTTTAAGTTG – 3'. The
NotI and *XhoI* sites present in the sense and anti-sense primers respectively are underlined.
The amplified fragments of GPR41 and G α_{i3} were digested with the appropriate enzymes
and ligated, in frame, into pcDNA3.

2.5.4 Basic mutants

GPR41 Arg⁷¹Ala

Using the Stratagene QuikChange method, primers were designed to mutate Arg⁷¹ in
GPR41 to Ala, with the mutated bases shown in bold italics;

Sense 5' – GCTGTTCTGCCTTTC**GCC**ATGGTGGAGGCAGCC – 3'

Anti-sense 5' – GGCTGCCTCCACCATG**GCG**AAAGGCAGGAACAGC -3'.

The primers were used to introduce the mutation into GPR41-eYFP or GPR41-G α_{i3}
Cys³⁵¹Ile in pcDNA3 and the template digested with *DpnI* to leave mutated plasmid.
Sequencing was carried out to confirm the introduction of the mutation.

GPR41 His¹⁴⁶Ala

Using the Stratagene QuikChange method, primers were designed to mutate His¹⁴⁶ in
GPR41 to Ala, with the mutated bases shown in bold italics;

Sense 5' – GCTGTTGGCCTCTGCT**GC**CTGCAGCGTGGTCTACG – 3'

Anti-sense 5' – CGTAGACCACGCTGCAG**GC**CAGCAGAGGCCAACAGC – 3'.

The primers were used to introduce the mutation into GPR41-eYFP or GPR41-G α_{i3} Cys³⁵¹Ile in pcDNA3 and the template was digested with *DpnI* to leave mutated plasmid. Sequencing was carried out to confirm the introduction of the mutation.

GPR41 Arg¹⁸⁵Ala

Using the Stratagene QuikChange method, primers were designed to mutate Arg¹⁸⁵ in GPR41 to Ala, with the mutated bases shown in bold italics;

Sense 5' – CCTCCTGCCCCGTG**GC**GCTGGAGATGGC – 3'

Anti-sense 5' – GCCATCTCCAGC**GC**CACGGGCAGGAGG – 3'.

The primers were used to introduce the mutation into GPR41-eYFP or GPR41-G α_{i3} Cys³⁵¹Ile in pcDNA3 and the template digested with *DpnI* to leave mutated plasmid. Sequencing was carried out to confirm the introduction of the mutation.

2.6 Generation of GPR43 constructs

2.6.1 N-terminally epitope tagged

Flag-GPR43

Primers encoding the Flag epitope sequence were used to generate N-terminally tagged Flag-GPR43;

Sense 5' –

CCCAAGCTT***ATGGACTACAAGGACGACGATGATAAGTGT***CTGCCCCGACTTGAAG

AGCTCCTTGATC - 3', anti-sense 5'-

CTAGTCTAGACTACTCTGTAGTGAAGTCCGAACTTGG – 3. The region encoding

the Flag epitope tag is shown in bold italics. The *HindIII* and *XbaI* sites present in the

sense and anti-sense primers respectively are underlined and the amplified fragment was

digested and ligated into pcDNA3.

c-Myc-GPR43

Primers encoding the c-Myc epitope sequence were used to generate N-terminally tagged c-Myc-GPR43;

sense 5' –

CCCAAGCTT***ATGGAACAAAACTTATTTCTGAAGAAGATCTG***CTGCCCCGACTGG

AAGAGCTCCTTGATC – 3', anti-sense 5' –

CTAGTCTAGACTACTCTGTAGTGAAGTCCGAACTTGG – 3'. The region encoding the c-Myc epitope tag is shown in bold italics. The *Hind*III and *Xba*I sites presents is the sense and anti-sense primers respectively are underlined and the amplified fragment was digested and ligated into pcDNA3.

2.6.2 C-terminally epitope tagged

GPR43-Flag

Primers to remove the stop codon of GPR43 and to introduce the Flag epitope sequence were used to generate C-terminally tagged GPR43-Flag;

sense 5' – CCCAAAGCTTATGCTGCCGGACTGGAAGAGCTCCTTGATC – 3',

anti-sense 5' –

CTAGTCTAGACTA**AGACTTATCATCGTCGTCCTTGTAGTCCTCTGTAGTGAAGTCCGAACTTGGCATCCCTTC** – 3'. The region encoding the Flag epitope tag is shown in bold italics. The *Hind*III and *Xba*I sites present in the sense and anti-sense primers respectively are underlined and the amplified fragment was digested and ligated into pcDNA3.

GPR43-c-Myc

Primers to remove the stop codon of GPR43 and to introduce the c-Myc epitope sequence were used to generate C-terminally tagged GPR43-c-Myc;

sense 5' – CCGGGTACCATGGATACAGGCCCGACCAGTCCTACTTC – 3',

anti-sense 5' –

CTAGTCTAGACTA**CAGATCTTCTTCAGAAATAAGTTTTGTTCCCTCTGTAGTGAA**GTCCGAACTTGG – 3'. The region encoding the c-Myc epitope tag is shown in bold italics. The *Hind*III and *Xba*I sites present in the sense and anti-sense primers respectively are underlined and the amplified fragment was digested and ligated into pcDNA3

2.6.3 Fluorescent fusions

GPR43-eCFP

Primers were designed to amplify GPR43 and to remove the stop codon;

sense 5' – CCCCCAAAGCTTCCACCATGCTGCCGGACTGGAAGAGC – 3',

anti-sense 5' – AAAAAGATATCCTCTGTAGTGAAGTCCGAACTTGG – 3'. The *Hind*III and *Eco*RV sites present in the sense and anti-sense primers respectively are

underlined. The amplified fragment was digested and ligated into pcDNA3, in frame, with eCFP ligated between *NotI* and *XhoI*.

GPR43-eYFP

Primers were designed to amplify GPR43 and to remove the stop codon;

sense 5' – CCCCCAAGCTTCCACCATGCTGCCGGACTGGAAGAGC – 3',

anti-sense 5' – AAAAAGATATCCTCTGTAGTGAAGTCCGAACTTGG – 3'.

The *HindIII* and *EcoRV* sites present in the sense and anti-sense primers respectively are underlined. The amplified fragment was digested and ligated into pcDNA3, in frame, with eCFP ligated between *NotI* and *XhoI*.

2.6.4 Basic mutations

GPR43 Lys⁶⁵Ala

Using the Stratagene QuikChange method, primers were designed to mutate Lys⁶⁵ in GPR43 to Ala, with the mutated bases shown in bold italics;

Sense 5' – GCTGCTGCTGCCCTT***CG***GATCATCGAGGCTGCG – 3'

Anti-sense 5' – CGCAGCCTCGATGATC***CG***GAAGGGCAGCAGCAGC – 3'.

The primers were used to introduce the mutation into GPR43-eYFP in pcDNA3 and the template was digested with *DpnI* to leave mutated plasmid. Sequencing was carried out to confirm the introduction of the mutation.

GPR43 His¹⁴⁰Ala

Using the Stratagene QuikChange method, primers were designed to mutate His¹⁴⁰ in GPR43 to Ala, with the mutated bases shown in bold italics;

Sense 5' - GGTTATGTCCTTTGGT***GC***CTGCACCATCGTGATCATC – 3'

Anti-sense 5' – GATGATCACGATGGTGCAG***GC***ACCAAAGGACATAACC – 3'

The primers were used to introduce the mutation into GPR43-eYFP in pcDNA3 and the template digested with *DpnI* to leave mutated plasmid. Sequencing was carried out to confirm the introduction of the mutation.

GPR43 Arg¹⁸⁰Ala

Using the Stratagene QuikChange method, primers were designed to mutate Arg¹⁷⁵ in GPR43 to Ala, with the mutated bases shown in bold italics;

Sense 5' – GGTGCTGCCCGTG***CG***CTGGAGCTGTGC – 3'

Anti-sense 5' – GCACAGCTCCAGC***GC***CACGGGCAGCACC – 3'.

The primers were used to introduce the mutation into GPR43-eYFP in pcDNA3 and the template was digested with *DpnI* to leave mutated plasmid. Sequencing was carried out to confirm the introduction of the mutation.

GPR43 Arg¹⁸⁰Leu

Using the Stratagene QuikChange method, primers were designed to mutate Arg¹⁷⁵ in GPR43 to Leu, with the mutated bases shown in bold italics;

Sense 5' – GGTGCTGCCCCGTGCT**GT**GCTGGAGCTGTGC – 3'

Anti-sense 5' – GCACAGCTCCAGC**AG**CACGGGCAGCACC – 3'.

The primers were used to introduce the mutation into GPR43-eYFP in pcDNA3 and the template digested with *DpnI* to leave mutated plasmid. Sequencing was carried out to confirm the introduction of the mutation.

GPR43 Arg¹⁸⁰Lys

Using the Stratagene QuikChange method, primers were designed to mutate Arg¹⁷⁵ in GPR43 to Lys, with the mutated bases shown in bold italics;

Sense 5' – GGTGCTGCCCCGTG**AA**GCTGGAGCTGTGC – 3'

Anti-sense 5' – GCACAGCTCCAGC**TT**CACGGGCAGCACC – 3'.

The primers were used to introduce the mutation into GPR43-eYFP in pcDNA3 and the template digested with *DpnI* to leave mutated plasmid. Sequencing was carried out to confirm the introduction of the mutation.

GPR43 Arg¹⁸⁰Ser

Using the Stratagene QuikChange method, primers were designed to mutate Arg¹⁷⁵ in GPR43 to Ser, with the mutated bases shown in bold italics;

Sense 5' – GGTGCTGCCCCGTG**TC**GCTGCTGTGC – 3'

Anti-sense 5' – GCACAGCTCCAGC**GA**CACGGGCAGCACC – 3'.

The primers were used to introduce the mutation into GPR43-eYFP in pcDNA3 and the template was digested with *DpnI* to leave mutated plasmid. Sequencing was carried out to confirm the introduction of the mutation.

2.6.5 TM3 mutations

GPR43 Trp⁹⁸Gly

Using the Stratagene QuikChange method, primers were designed to mutate Trp⁹⁸ in GPR43 to Gly, with the mutated bases shown in bold italics;

Sense 5' – C T A C T G C A G C A C G **G G G G** C T C C T G G C G G G C – 3'

Anti-sense 5' – G C C C G C C A G G A G C C C C G T G C T G C A G T A G – 3'.

The primers were used to introduce the mutation into GPR43-eYFP in pcDNA3 and the template was digested with *DpnI* to leave mutated plasmid. Sequencing was carried out to confirm the introduction of the mutation.

GPR43 Thr⁹⁷Gly, Trp⁹⁸Gly

Using the Stratagene QuikChange method, primers were designed to mutate Thr⁹⁷ to Gly in GPR43 already containing a Trp⁹⁸Gly mutation, with the mutated bases shown in bold italics;

Sense 5' – C T A C T G C A G C **G G G G G G** C T C C T G G C G G G C – 3'

Anti-sense 5' – G C C C G C C A G G A G C C C C C **C C** G T G C T G C A G T A G – 3'.

The primers were used to introduce the mutation into GPR43 Trp⁹⁸Gly-eYFP in pcDNA3 and the template was digested with *DpnI* to leave mutated plasmid. Sequencing was carried out to confirm the introduction of the mutation.

GPR43 Ser, Thr, Trp⁹⁶⁻⁹⁸Gly, Gly, Gly

Using the Stratagene QuikChange method, primers were designed to mutate Ser⁹⁶ to Gly in GPR43 already containing Thr⁸⁷Gly and Trp⁹⁸Gly mutations, with the mutated bases shown in bold italics;

Sense 5' – G C A T C T A C T G C **G G C G G G G G G G** C T C C T G G – 3'

Anti-sense 5' – C C A G G A G C C C C C C C G C C G C A G T A G A T G C – 3'.

The primers were used to introduce the mutation into GPR43 Thr⁹⁷Gly, Trp⁹⁸Gly-eYFP in pcDNA3 and the template was digested with *DpnI* to leave mutated plasmid. Sequencing was carried out to confirm the introduction of the mutation.

2.7 Cell culture

2.7.1 Cell maintenance

2.7.1.1 HEK293T

Human embryonic kidney cells stably expressing the SV40 large T-antigen (HEK293T) were grown in Dulbecco's modified Eagle's medium supplemented with 10% newborn calf serum and 2mM L-glutamine. Cells were grown in a humidified incubator of 95% air/5% CO₂ at 37°C.

2.7.1.2 HEK293 MSRII

Human embryonic kidney cells (HEK293 MSRII) transformed with the macrophage scavenger receptor (Class A, type1; GenBank Accession no. D90187) were maintained in minimal essential medium containing 2mM L-glutamine supplemented with 10% foetal calf serum, 1% non-essential amino acids and 0.8% G418. Cells were grown in a humidified incubator of 95% air/5% CO₂ at 37°C. The expression of this receptor by the HEK293 cells enhances their ability to stick to tissue culture treated plasticware.

2.7.1.3 Flp-In T-REx HEK293

Cell were maintained in Dulbecco's modified Eagle's medium without sodium pyruvate, 4500mg/litre glucose, and L-glutamine supplemented with 10% (v/v) foetal calf serum, 1% antibiotic mixture, and 10µg/ml blasticidin at 37°C in a humidified atmosphere of air/CO₂ (19:1).

2.7.1.4 INS-1E

The transformed rat pancreatic β-cell line INS-1E was maintained in RPMI 1640 medium with L-glutamine supplemented with 10% foetal calf serum, 10mM HEPES, 1mM sodium pyruvate, 50µM 2-mercaptoethanol and 1% antibiotic mixture at 37°C in a humidified atmosphere of air/CO₂ (19:1). Cells were grown in Falcon flasks and passaged once a week.

2.7.2 Passage of cells

Confluent HEK293T, Flp-In T-Rex HEK293 and INS-1E cells were passaged by the addition of sterile 0.25% trypsin-EDTA after removal of growth media. HEK293 MSRII cells were washed once with sterile PBS before the addition of versene to detach the cells. Flasks were gently rotated to cover the monolayer and placed in the incubator for 5 minutes. Once detached, 7ml of fresh media was added and the cells centrifuged at 288 x g for 5 minutes. The resulting pellet was resuspended in fresh media. The suspension was split into flasks, dishes, plates or coverslips as required.

2.7.3 Transient transfection

Transfection of cells was performed when the cells had reached 60-70% confluency. Plasmid DNA was transfected using Lipofectamine in accordance with the manufacturer's instructions.

2.7.4 Generation of Flp-In T-Rex HEK293 inducible cell line

Flp-In T-Rex HEK293 cells were transfected with a mixture of GPR40-eYFP in the pcDNA5/FRT/TO vector and the pOG44 vector in a 1:9 ratio with Lipofectamine as described in section 2.7.3. After 48 hours, the medium was changed to medium as described in section 2.7.1.3 supplemented with 200 μ g/ml hygromycin to initiate selection of stably transfected selected cells. To initiate expression of GPR40-eYFP, cells were treated with 1 μ g/ml doxycycline for 24 hours.

2.7.5 Cell harvesting

Transfected cells were harvested 24-48 hours post-transfection. The media was discarded and cells washed 3 times in ice cold 1 x PBS. Cells were scraped from the flask using a disposable cell scraper and transferred to a 15ml centrifuge tube. The detached cells were centrifuged for 5 minutes at 288 x g at 4°C. After discarding the supernatant, the cell pellet was frozen at -80°C until required.

2.8 Biochemical assays and other methods of analysis

2.8.1 Preparation of cell membranes

Harvested pellets were thawed and resuspended in Tris/EDTA buffer. The cells were homogenised by 50 passes of a glass-on-Teflon homogeniser. The resulting suspension was centrifuged at 288 x g for 10 minutes to remove unbroken cells and nuclei. The supernatant was subsequently ultracentrifuged at 50,000 x g for 30 minutes in a Beckman Optima TLX Ultracentrifuge (Palo Alto, CA). The resulting pellet was resuspended in Tris/EDTA buffer and passed 10 times through a 25 gauge needle. The protein concentration was determined as detailed in section 2.8.2 and the membranes diluted to 1 μ g/ μ l and stored at -80°C until required.

2.8.2 BCA protein quantification

The protein concentration in samples was quantified using the BCA assay. This assay utilises bincinhoninic acid (BCA) and copper sulphate solutions, in which proteins reduce the Cu(II) ions to Cu(I) ion in a concentration dependent manner and the reduced Cu(I) can be bound by BCA. When BCA binds Cu(I) a colour change occurs which has an absorption maximum of 562nm. Using solutions of known protein concentrations a standard curve was constructed, which allows the concentrations of unknown samples to be established. Solutions used in this assay consisted of: Reagent A – 1% (w/v) BCA, 2% (w/c) Na₂CO₃, 0.16% (w/v) sodium tartrate, 0.4% NaOH, 0.95% NaHCO₃, pH 11.25 and Reagent B – 4% CuSO₄. 1 part reagent B was mixed with 49 parts reagent A and 200µl of this solution added to 10µl of protein standard or unknown sample in a 96 well ELISA plate. The assay was incubated at 37°C before the absorbance was read.

2.8.3 Co-immunoprecipitation

Cells were harvested as described in section 2.7.4 and the resulting pellets resuspended in 1ml of 1 x RIPA buffer supplemented with 10mM NaF, 5mM EDTA pH 8, 10mM NaH₂PO₄, 5% ethylene glycol and a complete EDTA-free protease inhibitor tablet. The resuspended pellet was rotated for 1 hour at 4°C on a rotating wheel. After 1 hour, the samples were centrifuged at 100,000 x g for 30 minutes. To the supernatant, 200µl of 1 x RIPA and 50µl of protein G were added and rotated for 1 hour at 4°C to pre-clear the samples. The samples were centrifuged at 16,000 x g for 10 minutes at 4°C and the protein concentration of the samples determined as detailed in section 2.8.2. The protein concentration of the samples was equalised to 1µg/µl using 1 x RIPA. To 600µl of each sample 40µl of protein G and 5µl M2 anti-Flag antibody was added and incubated overnight at 4°C on a rotating wheel. To investigate protein expression 100µl of the equalised supernatant was reserved and to this 20µl of 5 x Laemmli buffer was added. After approximately 16 hours of rotation, the samples were centrifuged at 16,000 x g for 1 minute at 4°C and the supernatant removed and the protein G beads washed in 1 x RIPA buffer. This was repeated twice before addition of 40µl Laemmli buffer. Both immunoprecipitated samples and cell lysates were then subjected to SDS-PAGE and western blotting.

2.8.4 Sodium dodecylsulphate polyacrylamide gel electrophoresis

Protein samples were resolved using sodium dodecylsulphate polyacrylamide gel electrophoresis (SDS-PAGE). After the addition of Laemmli buffer samples were heated at 65°C for 10 mins then left overnight at room temperature before loading. Samples were loaded onto precast NuPage Novex Bis-Tris gels with 4-12% acrylamide concentration alongside full range Rainbow molecular weight markers. NuPage MOPS SDS buffer was used for electrophoresis at 200V using the XCell Surelock mini-cell gel tank until the dye front reached the foot of the gel.

2.8.5 Western blotting

Following separation of samples by SDS-PAGE as detailed in section 2.8.4, proteins were electrophoretically transferred onto nitrocellulose using the XCell II blot module. Proteins were transferred at 30V for at least 1 hour in transfer buffer (0.2M glycine, 25mM Tris and 20% (v/v) methanol). Efficient transfer was monitored using Ponceau stain (0.1% (w/v) Ponceau S, 3% (w/v) trichloroacetic acid). To block non-specific binding sites, the nitrocellulose was incubated in 5% (w/v) low fat milk, PBS/0.1% (v/v) Tween 20 at room temperature on a rotating shaker for two hours. The membrane was incubated with primary antibody overnight in 5% (w/v) low fat milk, PBS/0.1% (v/v) Tween 20 containing the required antibody (Table 2.1) at 4°C. After overnight incubation, the membrane was washed 4 times in PBS/0.1% (v/v) Tween 20 over a 30 minute period. The horseradish peroxidase linked secondary antibody (Table 2.1) in 5% (w/v) low fat milk, PBS/0.1% (v/v) Tween 20 was incubated at room temperature for 20 minutes. Again the membrane was washed 4 times in PBS/0.1% (v/v) Tween 20 over a 30 minute period. The nitrocellulose was then incubated for 5 minutes with ECL solution and then exposed to blue Kodak film and developed. For co-immunoprecipitation experiments the blot was stripped and re-probed using different antibodies. To strip the antibodies from the nitrocellulose the membrane was incubated for 15 minutes in 10% (v/v) ReBlot Plus solution and then the non-specific sites blocked as described above.

Primary Antibody	Dilution Factor	Secondary Antibody	Dilution Factor
Anti-c-Myc	1:1000	Anti-rabbit	1:10000
Anti-Flag M2	1:2000	Anti-mouse	1:10000

Table 2.1 Primary and secondary antibody dilutions for western blotting

2.8.6 Time resolved FRET

HEK293T cells were singly transfected to express c-Myc or Flag epitope tagged versions of GPR40 or GPR43, or co-transfected with c-Myc tagged GPR40 or GPR43 and Flag tagged GPR40 or GPR43. Cells were harvested 48 hours post-transfection and samples containing singly tagged receptors mixed to form a negative control. Membranes were prepared as detailed in section 2.8.1 but the membrane pellet was resuspended in PBS. Protein concentrations were equilibrated to 1 μ g/ μ l. To investigate energy transfer antibodies directed against the c-Myc and Flag epitope tagged versions conjugated to the donor, europium³⁺ (Eu³⁺) and acceptor, allophycocyanin (APC) fluorophores respectively. The antibodies were diluted in 50% newborn calf serum:50% PBS to a final concentration of 5nM anti-c-Myc Eu³⁺ and 15nM anti-Flag. A dilution containing only the anti-c-Myc Eu³⁺ antibody at a concentration of 5nM was also prepared. To 250 μ l of the antibody dilutions 50 μ l of membranes were added resulting in antibody incubations containing only anti-c-Myc Eu³⁺ or containing both anti-c-Myc Eu³⁺ and anti-Flag APC antibodies for each sample. The samples were incubated on a rotating wheel at room temperature for 2 hours. The samples were covered in aluminium foil to minimise exposure of the fluorophores to light. After incubation the sample were centrifuged at 16,000 x g for 15 minutes and the antibody mix removed from the membrane pellet. The pellet was washed in ice-cold PBS and centrifuged again at 16,000 x g for 15 minutes. The samples were resuspended in 250 μ l of PBS and passed through a 25 gauge needle. In order to measure the energy transfer, 40 μ l of each sample was dispensed in triplicate into a black 384-well plate. Background readings were performed on wells containing PBS.

Tr-FRET was determined using a Victor² plate reader (PackardBioscience). Excitation was at 340nm and emission filters generated data representing donor (615nm) and acceptor (665nm) emission. Normalized FRET was calculated using the following equation;

$$\text{Normalized FRET} = ((A_{665}-\text{BLK})/D_{615})-C$$

Where A_{665} is the fluorescent emission from the acceptor, D_{615} is the fluorescent emission from the donor and BLK represents the background reading at 665nm from the wells containing PBS. C represents the crosstalk between the donor and acceptor windows for the samples incubated with only anti-c-Myc Eu³⁺ and is equal to $A_{665}-\text{BLK}/D_{615}$.

2.8.7 FRET imaging in single living cells

HEK293T cells were grown on coverslips treated with poly-D-lysine and transiently transfected to express the receptor or receptors of interest. Coverslip fragments were placed into a microscope chamber containing physiological saline solution. Cells were visualised using a Nikon Eclipse TE2000-E fluorescence inverted microscope and images obtained individually for eYFP, eCFP and FRET filter channels using a Optoscan monochromator (Cairn Research, Faversham, Kent, UK) and a dichroic mirror 86002v2bs (Chroma Inc., Rockingham, VT). The filter sets used were; eYFP (excitation – 500/5 nm; emission – 535/30 nm), eCFP (excitation 430/12 nm; emission – 470/30 nm) and FRET (excitation 430/12 nm; emission 535/30 nm). The illumination time was 250 ms and binning modes 2x2. MetaMorph imaging software (Universal Imaging Corp., West Chester, PA) was used to quantify FRET images using the donor only specified bleed through FRET method.

Bleed through coefficients were calculated using cells singly transfected with either the eCFP (donor in FRET) or eYFP (donor in acceptor) fused receptors. The values obtained for the constructs used in this study are shown in table 2.2.

Construct	Coefficient
GPR40-eYFP	0.653
GPR40-eCFP	0.0092
GPR43-eYFP	0.6253
GPR43-eCFP	0.0078
H ₁ -eYFP	0.0155

Table 2.2 FRET bleedthrough coefficients

To correct the FRET levels for the varying amounts of donor (CFP) and acceptor (eYFP), normalised FRET was calculated using the following equation;

$$\text{FRET}_n = \text{FRET}_c / \text{CFP} \times \text{eYFP}$$

Where FRET_c, CFP and eYFP are equal to the fluorescence values measured for each individual cell. FRET was measured for 30-50 cells.

2.8.8 [³⁵S]GTP γ S binding assays

[³⁵S]GTP γ S binding experiments were initiated by the addition a given amount of membranes expressing the required construct (2.5 μ g for GPR40 constructs and 5 μ g for GPR41 constructs) to an assay buffer (20mM HEPES (pH 7.4), 3mM MgCl₂, 100mM NaCl, 1 μ M GDP, 0.2mM ascorbic acid, and 50nCi [³⁵S]GTP γ S) containing the given concentration of agonist or antagonist. Non-specific binding was determined in the above condition with the addition of 100 μ M GTP γ S. Reactions were incubated for 30 minutes at 30°C and were terminated by the addition of 500 μ l of ice-cold buffer containing 20mM HEPES (pH 7.4), 3mM MgCl₂, 100mM NaCl and 0.2mM ascorbic acid. The samples were centrifuged at 16,000 x g for 10 minutes at 4°C. The resulting pellets were resuspended in 50 μ l solubilisation buffer (100mM Tris, 200mM NaCl, 1mM EDTA, and 1.25% Nonidet P-40) plus 0.2% SDS. Samples were pre-cleared with pansorbin followed by immunoprecipitation with the required anti-serum against the C-terminus of the given G protein. Finally, the immunocomplexes were washed once with solubilisation buffer, and bound [³⁵S]GTP γ S was estimated by liquid-scintillation spectrometry.

2.8.9 Single cell calcium assay

HEK293T cells grown on poly-D-lysine coated coverslips were transiently transfected to express the receptor of interest. 24 h after transfection cells were loaded with the calcium sensitive dye fura-2. 1.5 μ M fura-2 was added to normal growth media and the cells incubated at 37°C for 30 minutes. After loading of the dye, fragments of coverslips were placed into a microscope chamber containing physiological saline solution and illuminated with an ultra high point intensity 75-watt xenon arc lamp (Optosource, Cairn Research, Faversham, Kent, UK) and imaged using a Nikon Diaphot inverted microscope equipped with a Nikon 40 \times oil immersion Fluor objective lens (NA = 1.3) and a monochromator (Optoscan, Cairn Research), which was used to alternate the excitation wavelength between 340/380nm and to control the excitation band pass (340nm band pass = 10nm; 380nm band pass = 8nm). Fura-2 fluorescence emission at 510nm was monitored using a high resolution interline-transfer cooled digital CCD camera (Cool Snap-HQ, Roper Scientific/Photometrics, Tucson, AZ). MetaFluor imaging software (Universal Imaging Corp., Downing, PA) was used for control of the monochromator, CCD camera, and for processing of the cell image data. Sequential images (2 \times 2 binning) were collected every 2s, exposure to excitation light was 100 ms/image. Agonist was added after 60s (after 30

images) for 60s using a perfusion system. Experiments were ran for 5 minutes in total. MetaFluor software was used to analyse the images

2.8.10 FLIPR based calcium assay

HEK293 MSRII cells were transiently transfected to express the receptor of interest. 24 h after transfection cells were detached from flasks and counted on a Cedex AS²⁰ cell counter (Innovatis Inc, Malvern, PA) using the tryptan blue exclusion method. Cells were seeded at 15,000 cells/well into poly-D-lysine coated 384-well black-wall, clear-bottom microtiter plates (Greiner Bio-One, Kremsmünster, Austria) using a Multidrop dispenser. The following day the media was aspirated from the cells and 40µl of assay buffer (Hanks' balanced salts solution, 10mM HEPES, 200µM Ca²⁺, 2.5mM probenecid, 0.5M brilliant black, 1µM fluo-4 AM) was added to each well, this was repeated once and the cells incubated at 37°C for 1 hour to allow loading of the fluorescent dye. After 1 hour the assay was ran on a fluorometric imaging plate reader (FLIPR, Molecular Devices, Sunnyvale, CA). Images were collected every 2s and agonist was added after 10s, a total of 60 images were collected. The data was analysed using the following equation and plotted using XLfit curve fitting software (IDBS, Guildford, Surrey)

2.8.11 RT-PCR

Total RNA was extracted from INS-1E cells using the RNeasy miniprep procedure as per manufacturer's instructions. Prior to reverse transcription, RNA was treated with deoxyribonuclease to ensure that there was no contamination with genomic DNA. First strand cDNA was produced using the 1st Strand cDNA synthesis kit. Detection of specific mRNA transcripts was carried out by PCR using 50ng cDNA and 200nM oligonucleotides corresponding to rat GPR40, rat GPR41, rat GPR43 or rat cyclophilin. The primers used for PCR are as follows;

rat GPR40 5' – CCCTGCCCCGACTCAGTTTC – 3',
 5' – GGCAGCCCACATAGCAGAA – 3',
 rat GPR41 5' – GTGCGACTGGAAATGGCTG – 3',
 5' – CACACCAGGCGACTGTAGC – 3',
 rat GPR43 5' – GAGCTGTGCCTGGCCTC – 3',
 5' – GCATGATCCATACAAAGC – 3',
 rat cyclophilin 5' – TCACCATCTCCGACTGTGGA – 3',
 5' – AAATGCCCCGCAAGTCAAAGA – 3'.

cDNA was amplified using the following cycling conditions: 10 minutes at 95°C, then 40 cycles of 1 minute at 95°C, 1 minute at 52°C, 2 minutes at 72°C, which was followed by 5 minutes at 72°C. Samples were resolved on a 1% agarose gel as described in section 2.3.7.

3 Development of functional assays to monitor activation of GPR40, GPR41 and GPR43

3.1 Introduction

Fatty acids have recently been described as the likely endogenous ligands for GPR40 (Briscoe et al., 2003; Itoh et al., 2003; Kotarsky et al., 2003), GPR41 and GPR43 (Brown et al., 2003; Le Poul et al., 2003; Nilsson et al., 2003). The recent de-orphanisation of the receptors means that there are many areas of their pharmacology and function that are poorly understood. In order to investigate the pharmacology of the receptors and to determine the function of mutants generated to identify areas important in fatty acid binding, assays that monitor the activation of each of the three receptors had to be optimised. Also, to investigate the possible oligomerisation of the receptors, a variety of modified versions of the receptors were generated to allow assays to determine protein-protein interactions to be carried out. Therefore, in this chapter, a variety of modified versions of each of the receptors were generated and their usefulness and function assessed.

Epitope tags are a useful tool in studying GPCRs as they facilitate detection of the protein by immunocytochemistry or by immunoblotting without the need for receptor specific antibodies. Epitope tags consist of a short sequence of amino acids that may be added at the N- or C-terminus of a receptor. Addition of the epitope tag at the N-terminus enables visualisation of the receptor at the cell surface using commercially available antibodies generated to recognise the specific sequence. In this study c-Myc and Flag epitopes have been used. The c-Myc epitope consists of a 10 amino acid sequence of the human proto-oncogene myc (Evan et al., 1985), whereas the Flag epitope is a synthetic octapeptide (Chubet and Brizzard, 1996).

A number of proteins have been fused onto the C-terminus of GPCRs without disrupting their ligand binding and signal transduction. Fusion of a G protein α subunit onto the C-terminus of a GPCR provides a way by which [35 S]GTP γ S binding studies can be performed with receptors that couple to $G\alpha_{q/11}$ or $G\alpha_s$, as historically it has proved difficult to use any receptor that does not couple to the $G\alpha_{i/o}$ family of G proteins due to the low levels of [35 S]GTP γ S binding observed. Using the combination of a receptor-G protein

fusion and an immunocapture step with antibodies generated towards the G protein helps to overcome this problem (Milligan, 2003).

It is becoming increasingly common to fuse a fluorescent protein to the C-terminus of a GPCR. There is a wide range of fluorescent proteins, with many of them based on GFP from the jellyfish *Aequoria victoria* as it folds into a fully functioning fluorescent protein without the need for a substrate or accessory protein (Giepmans et al., 2006). There are many variants of GFP, each possessing distinct spectral properties and these have been exploited in several resonance energy transfer techniques. The two variants used in this study are enhanced cyan fluorescent protein (eCFP) and enhanced yellow fluorescent protein (eYFP). eCFP has a blue-green colour with an excitation maximum of 430nm and emission maximum of 470nm (Cubitt et al., 1999; Heim and Tsien, 1996). eYFP is a red-shifted GFP variant which presents an excitation maximum of 500nm and an emission maximum of 535nm. The spectral properties of eCFP and eYFP have been extensively exploited as donor and acceptor moieties in FRET to demonstrate molecular interactions between proteins (Tsien, 1998; Zhou et al., 2003; Dinger et al., 2003).

The limited number of previous studies into the pharmacology of GPR40 have taken advantage of its selective coupling to the $G\alpha_{q/11}$ family of G proteins, as activation of these G proteins results in the elevation of intracellular calcium ($[Ca^{2+}]_i$). Changes in $[Ca^{2+}]_i$ levels are relatively easy to measure due to the wide range of Ca^{2+} sensitive dyes on the market and the availability of high throughput systems based on this technology. In this study two assays have been used that monitor mobilisation of $[Ca^{2+}]_i$ as an end point; a single cell based approach using the ratiometric dual wavelength dye Fura-2 (Roe et al., 1990) and a fluorescent microscope, and a high throughput method using a Fluorometric Imaging Plate Reader (FLIPR) and a single wavelength dye, Fluo-4 (Gee et al., 2000). Both systems have advantages and disadvantages which will be discussed later. To monitor activation of GPR41, which is predominately $G\alpha_{i/o}$ coupled, by measuring changes in $[Ca^{2+}]_i$, a G protein that allows a switch to the activation of this cascade had to be co-expressed with the receptor. This can be a promiscuous G proteins α subunit, such as $G\alpha_{15}$ or $G\alpha_{16}$ which couple to many GPCRs, or a G protein chimera in which the last five amino acids of $G\alpha_q$ have been replaced by the corresponding sequence from $G\alpha_{i1}$ or $G\alpha_s$ (Kostenis et al., 2005). The G protein chimera used in this study is a recently described $G\alpha_{q15}$ mutant that has a glycine to aspartic acid mutation introduced at position 66 that allows it to more effectively couple to a panel of $G\alpha_{i/o}$ coupled receptors (Kostenis et al., 2004). However, $[Ca^{2+}]_i$ mobilization assays are not ideally suited to monitoring activation of these receptors due to the relatively low potency of the fatty acids at the receptors.

3.2 Functional assays to monitor activation of GPR41

As GPR41 is a predominately $G_{i/o}$ coupled receptor, a [^{35}S]GTP γ S binding assay using this receptor was developed. GPR41 was co-transfected with a panel of $G_{i/o}$ α subunits ($G\alpha_{i1}$, $G\alpha_{i2}$, $G\alpha_{i3}$ or $G\alpha_o$) and a [^{35}S]GTP γ S binding assay carried out on the membranes prepared from these cells. The increase in [^{35}S]GTP γ S binding obtained on the addition of a high concentration of propionate (10mM) was small although it appeared that GPR41 showed some selectivity towards $G\alpha_{i3}$ over any of the other α subunits tested (data not shown). When using membranes co-expressing GPR41 and $G\alpha_{i3}$, concentration-response curves were generated to propionate (Figure 3.1). [^{35}S]GTP γ S binding at maximally effective concentrations was only $58\pm 3\%$ higher than basal binding and due to this small activation window a fusion protein between GPR41 and $G\alpha_{i3}$ was generated, with the aim to improve the activation window. When this fusion protein was transfected into HEK293T cells and [^{35}S]GTP γ S binding studies carried out on membranes prepared from these cells in the presence of increasing concentrations of propionate, a maximal increase in [^{35}S]GTP γ S binding of $661\pm 26\%$ was observed. The pEC_{50} value for propionate at the GPR41- $G\alpha_{i3}$ Cys 351 Ile fusion protein was 3.6 ± 0.1 and at GPR41 when co-transfected with $G\alpha_{i3}$ the pEC_{50} was 3.7 ± 0.2 . The increase in binding was much more robust when using the receptor-G protein fusion protein and allowed potencies of other short chain fatty acids to be determined with greater accuracy (Figure 3.2 and Table 3.1). Using this method the rank order of potencies for short chain fatty acids at GPR41 was valerate > butyrate = propionate > acetate.

Most of the work on GPR41 has concluded that it is a predominately $G\alpha_{i/o}$ coupled receptor (Brown et al., 2003, Le Poul et al., 2003, Xiong et al., 2004). To confirm this, GPR41-eYFP was transiently expressed in HEK293T grown on coverslips. 24h post transfection cells were loaded with the Ca^{2+} sensitive dye Fura-2 for 30mins. Cells were mounted into a chamber containing live cell buffer and the changes in Fura-2 fluorescence monitored. Cells were exposed to 10mM propionate, added using a perfusion system, after 60s of basal readings and data collected for a further 240s. The cells were exposed to propionate for 60s. In the absence of a co-expressed promiscuous or chimeric G protein α subunit, only a negligible change in $[\text{Ca}^{2+}]_i$ was observed in cells positively transfected with GPR41 selected on the basis of eYFP fluorescence (Figure 3.3). Upon co-expression with the chimeric G protein α subunit, $G\alpha_{qG66Di5}$, challenge with 10mM propionate resulted in a rapid, transient rise in $[\text{Ca}^{2+}]_i$ only in cells expressing GPR41-eYFP. When GPR41-eYFP was co-expressed with the promiscuous G protein α subunit, $G\alpha_{16}$, a rise in $[\text{Ca}^{2+}]_i$

was also observed, although the kinetics of the increase in $[Ca^{2+}]_i$ were different from those in cells co-expressing GPR41-eYFP and $G\alpha_{qG66Di5}$ (Figure 3.3).

3.3 Function of N- and C-terminally modified forms of GPR43 and C-terminally modified forms of GPR40

To confirm that GPR43 was able to couple to $G\alpha_q$, the receptor was transiently expressed with $G\alpha_q$ in mouse embryonic fibroblasts that lack expression of both $G\alpha_q$ and $G\alpha_{11}$, called EF88 cells herein (Liu et al., 2002). A large, transient rise in $[Ca^{2+}]_i$ was recorded in response to the addition of 10mM acetate (Figure 3.4). EF88 cells were difficult to transfect with high efficiency and for the purpose of developing an assay to monitor function of modified versions of GPR43, they were poorly suited. To overcome this, HEK293T cells were used in further assays as transfection was much more efficient.

The effect of N-terminally epitope tagging GPR43 was assessed (Figure 3.5). Flag-GPR43 and c-Myc-GPR43 were generated and the sequence confirmed by DNA sequencing. The modified versions of GPR43 were transfected into HEK293T cells, membranes prepared and samples resolved using SDS-PAGE. Proteins were transferred onto nitrocellulose membrane and an immunoblot performed using commercial versions of anti-Flag or anti-c-Myc antibodies. A band of approximately 35kDa was observed in the Flag-GPR43 sample lane but no band was present in the lane corresponding to c-Myc-GPR43. c-Myc-CXCR1 and Flag-CXCR1 (Wilson et al., 2005) were included as positive or negative controls depending on the antibody used. The apparent lack of expression of c-Myc-GPR43 may have been due to the inability of the antibody to identify the epitope therefore to explore this finding, HEK293T cells were transiently transfected with wild type GPR43, Flag-GPR43 and c-Myc-GPR43, loaded with Fura-2 and changes in $[Ca^{2+}]_i$ monitored in response to 10mM acetate. Wild type GPR43 was able to elicit a rapid, transient rise in $[Ca^{2+}]_i$ similar to that seen in the EF88 cells. The magnitude of the response from Flag-GPR43 was slightly reduced compared to the wild type receptor whereas no signal could be detected in cells transfected with the c-Myc-GPR43 construct. From these data, it appears that c-Myc-GPR43 does not express when transfected into HEK293T cells whereas Flag-GPR43 was expressed and rise in $[Ca^{2+}]_i$ could be detected. It was therefore concluded that N-terminally tagging GPR43 was detrimental to the function of the receptor and as a fully functioning receptor was required for future experiments they were not used further.

To address the problem of not being able to effectively epitope tag GPR43 at its N-terminus with multiple distinct tags, constructs were generated with c-Myc and Flag fused to the C-terminus of GPR43. These constructs were transfected into HEK293T cells and their ability to mediate a rise in $[Ca^{2+}]_i$ compared to that of the wild type receptor assessed (Figure 3.6). Both GPR43-Flag and GPR43-c-Myc were able to mediate a rapid, transient rise in $[Ca^{2+}]_i$ and this Ca^{2+} mobilisation was very similar to that mediated by the wild type receptor. In addition, immunoblot analysis of the C-terminally tagged versions of GPR43 confirmed their expression (data shown in Chapter 6). Fusion proteins between GPR43 and eCFP, eYFP or $G\alpha_q$ were also constructed (GPR43-eCFP, GPR43-eYFP and GPR43- $G\alpha_q$) and tested for their ability to induce a rise in $[Ca^{2+}]_i$ levels in response to 10mM acetate. Each of these fusion proteins was able to produce a transient rise $[Ca^{2+}]_i$, comparable to that of the wild type receptor (Figure 3.6). Using GPR43-eCFP allowed positively transfected cells to be identified and tested for their response to various short and long chain fatty acids (Figure 3.7). Acetate, butyrate and propionate (all at 10mM) were able to mediate a rise in $[Ca^{2+}]_i$ via GPR43. Whereas, when cells expressing GPR43-eCFP were exposed to 100 μ M lauric acid no change in $[Ca^{2+}]_i$ levels was detected.

Monitoring $[Ca^{2+}]_i$ mobilisation in single cells is poorly suited to investigate the potency of fatty acids at GPR43 due to its time consuming nature, therefore a high throughput FLIPR-based method was employed. This method enabled a panel of short and long chain fatty acids to be tested for their ability to mediate a rise in $[Ca^{2+}]_i$ via GPR43. GPR43-eYFP and a G protein cocktail (consisting of $G\alpha_{q05}$, $G\alpha_{q15}$, $G\alpha_{qz5}$, $G\alpha_{qs5}$, $G\alpha_{15}$ and $G\alpha_{16}$) was transiently transfected into HEK293 MSRII cells and the ability of a variety of fatty acids to mediate a rise in $[Ca^{2+}]_i$ monitored by a change in Fluo-4 fluorescence measured by the FLIPR. Figure 3.8 shows that acetate, propionate and butyrate were all able to mediate a rise in $[Ca^{2+}]_i$ in a concentration-dependent manner and relative potencies were ascribed (Table 3.2). Only at high concentrations was formate able to transiently rise $[Ca^{2+}]_i$ levels. None of the longer chain fatty acids tested were able to activate GPR43 and no change in fluorescence was seen when short chain fatty acids were added to control cells transfected with GPR40-eYFP or the neuromedin U receptor (NMU-R). The rank order of potency of the short chain fatty acids at GPR43 using this method was propionate>acetate>butyrate>formate.

When GPR40 is co-expressed with $G\alpha_q$ in EF88 cells that lack endogenous expression of $G\alpha_q$ or $G\alpha_{11}$, caproic acid (C6:0) allowed rapid and transient elevation of $[Ca^{2+}]_i$ (Figure 3.9). In HEK293T cells, co-transfection with $G\alpha_q$ was not required for caproic acid to generate a Ca^{2+} signal as these cells express both $G\alpha_q$ and $G\alpha_{11}$ endogenously. A range of

C-terminal modifications were introduced onto GPR40, including c-Myc and Flag epitope tags, and the in-frame fusion of eCFP, eYFP or $G\alpha_q$. When the modified versions of GPR40 were transfected into HEK293T cells and challenged with caproic acid, no loss of agonist function could be detected (Figure 3.10). Caproic acid has been described as a low affinity agonist for GPR40 and the shortest chain length fatty acid able to activate this receptor (Briscoe et al., 2003). A range of other fatty acids were tested for their capacity to elevate $[Ca^{2+}]_i$ in HEK293T cells expressing GPR40-eCFP. Each of lauric acid (C12:0), palmitic acid (C16:0) and elaidic acid (C18:1) were able to mediate a rise in $[Ca^{2+}]_i$ only in positively transfected cells displaying eCFP fluorescence (Figure 3.11). It was noted that slower elevation of $[Ca^{2+}]_i$ was observed with increasing fatty acid chain length and that the signal generated by each of the fatty acids displayed distinct kinetics. This was particularly clear with elaidic acid, with a slower increase in $[Ca^{2+}]_i$ compared to the other fatty acids and the Ca^{2+} levels within the cells did not return to baseline during the duration of the assay. This difference may reflect variations in the affinity or ligand association rate of the fatty acids, or variations in their solubility characteristics. As the fatty acids were solubilised in 100% ethanol and diluted down to the required concentration, it was necessary to confirm that the signal generated was specific to the addition of a fatty acid. Therefore, 1% ethanol was added to cells expressing GPR40-eCFP and no change in $[Ca^{2+}]_i$ was detected (Figure 3.11).

As mentioned above, single cell Ca^{2+} experiments are poorly suited to determine potencies of agonists at a specific receptor. Therefore, to determine the potencies of a variety of saturated and un-saturated fatty acids at GPR40, a FLIPR-based Ca^{2+} release assay was developed. GPR40-eYFP was transiently expressed in HEK293 MSRII cells and the ability of a variety of fatty acids to mediate a change in Fluo-4 fluorescence monitored. The resulting potencies are detailed in Table 3.3. As expected, GPR40 was able to mediate a rise in $[Ca^{2+}]_i$ in response to increasing concentrations of both saturated and un-saturated fatty acids.

The majority of fatty acids circulating in the body are complexed with albumin and other serum proteins and it is important to take this into consideration when studying fatty acids and experiments were carried out to address this issue (Figure 3.12). HEK293T cells transiently expressing either GPR40-eCFP or GPR43-eCFP were exposed to fatty acids with increasing concentrations of fatty acid free bovine serum albumin (BSA). The addition of 0.1% fatty acid free BSA reduced the signal generated by 100 μ M lauric acid at GPR40-eCFP but had little effect on the magnitude of signal generated by GPR43-eCFP in response to 10mM acetate. With 0.5% fatty acid free BSA added to 100 μ M lauric acid no

detectable signal was produced by GPR40-eCFP and when GPR43-eCFP was exposed to 10mM acetate and 0.5% fatty acid free BSA a reduction in the maximal signal was observed.

3.4 BSA allows the pharmacology of GPR40 to be uncovered

The differing kinetics of fatty acids at GPR40 in single cell Ca^{2+} imaging studies demonstrated that this method is not well suited for examining ligand concentration-dependence, especially for these low affinity ligands. To overcome this and to carry out detailed pharmacological assessment of ligands at GPR40, the GPR40- $\text{G}\alpha_q$ fusion protein was employed and a [^{35}S]GTP γ S binding assay developed.

Historically, it has been difficult to carry out [^{35}S]GTP γ S binding studies on GPCRs that couple to $\text{G}\alpha_q$ or $\text{G}\alpha_{11}$. Using a GPCR-G protein fusion in combination with an immunocapture step with G protein specific antibodies, enriches the levels of $\text{G}\alpha_{q/11}$ and allows monitoring of activation of the receptor (Carrillo et al., 2002, Milligan et al., 2004, Canals et al., 2006). GPR40- $\text{G}\alpha_q$ was transiently expressed in HEK293T cells and membranes prepared. [^{35}S]GTP γ S binding studies were performed with subsequent immunoprecipitation using the anti $\text{G}\alpha_{q/11}$ antiserum CQ (Mitchell et al., 1991). High levels of [^{35}S]GTP γ S were present in the GPR40- $\text{G}\alpha_q$ immunoprecipitates in the absence of an added agonist. When 30 μM palmitic acid or elaidic acid were present in the assay, no increase in levels of [^{35}S]GTP γ S was detected (Figure 3.13). This is unlike a range of other GPCR- $\text{G}\alpha_q$ or GPCR- $\text{G}\alpha_{11}$ fusion proteins that have been studied, where loading of [^{35}S]GTP γ S is very low in the absence of receptor stimulation (Carrillo et al., 2002, Milligan et al., 2004, Canals et al., 2006).

As the reported endogenous agonists at GPR40 are medium and long chain free fatty acids and fatty acid free BSA was able to inhibit the function of free fatty acids in the Ca^{2+} mobilization assay, it was therefore possible that the high level of basal loading of [^{35}S]GTP γ S onto GPR40- $\text{G}\alpha_q$ might reflect the presence of endogenous agonist in the assay which could activate GPR40- $\text{G}\alpha_q$ and give the appearance of high levels of [^{35}S]GTP γ S binding in basal conditions. The most obvious means by which the endogenous agonist could be present is via the release of free fatty acids during cell rupture and membrane preparation. To explore this possibility, fatty acid free BSA was added to GPR40- $\text{G}\alpha_q$ expressing membranes in increasing concentrations and [^{35}S]GTP γ S

incorporation onto GPR40-G α_q measured. Levels of bound [35 S]GTP γ S decreased with increasing concentrations of fatty acid free BSA over the full concentration range tested. At high levels of fatty acid free BSA (300 μ M), the levels of bound [35 S]GTP γ S were very low (Figure 3.14). As noted earlier, in the absence of BSA the stimulation of [35 S]GTP γ S binding induced by the addition of 30 μ M palmitic acid was very limited. In the presence of concentrations of fatty acid free BSA up to 1 μ M, 30 μ M palmitic acid was now able to increase [35 S]GTP γ S binding up to the levels observed in the absence of fatty acid free BSA. At concentrations of fatty acid free BSA between 1-10 μ M, basal [35 S]GTP γ S binding continued to decrease but although 30 μ M palmitic acid was still able to stimulate [35 S]GTP γ S binding it was unable to achieve the same maximal level. This is likely to be due to substantial amounts of palmitic acid now being bound by the excess of fatty acid free BSA. Also, when membranes expressing GPR40-G α_q were treated with the selective G $\alpha_{q/11}$ inhibitor, YM254890, which blocks guanine nucleotide exchange on the G protein (Takasaki et al., 2004, Canals et al., 2006), the presence of [35 S]GTP γ S in the immunoprecipitates was virtually eliminated (Figure 3.15). This demonstrates that the high levels of [35 S]GTP γ S bound at GPR40-G α_q in basal conditions reflects direct exchange of the guanine nucleotide on the G protein. Taken together, these results suggest that high levels of [35 S]GTP γ S binding in basal conditions are a consequence of an endogenous agonist being present which can be stripped away by fatty acid free BSA and this results in a window in which detailed pharmacology of ligands at GPR40 could be measured in [35 S]GTP γ S binding studies.

To demonstrate that concentration-response curves could be generated by reducing the basal activation of GPR40-G α_q , [35 S]GTP γ S binding studies were performed on membranes expressing GPR40-G α_q in the presence of increasing concentrations of palmitic acid and three concentrations of fatty acid free BSA. In the presence of a low concentration of fatty acid free BSA (100nM), basal [35 S]GTP γ S binding was high and no increase in binding was observed with increasing concentrations of palmitic acid. By contrast, in the presence of either 10 μ M or 100 μ M fatty acid free BSA, basal [35 S]GTP γ S binding was greatly reduced, with a larger reduction seen on the addition of 100 μ M fatty acid free BSA. When increasing concentrations of palmitic acid were added a concentration response curves was seen and allowed the potency of palmitic acid to be determined (Figure 3.16 and Table 3.4). At the higher concentration of fatty acid free BSA, the concentration-response curve to palmitic acid was shifted to higher apparent concentrations which is consistent with the higher amounts of fatty acid free BSA binding a greater amount of the added palmitic acid. The potency of palmitic acid achieved with

the addition of 10 μ M fatty acid free BSA is similar to that observed using other methods (Briscoe et al., 2003; Itoh et al., 2003; Nilsson et al., 2003) and therefore was used in further experiments to examine the pharmacology of a range of fatty acids (Figure 3.17). The potencies of the fatty acids examined using the [³⁵S]GTP γ S binding assay are shown in Table 3.5. Due to time constraints a full panel of fatty acids could not be tested against GPR40-G α_q .

Compared to GPR40-G α_q , the GPR41-G α_{i3} Cys³⁵¹Ile fusion protein did not display unusually high levels of basal [³⁵S]GTP γ S binding and a large increase in [³⁵S]GTP γ S binding upon addition of agonist could be observed. [³⁵S]GTP γ S binding studies were performed on membranes expressing GPR41-G α_{i3} Cys³⁵¹Ile, with the addition of increasing concentrations of fatty acid free BSA in the absence or presence of 10mM propionate. Figure 3.18 shows that the addition of fatty acid free BSA had little effect on the basal binding of [³⁵S]GTP γ S to GPR41-G α_{i3} Cys³⁵¹Ile and only at high concentrations of fatty acid free BSA was a reduction in the levels of stimulation observed. This was likely to be due to the binding of propionate to BSA and therefore to reduce the amount available to activate the receptor. To confirm this observation, membranes expressing GPR41-G α_{i3} Cys³⁵¹Ile were used in [³⁵S]GTP γ S binding studies where increasing concentrations of propionate were added in the presence of three concentrations of fatty acid free BSA (Figure 3,19). Only a slight shift in apparent potency of propionate was observed on the addition of 100 μ M fatty acid free BSA (Table 3.6). It was therefore deemed unlikely that GPR41-G α_{i3} Cys³⁵¹Ile is activated by an endogenous ligand in [³⁵S]GTP γ S binding studies.

3.5 Detection of GPR40, GPR41 and GPR43 in a β -cell line and the function of GPR40 in these cells

The expression of GPR40 in β -cells has been well documented in many studies using a range of β -cell lines and human tissue. To confirm the expression of GPR40 in β -cells, a rat insulinoma cell line (INS-1E) was used, as human pancreatic cell lines are not generally available. RNA from these cells was isolated and cDNA generated via reverse transcription. The cDNA was probed using primers specific for rat GPR40 and a protein accepted to be expressed in β -cells, cyclophilin (Figure 3.20(a-b)). This confirmed the expression of GPR40 in these cells. In the absence of reverse transcriptase no band was observed (data not shown). To date the only evidence of GPR41 and GPR43 being

expressed in pancreatic β cells comes from a patent applications by Arena Pharmaceuticals, to investigate if these receptors were also expressed in the INS-1E cells cDNA from these cells was probed using primers specific for rat GPR41 and rat GPR43, and bands corresponding to each of these receptors were present (Figure 3.20 c-d).

The proceeding studies on GPR40 were performed on cells and cell membranes into which forms of GPR40 has been introduced and it was of interest to assess if similar results would be obtained in INS-1E cells endogenously expressing GPR40. It was confirmed that 100 μ M lauric acid could activate GPR40 in these cells by generation of a robust and transient elevation of $[Ca^{2+}]_i$ (Figure 3.21). Membranes from INS-1E cells were prepared and used in [35 S]GTP γ S binding studies. With end of assay immunoprecipitation of $G\alpha_{q/11}$, levels of bound [35 S]GTP γ S in the basal state were again very high and little stimulation was produced by the addition of 100 μ M palmitic acid (Figure 3.22). As with HEK293T membranes transiently expressing GPR40- $G\alpha_q$, addition of fatty acid free BSA resulted in a large reduction in the apparent basal [35 S]GTP γ S binding in $G\alpha_q$ immunoprecipitates and these levels were now markedly increased by the addition of palmitic acid.

3.6 Discussion

There are many difficulties in studying newly orphanised GPCRs. In the case of GPR40, GPR41 and GPR43 the recent description of their activating ligands means that there is a vast amount to be discovered about them but the availability of tool compounds and well developed assay systems makes this difficult. To be able to investigate their function and pharmacology, robust methods of monitoring their activation and expression were developed.

GPR41 mainly couples to the $G\alpha_{i/o}$ family of $G\alpha$ subunit and this allowed [35 S]GTP γ S binding studies to be carried out by Brown et al., (2003) and Le Poul et al., (2003) with GPR41 co-transfected with $G\alpha_{i1}$ or in membranes prepared from CHO cells stably expressing GPR41 respectively. In this present study, when GPR41 was co-transfected with $G\alpha_{i3}$ and [35 S]GTP γ S binding studies performed on the resulting membranes using immuno-capture of $G\alpha_{i3}$ only a small rise in [35 S]GTP γ S binding (60% increase over basal binding) was observed at high concentrations of propionate (Figure 3.1). This level of activation was not robust enough to allow good pharmacological assessment to be carried out. To overcome this, a GPR41- $G\alpha_{i3}$ Cys 351 Ile fusion protein was constructed and this fusion protein showed a 661 \pm 26% increase in [35 S]GTP γ S binding over basal in response

to propionate. This provided an effective means to measure ligand-stimulated binding of [³⁵S]GTPγS. Using this fusion protein, potencies of four short chain fatty acids were determined (Table 3.1). The potencies observed using this assay system were similar to those seen by Brown et al., (2003) in a [³⁵S]GTPγS binding assay. The rank order of potency differs slightly but this is likely to be due to the similar potencies observed for propionate, valerate and butyrate.

The use of promiscuous and chimeric G proteins allows receptors that do not naturally couple to G protein α subunits that activate PLC-β to be used in assays that monitor the mobilization of [Ca²⁺]_i. The Gα subunit Gα₁₆ is viewed as being promiscuous, although it has been shown to be unable to couple to a subset of GPCRs and the majority of these receptors are Gα_{i/o} selective (Kostenis, 2001). When GPR41 was co-transfected with Gα₁₆ the kinetics of [Ca²⁺]_i release in response to propionate was slower than observed upon co-transfection with Gα_{qG66Di5}. Gα_{qG66Di5} has been shown to be more effective in coupling to a set of Gα_{i/o} coupled receptors than Gα_{qi5} (Kostenis et al., 2005). Although Gα_{qi5} was not tested in this study, it does appear that GPR41 coupled better to Gα_{qG66Di5} than Gα₁₆, although this could also be due to expression levels and the scope of this study did not look into this. Therefore, in further experiments with GPR41 where [Ca²⁺]_i mobilization was measured, Gα_{qG66Di5} was co-expressed.

To investigate cell surface expression of GPR43, N-terminally modified forms of the receptor were generated. Unusually, the addition of the c-Myc epitope tag resulted in the loss of expression of the receptor monitored by immunoblotting and no rise in [Ca²⁺]_i could be initiated in cells transfected with c-Myc-GPR43 upon the addition of acetate. The inability to detect c-Myc-GPR43 by immunoblotting may be due to low levels of expression of the receptor rather than the receptor not expressing at all. The single cell Ca²⁺ assay is a sensitive assay system and no rise in [Ca²⁺]_i could be detected in any cell transfected with c-Myc-GPR43 cDNA, which supports a loss of expression rather than low levels of expression that may fall below expression levels required to be detected by immunoblotting. The addition of the Flag epitope tag to GPR43 allowed detection of the receptor by immunoblotting and the signal generated in response to acetate was similar to that generated by the wild type receptor. For many GPCRs, the addition of N-terminally epitope tags has been shown to have no or limited effects on expression or ligand binding. These include the α_{1A} adrenoceptor (Stanasila et al., 2002), β₂ adrenoceptor (Hebert et al., 1996), CXCR1 and CXCR2 chemokine receptors (Wilson et al., 2005), D1 dopamine receptor (George et al., 1998), and MT₁ and MT₂ melatonin receptors (Ayoub et al., 2002).

The large effect seen when N-terminally tagging GPR43 may be due to its relatively short N-terminal extracellular domain. The addition of an epitope tag onto this short N-terminal may affect the receptor synthesis and maturation. It was shown in single cell $[Ca^{2+}]_i$ experiments that the addition of a variety of C-terminal tags did not have an effect on the function of GPR43. The addition of the fluorescent proteins, eCFP and eYFP to the C-terminus of GPR43 provided an ideal way to monitor the expression of the receptor and allowed only positively transfected cells to be selected when analysing the single cell Ca^{2+} experiments.

Using the GPR43-eYFP fusion, potencies of short chain fatty acids at the receptor were determined using a FLIPR-based $[Ca^{2+}]_i$ mobilization assay. The potencies determined were very close to those reported by Brown et al., (2003) and Le Poul et al., (2003) when using a Ca^{2+} -based assay with propionate being the most potent in all three studies. The data generated by Nilsson et al., (2003) on the potency of short chain fatty acids at GPR43 found that they were less potent using both a reporter gene assay and a Ca^{2+} mobilisation based assay. In HEK293T cells, it was not necessary to co-transfect GPR43 with additional G protein, as a robust signal could be generated upon the expression of GPR43 alone. Whereas, in the FLIPR-based assay system, expression of GPR43-eYFP in HEK293 MSRII cells was not sufficient to generate a change in fluorescence upon the addition of an activating ligand that could be detected by the FLIPR. Only upon the co-transfection of a G protein cocktail could a signal be detected. This highlights the differing sensitivities of the two assay systems used in this study to monitor agonist induced Ca^{2+} release. The single cell Ca^{2+} mobilization assay allowed single cells to be measured for their response to agonist. In the FLIPR based assay, the change in fluorescence is measured over a field of cells. Comparing the change in Fura-2 ratio generated by GPR43 and GPR40, GPR43 does not produce as large an increase in $[Ca^{2+}]_i$ compared to GPR40. It may also be due to the transient expression of the receptor in these cells or due to low levels of receptor expression. This signal, although robust enough to be measured in single cells, is likely to have been too small an average change over a field of cells to be measured by the FLIPR.

Agonist ligands act to stabilize and enrich populations of active states of GPCRs (Milligan, 2003). In the case of opsins, 11-cis retinal is bound by the receptor as an endogenous inverse agonist to virtually eliminate active states in the absence of light, however, other GPCRs display varying levels of agonist-independent or constitutive activity (Milligan, 2003, Bond and IJzerman, 2006). When studying GPCRs in transfected cell systems this constitutive activity can be extensive and may virtually occlude detection of effects of

agonists above such high basal activity. The importance of constitutive activity in native tissue is not fully understood but there is significant evidence that for some receptors it may be relevant to their physiological effect and the effects of therapeutic medicines (Bond and IJzerman, 2006). The role of constitutive activity, the ability of inverse agonists to reduce this activity and the advantages this may have as a therapeutic strategy has been difficult to interpret due the possibility that 'basal' activity may reflect the presence of an endogenous agonist that is difficult to eliminate or remove.

It is now well appreciated that a substantial number of GPCRs respond to hydrophobic, lipid or lipid-like endogenous mediators and these have the potential to be difficult to remove from cell preparations if they are long lived. Taking this into consideration when developing the [³⁵S]GTPγS binding assay using GPR40-Gα_q the detection of very high levels of apparent constitutive activity were of considerable interest not only because of the hydrophobic nature of the proposed endogenous agonist but also because high levels of constitutive activity has been reported for other GPCRs that are of therapeutic interest in the areas of feeding, obesity and the metabolic syndrome, such as the ghrelin receptor (Holst and Schwartz, 2004, Holst et al., 2004).

It may be argued that the apparent high constitutive activity of GPR40 in these assays could relate to the close proximity enforced between the GPCR and G protein in the use of the GPR40-Gα_q fusion protein. This is unlikely as in other GPCR-Gα_q or Gα₁₁ fusions studied only low levels of [³⁵S]GTPγS were bound in the absence of ligand (Carrillo et al., 2002, Milligan et al., 2004, Canals et al., 2006) and when using membranes prepared from INS-1E high levels of basal binding of [³⁵S]GTPγS were also seen. A common feature of constitutively active GPCRs is constitutive internalisation of the receptor seen using GPCR-fluorescent protein fusions. When GPR40-eYFP is transiently expressed in HEK293T cells or inducibly expressed in Flp-In TRex cells it is membrane delineated and only low levels of the receptor are internalised (seen in Figure 4.1). Thus, although not providing definitive evidence these observations would be consistent with GPR40 having low levels of constitutive activity.

Ca²⁺ mobilization assays are inherently unsuited to the detection of receptor constitutive activity because the capacity and requirement of intact cells to dynamically re-equilibrate alterations in Ca²⁺ levels. A key issue in these studies is that the high basal activity of GPR40 was only detected using the [³⁵S]GTPγS binding assays and not in either of the [Ca²⁺]_i mobilization assays. The potential key difference in the two assays is that the

[³⁵S]GTPγS binding assay employed membrane preparation. Although not addressed in this study, it may be that fatty acids released upon cell breakage during membrane preparation can remain in the membranes, rather than in the supernatant fraction, and therefore potentially bind and activate GPR40 during the assay. This is supported by the ability of fatty acid free BSA to reduce the basal loading of [³⁵S]GTPγS as it could bind and prevent the unappreciated fatty acids from activating the receptor. The addition of palmitic or lauric acid was unable to significantly increase binding of [³⁵S]GTPγS. With the addition of fatty acid free BSA, the effect of these fatty acids in combination the BSA was to elevate [³⁵S]GTPγS binding back to the basal level. If there is an endogenous ligand binding and activating this receptor then it is activating the receptor to its maximum which cannot be increased by the presence of additional fatty acid.

The addition of increasing concentrations of fatty acid free BSA and the recovery of maximal stimulation by additional fatty acid only occurred over a limited range of BSA and the effects of the added fatty acids were eventually decreased, presumably as the added fatty acid also became bound to BSA. To confirm this effect of fatty acid free BSA binding to the added fatty acid, the observed concentration response curve for palmitic acid moved to higher concentrations as greater concentrations of BSA were added to further reduce basal [³⁵S]GTPγS binding but the additional BSA in turn bound the added fatty acid and prevented it from activating the receptor. Using membranes prepared from INS-1E cells that endogenously express GPR40 it was found that they also showed high levels of basal [³⁵S]GTPγS binding and as with the membranes transiently expressing GPR40, no increase in [³⁵S]GTPγS binding was detected with addition of fatty acid. Fatty acid free BSA was again able to reduce the basal loading of [³⁵S]GTPγS and levels of incorporated [³⁵S]GTPγS could be returned to that seen in the basal state when fatty acids were added in combination with BSA. Therefore, the observations using transiently expressed GPR40 are unlikely to be due to an artefact of over-expression of the receptor or from the use of the receptor-G protein fusion.

If the endogenous ligand is a medium or long chain fatty acid, due to their hydrophobic nature, it might partition into the membranes rather than into the supernatant wash buffer. By contrast, for GPR41 there was no high basal levels of [³⁵S]GTPγS binding and stimulation was seen in the presence of added fatty acid. There was little effect of increasing concentrations of fatty acid free BSA on the basal [³⁵S]GTPγS loading of GPR41-Gα₁₃ Cys³⁵¹Ile or on the increase in binding of [³⁵S]GTPγS stimulated by propionate. In addition, there was no significant change in the concentration-response

curves to propionate on addition of varying concentrations of fatty acid free BSA. During membrane preparation, any short chain fatty acid are likely to be found in the wash buffer, as they are more water soluble, and therefore be removed and unable to activate GPR41. These findings support the hypothesis that the high levels of basal loading of GPR40-G α_q are due to an endogenous ligand, which is likely to be a fatty acid or lipid, being present in membrane preparations.

Two further GPCRs, GPR120 and GPR84 (Katsuma et al., 2005, Wang et al., 2006) have been described whose endogenous ligands appear to be medium to long chain fatty acids. Wang et al., (2006) performed [³⁵S]GTP γ S binding studies using GPR84. Rather than using an immunocapture step at the end of assay, they terminated the assay by filtration. They were able to show fatty acid-mediated increases in [³⁵S]GTP γ S binding in a concentration-dependent manner, which could be completely abolished by the addition of PTX. In their study GPR84 was shown to respond to fatty acids of between 9 and 14 carbons in length whereas GPR40 can be activated by longer chain fatty acids. If GPR40 is being activated by an endogenous ligand released upon cell rupture then this ligand does not appear to activate GPR84.

The expression of GPR40 in pancreatic β -cell lines (Briscoe et al., 2003, Itoh et al., 2003, Itoh and Hinuma, 2006, Shapiro et al., 2005) and in human pancreatic tissue (Tomita et al., 2006) has been well documented. In this study I have confirmed the expression of GPR40 in INS-1E cells but I have also shown that mRNA corresponding to rat GPR41 and GPR43 could also be detected. Although, Brown et al., (2003) were able to identify low levels of expression of human GPR41 in the pancreas they did not determine if expression was localised to the β -cells. None of the other studies looking into the tissue distribution of GPR41 and GPR43 have reported expression of either of these receptors in the pancreas (Le Poul et al., 2003, Kotarsky et al., 2003, Hong et al., 2005). Recent patents by Arena Pharmaceuticals also reported expression of all three receptors in pancreatic islet cells. This is the first time that all three receptors have been shown to be expressed in the same cell line and leads to the possibility that they may form hetero-dimers, which in turn may affect their function.

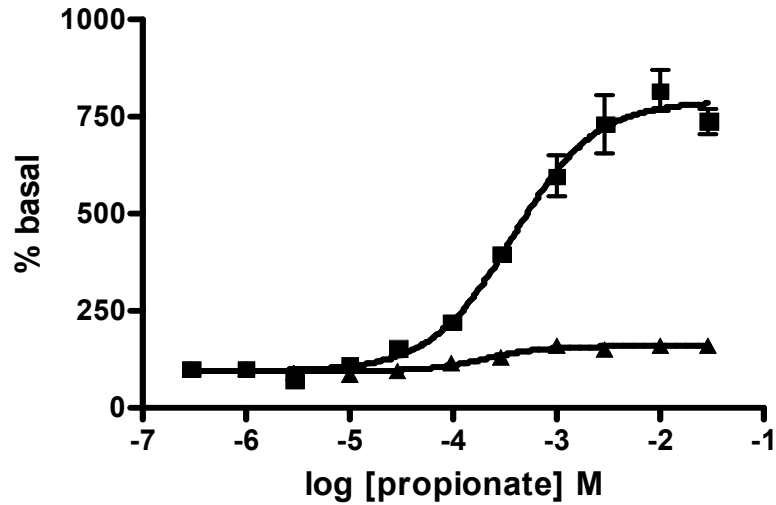


Figure 3.1 Comparison of levels of [³⁵S]GTP γ S binding using a GPR41-G α_{i3} Cys³⁵¹Ile fusion protein to that when GPR41 is co-transfected with G α_{i3}

HEK293T cells were co-transfected with GPR41 and G α_{i3} Cys³⁵¹Ile (triangles) or transfected with a GPR41-G α_{i3} Cys³⁵¹Ile fusion (squares) and membranes prepared. Membranes were exposed to increasing concentrations of propionate and levels of [³⁵S]GTP γ S bound in G α_{i3} immunoprecipitates determined. Graph shown is representative of three individual experiments performed in triplicate. Data points represent means \pm SEM.

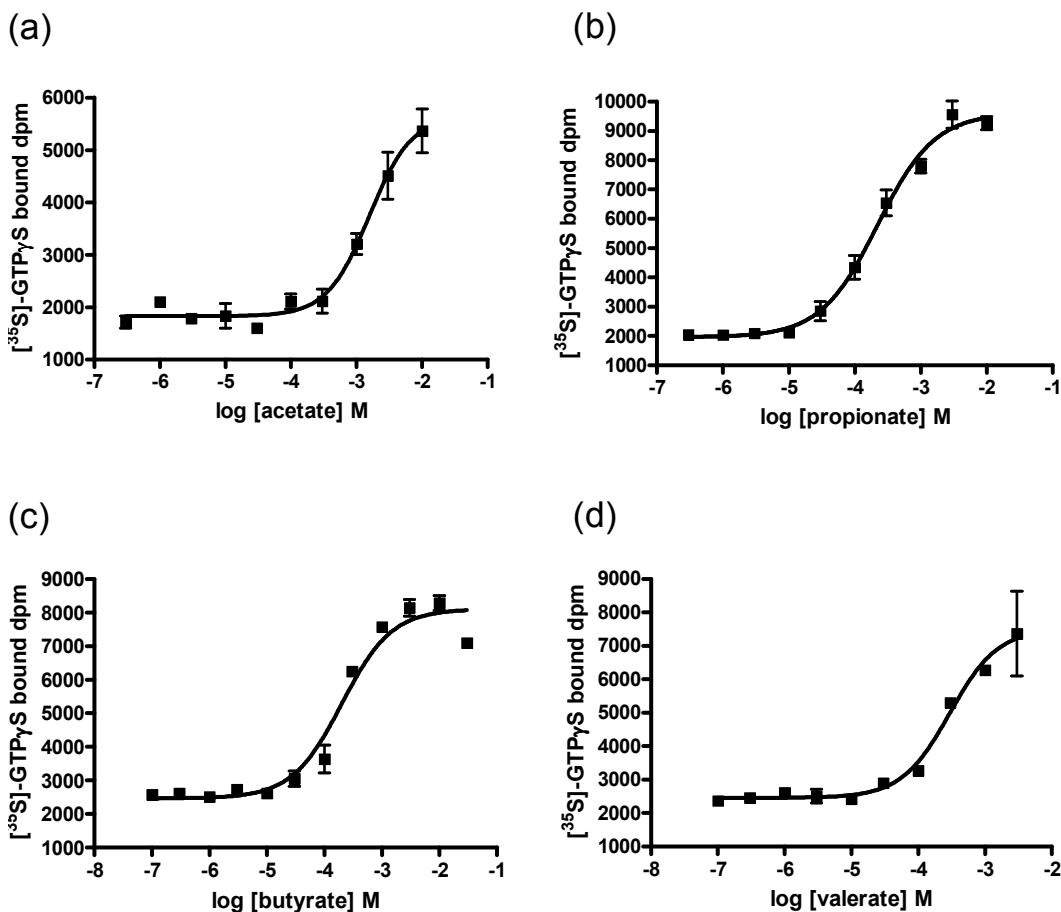


Figure 3.2 Potency of various short chain fatty acids at GPR41-G α_{13} Cys³⁵¹Ile measured by $[^{35}\text{S}]\text{GTP}\gamma\text{S}$ binding

HEK293T cells were transfected with GPR41-G α_{13} Cys³⁵¹Ile and membranes prepared. $[^{35}\text{S}]\text{GTP}\gamma\text{S}$ binding studies were performed in the presence of increasing concentrations of (a) acetate, (b) propionate, (c) butyrate and (d) valerate. Assay samples were immunoprecipitated with the G α_{13} antiserum I3 before scintillation counting. Graphs shown are representative of results obtained for three individual experiments performed in triplicate. Data points represent means \pm SEM.

SCFA	pEC ₅₀
Acetate (C ₂)	1.83±0.69
Propionate (C ₃)	3.61±0.11
Butyrate (C ₄)	3.63±0.16
Valerate (C ₅)	3.94±0.22

Table 3.1 Potency of short chain fatty acids at GPR41 measured in the [³⁵S]GTPγS binding assay

[³⁵S]GTPγS binding studies were performed on membranes expressing GPR41-Gα_{i3} Cys³⁵¹Ile in the presence of the specified short chain fatty acid. Data represent mean±SEM from three individual experiments.

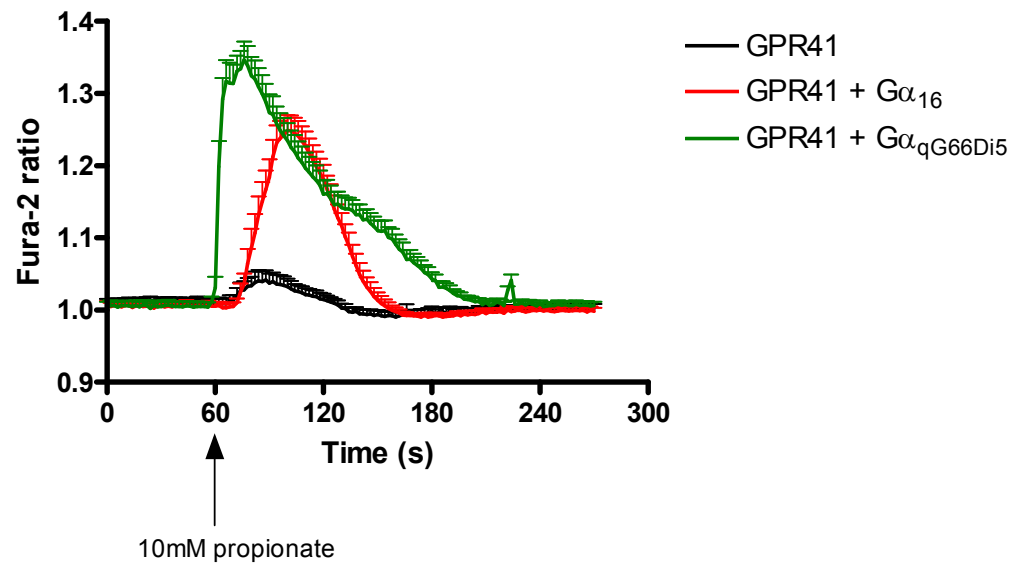


Figure 3.3 Co-transfection of GPR41 with either G α_{16} or a G α_q /G α_{i1} chimera (G $\alpha_{qG66Di5}$) allows the response to agonist to be observed by monitoring [Ca²⁺]_i.

HEK293T grown on coverslips were transfected to express GPR41-eYFP (black line), GPR41-eYFP and G α_{16} (red line), or GPR41-eYFP and G $\alpha_{qG66Di5}$ (green line). Cells were loaded with Fura-2. Images were collected every 2s and 10mM propionate was added at the 60s time point. Alterations in Fura-2 fluorescence was monitored for a further 240s. Data represent means \pm SEM from 20 positively transfected cells selected on the basis of eYFP fluorescence.

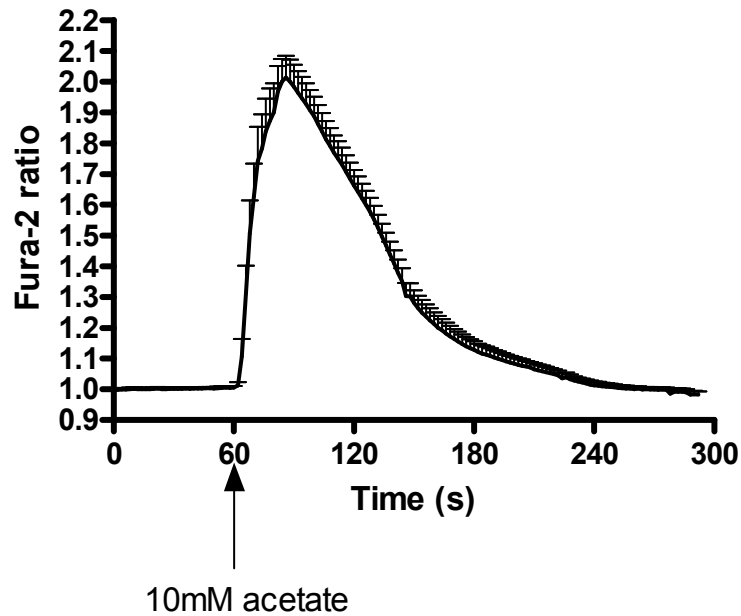


Figure 3.4 GPR43 can mediate mobilisation of $[Ca^{2+}]_i$ in $G\alpha_{q/11}$ knock out cells when co-transfected with $G\alpha_q$.

EF88 mouse embryonic fibroblasts lacking expression of both $G\alpha_q$ and $G\alpha_{11}$ were transiently transfected using the Amaxa nucleofection system to express both GPR43 and $G\alpha_q$. Cells were loaded with Fura-2. 10mM acetate was added at the 60s time point and alterations in Fura-2 fluorescence measured over the following 240s. Images were collected every 2s. Data shown represent means \pm SEM from 20 individual cells.

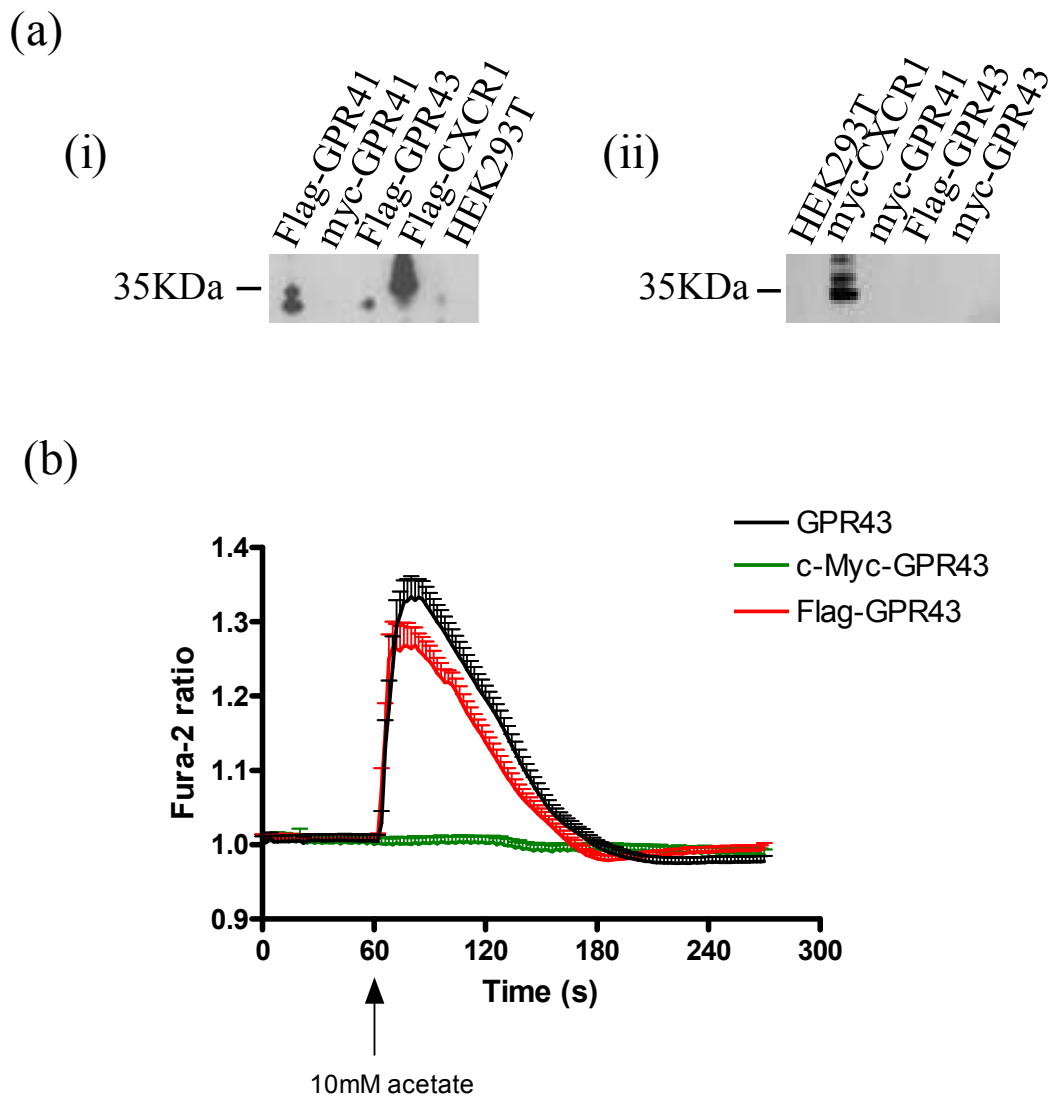


Figure 3.5 Detrimental effect of N-terminally tagging GPR43

(a) HEK293T cells were transiently transfected with cDNA encoding the required tagged receptor. Cells were harvested 24h after transfection and membranes prepared. 10 μ g of protein was loaded per well and resolved by SDS-PAGE and immunoblotted with (i) anti-Flag antibody and (ii) anti c-myc antibody. (b) HEK293T cells were grown on coverslips and transiently transfected with cDNA encoding GPR43 (black line), c-Myc-GPR43 (green line) or Flag-GPR43 (red line). After loading with the Ca²⁺ sensitive dye Fura-2, 10mM acetate was added at the 60s time point and alterations in [Ca²⁺]_i measured by monitoring changes in Fura-2 fluorescence over a further 240s. Data shown represent means \pm SEM from 20 individual cells.

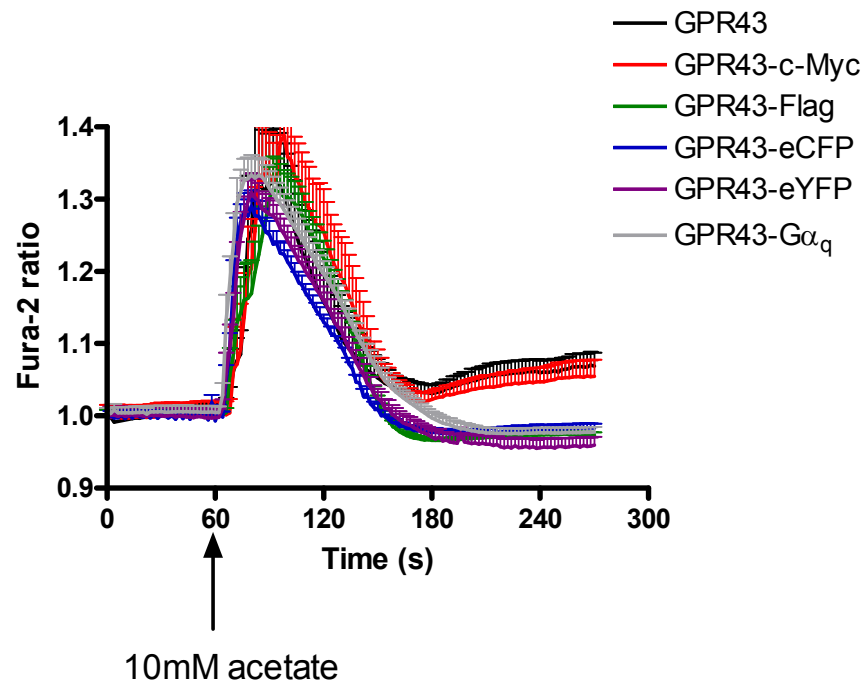


Figure 3.6 A variety of C-terminal tags do not affect the ability of GPR43 to mediate a rise in $[Ca^{2+}]_i$ in response to acetate

HEK293T cells grown on coverslips were transfected with GPR43 (black line), GPR43-c-Myc (red line), GPR43-Flag (green line), GPR43-eCFP (blue line), GPR43-eYFP (purple line) or GPR43-G α_q (grey line). Cells were loaded with Fura-2 and 10mM acetate added after 60s of basal readings. Alterations in Fura-2 fluorescence were monitored for a further 240s. Images were collected every 2s. Data shown represent means \pm SEM from at least 15 individual cells.

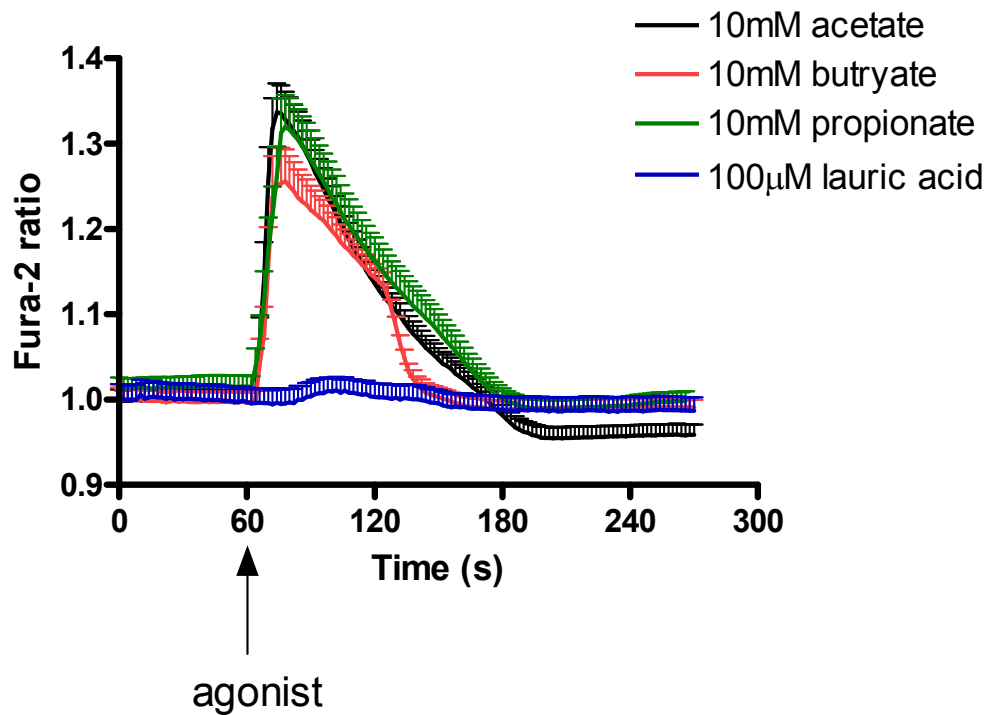


Figure 3.7 Stimulation of GPR43 specifically with various short chain fatty acids causes a transient rise in $[Ca^{2+}]_i$ in HEK293T cells

HEK293T cells were transiently transfected to express GPR43-eCFP. Cells were loaded with Fura-2. Cells were exposed to 10mM acetate (black line), 10mM butyrate (red line), 10mM propionate (green line) or 100µM lauric acid (blue line) at the 60s time point. Alterations in Fura-2 ratio were monitored over a further 240s. Images were collected every 2s. Data represent means \pm SEM from 20 positively transfected cells selected on the basis of eCFP fluorescence.

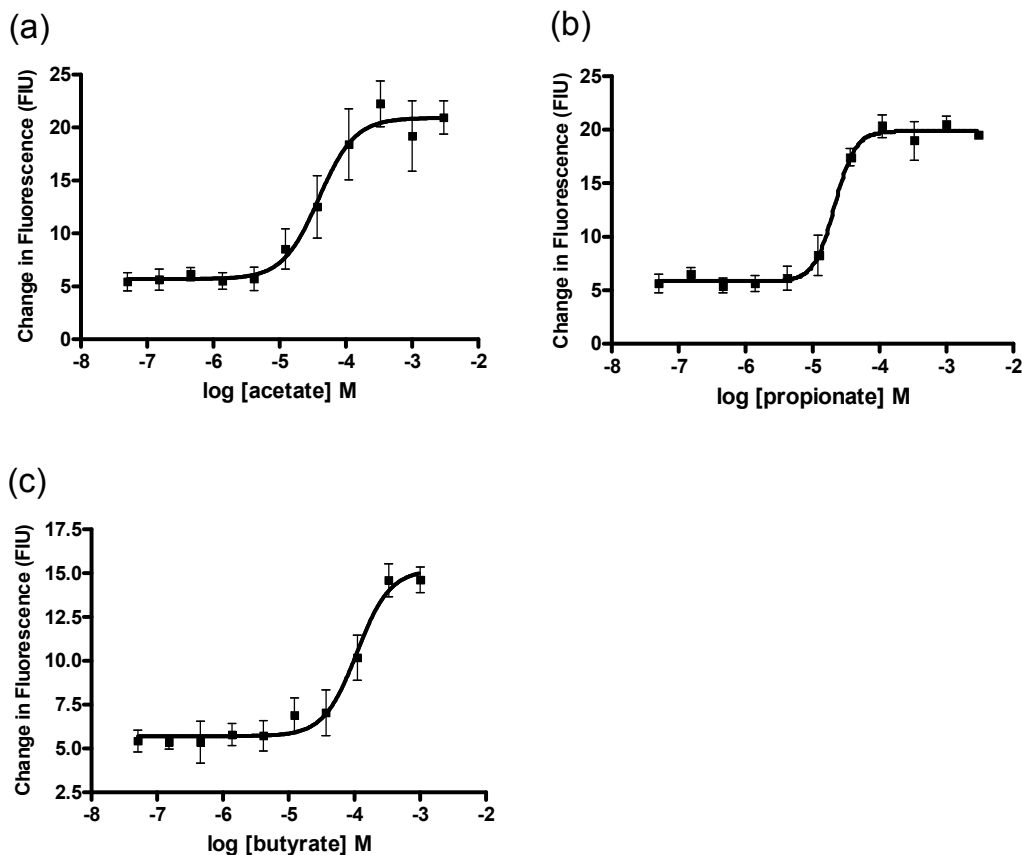


Figure 3.8 Short chain fatty acids can activate GPR43 in a concentration-dependent manner in a FLIPR based $[Ca^{2+}]_i$ mobilization assay

HEK293 MSRII cells were transiently transfected to express GPR43-eYFP and a G protein cocktail consisting of $G\alpha_{q05}$, $G\alpha_{qi5}$, $G\alpha_{qz5}$, $G\alpha_{qs5}$, $G\alpha_{15}$ and $G\alpha_{16}$. 24h post transfection cells were seeded at 15,000 cells per well into 384 well microtitre plates. Changes in $[Ca^{2+}]_i$ levels were measured using the FLIPR apparatus following challenge with increasing concentrations of (a) acetate, (b) propionate or (c) butyrate added at the 10s time point and data collected for a further 110s. Graph shown are representative of data obtained from three individual experiments performed in duplicate. Data points represent means \pm SEM.

SCFA	pEC ₅₀
Formate (C ₁)	2.8±1.0
Acetate (C ₂)	4.6±0.2
Propionate (C ₃)	4.9±0.2
Butyrate (C ₄)	4.4±0.5

Table 3.2 Potency of various short chain fatty acids at GPR43 measured by a FLIPR based [Ca²⁺]_i mobilization assay

HEK293 MSRII cells were transiently transfected to express GPR43-eYFP. 24h post transfection, cells were seeded at 15,000 cells per well into 384 well microtitre plates. Changes in [Ca²⁺]_i levels were measured using the FLIPR apparatus following challenge with test ligands added at the 10s time point and data collected for a further 110s. Data represent mean±SEM of three individual experiments.

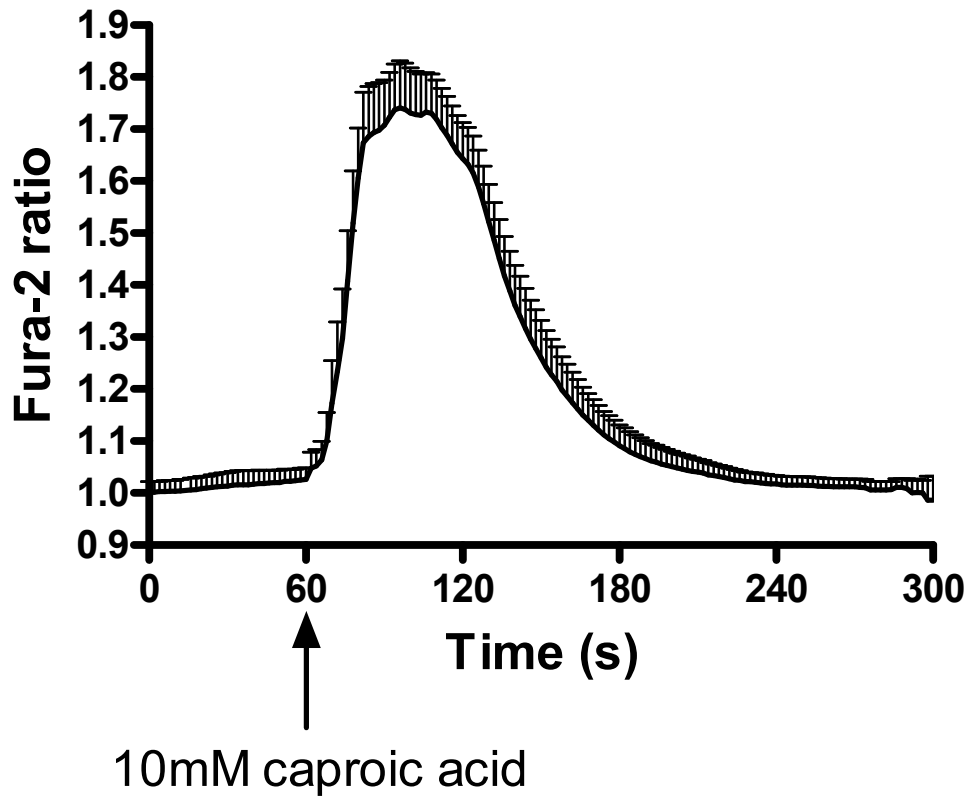


Figure 3.9 GPR40 can mediate mobilisation of $[Ca^{2+}]_i$ in response to caproic acid in $G\alpha_{q/11}$ knock out cells when co-transfected with $G\alpha_q$

EF88 mouse embryo fibroblasts lacking expression of both $G\alpha_q$ and $G\alpha_{11}$ were transiently transfected using the Amaxa nucleofection system to express both GPR40 and $G\alpha_q$.

Following loading with Fura-2, 10mM caproic acid was added at the 60s time point and the alteration in Fura-2 fluorescence monitored over the following 240s. Images were collected every 2s. Data represent means \pm SEM. from 15 individual cells.

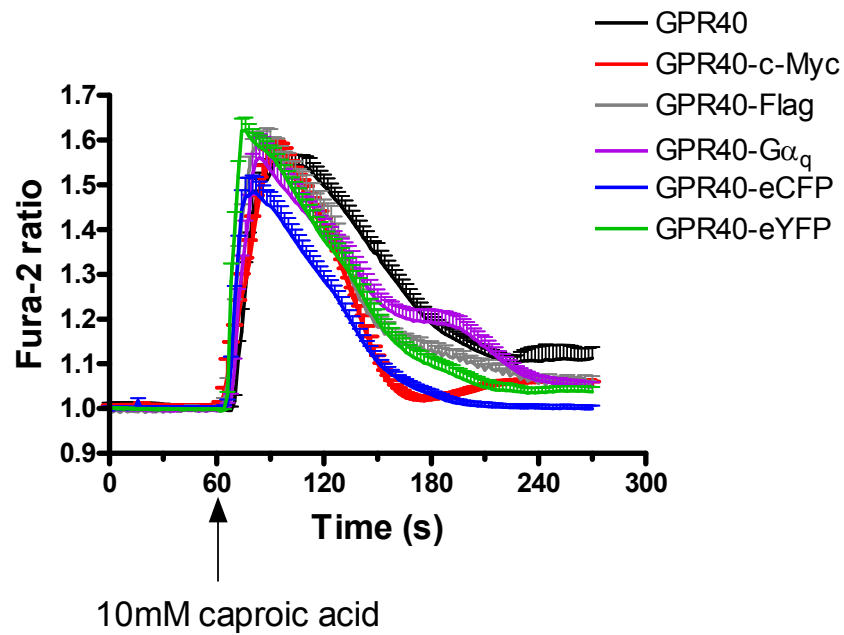


Figure 3.10 A variety of C-terminal modifications do not affect the ability of GPR40 to mediate a rise of $[Ca^{2+}]_i$ in response to caproic acid

HEK293T cells were transfected to transiently express GPR40 (black), GPR40-c-myc (red), GPR40-Flag (grey), GPR40-Gα_q (purple), GPR40-eCFP (blue) or GPR40-eYFP (green). Following loading of the cells with Fura-2, cells were exposed to 10mM caproic acid at the 60s time point. Changes in Fura-2 fluorescence were monitored over a further 240s. Images were collected every 2s. Data shown represent means±SEM from at least 20 individual cells.

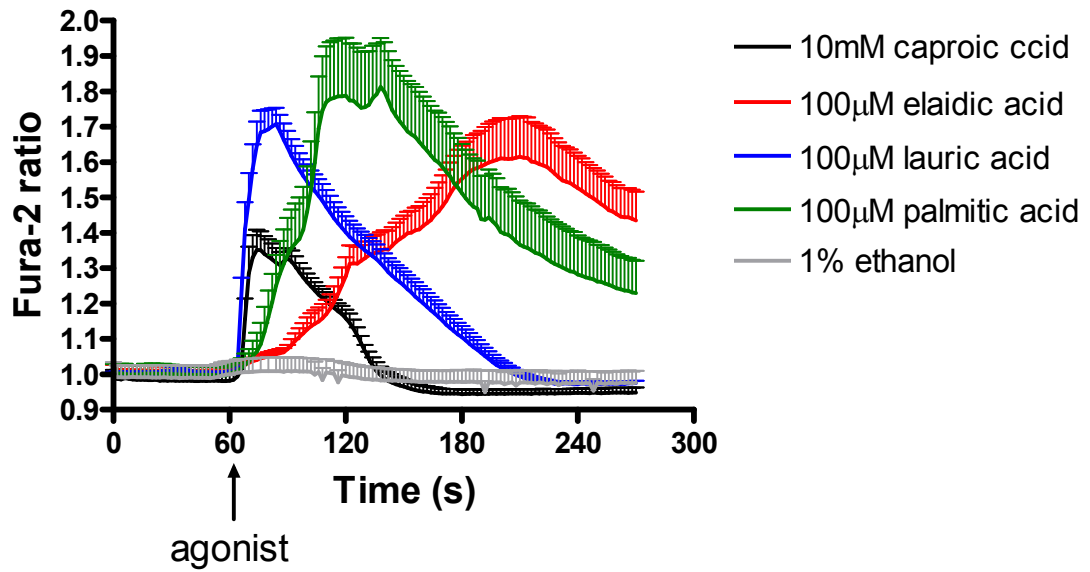


Figure 3.11 GPR40-eCFP responds to different fatty acids but kinetics of Ca^{2+} mobilisation depends on the identity of the fatty acid used

GPR40-eCFP was transiently transfected into HEK293T cells. Cells were loaded with Fura-2 and were exposed to 100µM lauric acid (blue), 100µM palmitic acid (green), 100µM elaidic acid (red), 10mM caproic acid (black) or 1% ethanol (grey) at the 60 sec time point and the alteration in Fura-2 fluorescence monitored over time. Images were collected every 2s. Data shown represent means±SEM from at least 20 individual positively transfected cells selected on the basis of eCFP fluorescence.

Fatty Acid	pEC50
Caproic Acid (C6:0)	4.0±0.1
Caprylic Acid (C8:0)	4.3±0.3
Capric Acid (C10:0)	5.5±0.6
Lauric Acid (C12:0)	5.3±0.4
Myristic Acid (C14:0)	5.4±0.5
Palmitic Acid (C16:0)	5.5±0.8
Stearic Acid (C18:0)	4.9±0.7
Palmitoleic Acid (C16:1)	5.3±0.3
Linolenic Acid (C18:3)	5.6±0.3
γ -Linolenic Acid (C18:3)	5.5±0.2
Linoleic Acid (C18:2)	5.6±0.2
Elaidic Acid (C18:1)	5.2±0.2
Retinoic Acid (C20:1)	5.3±0.4
Arachidonic Acid (C20:4)	5.4±0.3
Docosapentaenoic Acid (C22:5)	5.3±0.2

Table 3.3 Potency of various fatty acids at GPR40 measured by a FLIPR-based $[Ca^{2+}]_i$ mobilisation assay

HEK293 MSRII cells were transiently transfected to express GPR40-eYFP. 24h post transfection, cells were seeded at 15,000 cells per well into 384 well microtitre plates. Changes in $[Ca^{2+}]_i$ levels were measured using the FLIPR apparatus following challenge with the test ligands added at the 10s time point and data collected for a further 110s. Data represent mean±SEM of three individual experiments.

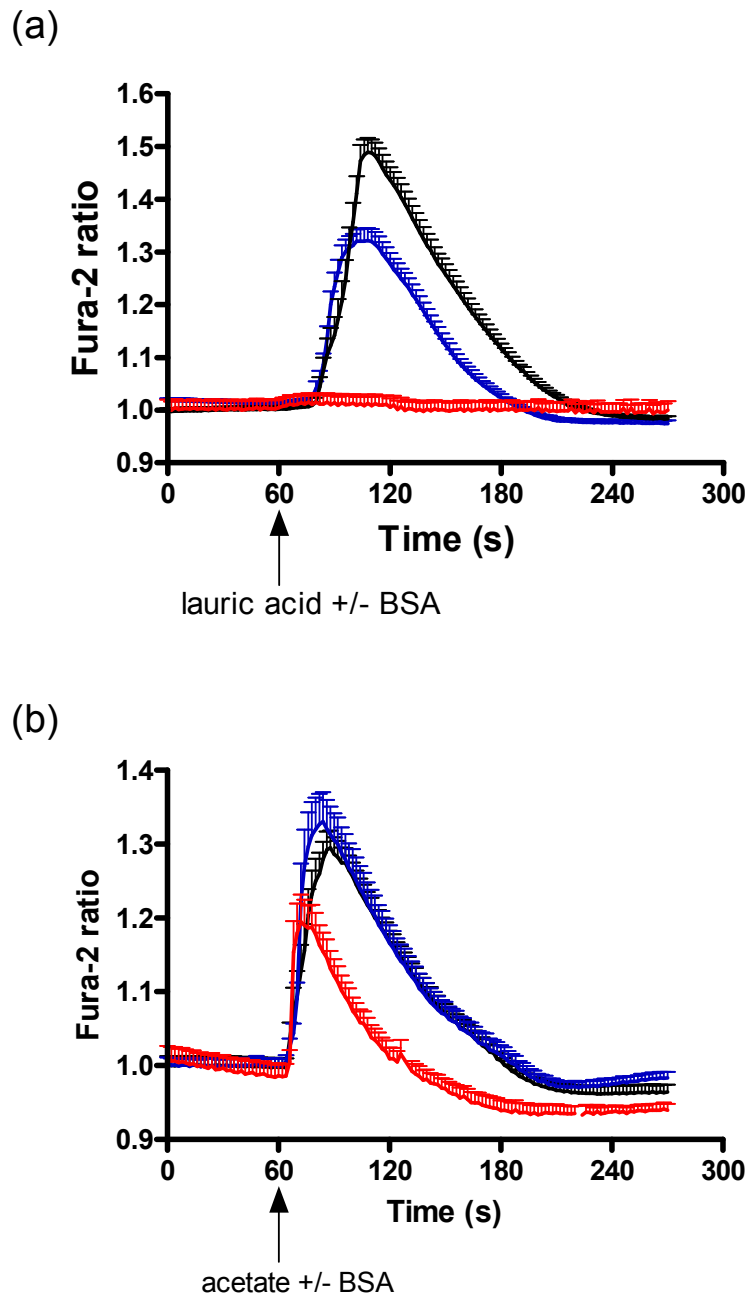


Figure 3.12 Increasing concentrations of fatty acid free BSA reduces the magnitude of $[Ca^{2+}]_i$ release generated by GPR40 and GPR43 in response to fatty acids

HEK293T cells were transfected to transiently express (a) GPR40-eCFP or (b) GPR43-eCFP. Cells were loaded with Fura-2. At the 60s time point cells were exposed to (a) 100 μ M lauric acid or (b) 10mM acetate in the absence (black line) or presence of 0.1% fatty acid free BSA (blue line) or 0.5% fatty acid free BSA (red line) and changes in Fura-2 fluorescence monitored for a further 240s. Images were collected every 2s. Data represent means \pm SEM from at least 20 positively transfected cells selected on the basis of eCFP fluorescence.

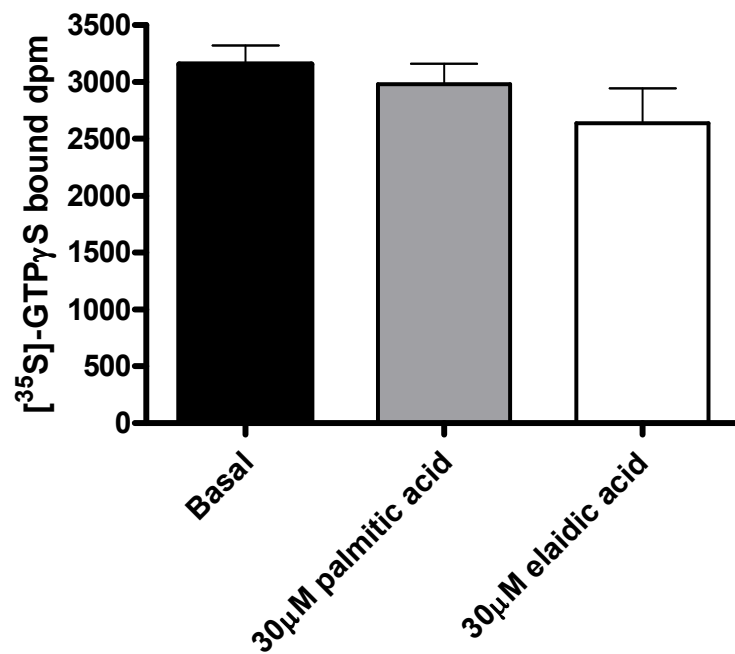


Figure 3.13 GPR40 appears to display high constitutive activity in [³⁵S]GTPγS binding studies

HEK293 cells were transfected to express GPR40-Gα_q and membranes prepared.

[³⁵S]GTPγS binding studies were performed. Assay samples were immunoprecipitated with the Gα_{q/11} antiserum, CQ. Basal (black bar) [³⁵S]GTPγS binding in Gα_{q/11}

immunoprecipitates was determined and the effect of 30μM palmitic acid (grey bar) and

30μM elaidic acid (white bar) assessed. Graph shown is representative of three individual experiments and data points represent means±SEM.

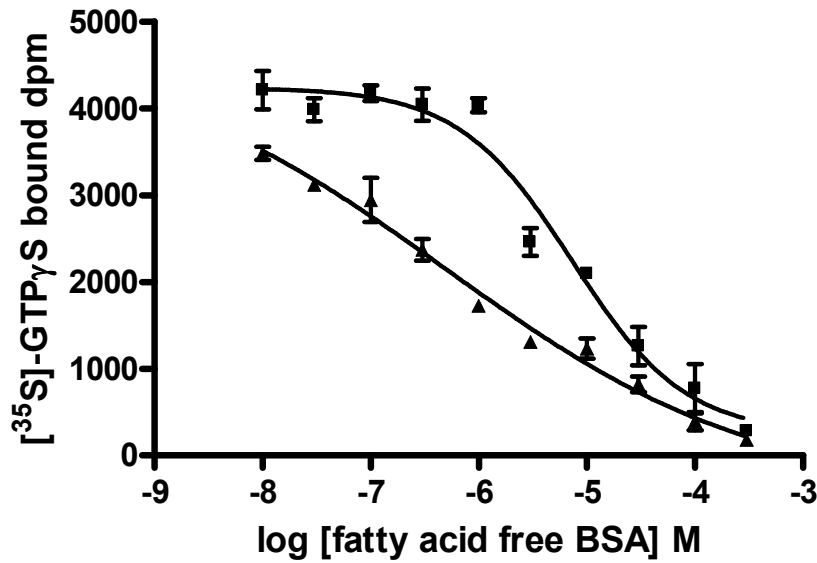


Figure 3.14 Increasing concentrations of fatty acid free BSA reduces the ‘basal’ [³⁵S]GTP_γS binding of GPR40-G_{αq}

HEK293T cells were transfected to transiently express GPR40-G_{αq} and membranes prepared. [³⁵S]GTP_γS binding studies were performed with the addition of varying concentrations of fatty acid free BSA in the absence (triangles) or presence (squares) of 30 μM palmitic acid. At the end of assay GPR40-G_{αq} was recovered by immunoprecipitation with the anti G_{αq/11} antiserum CQ and bound [³⁵S]GTP_γS estimated using scintillation counting. Graph shown is representative of results obtained from three individual experiments performed in triplicate. Data points represent means±SEM.

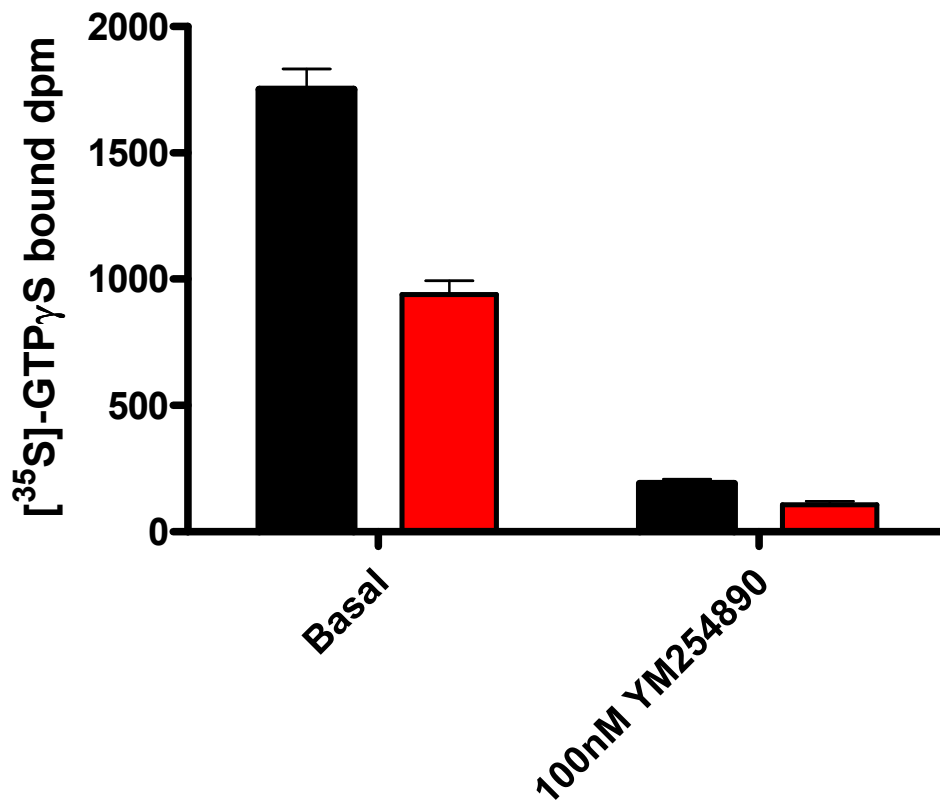


Figure 3.15 The $G\alpha_{q/11}$ specific inhibitor YM254890 reduces the basal [³⁵S]GTP γ S loading of GPR40- $G\alpha_q$

HEK293T cells were transiently transfected with GPR40- $G\alpha_q$ and membranes prepared. [³⁵S]GTP γ S binding studies were performed in the absence (black bar) or presence (red bar) of 10 μ M fatty acid free BSA. The effect of the $G\alpha_{q/11}$ inhibitor YM254890 (100nM) was assessed. All assay samples were immunoprecipitated with the $G\alpha_{q/11}$ antiserum CQ before scintillation counting. Data shown are representative of results obtained for three individual experiments performed in triplicate. Data points represent means \pm SEM.

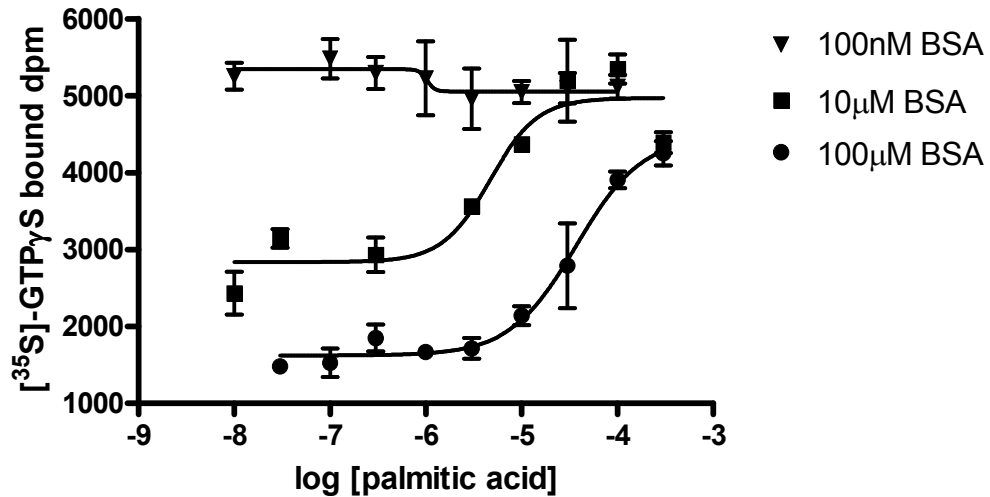


Figure 3.16 Varying concentrations of fatty acid free BSA alter the potency of palmitic acid at GPR40-Gα_q

HEK293T cells were transiently transfected to express GPR40-Gα_q and membranes were prepared. [³⁵S]GTPγS binding studies were performed in the presence of varying concentrations of palmitic acid and differing concentrations of fatty acid free BSA, 100nM (triangles), 10μM (squares) or 100μM (circles). All assay samples were immunoprecipitated with the Gα_{q/11} antiserum CQ before scintillation counting. Graph shown is representative of three individual experiments. Data points represent means±SEM.

[Fatty acid free BSA] added	pEC ₅₀ (palmitic acid)
100nM	inactive
10μM	4.4±0.5
100μM	3.8±0.5

Table 3.4 Potency of palmitic acid in the presence of varying concentrations of fatty acid free BSA

[³⁵S]GTPγS binding studies were performed on membranes expressing GPR40-Gα_q in the presence of increasing concentrations of palmitic acid and 100nM, 10μM or 100μM fatty acid free BSA. Data represent means±SEM from three individual experiments.

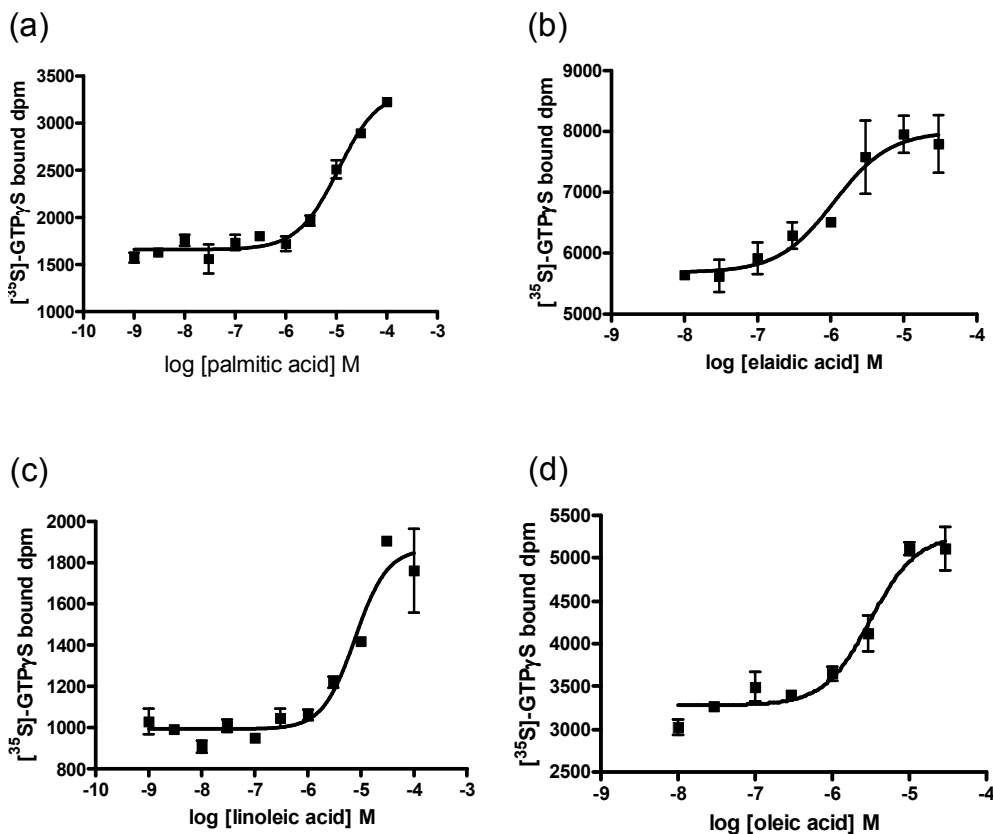


Figure 3.17 The addition of fatty acid free BSA allows the potency of fatty acids at GPR40-G α_q to be determined

Membranes were prepared from HEK293T cells transiently transfected to express GPR40-G α_q . $[^{35}\text{S}]\text{GTP}\gamma\text{S}$ binding studies were performed the presence of $10\mu\text{M}$ fatty acid free BSA and increasing concentrations of (a) palmitic acid, (b) elaidic acid, (c) linoleic acid or (d) oleic acid. Bound $[^{35}\text{S}]\text{GTP}\gamma\text{S}$ in G α_q immunoprecipitates was estimated by scintillation counting. The graphs shown are representative of three individual experiments performed in triplicate. Data points represent means \pm SEM.

Fatty Acid	pEC ₅₀
Palmitic Acid (C16:0)	4.94±0.13
Elaidic Acid (C18:1)	5.76±0.12
Linoleic Acid (C18:2)	5.41±0.10
Oleic Acid (C18:1)	5.24±0.26

Table 3.5 Potency of various fatty acids at GPR40-G α_q measured by a [³⁵S]GTP γ S binding assay in the presence of 10 μ M fatty acid free BSA

[³⁵S]GTP γ S binding studies were performed on HEK293T cell membranes expressing GPR40-G α_q in the presence of 10 μ M fatty acid free BSA and the specified fatty acid. Data represent means \pm SEM from three individual experiments

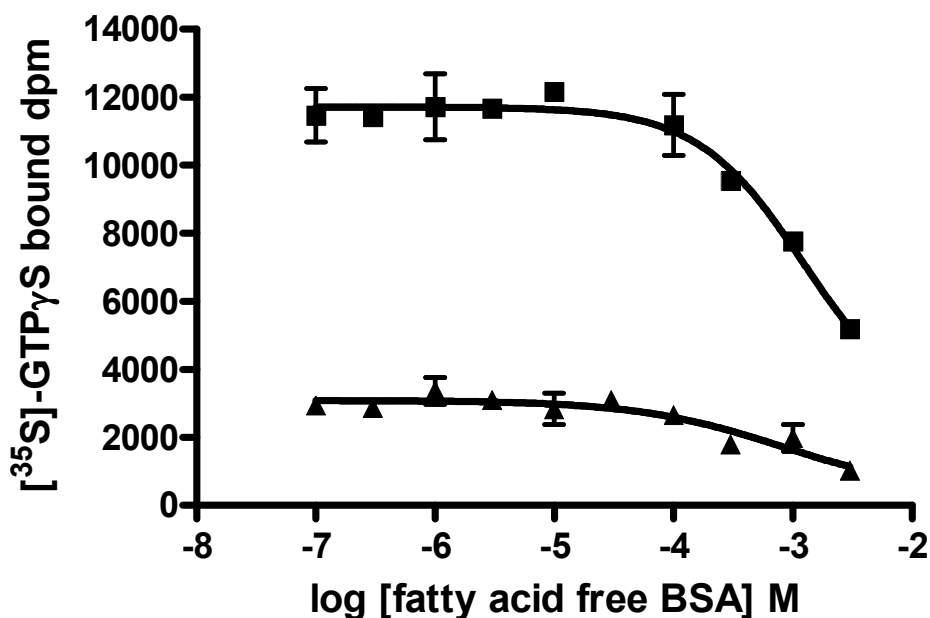


Figure 3.18 Fatty acid free BSA has no effect on the basal [³⁵S]GTPγS loading of GPR41-Gα_{i3} Cys³⁵¹Ile and only reduces stimulated levels at high concentrations

HEK293T cells were transfected to transiently express GPR41-Gα_{i3} Cys³⁵¹Ile and membranes prepared. [³⁵S]GTPγS binding studies were performed with the addition of varying concentrations of fatty acid free BSA in the absence (triangles) or presence (squares) of 10mM propionate. At the end of assay GPR41-Gα_{i3} Cys³⁵¹Ile was recovered by immunoprecipitation with the anti Gα_{i3} antiserum I3 and bound [³⁵S]GTPγS estimated using scintillation counting. Graph shown is representative of results obtained from three individual experiments performed in triplicate. Data points represent means±SEM.

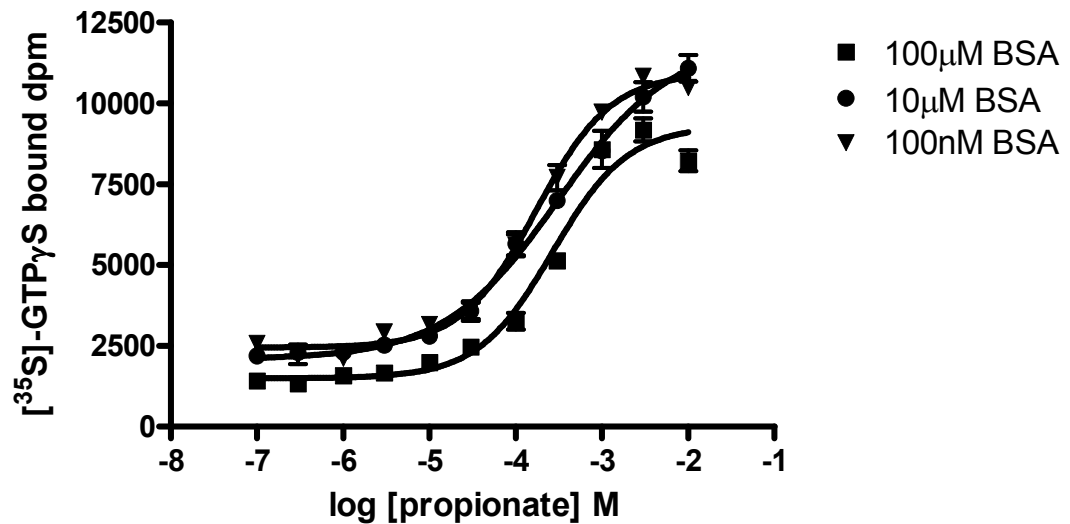


Figure 3.19 Varying concentrations of fatty acid free BSA have little effect on the potency of propionate at GPR41-G α _{i3} Cys⁶Ile

HEK293T cells were transiently transfected to express GPR41-G α _{i3} Cys³⁵¹Ile and membranes were prepared. [³⁵S]GTP γ S binding studies were performed in the presence of varying concentrations of propionate and differing concentrations of fatty acid free BSA, 100nM (triangles), 10 μ M (circles) or 100 μ M (squares). All assay samples were immunoprecipitated with the G α _{i3} antiserum I3 before scintillation counting. Graph shown is representative of results obtained from three individual experiments performed in triplicate. Data points represent means \pm SEM.

[Fatty acid free BSA] added	pEC ₅₀ (propionate)
100μM	3.37±0.11
10μM	3.74±0.08
100nM	3.79±0.10

Table 3.6 Potency of propionate at GPR41-Gα_{i3} Cys³⁵¹Ile in the presence of varying concentrations of fatty acid free BSA

[³⁵S]GTPγS binding studies were performed on membranes expressing GPR41-Gα_{i3} Cys³⁵¹Ile in the presence of increasing concentrations of propionate and 100nM, 10μM or 100μM fatty acid free BSA. Data represent mean±SEM of three individual experiments.

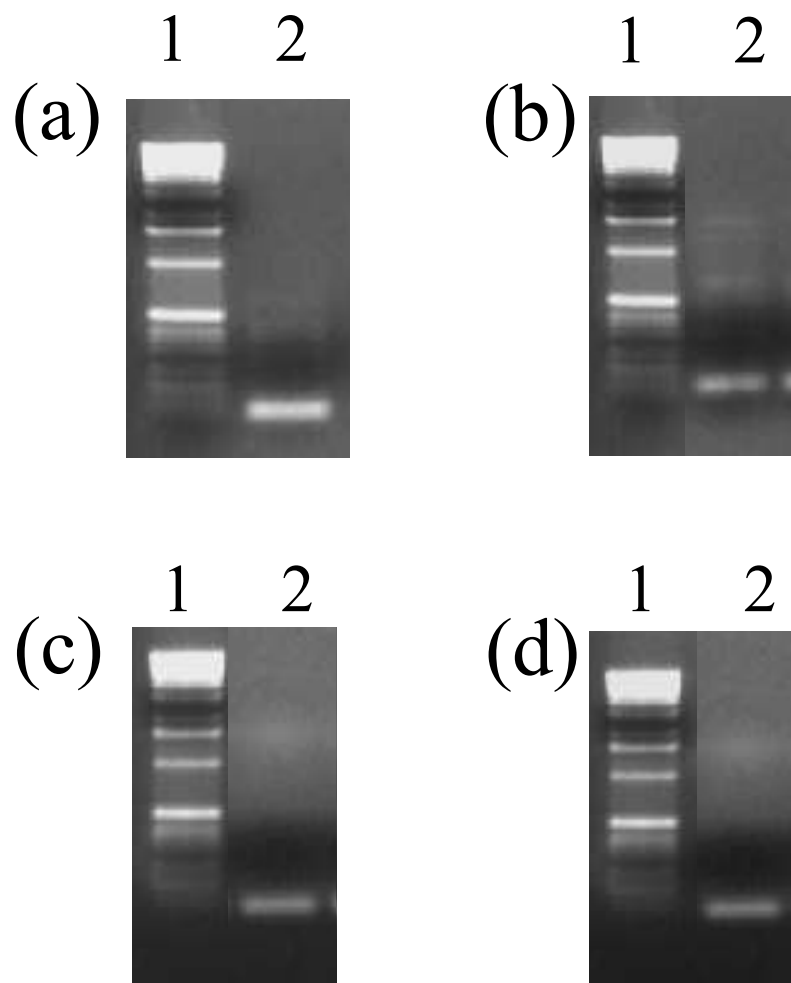


Figure 3.20 Expression of GPR40, GPR41 and GPR43 in INS-1E cells

mRNA was isolated from INS-1E cells using the Qiagen RNeasy Mini Kit. First strand cDNA was synthesised using the First Strand cDNA synthesis kit. Detection of (a) rGPR40, (b) rGPR41, (c) rGPR43 and (d) rCyclophilin specific mRNA transcripts was carried out by PCR and samples resolved on a 1% agarose gel. Lane 1, DNA markers, Lane 2, plus cDNA. In each case the expected size of the amplified fragment was 75 bp.

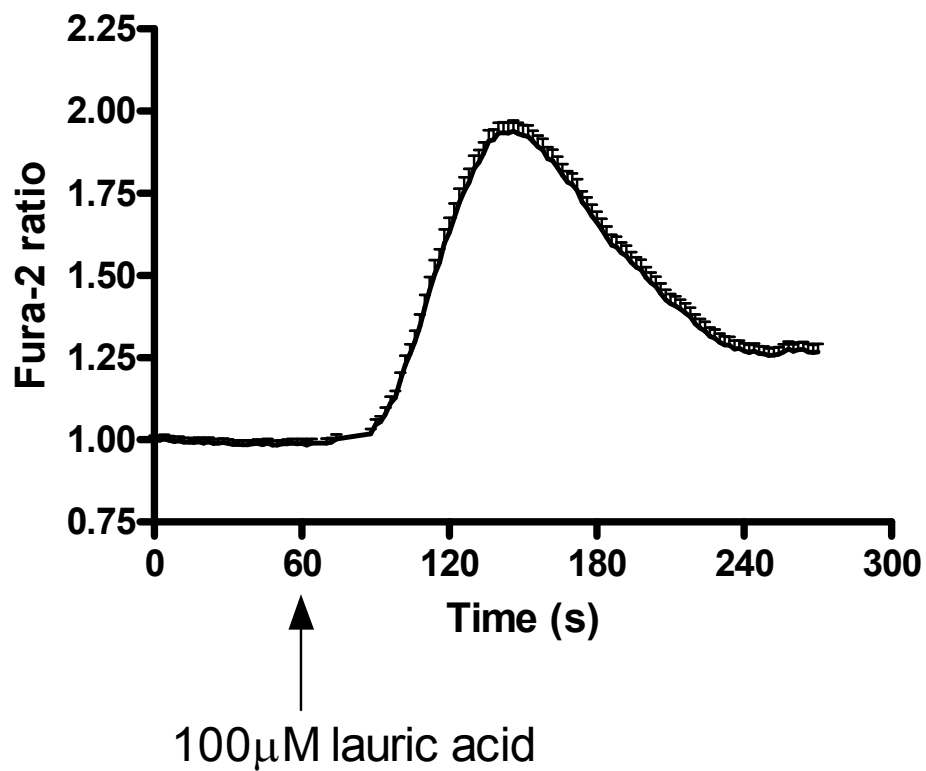


Figure 3.21 Elevation of $[Ca^{2+}]_i$ by lauric acid in INS-1E cells

INS-1E cells were grown on coated coverslips and loaded with Fura-2. Cells were exposed to 100µM lauric acid at the 60s time point and data collected for a further 240 sec. Images were collected every 2s. Data represents means±SEM from 50 cells.

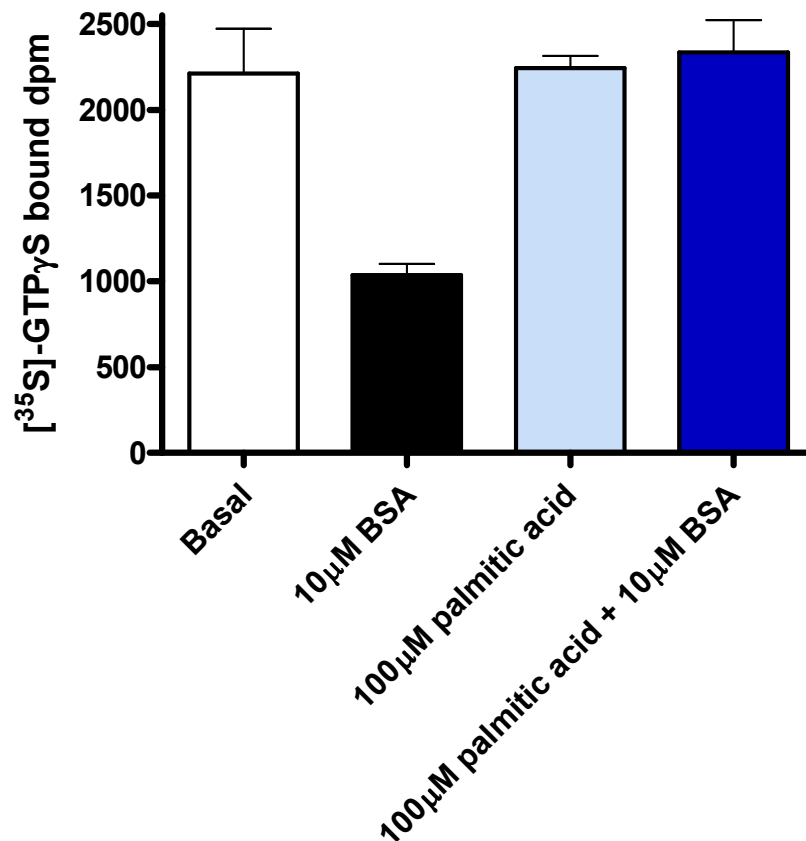


Figure 3.22 Endogenously expressed GPR40 also displays high levels of basal [³⁵S]GTP γ S

Membranes were prepared from INS-1E cells. Basal (white bar) levels of [³⁵S]GTP γ S binding in G $\alpha_{q/11}$ immunoprecipitates was determined and the effects of 10 μ M fatty acid free BSA (black bar), 100 μ M palmitic acid (light blue bar) and a combination of 10 μ M fatty acid free BSA and 100 μ M palmitic acid (dark blue bar) on levels of [³⁵S]GTP γ S binding were assessed. Graph shown is representative of three individual experiments performed in triplicate. Data points represent means \pm SEM.

4 Characterisation of GPR40 synthetic agonists and antagonist

4.1 Introduction

Of the three receptors within the GPR40 family, it is GPR40 that has attracted the most interest since fatty acids were shown to be the likely endogenous agonists for this family of receptors (Covington et al., 2006; Milligan et al., 2006). The expression profile of GPR40 has shown GPR40 mRNA to be present in high levels in the insulin secreting β -cells of the pancreas, both in a large range of pancreatic β -cell lines (Briscoe et al., 2003, Itoh et al., 2003, Itoh and Hinuma, 2006, Shapiro et al., 2005) as well as in human pancreatic tissue (Tomita et al., 2006). The chronic detrimental effects of fatty acids on pancreatic islets have been well documented and the role of GPR40 in this is still under debate. At present, GPR40 is a potential therapeutic target in the regulation of insulin secretion and diabetes.

Interestingly, a report by Kotarsky et al. (2003) identified that rosiglitazone, a compound that has antidiabetic effects, was able to act as an agonist at GPR40 in a reporter gene assay. Rosiglitazone belongs to a class of drugs termed thiazolidinediones that have been shown to reduce plasma glucose levels and improve insulin sensitivity in adipose tissue, liver and muscle (Lehmann et al., 1995). The thiazolidinediones are accepted as agonists at peroxisome proliferator activated receptor gamma (PPAR γ). There are three major isoforms of the PPAR family; α , β/δ and γ although most is known about PPAR γ due to its therapeutic potential for treatment of diabetes (Rangwala et al., 2004). There are four main thiazolidinediones, rosiglitazone, troglitazone, pioglitazone and ciglitazone, that have been employed clinically. Ciglitazone was the first thiazolidinedione identified but it was never marketed. Troglitazone was the first of the thiazolidinediones to be licensed for use but was withdrawn from all markets due to its association with acute liver failure (Graham et al., 2002). At present both rosiglitazone and pioglitazone are being used for the treatment of type 2 diabetes. There is also a growing body of evidence that indicates that there are PPAR γ -independent effects of thiazolidinediones (Feinstein et al., 2005). The interpretation of the observation that rosiglitazone is an agonist at GPR40 is hampered by the possible expression of PPAR γ in the pancreatic cell lines used (Kotarsky et al., 2003). They did not attempt to determine the structure-activity relationship of various thiazolidinediones at GPR40 and this is required to dissect out the role of GPR40 agonism by these compounds *in vivo*.

The interest in GPR40 as a therapeutic target has led to the synthesis of a number of small molecule agonists of GPR40 (Garrido et al., 2006). These have been shown to be more potent than any fatty acid at GPR40 in an assay based on the measurement of $[Ca^{2+}]_i$. One of these compounds, GW9508 (called GW839508 herein) was further characterised, along with a GPR40 specific antagonist, GW1100, in a follow up study (Briscoe et al., 2006). They showed that the agonist was able to potentiate glucose-stimulated insulin release in the pancreatic β cell line, MIN6 and that these effects could be reversed by the inclusion of the antagonist GW1100.

4.2 Agonist activity of thiazolidinediones at GPR40

To demonstrate that troglitazone has agonistic activity at human GPR40 as shown by Kotarsky et al (2003) for rat GPR40, HEK293T cells grown on coverslips were transiently transfected with GPR40-eYFP, challenged with 10 μ M troglitazone and the effect on $[Ca^{2+}]_i$ monitored (Figure 4.1a). Troglitazone caused a rapid and transient elevation of $[Ca^{2+}]_i$ only in cells positively transfected with GPR40-eYFP as monitored by eYFP fluorescence. To confirm that expression of GPR40 was required to allow elevation of $[Ca^{2+}]_i$ in response to troglitazone, Flp-In T-Rex-HEK293 cells with GPR40-eYFP located at the Flp-In locus were generated and employed as in this system GPR40-eYFP expression is controlled by the addition of doxycycline. In the absence of antibiotic treatment no auto-fluorescence corresponding to eYFP could be detected and when exposed to troglitazone no change in $[Ca^{2+}]_i$ was observed (Figure 4.1b(i)). By contrast, following doxycycline treatment (1 μ g/ml, 24 h) GPR40-eYFP was apparently present at the cell surface, and when challenged with troglitazone produced a robust and rapid elevation of $[Ca^{2+}]_i$ (Figure 4.1b(ii)) similar to that seen in transiently transfected cells.

The ability of troglitazone to mediate a rise in $[Ca^{2+}]_i$ in cells expressing GPR40 led to the question of whether other thiazolidinediones could also act as agonists at this receptor. In cells expressing GPR40-eYFP, rosiglitazone and pioglitazone were also able to mediate a rise in $[Ca^{2+}]_i$ only in positively transfected cells (Figure 4.2).

As mentioned previously, single cell $[Ca^{2+}]_i$ mobilization experiments are poorly suited to measure potency of agonists therefore to investigate the potency of the thiazolidinediones at human GPR40 [35 S]GTP γ S binding experiments had to be performed. In chapter 3, it was shown that an increase in [35 S]GTP γ S binding in response to a fatty acid agonist could only be observed in the presence of 10 μ M fatty acid free BSA and Figure 4.3a shows that

this is also true for troglitazone. The basal loading of [³⁵S]GTPγS onto GPR40-Gα_q was high and with the addition of 10μM troglitazone, which is able to elicit a large increase in [Ca²⁺]_i, the levels of [³⁵S]GTPγS binding were similar to those observed in basal conditions. The basal loading of GPR40-Gα_q was reduced by the addition of 10μM fatty acid free BSA and when 10μM troglitazone was also included there was an increase in [³⁵S]GTPγS binding. To determine the potency of four thiazolidinediones, troglitazone, rosiglitazone, ciglitazone and pioglitazone, their ability to increase [³⁵S]GTPγS binding in a concentration dependent manner was assessed (Figure 4.3b(i-iv)). Each of these thiazolidindiones was able to increase [³⁵S]GTPγS binding, although ciglitazone and pioglitazone did not give sigmoidal concentration response curves with Hill slopes approaching a value of 1 (Table 4.1). The potency of these compounds varied, with the rank order of potency being troglitazone >rosiglitazone=pioglitazone>ciglitazone (Table 4.1). In order to confirm the potencies seen in the [³⁵S]GTPγS binding experiments, HEK293 MSRII cells were transiently transfected with GPR40-eYFP and loaded with the calcium sensitive dye Fluo-4 and changes in Fluo-4 fluorescence measured using the FLIPR, which corresponds to a change in [Ca²⁺]_i. Using this method both troglitazone and rosiglitazone were able to produce a measurable signal and the observed potencies are shown in Table 4.2. Again, troglitazone was shown to be more potent at GPR40-eYFP than rosiglitazone. Neither ciglitazone nor pioglitazone produced a change in [Ca²⁺]_i and were consequently concluded to be inactive at GPR40-eYFP using this technique. In addition, control cells transiently transfected with GPR43-eYFP or the neuromedin U receptor (NMU-R) showed no change in [Ca²⁺]_i in response to any of the thiazolidinediones.

4.3 Potency of small molecule agonists of GPR40

A variety of synthetic small molecule agonists of GPR40 have recently been described. I was able to test five (a-e in Figure 1.3) of these compounds in a [Ca²⁺]_i based FLIPR assay and six (a-f in Figure 1.3) in [³⁵S]GTPγS binding experiments. I was unable to test GSK248257A in the FLIPR based assay due to problems in obtaining the compound. In order to determine the ability of these compounds to mediate a rise in [Ca²⁺]_i in a concentration dependent manner HEK293 MSRII cells were transiently transfected with GPR40-eYFP, loaded with Fluo-4 and the changes in [Ca²⁺]_i in response to test compound were measured using the FLIPR. With this assay method three of the five compounds; GW839508X, GSK250089A and GSK223112A, were able to generate robust, transient rises in [Ca²⁺]_i in cells transfected with GPR40-eYFP and relative potencies could be

ascribed (Table 4.3). GW839508X was shown to be the most potent, followed by GSK250089A and then GSK223112A. Neither GSK272235A nor GSK269778A were able to mediate a rise in $[Ca^{2+}]_i$ in cells transfected with GPR40-YFP and were therefore deemed inactive using this method. In addition, control cells transiently transfected with GPR43-eYFP or NMU-R showed no change in $[Ca^{2+}]_i$ in response to any of these compounds. To confirm these observed potencies $[^{35}S]GTP\gamma S$ binding experiments were performed on membranes prepared from cells transiently transfected to express GPR40-G α_q . As with fatty acids and thiazolidinediones, GSK250089A only showed agonistic effects in the presence of fatty acid free BSA (Figure 4.4). Of the six compounds tested in the $[^{35}S]GTP\gamma S$ binding experiments, GW839508X, GSK258257A and GSK250089A were able to produce sigmoidal concentration response curves that reached saturation (Figure 4.5 a-c). Two further compounds, GSK223112A and GSK269778A (Figure 4.5 d-e), showed some agonist activity by increasing $[^{35}S]GTP\gamma S$ binding at the highest concentrations tested (10 μ M). The assays were never performed at higher concentrations to determine if saturation could be reached. As in the FLIPR assay, GSK272235A was unable to increase $[^{35}S]GTP\gamma S$ binding at any concentrations and therefore was inactive at GPR40-G α_q (Figure 4.5f). The rank order of potency differed from that obtained in the FLIPR assay, with GSK250089A being the most potent giving a pEC₅₀ of 8.5 \pm 0.02, followed by GSK248257A, then GW839508X, GSK269778A and finally GSK223112A (Table 4.4).

4.4 Characterisation of GW1100 as an antagonist at GPR40

GW1100 has recently been described as an antagonist at GPR40 (Briscoe et al., 2006) mainly using $[Ca^{2+}]_i$ mobilization based assays. As I have developed a robust $[^{35}S]GTP\gamma S$ binding assay it provided an ideal way to further characterise GW1100 as an antagonist of GPR40. Firstly, HEK293T membranes expressing GPR40-G α_q were exposed to 10 μ M GW1100 and the effect on basal loading of $[^{35}S]GTP\gamma S$ in the presence or absence of fatty acid free BSA determined (Figure 4.6). GW1100 reduced the basal binding of $[^{35}S]GTP\gamma S$ at GPR40-G α_q in the absence of fatty acid free BSA. The combination of 10 μ M GW1100 and 10 μ M fatty acid free BSA had an additive effect and reduced $[^{35}S]GTP\gamma S$ binding to minimal levels. As shown earlier, the agonist effect of GSK250089A could only be seen in the presence of fatty acid free BSA but this agonist effect could be reduced by the addition of 10 μ M GW1100, both in the absence and presence of fatty acid free BSA. This

also showed that GSK250089A can increase the low levels [35 S]GTP γ S bound in the presence of GW1100 and fatty acid free BSA, potentially indicative of the competitive nature of these ligands.

HEK293T membranes expressing GPR40-G α_q were used to investigate the ability of GW1100 to reduce the basal [35 S]GTP γ S binding of GPR40-G α_q in a concentration dependent manner. In the absence of fatty acid free BSA, the curves did not level off and concentrations higher than shown were not tested (Figure 4.7). In the presence of 10 μ M fatty acid free BSA, the maximum decrease in [35 S]GTP γ S binding was observed at 10 μ M GW1100 and higher concentrations did not result in a further decrease of [35 S]GTP γ S binding. Even in the presence of 10 μ M fatty acid free BSA, [35 S]GTP γ S binding was substantially reduced by GW1100 in a concentration-dependent manner. This suggest that GW1100 is either an inverse agonist at GPR40 or that GW1100 is able to compete with remaining endogenous agonist not removed by treatment with fatty acid free BSA.

As shown above, agonist activity of GSK250089A could only be detected in the presence of fatty acid free BSA. However, in the absence of BSA, the agonist activity of GSK250089A could also be detected when 10 μ M GW1100 was also present (Figure 4.6). Figure 4.8 demonstrates that this effect was concentration dependent. When GSK250089A was added to membranes expressing GPR40-G α_q in increasing concentrations in the absence of GW1100 no increase in [35 S]GTP γ S binding was observed but an increase in [35 S]GTP γ S binding, and consequently a concentration response curve, could be observed when 10 μ M GW1100 was added (Figure 4.8). Interestingly, even very high concentrations of GSK250089A were unable to stimulate [35 S]GTP γ S binding to the levels observed in the absence of GW1100. The apparent pEC50 of GSK250089A when 10 μ M GW1100 was present was 7.1 \pm 0.2. In a similar fashion, the presence of either fatty acid free BSA or GW1100 allowed 1 μ M troglitazone to elevate [35 S]GTP γ S binding to GPR40-G α_q (Figure 4.9a). GW1100 was able to inhibit the rise in [35 S]GTP γ binding mediated by 1 μ M troglitazone in a concentration-dependent fashion and at 10 μ M appeared to be the concentration where maximum reduction was observed (Figure 4.9b).

4.5 Ability of synthetic agonists to activate endogenously expressed GPR40

As shown in Chapter 3, GPR40 is endogenously expressed in the rat β cell line, INS-1E and shows the same high levels of basal [35 S]GTP γ S binding as transfected human GPR40. To assess whether the effects of troglitazone and GSK250089A could be reproduced in these cells, the effects of these compounds were first evaluated by investigating their ability to mediate a rise in [Ca^{2+}] $_i$ in this cell line. INS-1E cells were grown on coated coverslips and their response to 10 μ M troglitazone or 1 μ M GSK250089A measured by the change in Fura-2 ratio (Figure 10a). Troglitazone was able to induce a transient, large rise in [Ca^{2+}] $_i$. GSK250089A was unable to mediate a rise in [Ca^{2+}] $_i$. To confirm the observations seen in the [Ca^{2+}] $_i$ mobilization assay, cell membranes prepared from INS-1E cells were used in [35 S]GTP γ S binding assays. As observed in Chapter 3, in basal conditions a high level of [35 S]GTP γ S was bound and this could be reduced by the addition of 10 μ M fatty acid free BSA (Figure 10b). There was no increase in [35 S]GTP γ S binding upon the addition of saturating concentration of troglitazone (1 μ M) or GSK250089A (100nM) in the absence of fatty acid free BSA. The combination of 1 μ M troglitazone and 10 μ M fatty acid free BSA resulted in an increase of [35 S]GTP γ S binding compared to that with the BSA alone. Whereas the combination of 100nM GSK230089A and 10 μ M fatty acid free BSA gave [35 S]GTP γ S binding levels similar to BSA alone.

4.6 Discussion

The interest in GPR40 as a potential therapeutic target for the treatment of type 2 diabetes demands full understanding of the pharmacology and activation of the receptor. The endogenous fatty acid ligands for the receptor display relatively low potency which hampers their use as pharmacological tools. The recent description of small molecule agonists of GPR40 which are significantly more potent than any of the fatty acids (Garrido et al., 2006) and the observation that rosiglitazone appeared to display agonist activity at rat GPR40 (Kotarsky et al., 2003) provided tools to uncover some of the pharmacology of this receptor which cannot easily be investigated using fatty acids.

To date, only Kotarsky et al., (2003) have shown that rosiglitazone is able to act as an agonist at GPR40. This was confirmed for human GPR40 in two [Ca^{2+}] $_i$ mobilization based assays (Figure 4.2 and Table 4.2) and in the [35 S]GTP γ S binding assay (Figure 4.3).

In addition to rosiglitazone, three further members of the thiazolidinedione family (troglitazone, ciglitazone and pioglitazone) were tested. Troglitazone was shown to be the most potent of the thiazolidinediones tested here with a pEC_{50} of 6.5 ± 0.1 measured in a [^{35}S]GTP γ S binding assay and 5.9 ± 0.1 measured by the FLIPR-based Ca^{2+} release assay. Taking the [^{35}S]GTP γ S binding and Ca^{2+} mobilization data together, the rank order of potency of these compounds at GPR40 is troglitazone > rosiglitazone > pioglitazone > ciglitazone. The observation that the thiazolidinediones are able to act as agonists at GPR40 with varying degrees of potency according to their structure poses interesting questions as to possible contributions of GPR40 to their *in vivo* actions rather than PPAR γ . Interpretation of the results from Kotasky et al., (2003) is hampered by the accompanying PPAR activity of the tool compounds. By using an inducible cell line I demonstrated that only in the presence of GPR40-eYFP could troglitazone mediate a rise in $[Ca^{2+}]_i$ (Figure 4.1). This confirmed that the rise in $[Ca^{2+}]_i$ in response to troglitazone must be mediated by GPR40.

The thiazolidinediones were first described as agonists for PPAR γ by Lehmann et al., (1995) and since then much work has been undertaken to understand the mode of action of these compounds. Activated PPAR γ binds and activates peroxisome proliferator responsive elements (PPREs) in the promoter region of target genes and increases gene transcription. Genes with PPREs include those in glucose and lipid metabolism pathways, which reduce adipocyte lipolysis, reduce plasma free fatty acids and improve insulin-stimulated glucose disposal (Kliwer et al., 1992). Although much of the research into thiazolidindiones has focused on their insulin-sensitizing properties (Rangwala et al., 2004), they have also been shown to have anti-inflammatory properties (Genolet et al., 2004; Youssef et al., 2004) and display antiproliferative activity against a variety of cancer cell lines (Grommes et al., 2004; Theocharis et al., 2004; Rume et al., 2004). Although there is good correlation between the EC_{50} of various thiazolidinediones at PPAR γ and the *in vivo* minimum effective antihyperglycemic dose (Willson et al., 1996) developments in the field have uncovered a series of rapid, apparently PPAR γ independent effects, of these compounds (Feinstein et al., 2005; Gardner et al., 2005). The activation of GPR40 by various thiazolidinediones may help to explain some of these effects. Palakurthi et al., (2001) showed that troglitazone and ciglitazone were able to mediate a rise in $[Ca^{2+}]_i$ in both PPAR $\gamma^{+/+}$ and PPAR $\gamma^{-/-}$ mouse embryonic stem cells. The kinetic of this $[Ca^{2+}]_i$ release was similar to that observed in GPR40-eYFP transfected HEK293T cells (Figure 4.1a) and in INS-1E cells endogenously expressing GPR40 (Figure 4.10b).

There are marked differences in the potency of the thiazolidinediones at GPR40 and PPAR γ and these are shown in Table 4.5. It has been noted that the anti-inflammatory effects of thiazolidinediones are often observed at concentrations much higher than their EC₅₀ values for binding to (Willson et al., 1996) or activating PPAR γ (Pershadsingh et al., 2004). In activated macrophage, 30 μ M troglitazone has been shown to inhibit induction of the inducible form of nitric oxide synthase (Ricote et al., 1998), which is significantly higher than the EC₅₀ at PPAR γ . The concentrations of troglitazone required to reduce cytokine release from activated human monocytes was 100 μ M (Jiang et al., 1998) which is again significantly higher than the EC₅₀ value at PPAR γ . The expression of GPR40 in monocytes was shown by Briscoe et al., (2003) and these levels of troglitazone may be activating GPR40. To separate the contribution of GPR40 from that of PPAR γ to the mode of action of the thiazolidinediones requires much more work. The knowledge of the structure-activity relationship of these compounds at GPR40 and PPAR γ , along with analysis of the effects of these compounds in GPR40 knock-out animals and selective knock-down of GPR40 in model systems will help answer this question. The recent development of PPAR γ inactive thiazolidinedione analogues which retain the ability to cause apoptosis of cancer cell lines but have no PPAR γ activity (Huang et al., 2005) may provide interesting tools in this field if they can be shown to have activity at GPR40.

It is also important to consider whether levels of thiazolidinediones reached *in vivo* would be sufficient to activate GPR40. In humans, maximum serum concentrations of troglitazone can reach about 7-8 μ M (Plosker et al., 1999) and for pioglitazone levels reach about 2.2 μ M (Gillies et al., 2000). With the data generated in this study on the potency of these compounds, the serum levels of pioglitazone would not be expected to have any effect on GPR40 but with troglitazone this concentration should be able to activate GPR40 extensively. Figure 4.10 shows that 10 μ M troglitazone can activate a large and rapid increase in [Ca²⁺]_i in cells that endogenously express GPR40 and only 1 μ M troglitazone is required to increase [³⁵S]GTP γ S in membranes prepared from these cells.

The recently described small molecule agonists for GPR40 may also provide tools for investigating the role of GPR40 *in vivo*. The six compounds tested in this study were shown to be GPR40 agonists in a reporter gene assay (Garrido et al., 2006), it was therefore necessary to test these compounds in assays that measure signals produced further upstream. Only GW839508X had previously been tested in a [Ca²⁺]_i release assay (Briscoe et al., 2006). Table 4.6 shows the comparison between the potencies seen for each of the compounds in the three difference assay systems in which they have been

tested. GW839508X, GSK248257A and GSK250089A all show similar potency in the reporter gene assay and the [^{35}S]GTP γ S binding assay. By contrast, of the other three compounds GSK272235A was shown to be inactive in both the FLIPR based [Ca^{2+}]_i release assay and the [^{35}S]GTP γ S binding assay, GSK269778A inactive in the [Ca^{2+}]_i based assay and much less potent in the [^{35}S]GTP γ S binding than reported in the published data. GSK223112A was less potent in the [Ca^{2+}]_i release assay than in the reporter gene assay but was basically inactive in the [^{35}S]GTP γ S binding assay. The six compounds tested here fall into two broad categories, those with a carboxylate group (GW839508X, GSK250089A and GSK248257A) and those with an amide group in place of the carboxylic acid headgroup (GSK223112A, GSK272235A and GSK269778A). Garrido et al., (2006) found little difference when replacing the carboxylic acid with an amide but the data in this study argues against this. The three compounds that showed little or no activity in the two assay systems tested were the ones with the amide group, whereas the compounds containing the carboxylic acid proved to be potent agonists of GPR40. The importance of the carboxylic group for activation of the receptor by fatty acids has not been fully assessed in the literature and time constraints prevented this been investigated in this study.

These small molecule ligands may help in dissecting the role GPR40 plays in fatty acid-potentiated, glucose-stimulated insulin release. Briscoe et al., (2006) were able to show in a mouse β -cell line a concentration-dependent stimulation of insulin secretion in the presence of glucose by GW839508X but they were unable to reproduce these results in isolated rat or mouse islets. This is consistent with the observation in this study where GSK250089A was unable to mediate a rise in [Ca^{2+}]_i in single INS-1E cells or increase [^{35}S]GTP γ S binding in membranes prepared from these cells. This may reflect a difference in the binding of these compounds to rat or mouse GPR40 compared to human GPR40. If this is shown to be true, it would reduce their potential as compounds to unravel the pharmacology and function of GPR40 *in vivo* as many of the model systems for insulin release are rodent based. Although this may have an impact on the usefulness of these compounds, they still are at least 100 times more potent than any of the fatty acids at GPR40 and will definitely play a part in uncovering the true role of GPR40 *in vivo* and detailed comparisons of the activation of human and rat GPR40 by these compounds will provide insights into the mechanisms of ligand binding.

Briscoe et al., (2006) also described GW1100 as an antagonist of GPR40. This was shown by its ability to reduce GW839598X-stimulated increases in [Ca^{2+}]_i and glucose-stimulated

insulin secretion in a concentration-dependent manner. The observation that the GPR40-G α_q fusion protein displayed apparent high levels of constitutive activity that could be reduced by treatment with fatty acid free BSA provided an assay system to define both the role of GW1100 as an antagonist of GPR40 and the basis for the high levels of basal [35 S]GTP γ S binding. In this study it was confirmed that GW1100 is an antagonist of GPR40-G α_q by using the [35 S]GTP γ S binding assay. GW1100 can reduce the basal [35 S]GTP γ S binding to this protein in a concentration-dependent manner in the absence of fatty acid free BSA. In the presence of fatty acid free BSA, GW1100 was able to reduce basal loading further, which was comparable to the levels of [35 S]GTP γ S binding seen when GPR40-G α_q was treated with the G $\alpha_{q/11}$ inhibitor YM254890 (Figure 3.15). In the presence of BSA, GW1100 appeared to be a more potent antagonist, with saturation of reduction of binding being reached (Figure 4.7). The conventional interpretation of GW1100's ability to reduce basal [35 S]GTP γ S loading of GPR40 would be to describe GW1100 as an inverse agonist at GPR40. Consideration of the data obtained using fatty acid free BSA prevents GW1100 to be defined in this way as it is not possible to assess clearly whether this effect reflects competition with an endogenous agonist which binds to the receptor or if it is suppression of a high level of constitutive activity. The only way that this could be resolved would be if both inverse agonists and neutral antagonist are available for GPR40 but as it is a recently characterised GPCR the availability of small molecule modulators is limited and to date the only antagonist of GPR40 described is GW1100. The lack of inverse agonists and neutral antagonists has been the most limiting issue in defining the contribution of constitutive activity to the physiological function of GPCRs (Gardner and Mallet., 2006; Negus, 2006). It is therefore only possible to refer to GW1100 as a GPR40 antagonist until this issue can be clearly defined.

The detrimental effect of chronic exposure of β -cells to fatty acids is well documented (Lee et al., 1994; El Assaad et al., 2003; Prentki et al., 2003). The use of a GPR40 antagonist may be of use to help in the understanding of this effect and establish the role GPR40. It has recently been shown that mice expressing GPR40 under the control of the PDX-1 (pancreatic duodenal homobox-1) promoter had impaired beta-cell function and developed diabetes (Steneberg et al., 2005). Hence development of a GPR40 antagonist may be an attractive approach for the treatment of diabetes.

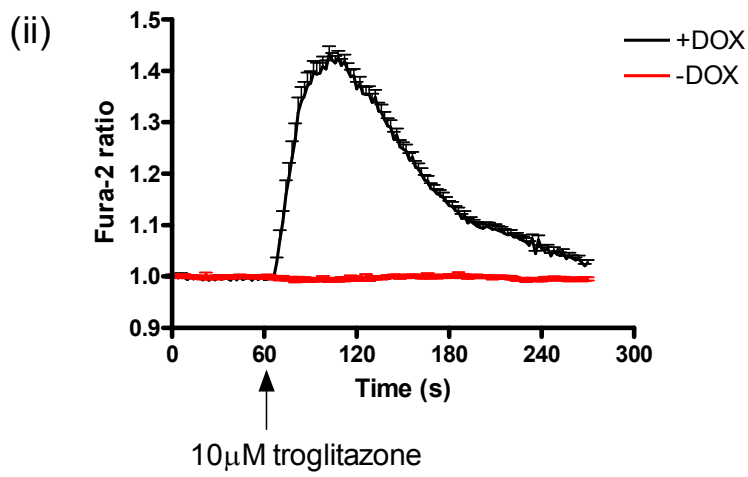
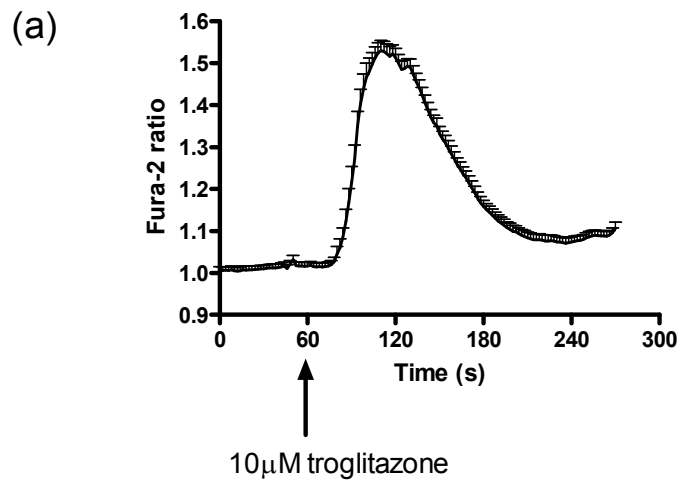


Figure 4.1 Troglitazone can produce a rise in $[Ca^{2+}]_i$ via GPR40

(a) HEK293T cells were transfected to transiently express GPR40-eYFP. Following loading with Fura-2, 10 μ M troglitazone was added at the 60 second time point and the alteration in Fura-2 fluorescence monitored over the following 240 seconds with images collected every 2 seconds. Data represent means \pm SEM from 20 positively transfected cells selected on the basis of eYFP fluorescence. (b) (i) Cells of a clone of Flp-In T-REx-HEK293 cells with GPR40-eYFP located at the Flp-In locus were grown on poly-D lysine coated coverslips and treated with (+ DOX) (right panel) or without (- DOX) (left panel) 1 μ g/ml doxycycline for 24h. Cells were visualized to detect expression of GPR40-eYFP. (ii) Cells were loaded with Fura-2 and 10 μ M troglitazone added at the 60s time point. Alterations in Fura-2 fluorescence were monitored for a further 240s in at least 20 + DOX (black) and - DOX (red) cells.

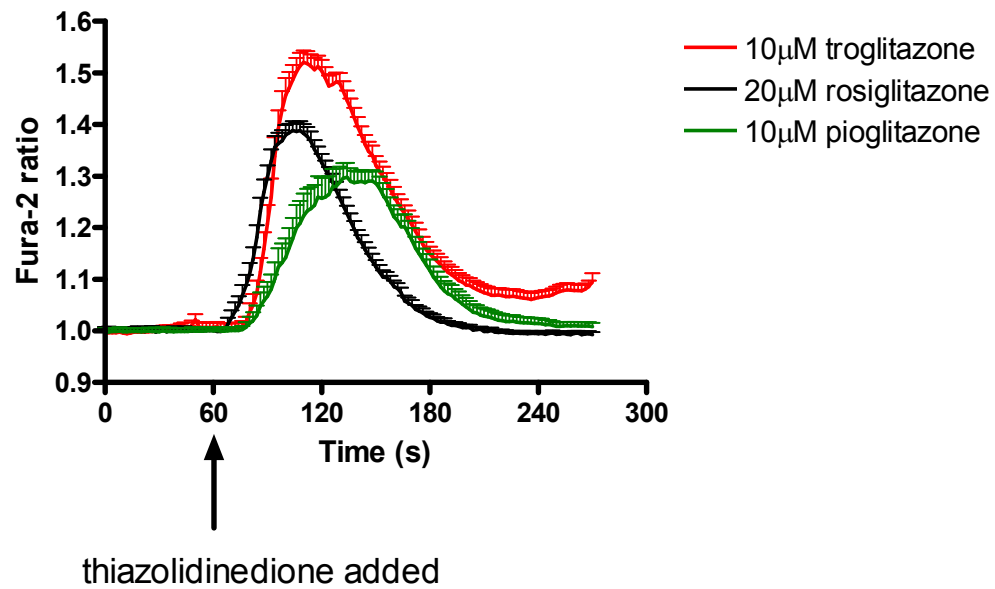


Figure 4.2 Other thiazolidinediones can act as agonists at GPR40 in a single cell calcium assay

HEK293T cells were transfected to transiently express GPR40-eYFP. Following loading with Fura-2, 10µM troglitazone (red), 10µM pioglitazone (green) or 20µM rosiglitazone (black) were added at the 60 second time point and the alteration in Fura-2 fluorescence monitored over the following 240 seconds with images collected every 2 seconds. Data represent means±SEM from at least 20 positively transfected cells selected on the basis of eYFP fluorescence

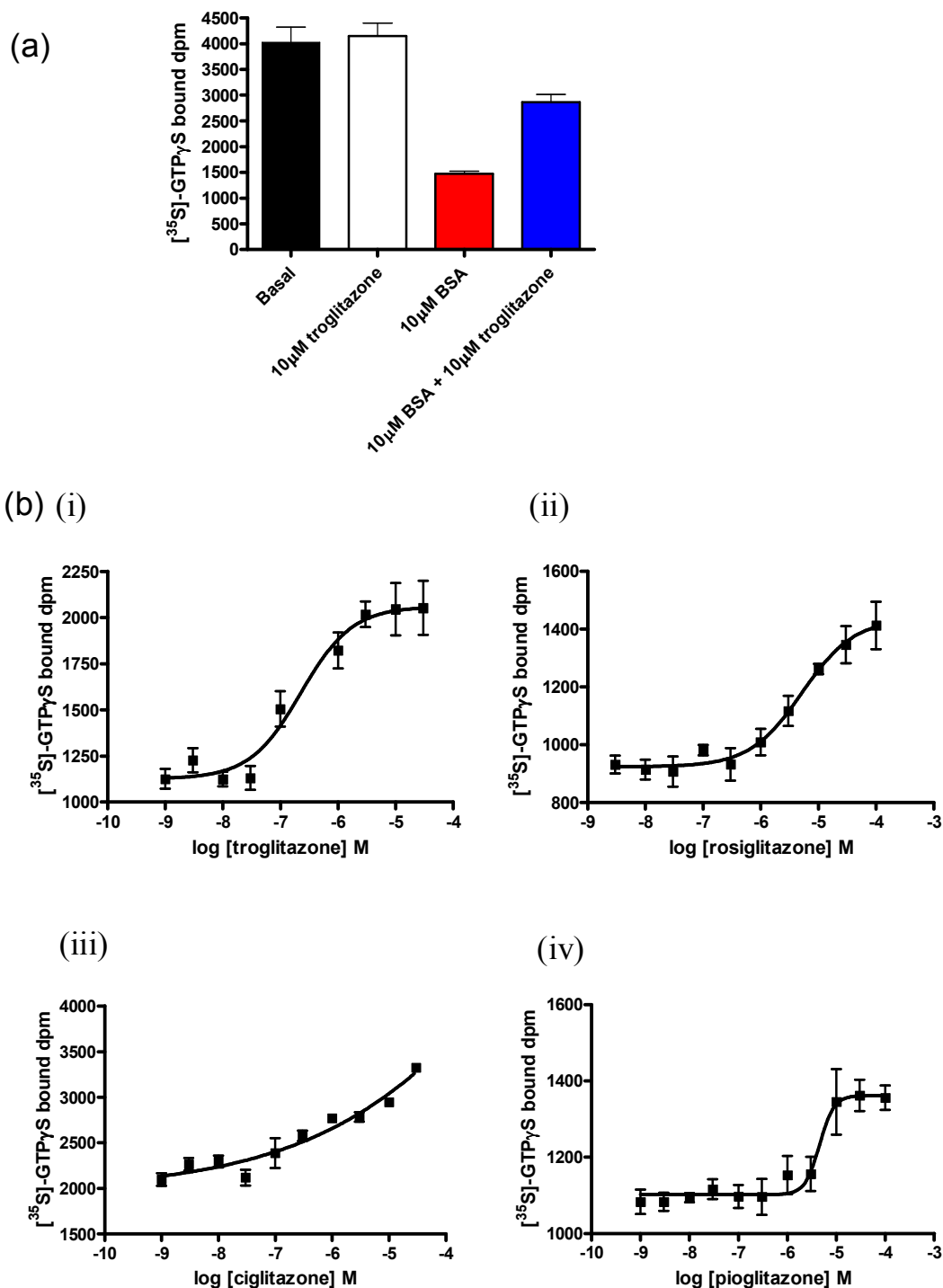


Figure 4.3 Thiazolidinediones activate GPR40 in a concentration-dependent manner in a [³⁵S]GTP_γS binding assay with varying degrees of potency but only in the presence of fatty acid free BSA

HEK293T cells were transfected to express GPR40-Gα_q and membranes prepared. (a) Basal (black bar) [³⁵S]GTP_γS binding in Gα_q immunoprecipitates was determined and the effects of 10 μM troglitazone (white), 10 μM fatty acid free BSA (red), and 10 μM fatty acid free BSA plus 10 μM troglitazone (blue) on levels of [³⁵S]GTP_γS bound were determined.

(b) [^{35}S]GTP γ S binding studies were performed in the presence of 10 μM fatty acid free BSA and increasing concentrations of (i) troglitazone, (ii) rosiglitazone, (iii) ciglitazone and (iv) pioglitazone. Graphs shown are representative of results obtained for three individual experiments performed in triplicate. Data points represent means \pm SEM.

Compound	pEC50	Hill Slope
Troglitazone	6.5±0.1	0.96±0.2
Rosiglitazone	5.5±0.2	0.90±0.1
Ciglitazone	>4	0.34±0.1
Pioglitazone	5.5±.0.1	4.53±1.1

Table 4.1 Potency of thiazolidinediones at GPR40-G α_q measured by in the [³⁵S]GTP γ S binding assay

[³⁵S]GTP γ S binding studies were performed on membranes expressing GPR40-G α_q in the presence of 10 μ M fatty acid free and the specified thiazolidinedione. Data represent means \pm SEM of three individual experiments.

Compound	pEC50
Troglitazone	5.9±0.1
Rosiglitazone	5.7±0.3
Ciglitazone	inactive
Pioglitazone	inactive

Table 4.2 Potency of thiazolidinediones at GPR40 measured in a FLIPR based $[Ca^{2+}]_i$ mobilisation assay

HEK293 MSRII cells were transiently transfected to express GPR40-eYFP. 24h post transfection cells were seeded at 15,000 cells per well into 384 well microtitre plates. Changes in $[Ca^{2+}]_i$ levels were measured using the FLIPR apparatus following challenge with test ligands added at the 10s time point and data collected for a further 110s. Data represent mean±SEM of three individual experiments.

Compound	pEC50
GW839508X	7.6±0.3
GSK248257A	ND
GSK250089A	7.0±0.2
GSK223112A	5.7±0.7
GSK272235A	inactive
GSK269778A	inactive

Table 4.3 Potency of synthetic small molecules at GPR40 measured in a FLIPR based $[Ca^{2+}]_i$ assay

HEK293 MSRII cells were transiently transfected to express GPR40-eYFP. 24h post transfection cells were seeded at 15,000 cells per well into 384 well microtitre plates. Changes in $[Ca^{2+}]_i$ levels were measured using the FLIPR apparatus following challenge with test ligands added at the 10s time point and data collected for a further 110s. Data represent mean±SEM of three individual experiments. ND = not determined.

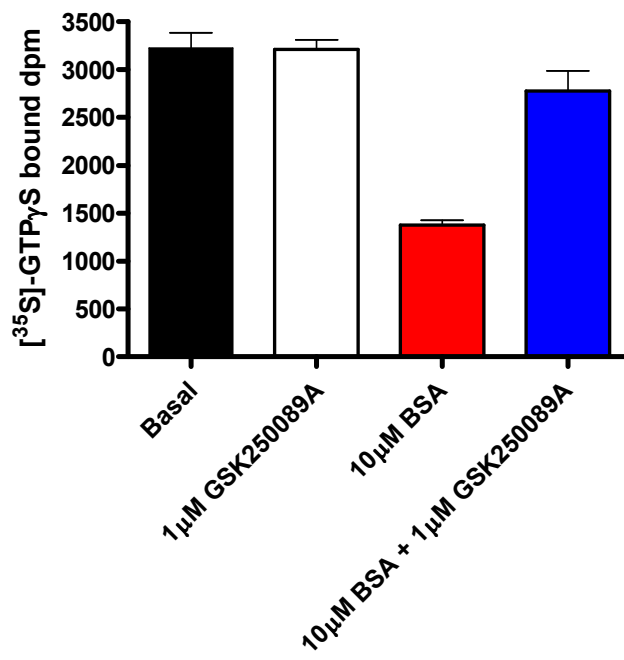


Figure 4.4 GSK250089A can apparently only act as an agonist of GPR40-Gα_q in the presence of fatty acid free BSA

HEK293T cells were transfected to express GPR40-Gα_q and membranes prepared. Basal (black bar) [³⁵S]GTPγS binding in Gα_q immunoprecipitates was determined and the effects of 1 μM GSK250089A (white), 10 μM fatty acid free BSA (red), and 10 μM fatty acid free BSA plus 1 μM GSK250089A (blue) on levels of [³⁵S]GTPγS bound were determined.

Graph shown is representative of three experiments performed in triplicate and data points shown are means±SEM.

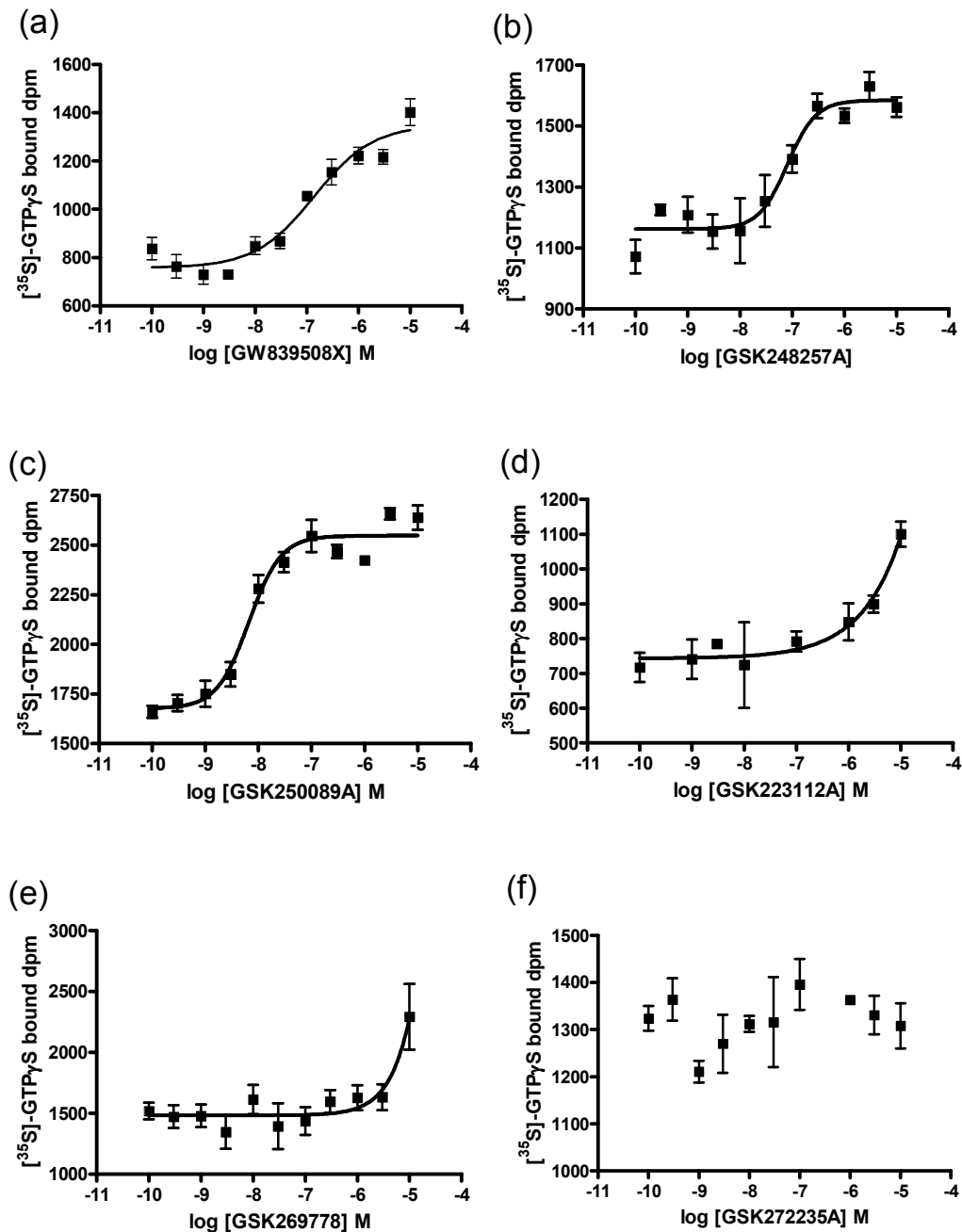


Figure 4.5 Potency of synthetic small molecules agonists at GPR40 measured in the $[^{35}\text{S}]\text{-GTP}\gamma\text{S}$ binding assay

HEK293T cell membranes expressing GPR40- $\text{G}\alpha_q$ were used to measure the ability of increasing concentrations of (a) GW839508X, (b) GSK248257A, (c) GSK250089A, (d) GSK223112A, (e) GSK269778A and (f) GSK272335A to mediate alterations in $[^{35}\text{S}]\text{-GTP}\gamma\text{S}$ binding. All assay samples were immunoprecipitated with the $\text{G}\alpha_{q/11}$ antiserum CQ before scintillation counting. Graph shown is representative of results obtained for three individual experiments performed in triplicate. Data points represent means \pm SEM.

Compound	pEC50
GW839508X	6.9±0.2
GSK248257A	7.2±0.1
GSK250089A	8.5±0.1
GSK223112A	>5
GSK272235A	inactive
GSK269778A	>5

Table 4.4 Potency of synthetic small molecules at GPR40 measured in a [³⁵S]GTPγS binding assay

[³⁵S]GTPγS binding studies were performed on HEK293T cell membranes expressing GPR40-Gα_q in the presence of 10μM fatty acid free and the specified synthetic agonist. Data represent mean±SEM from three individual experiments

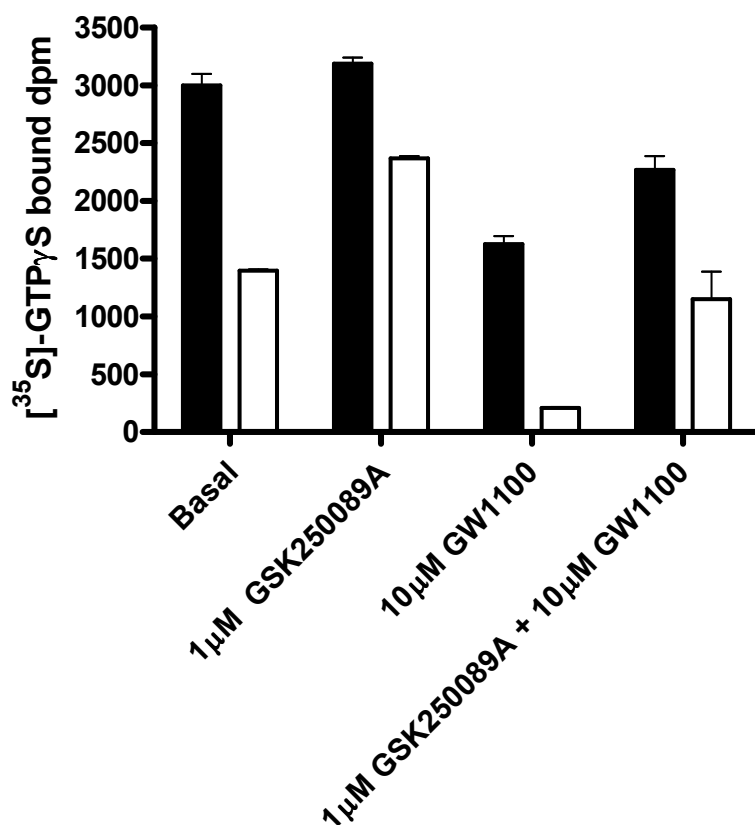


Figure 4.6 GW1100 is an antagonist of GPR40-Gα_q

HEK293T cells were transiently transfected to express GPR40-Gα_q and membranes were prepared. Basal [³⁵S]GTPγS binding in Gα_q immunoprecipitates was determined in the presence (white bar) and absence (black bar) of 10 μM fatty acid free BSA. The effect of 1 μM GSK250089A, 10 μM GW1100 and the combination of 1 μM GSK250089A and 10 μM GW1100 in the presence (black bars) and absence (white bars) of 10 μM fatty acid free BSA was determined. The graph shown is representative of three individual experiments performed in triplicate. Data shown are means ± SEM.

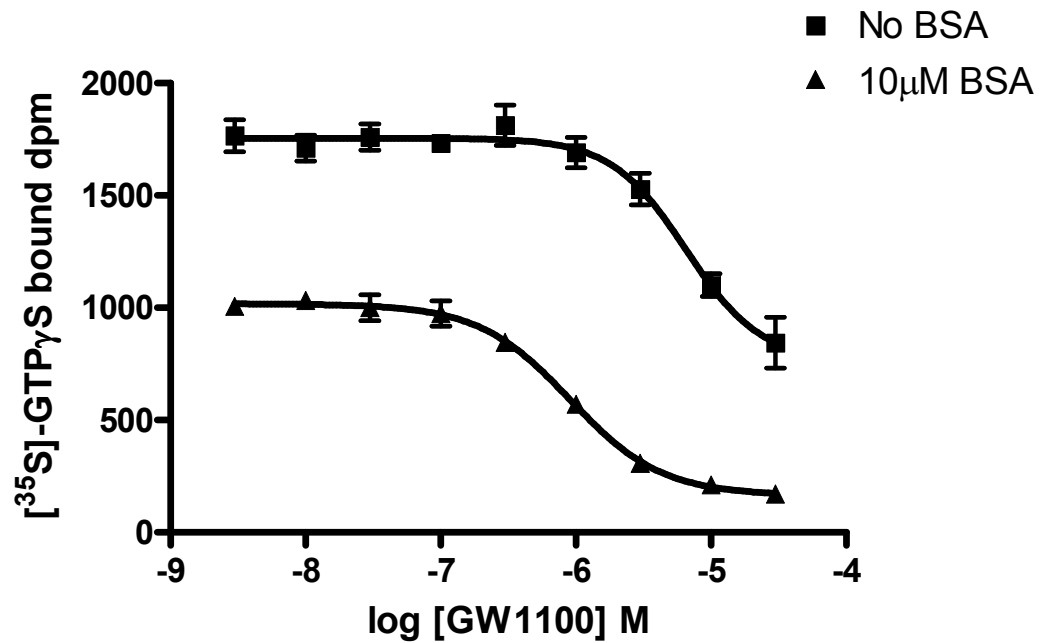


Figure 4.7 'Basal' [³⁵S]GTP_γS binding at GPR40-Gα_q is substantially reduced by GW1100 in the presence and absence of fatty acid free BSA in a concentration dependent manner

HEK293T cells were transiently transfected with GPR40-Gα_q and membranes were prepared. [³⁵S]GTP_γS binding assays were performed in the presence of varying concentrations of GW1100 and the absence (squares) or presence (triangles) of 10μM fatty acid free BSA. [³⁵S]GTP_γS binding in Gα_q immunoprecipitates was estimated by scintillation counting. The graph show is representative of three individual experiments performed in triplicate. Data points represent means±SEM.

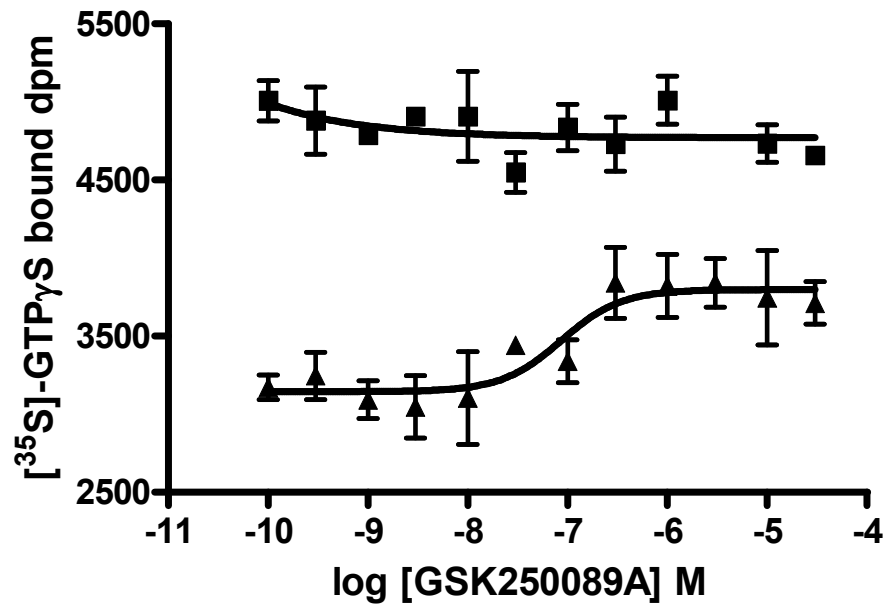
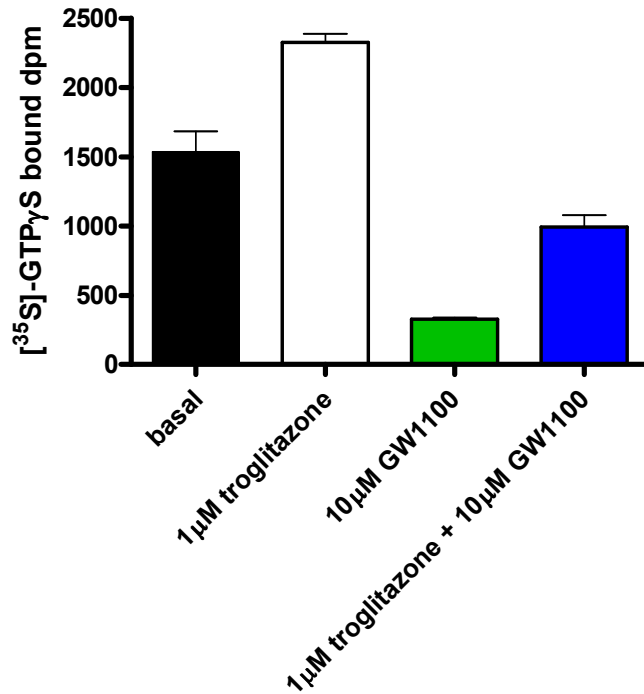


Figure 4.8 Agonist activity of GSK250089A can be detected in the presence of GW1100

HEK293T cells were transiently transfected to express GPR40-G α_q and membranes were prepared. [35 S]GTP γ S binding in G α_q immunoprecipitates was determined and the effect of increasing concentrations of GSK250089A in the presence (triangles) or absence (squares) of 10 μ M GW1100. The graph shown is representative of three individual experiments performed in triplicate. Data points represent means \pm SEM.

(a)



(b)

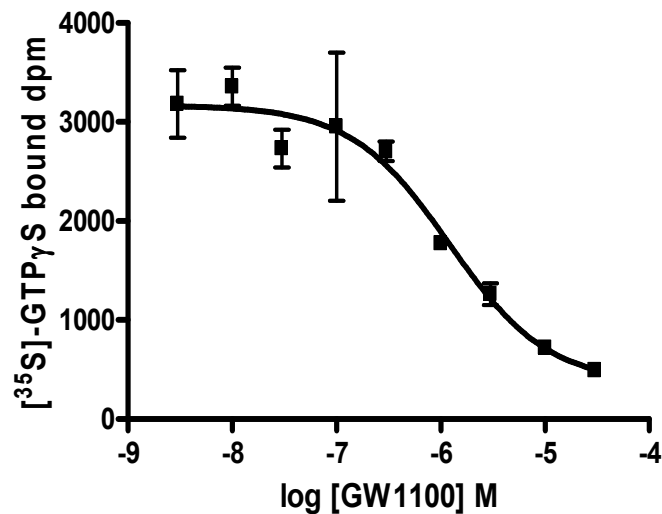


Figure 4.9 GW1100 can inhibit troglitazone-mediated activation of GPR40

HEK293T cells transiently transfected with GPR40-G α_q were used to prepare membranes.

(a) Basal [35S]GTP γ S binding was assessed in G α_q immunoprecipitates in the presence 10 μ M of fatty acid free BSA. The effects of 1 μ M troglitazone (white bar), 10 μ M GW1100 (green bar) or the combination of 1 μ M troglitazone and 10 μ M GW1100 (blue bar) were assessed. (b) The effect of increasing concentrations of GW1100 on the ability of 1 μ M troglitazone to increase [35S]GTP γ S binding. Graphs shown are representative of three individual experiments performed in triplicate. Data points represent mean \pm SEM.

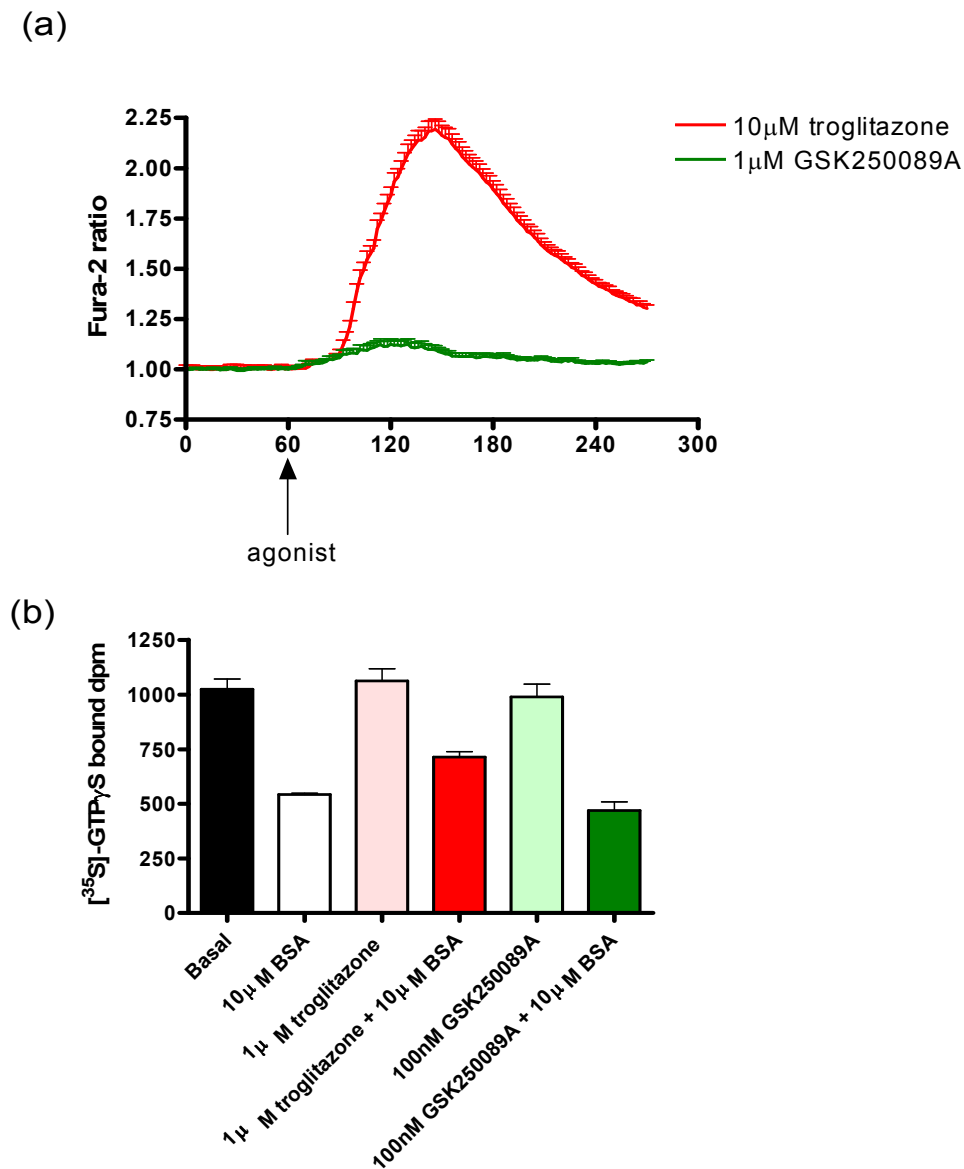


Figure 4.10 Ability of troglitazone and GSK250089A to elicit mobilization of $[Ca^{2+}]_i$ in INS-1E cells and increase $[^{35}S]GTP\gamma S$ binding in INS-1E cell membranes

(a) INS-1E cells were grown on coverslips. Following loading with Fura-2, 10 μ M troglitazone (red line) or 1 μ M GSK250089A (green line) was added at the 60s time point and the alteration in Fura-2 fluorescence monitored over the following 240s with images collected every 2s. Data represents means \pm SEM from 50 cells. (b) Cell membranes were prepared from INS-1E cells. Basal (black bar) binding of $[^{35}S]GTP\gamma S$ in $G\alpha_q$ immunoprecipitates and the effects of 10 μ M fatty acid-free BSA alone (white bar), 1 μ M troglitazone (pink bar), 100nM GSK250089A (light green bar) and combination of 10 μ M fatty acid free BSA and 1 μ M troglitazone (red bar) or 100nM GSK250089A (green bar) on levels of $[^{35}S]GTP\gamma S$ bound were assessed.

Agonist	EC ₅₀ (μM) at	
	GPR40	PPAR _γ
Troglitazone	0.32	0.78
Rosiglitazone	3.16	0.076
Pioglitazone	3.26	0.55
Ciglitazone	3162	3

Table 4.5 Comparison of potency of various thiazolidinediones at GPR40 and PPAR_γ

EC₅₀ values for GPR40 determined using [³⁵S]GTP_γS binding assay as shown in Table 4.1.

EC₅₀ values for PPAR_γ were determined using reporter gene chimera genes at mouse PPAR_γ (Pershadsingh, 2004).

Agonist	pEC ₅₀ determined by		
	[³⁵ S]GTP _γ S binding	[Ca ²⁺] _i release	Reporter gene activation
GW839508X	6.9	7.6	7.2
GSK248257A	7.2	ND	7.9
GSK250089A	8.5	7.0	8.3
GSK223112A	>5	5.7	7.3
GSK272235A	inactive	inactive	7.4
GSK269778A	>5	inactive	7.0

Table 4.6 Potency of various small molecule ligands determined in three different assay systems

pEC₅₀ values for six small molecule ligands was determined in [³⁵S]GTP_γS binding assays (taken from Table 4.4), FLIPR based [Ca²⁺]_i release assays (taken from Table 4.3) and in a reporter gene assay (taken from Garrido et al., 2006)

5 Mutagenesis to identify residues important in fatty acid binding and fatty acid chain length selectivity

5.1 Introduction

There is no mutational data available on the regions and residues that play a role in fatty acid binding to GPR40, GPR41 and GPR43. Studies on other receptors whose ligands contain carboxyl groups indicate that a positively charged amino acid is very important in ligand binding. Tunaru et al. (2005) demonstrated that an arginine residue in TM3 of the high affinity nicotinic acid receptor, HM74A provides a positive charge by which the carboxylate group of nicotinic acid can bind. Studies on GPR91 have shown that four arginine residues are required for binding the dicarboxylate groups of succinate (He et al., 2004). Basic residues have also been implicated in the binding of prostanoids to prostanoid receptors (Stitham et al., 2003) and of leukotriene B₄ to its receptor (Sabirsh et al., 2006). Sequence alignment of GPR40, GPR41 and GPR43 shows that there are three conserved basic residues in transmembrane regions; an arginine or lysine in TM2, histidine in TM4 and arginine in TM5 (Figure 5.1).

Homology models of GPR40, GPR41 and GPR43 were generated by GlaxoSmithKline based on the crystal structure of rhodopsin. They were generated using the automated GPCR_Builder programme and the process of developing the model is described in detail by Berkhout et al., (2003). The intracellular loops of the receptors were not modelled, due to their poor definition in the crystal structures of rhodopsin. The receptors were aligned based on key conserved residues in family A GPCRs, these include an Asn in TM1, a Cys residue in extracellular loop 1, the D(E)RY motif at the bottom TM3, a Cys in extracellular loop 2, a Pro residue in TM5 and in TM6. GPR43 contains an ERY motif in TM3 whereas in GPR40 a GRY triplet is found and in GPR41 it is an ERF motif. Figure 5.2 shows one of the small molecule agonists of GPR40 docked into the homology model of the receptor. This demonstrates the ability of the Arg in TM5 to interact with the carboxylate head group of the compound. The His in TM4 is found near the proposed binding site whereas the Lys in TM2 is quite far away. The size of the short chain fatty acids prevents them from being modelled with any degree of accuracy into the models of GPR41 and GPR43 and as there have been no small molecule ligands described at either receptor, the models shown in Figure 5.3 do not contain any ligand bound. The models of both receptors show

the Arg in TM5 pointing into the core of the receptor, again with the His in close proximity. The Arg/Lys in TM2 points away from the proposed binding site, which would make it unavailable for interaction with the carboxylate group of the fatty acid.

Another important issue is the differing fatty acid chain length specificity of GPR40, GPR41 and GPR43. Sequence alignment and homology modeling indicates a region in TM3 that may play a role in chain length specificity. Within TM3 of GPR40 a glycine triplet is found whereas in GPR43 the triplet comprises serine-threonine-tryptophan. Figure 5.4 illustrates the role of these residues in the homology models of GPR40 and GPR43. In GPR40, the triplet of glycine allows the synthetic small molecule agonist to bind down into the core formed by the TM helices. In GPR43, the Ser-Thr-Trp triplet protrudes into the proposed binding pocket of the receptor and makes the binding pocket smaller. This would prevent any compound binding down into the core of the receptor.

To facilitate comparison between GPR40, GPR41, GPR43 and other family A GPCRs the Ballesteros-Weinstein numbering scheme will be used (Ballesteros and Weinstein, 1995). This numbering scheme assigns the most conserved residue in each TM helix the number 50 and each residue is numbered according to its position relative to the most conserved residue in the helix. In GPR40, GPR41 and GPR43 the conserved Arg/Lys in TM2 is numbered 2.60, the His in TM4 is numbered 4.56 and the Arg in TM5 is numbered 5.39. The triplet in TM3 of GPR40 and GPR43 are numbered 3.39, 3.40 and 3.41. Within the discussion section of this chapter the Ballesteros-Weinstein numbering will be included to allow comparison between receptors.

To investigate the roles of each of the basic transmembrane residues a point mutagenesis approach was used. Using the Stratagene QuikChange mutagenesis protocol, initially each of the sequences corresponding to the basic residues were mutated to code for alanine. The mutations were introduced into the receptor-eYFP fusion protein. The receptor-eYFP fusions are a valuable tool for this study as they allowed monitoring of the expression of each of the mutants and selection of positively transfected cells during single cell Ca^{2+} experiments to assess the function of the mutant. For mutation of the triplet in TM3 of GPR40 all three residues were mutated together to the corresponding residues in GPR43 using the QuikChange method. With GPR43, each of the residues was mutated in turn to glycine, starting with the tryptophan, as it is the most bulky of the three residues.

5.2 Mutation of conserved transmembrane basic residues in GPR43

Three GPR43 mutants were generated in which the conserved transmembrane basic amino acids that are implicated in the coordination of the carboxyl group of the fatty acid were mutated to alanine in the GPR43-eYFP fusion protein. Each of the mutants was tested for its ability to mediate a rise in $[Ca^{2+}]_i$ in single cells in response to 10mM acetate, butyrate or propionate (Figure 5.5). To each of the short chain fatty acids tested, wild type GPR43 produced a rapid, transient increase in $[Ca^{2+}]_i$. The mutant with the TM2 lysine mutated to alanine, GPR43 Lys⁶⁵Ala-eYFP, was able to produce a transient rise in $[Ca^{2+}]_i$ when challenged with acetate or propionate but when exposed to butyrate no change in $[Ca^{2+}]_i$ was observed. Mutation of the histidine in TM4 to alanine to produce GPR43 His¹⁴⁰Ala-eYFP, was found to have no significant effect on the function of the receptor, with a similar rise in $[Ca^{2+}]_i$ as observed with the wild type receptor to all three fatty acids tested. The mutation of the TM5 arginine to generate, GPR43 Arg¹⁸⁰Ala-eYFP, resulted in a complete loss of function of the receptor to any of the short chain fatty acids tested. However, expression of the receptor was confirmed by eYFP fluorescence (see Figure 5.9).

To further investigate the role of the TM5 arginine, three additional mutants were generated with lysine (GPR43 Arg¹⁸⁰Lys), leucine (GPR43 Arg¹⁸⁰Leu) or serine (GPR43 Arg¹⁸⁰Ser) in place of arginine at position 180 in GPR43-eYFP. When transiently expressed in HEK293T cells, expression of each of the mutants was confirmed by eYFP fluorescence (Figure 5.9). Challenge of cells expressing the mutant receptors with acetate or propionate resulted in no change in $[Ca^{2+}]_i$ (Figure 5.6). Replacement of the arginine with another positively charged amino acid does not restore function to the receptor as GPR43 Arg¹⁸⁰Lys-eYFP was still unable to respond to either of the short chain fatty acids tested. Without the availability of assays to directly monitor the binding of the fatty acid to the receptor it is impossible to determine if the fatty acid is actually binding the mutant receptor. The data, therefore, indicates that the arginine in TM5 of GPR43 plays a key role in fatty acid mediated activation of GPR43.

As shown in Figure 5.5, GPR43 Lys⁶⁵Ala was unable to mediate a rise in $[Ca^{2+}]_i$ when challenged with butyrate but still retained the ability to respond to acetate or propionate. Expression of the mutant receptor could be confirmed by visualization of receptor but to further investigate the function of the mutant cells were challenged sequentially with butyrate then acetate or propionate (Figure 5.7). When challenged sequentially in this way,

GPR43 Lys⁶⁵Ala was still able to respond to acetate or propionate. The sequential addition of the fatty acids demonstrates GPR43 Lys⁶⁵Ala has lost the ability to respond to butyrate but not to acetate or propionate. It is therefore unlikely that Lys⁶⁵ is a charge partner for the carboxylic acid head group of the fatty acid due to this specific loss of function to butyrate.

In order to investigate the potency of various fatty acids at the GPR43 mutants generated, a FLIPR based Ca²⁺ mobilization assay was employed. As detailed in Chapter 3, HEK293 MSRII cells were transiently co-transfected to express GPR43-eYFP or one of the GPR43 mutant-eYFP fusions and a G protein cocktail, challenged with increasing concentrations of various chain length fatty acids and the change in fluorescence of the Ca²⁺ dye Fluo-4 monitored. Table 5.1 shows the potencies of short chain fatty acids at the GPR43 mutants. As anticipated from the single cell Ca²⁺ experiments, none of the Arg¹⁸⁰ mutants were able to respond to any of the fatty acids tested at any concentration. Carbachol was added to cells expressing the mutant receptors to confirm the viability of the cells, and in all cases a robust rise in [Ca²⁺]_i was seen upon the addition of this agonist. With cells transfected to express GPR43 Lys⁶⁵Ala, no rise in [Ca²⁺]_i could be observed on the addition of any of the fatty acids. This could be due to the reduced sensitivity of a FLIPR based assay compared to a single cell assay as in the single cell Ca²⁺ assays GPR43 Lys⁶⁵Ala did display a reduced ability to mediate a rise in [Ca²⁺]_i compared to the wild type receptor.

GPR43 His¹⁴⁰Ala displayed a loss of function towards formate but as this is a very low potency agonist at the wild type receptor any small change in the binding site is likely to be more apparent. This mutant also showed a significantly reduced potency towards acetate. As each of the mutants were tested against a panel of fatty acids with variable chain length, it was shown that GPR43 His¹⁴⁰Ala-eYFP was now able to mediate a rise in [Ca²⁺]_i when exposed to caproic acid or caprylic acid (Figure 5.8), which have carbon chain lengths of 6 and 7 respectively. The pEC₅₀ of caproic acid was 4.8±0.3 and for caprylic acid it was 4.8±0.4. These data suggests that GPR43 His¹⁴⁰Ala has increased affinity for longer chain fatty acids compared to the wild type receptor. This gain of function was not examined in the single cell [Ca²⁺]_i assay due to time constraints of the project.

Figure 5.9 shows that compared to the wild type receptor there was no obvious difference between the expression levels or expression pattern of any of the mutants. The wild type receptor did not appear to be effectively targeted to the cell surface in such transient assays which makes observations on the possible effects on trafficking of the mutant receptors hard to determine.

5.3 Mutation of conserved transmembrane basic residues in GPR41

GPR41 also contains three basic transmembrane residues. To investigate their role in the function of GPR41, initially each of the residues in the receptor-eYFP fusion protein was mutated to alanine. To assess their function, each of the mutants was transiently co-transfected with $G\alpha_{qG66D15}$ into HEK293T cells and their ability to mediate a rise in $[Ca^{2+}]_i$ in response to short chain fatty acids monitored (see Figure 3.3). Figure 5.10 shows the response each of the GPR41 mutants generated when challenged with butyrate or propionate. As with GPR43, mutation of the TM5 arginine in GPR41 to produce, GPR41 Arg¹⁸⁵Ala-eYFP, resulted in a receptor unable to respond to 10mM butyrate or propionate, again supporting the theory that the arginine in TM5 acts as a charge partner for the carboxyl group of the fatty acid. GPR41 His¹⁴⁶Ala-eYFP displayed similar ability as the wild type receptor to respond to both of the fatty acids tested, which indicates that it does not play a critical role in co-ordinating the fatty acid. GPR41 Arg⁷¹Ala-eYFP was also able to respond to butyrate with similar kinetics to the response generated by the wild type receptor. Whereas, when the mutant was challenged with propionate, the magnitude of the response was reduced compared to the wild type receptor.

Attempts were made to develop a FLIPR-based assay with GPR41 to allow the potencies of fatty acids to be determined at the GPR41 mutants. Even when co-transfecting GPR41-eYFP with $G\alpha_{qG66D15}$ or a G protein cocktail containing various G protein chimeras, no signal was generated by the wild type receptor that could be detected by the FLIPR in response to any of the fatty acids tested. In the single cell Ca^{2+} assay the signal generated by GPR41 when co-transfected with $G\alpha_{qG66D15}$ was relatively small and when using the FLIPR apparatus to measure the changes in $[Ca^{2+}]_i$, the signal may be below the threshold of detection. Therefore, to investigate the potency of propionate at the GPR41 mutants, the mutations were incorporated into the GPR41- $G\alpha_{i3}$ Cys³⁵¹Ile fusion protein (described in Figure 3.1) and concentration response curves were generated using the $[^{35}S]GTP\gamma S$ binding assay (Figure 5.11a). As shown in Chapter 3, the GPR41- $G\alpha_{i3}$ Cys³⁵¹Ile fusion protein produced a robust concentration-response curve to propionate. The incorporation of the His¹⁴⁶Ala into the GPR41- $G\alpha_{i3}$ Cys³⁵¹Ile fusion protein had little effect on the ability of the receptor to increase $[^{35}S]GTP\gamma S$ binding in a concentration-dependent manner and the potency of propionate remained unchanged (Table 5.2). When the Arg⁷¹Ala mutation was introduced into the GPR41- $G\alpha_{i3}$ Cys³⁵¹Ile fusion protein a much larger effect was observed, with only a very small increase in $[^{35}S]GTP\gamma S$ binding in response to increasing

concentrations of propionate observed and to be able to see the increase in binding a reduced scale had to be utilised (Figure 5.11b). The potency of propionate at this mutant receptor was significantly reduced compared to that at the wild type receptor (Table 5.2). As predicted from the data obtained in the single cell Ca^{2+} experiments, the introduction of the Arg¹⁸⁵Ala mutation into the fusion protein resulted in no increase in [³⁵S]GTP γ S binding upon the addition of increasing concentrations of propionate.

Like GPR43, transiently expressed GPR41-eYFP was not very well plasma membrane delineated (Figure 5.12). Figure 5.12 confirms that the GPR41 mutants express in a similar fashion to the wild type receptor although it is hard to determine if the mutant receptors are found at the cell surface.

5.4 Mutation of conserved basic transmembrane residues in GPR40

To investigate the importance of each of the basic transmembrane residues in the function of GPR40, each of the residues were mutated to alanine in a GPR40-eYFP fusion protein using the Stratagene QuikChange method. The mutant receptors were transiently transfected into HEK293T cells and their ability to mediate a rise in $[\text{Ca}^{2+}]_i$ in response to lauric acid monitored. As shown in Figure 3.11, GPR40-eYFP is able to generate a rapid and transient rise in $[\text{Ca}^{2+}]_i$ in response to the addition of 100 μM lauric acid (Figure 5.13). The mutation of Lys⁶² to Ala resulted in a slight slowing of the kinetics of the mobilisation signal compared to the wild type receptor. The GPR40 His¹³⁷Ala-eYFP mutant was not as efficacious as the wild type receptor in the mediation of a release of $[\text{Ca}^{2+}]_i$ in response to lauric acid, with a smaller increase in $[\text{Ca}^{2+}]_i$ recorded. Unlike GPR41 and GPR43, the mutation of the TM5 Arg in GPR40 did not result in complete loss of function of the receptor towards a fatty acid. GPR40 Arg¹⁸³Ala-eYFP still retained the ability to increase $[\text{Ca}^{2+}]_i$ upon the addition of lauric acid, although the signal was reduced compared to the wild type receptor.

As there are a large number of compounds that activate GPR40, to fully characterize the function of each of the mutants the high throughput FLIPR-based Ca^{2+} assay was utilised. Each of the mutants was transiently transfected into HEK293 MSRII cells, exposed to increasing concentrations of the test compound and changes in Fluo-4 fluorescence monitored. Using this method, potencies of a range of fatty acids (Table 5.3), small molecule agonists and thiazolidinediones (Table 5.4) could be ascribed to each of the

mutants. All of the mutants were able to respond to a range of fatty acids. As expected from the single cell Ca^{2+} experiments, GPR40 Arg¹⁸³Ala was able to respond to lauric acid and could also respond to the majority of fatty acids tested apart from caproic acid, palmitic acid and elaidic acid. Only some of the fatty acids (linolenic acid, linoleic acid and retinoic acid) showed a reduced potency at GPR40 Arg¹⁸³Ala. Of the saturated fatty acids tested, GPR43 His¹⁴⁰Ala was only able to respond to lauric acid and palmitic acid. In addition to this, many of the unsaturated fatty acids showed reduced potency at this mutant receptor. GPR40 Lys⁶²Ala was able to respond to all of the fatty acids tested, apart from caproic acid (which is one of the least potent of the fatty acids at the wild type receptor) and capric acid. Although, GPR40 Lys⁶²Ala was still able to respond to the fatty acids, a significant reduction in potency was recorded for many of the unsaturated fatty acids. The most marked difference observed with these GPR40 mutants was seen upon the addition of the small molecule agonists or thiazolidinediones (Table 5.4). GPR40 His¹³⁷Ala and GPR40 Arg¹⁸³Ala were unable to mediate a rise in $[\text{Ca}^{2+}]_i$ on the addition of any of the small molecule agonists or thiazolidinediones. GPR40 Lys⁶²Ala showed a reduced potency towards two of the small molecule agonists, GW839508X and GSK250089A, and was unable to respond to GSK223112A or either of the thiazolidinediones. All the mutants were also tested against short chain fatty acids, ciglitazone, pioglitazone, GSK272235A and GSK269778A and no rise in $[\text{Ca}^{2+}]_i$ was seen upon the addition of any of these compounds.

To confirm the observations on the function of the GPR40 mutants, the Lys⁶²Ala and Arg¹⁸³Ala mutations were incorporated into the GPR40-G α_q fusion protein (see section 3.4). Using the receptor-G protein fusion allows monitoring of the activation event further upstream in the cascade than Ca^{2+} release. The two GPR40-G α_q mutants and the wild type receptor-G α_q fusion were transiently transfected into HEK293T cells and [³⁵S]GTP γ S binding studies performed on the resulting membranes. Firstly, the effect of fatty acid free BSA on the basal loading of [³⁵S]GTP γ S onto the GPR40-G protein fusions was assessed (Figure 5.14). As shown in Chapter 3, the basal loading of [³⁵S]GTP γ S onto GPR40-G α_q is very high and this can be reduced by the addition of 10 μ M fatty acid free BSA. Both GPR40 Lys⁶²Ala-G α_q and GPR40 Arg¹⁸³Ala-G α_q also displayed this property, indicating that the mutant receptors still display apparent high constitutive activity and are therefore functional with respect to G protein activation by GPR40. To confirm the functionality of the mutant receptors, concentrations response curves were generated to three GPR40 agonists; a fatty acid (palmitic acid), a thiazolidinedione (troglitazone) and a small molecule agonist (GSK250089A) (Figure 5.15). Palmitic acid was able to increase

[³⁵S]GTPγS binding in both GPR40 Lys⁶²Ala-Gα_q and GPR40 Arg¹⁸³Ala-Gα_q, although a reduction in potency was observed at GPR40 Arg¹⁸³Ala-Gα_q. This supports the previous data that Arg¹⁸³ in GPR40 is not absolutely required for fatty acid binding and activation of the receptor. As expected from the FLIPR data, GSK250089A was unable to activate GPR40 Arg¹⁸³Ala-Gα_q and GPR40 Lys⁶²Ala-Gα_q displayed a significantly reduced potency towards this agonist. Although it appears that GSK250089A is more efficacious at GPR40 Lys⁶²Ala-Gα_q than the wild type receptor, this may be due to the larger reduction in basal [³⁵S]GTPγS binding seen upon the addition of fatty acid free BSA and the levels of [³⁵S]GTPγS binding at GPR40 Lys⁶²Ala-Gα_q in the presence of GSK250089A did not increase above the levels seen in the absence of fatty acid free BSA. Troglitazone was also able to increase [³⁵S]GTPγS binding in a concentration-dependent manner at GPR40 Lys⁶²Ala-Gα_q but it showed no activity at GPR40 Arg¹⁸³Ala-Gα_q. All the [³⁵S]GTPγS binding studies were performed in the presence of 10μM fatty acid free BSA to reduce the basal loading of [³⁵S]GTPγS onto the receptors. It is worth noting, that as with the wild type GPR40-Gα_q fusion, none of the agonists were able to increase the levels of [³⁵S]GTPγS binding above the levels of basal loading in the absence of fatty acid free BSA at GPR40 Lys⁶²Ala-Gα_q or GPR40 Arg¹⁸³Ala-Gα_q.

To determine the expression pattern of these GPR40 mutants, cells transiently expressing the receptor-eYFP fusion proteins were visualised. Compared to GPR41 and GPR43, the GPR40 wild type receptor was more membrane delineated (Figure 5.16). The mutant receptors appeared to be expressed in a similar pattern to the wild type receptor, with no obvious change in cell surface expression seen.

Unlike GPR41 and GPR43, mutation of the arginine in TM5 of GPR40 did not result in the loss of the ability of fatty acids to activate the receptor. To determine if a second amino acid residue may compensate for the loss of the TM5 basic residues, three double mutants were generated in which two of the basic transmembrane residues were substituted for alanine; GPR40 Lys⁶²Ala, His¹³⁷Ala, GPR40 Lys⁶²Ala, Arg¹⁸³Ala and GPR40 His¹³⁷Ala, Arg¹⁸³Ala. These mutations were introduced into the GPR40-eYFP fusion protein, transiently transfected into HEK293T cells and their ability to mediate a rise in [Ca²⁺]_i in response to lauric acid monitored (Figure 5.17). All three double GPR40 mutants were able to mediate a rise in [Ca²⁺]_i upon the addition of 100μM lauric acid. GPR40 Lys⁶²Ala, His¹³⁷Ala-eYFP was able to mediate a large, transient rise in [Ca²⁺]_i which was very similar to that generated by the wild type receptor, although a slight reduction in the maximal signal was observed. GPR40 His¹³⁷Ala, Arg¹⁸³Ala-eYFP also displayed similar

properties to the wild type receptor in its ability to mediate a change in $[Ca^{2+}]_i$ but the efficacy of the signal was markedly reduced compared to the wild type receptor. The double mutant which showed the most difference in the response to lauric acid was GPR40 Lys⁶²Ala, Arg¹⁸³Ala-eYFP, with a slower and reduced response to lauric acid than GPR40-eYFP.

To have a greater understanding of the function of these mutants, potencies of a range of compounds were determined as described for the initial GPR40 mutants using a FLIPR based Ca^{2+} assay. Table 5.6 shows the potencies determined for a range of fatty acids at all three of the GPR40 double mutants. Each of the mutants was able to respond to at least some of the fatty acids tested. GPR40 Lys⁶²Ala, His¹³⁷Ala was able to respond to all of the saturated fatty acids tested, except caproic acid. Of the eight unsaturated fatty acids tested, GPR40 Lys⁶²Ala, His¹³⁷Ala retained the ability to respond to six of them apart from palmitoleic acid and elaidic acid. Of the six unsaturated fatty acids that could activate this mutant receptor, three displayed a reduced potency in comparison to the wild type receptor; these being linolenic acid, linoleic acid and arachidonic acid. For GPR40 Lys⁶²Ala, Arg¹⁸³Ala, similar findings were recorded with the receptor displaying a degree of potency for the majority of fatty acids tested. Only caproic acid, capric acid and retinoic acid were unable to activate this mutant receptor. A significant shift in potency was also observed for three more fatty acids; caprylic acid, linolenic acid and linoleic acid. The small effects on the potencies of fatty acids at GPR40 Lys⁶²Ala, His¹³⁷Ala and GPR40 Lys⁶²Ala, Arg¹⁸³Ala were contrasted by the loss of ability of GPR40 His¹³⁷Ala, Arg¹⁸³Ala to respond to many of the fatty acid tested. This double mutant, GPR40 His¹³⁷Ala, Arg¹⁸³Ala, was unable to mediate a rise in $[Ca^{2+}]_i$ when challenged with any of the saturated fatty acid tested. In addition to this loss of potency of saturated fatty acids, four of the eight unsaturated fatty acids were also unable activate this mutant. Only linolenic acid, γ -linolenic acid, linoleic acid and docosapentaenoic acid were able to activate GPR40 His¹³⁷Ala, Arg¹⁸³Ala and their potencies remained unchanged compared to the wild type receptor.

The three double GPR40 mutants generated were also tested for their ability to mediate a rise in $[Ca^{2+}]_i$ in response to thiazolidinediones and small molecule agonists. These compounds were tested in a FLIPR-based Ca^{2+} assay on HEK293 MSRII cells transiently expressing the wild type or mutant receptor and potencies ascribed accordingly (Table 5.7). Unlike the GPR40 mutants where only one of the basic transmembrane residues was mutated and neither of the thiazolidinediones were able to activate them, two of the GPR40 double mutant, GPR40 Lys⁶²Ala, His¹³⁷Ala and GPR40 Lys⁶²Ala, Arg¹⁸³Ala, retained the

ability to mediate a rise in $[Ca^{2+}]_i$ when challenged with rosiglitazone. The potencies recorded were not significantly different to that seen at the wild type receptor. GPR40 His¹³⁷Ala, Arg¹⁸³Ala was unable to produce a change in levels of $[Ca^{2+}]_i$ in response to the addition of rosiglitazone. Although GPR40 Lys⁶²Ala, His¹³⁷Ala and GPR40 Lys⁶²Ala, Arg¹⁸³Ala possessed the ability to respond to rosiglitazone, all three GPR40 double mutants were inactive when challenged with the related compound troglitazone. The single mutant, GPR40 Lys⁶²Ala was shown to maintain the ability to respond to two of the small molecule agonists, GW839508X and GSK250089A. The introduction of the His¹³⁷Ala mutation into GPR40 Lys⁶²Ala did not abolish this response, although a reduction in potency was also observed to both of these compounds. In addition, when Arg¹⁸³ was mutated to Ala in GPR40 Lys⁶²Ala the double mutant was no longer able to be activated by GSK250089A and a further reduction in potency of GW839508X recorded. Alternatively, it could be that the incorporation of the Lys⁶²Ala to either the GPR40 His¹³⁷Ala or the GPR40 Arg¹⁸³Ala mutant restored the ability to respond to GW839508X and in the case of GPR40 Lys⁶²Ala, His¹³⁷Ala also, GSK250089A. None of the double mutants were able to mediate a rise in $[Ca^{2+}]_i$ when exposed to GSK223112A. In addition to the fatty acids, thiazolidinediones and small molecule agonists mentioned, the double mutants were also tested against short chain fatty acids, pioglitazone, ciglitazone, GSK272235A and GSK269778A but no change in $[Ca^{2+}]_i$ was measured in cells transiently expressing the GPR40 double mutants.

The expression pattern of the GPR40 double mutants was compared to the wild type receptor by visualisation of eYFP fluorescence in cells transiently expressing the receptor of interest (Figure 5.18). GPR40 Lys⁶²Ala, Arg¹⁸³Ala-eYFP express in a similar fashion to the wild type receptor, with the receptor apparently expressed at the cell surface. GPR40 Lys⁶²Ala, His¹³⁷Ala and GPR40 His¹³⁷Ala, Arg¹⁸³Ala do not appear to be as well expressed at the plasma membrane as the wild type receptor.

5.5 Mutation of the region implicated in fatty acid chain length selectivity in GPR40 and GPR43

As detailed in section 5.1, there is a region in TM3 of GPR40 and GPR43 that may be important in determining the chain length of the fatty acids that can activate each of the receptors. To investigate this, initially the glycine triplet in GPR40 was mutated to code for Ser, Thr, Trp which is the corresponding region of GPR43, in the GPR40-eYFP fusion protein. To start to determine the fatty acids that could activate this receptor, the mutant,

GPR40 GGG⁹³⁻⁹⁵STW, was transiently expressed in HEK293T cells and tested for its ability to mediate a rise in $[Ca^{2+}]_i$ in single cells in response to three long chain fatty acids; palmitic acid (C16:0), lauric acid (C12:0) and oleic acid (C18:1) (Figure 5.19 (a-c)). As expected, wild type GPR40-eYFP was able to produce a large, transient rise in $[Ca^{2+}]_i$ upon the addition of the specified long chain fatty acid. The mutant, GPR40 GGG⁹³⁻⁹⁵STW-eYFP, showed little difference in its response to oleic acid or lauric acid, showing that it can still respond to long chain fatty acids. In contrast, the response to palmitic acid was greatly reduced compared to the wild type receptor, with only a very small change in $[Ca^{2+}]_i$ mediated by GPR40 GGG⁹³⁻⁹⁵STW-eYFP in response to the addition of 100 μ M palmitic acid. When investigating the ability of the mutant to respond to the short chain fatty acid propionate, it was found that 12% of positively transfected cells expressing GPR40-eYFP possessed the ability to generate a small release of $[Ca^{2+}]_i$ upon the addition of 10mM propionate (Figure 5.19 (d)). The GPR40 GGG⁹³⁻⁹⁵STW mutant produced a larger increase in $[Ca^{2+}]_i$ compared to the wild type receptor and the number of cells producing a rise in $[Ca^{2+}]_i$ greatly increased, with 38% of cells expressing GPR40 GGG⁹³⁻⁹⁵STW-eYFP responding to propionate. A bigger separation between the wild type GPR40 receptor and the GPR40 GGG⁹³⁻⁹⁵STW mutant was seen when investigating their ability to respond to acetate (Figure 5.20). None of the imaged cells expressing GPR40-eYFP generated a signal in response the addition of 10mM acetate, whereas in 35 cells expressing GPR40 GGG⁹³⁻⁹⁵STW-eYFP a change in $[Ca^{2+}]_i$ levels was observed. Expression of GPR40 GGG⁹³⁻⁹⁵STW was confirmed by visualisation of eYFP fluorescence in cells transiently expressing the receptor (Figure 5.21)

As the residues in TM3 of GPR40 were replaced by those in the corresponding region of GPR43, it was necessary to generate the equivalent mutations in GPR43. The region coding for the Ser, Thr, Trp triplet in GPR43 was not suitable for mutation to three Gly using the Stratagene mutagenesis approach. To overcome this, each residue was mutated in turn to Gly, starting with the most bulky residue, Trp in the GPR43-eYFP fusion protein. This gave three GPR43 mutants; GPR43 Trp⁹⁸Gly, GPR43 Thr⁹⁷Gly, Trp⁹⁸Gly, and GPR43 Ser, Thr, Trp⁹⁶⁻⁹⁸Gly, Gly, Gly. To investigate the fatty acid chain length selectivity of these mutants and to further investigate the fatty acids that could activate GPR40 GGG⁹³⁻⁹⁵STW, the FLIPR based Ca^{2+} assay was used to test a number of long and short chain fatty acids for their ability to mediate a rise in $[Ca^{2+}]_i$ (Table 5.8). Unlike in the single cell Ca^{2+} mobilization assay, short chain fatty acids were unable to activate GPR40 GGG⁹³⁻⁹⁵STW-eYFP. Of the medium and long chain fatty acids tested, caproic acid, palmitic acid, palmitoleic acid, elaidic acid and retinoic acid were unable to mediate a rise in $[Ca^{2+}]_i$ in cells expressing GPR40 GGG⁹³⁻⁹⁵STW-eYFP. The majority of the fatty acids

tested were able to activate this GPR40 mutant, with linoleic acid, linolenic acid and docosapentaenoic acid showing a reduced potency compared to the wild type receptor. Docosapentaenoic acid (C22:5) was the longest chain length fatty acid tested against this mutant and for it to activate the receptor, albeit with a reduced potency, indicates that this region does not confer all the chain length specificity of GPR40. In addition to the fatty acids, the thiazolidinediones and small molecule agonists were also tested against GPR40 GGG⁹³⁻⁹⁵STW-eYFP and none of these compounds were able to mediate a change in $[Ca^{2+}]_i$ levels via this mutant.

The GPR43 mutants showed a bigger change in the chain length of fatty acids that could activate them (Table 5.8). GPR43 Trp⁹⁸Gly-eYFP still retained the ability to mediate a rise in $[Ca^{2+}]_i$ in response to acetate and propionate but a change in $[Ca^{2+}]_i$ was also recorded upon the addition of linolenic acid, γ -linolenic acid, linoleic acid and docosapentaenoic acid. Each of these longer chain fatty acids were of similar potency at GPR43 Trp⁹⁸Gly-eYFP than at GPR40. Further mutation of the TM3 triplet, Thr⁹⁷Gly, Trp⁹⁸Gly, resulted in none of the short chain fatty acids being able to mediate a change in $[Ca^{2+}]_i$ in cells expressing GPR43 Thr⁹⁷Gly, Trp⁹⁸Gly-eYFP. But now upon the addition of three of the long chain fatty acids, a change in $[Ca^{2+}]_i$ was detected and potencies could be determined for myristic acid, palmitoleic acid and elaidic acid. Replacement of the Ser, Thr, Trp triplet of GPR43 with three Gly was very detrimental to the receptors ability to respond to any of the fatty acids tested. Only elaidic acid was now able to mediate a rise in $[Ca^{2+}]_i$ in cells expressing GPR43 Ser, Thr, Trp⁹⁶⁻⁹⁸Gly, Gly, Gly, with all other fatty acids seen as inactive. None of GPR43 TM3 mutants were able to respond to any of the thiazolidinediones or GPR40 small molecule agonists.

5.6 Discussion

GPR40, GPR41 and GPR43 have been shown to be activated by fatty acids of varying chain length. It is thought that a carboxylate group is required for activation of GPR40 as Itoh et al., (2003) showed that methyl linolate was unable to activate the receptor. Sequence alignment and homology modelling of GPR40, GPR41 and GPR43 identified residues within TM regions that were predicted to potentially play a role in binding the carboxylate group of an activating fatty acid. The residue proposed to play an important role in binding of fatty acids was a conserved Arg in TM5 (5.39) of all three receptor. Sequence alignment identified two further conserved residues that had the potential to form ionic interactions with the fatty acid; an Arg or Lys in TM2 (2.60) and a His in TM4

(4.56). To establish their relative importance, a series of mutations were introduced into all three receptors and their function assessed.

Removing the charge in TM5 of GPR41 and GPR43 by mutating the arginine to alanine abolished the ability of both receptors to generate a signal in response to short chain fatty acids. Conservation of the charge in GPR43 by inserting a Lys in place of the Arg also generated a receptor that was unable to respond to short chain fatty acids. The loss of function of the GPR43 TM5 mutants was assessed in the single cell Ca^{2+} mobilization assay and in the FLIPR based Ca^{2+} assay. For GPR41, the inability of the TM5 mutant to respond to fatty acids was confirmed in the single cell Ca^{2+} mobilization assay and a [^{35}S]GTP γ S binding assay. This indicates that in GPR41 and GPR43, the conserved Arg in TM5 is absolutely necessary to allow activation of the receptor by fatty acid.

The requirement of a positively charged residue has been observed in other GPCRs whose ligands contain carboxylate groups. These include the high affinity nicotinic acid receptor, HM74A, in which Tunaru et al. (2005) demonstrated that an Arg in TM3 (3.35) of the receptor was absolutely required for binding of nicotinic acid and the human prostacyclin receptor in which the mutation of an Arg in TM7 (7.44) to Ala prevented binding of a synthetic agonist (Stitham et al., 2003). The requirement of positively charged residues to bind a carboxyl containing ligand was also observed for the receptor for succinate, GPR91. In GPR91, four positively charged residues are required for activation of the receptor, with an Arg (3.29) and His (3.33) in TM3 and an Arg in both TM6 (6.55) and 7 (7.49) proposed to bind the dicarboxylate groups of succinate (He et al., 2004).

Although the Arg in TM5 is conserved in GPR40, GPR41 and GPR43, unlike in GPR41 and GPR43 it is not a requirement to allow fatty acid activation of GPR40. Replacement of the Arg in TM5 of GPR40 with Ala gave a mutant receptor that was still able to respond to a range of fatty acids. In the range of fatty acids that were tested against this receptor, differing effects were observed, with a reduction in potency observed with some fatty acids, no change in potency detected for others and for three fatty acids a complete loss of potency recorded. In contrast to the ability of this mutant to respond to certain fatty acids, none of the thiazolidinediones or small molecule agonists were able to activate the mutant. The additional mutation of the His in TM4 of GPR40 resulted in a receptor that was unable to respond to the range of saturated fatty acids tested and only retained the ability to respond to certain unsaturated fatty acids. However, the introduction of the Lys⁶² to Ala mutation into GPR40 Arg¹⁸³Ala, appeared to restore the ability of the receptor to respond to some of the fatty acids and synthetic agonists. This suggests that there are other

residues important in the binding of agonists to GPR40 and its subsequent activation. This is similar to the finding by Sabirsh et al. (2006) on BLT₁, whereby an Arg in TM5 (5.35) was shown to be important in binding the carboxyl group of leukotriene B₄ but not essential. It was found that the Arg in TM5 of BLT₁ along with a Glu (5.42) were likely to bind the hydroxyl group in the ligand rather than the carboxyl head group. The recent description of a range of small molecule agonists at GPR40 found that a carboxyl group was not required (Garrido et al., 2006), although this was not confirmed in this study (see Chapter 4). Therefore, the results from the mutation of the TM5 Arg in GPR40 are not entirely unexpected when this is taken into consideration.

Many studies have shown that for most small molecule receptors, such as those for the biogenic amines, the binding sites are contained in a binding crevice formed by the TM helices. The TM helices that make up the binding sites are TM 3, 4, 5, 6 and 7 (Ji et al., 1998; Gether, 2000; Shi and Javitch et al., 2002; Stenkamp et al., 2002). Within the biogenic amine receptors, an aspartic acid residue in TM3 (3.32) is conserved and it has been proposed to interact with the positively charged head groups of the ligands for the adrenergic receptors (Strader et al., 1991), dopamine receptors (Mansour et al., 1992), histamine receptors (Gantz et al., 1992) and muscarinic acetylcholine receptors (Spalding et al., 1994). It is starting to appear that receptors for ligands containing a carboxylate group have a similar requirement for a charged residue, but unlike the biogenic amine receptors it is not conserved within a specific TM region.

Without the availability of a ligand binding assay for GPR40, GPR41 or GPR43, it is impossible to say if the fatty acids or synthetic ligands are binding the mutant receptors. It may be that they bind the mutant receptors but the receptor is no longer able to translate the binding of a ligand into a signal or that the mutant receptors can no longer bind the ligand. Therefore, the results of the mutagenesis studies can only indicate that a residue is required or important for activation rather than ligand binding.

To confirm the importance of the TM5 Arg in fatty acid mediated activation of GPR41 and GPR43, it was necessary to investigate the role of the other conserved TM basic residues. It was found that upon mutation of the TM4 His to Ala in GPR41 and GPR43, the mutant receptors responded to short chain fatty acids in a manner similar to the wild type receptor. By determining potencies of short chain fatty acids at GPR43 His¹⁴⁰Ala using the FLIPR based Ca²⁺ mobilization assay, it was found that the potency of propionate was reduced but in addition, the mutant was now capable of responding to two medium chain fatty acids, caproic and caprylic acid. The reduction in potency of short chain fatty acids and gain of

potency for medium chain fatty acids at this mutant taken together indicates that this residue of GPR43 may play a role in fatty acid chain length selectivity. This alteration in fatty acid chain length selectivity was not investigated in the equivalent GPR41 mutant due to time constraints, although no reduction in potency of propionate was observed in the [³⁵S]GTPγS binding assay. The effects of mutating the TM4 His in GPR41 and GPR43, was not entirely mirrored by the equivalent mutation in GPR40. When examining the potencies of a range of fatty acids, it was found that GPR40 His¹³⁷Ala was unable to respond to some of the long chain fatty acids tested. Interestingly, no response was observed upon challenge of the mutant receptor with the three shortest chain length fatty acids that were able to activate the wild type receptor, which again may suggest that this TM region may play a role in chain length selectivity. It may be that upon the mutation of the Arg in TM5 of GPR40, His¹³⁷ compensates for the loss of charge and vice versa, as in the model of GPR40 both His¹³⁷ and Arg¹⁸³ are found within the putative binding pocket for fatty acids as demonstrated by Figure 5.2. In addition to the loss of potency for some fatty acids, GPR40 His¹³⁷Ala was unable to respond to any of the synthetic agonists tested. This supports the observation that a series of residues are likely important in the activation of GPR40 by fatty acids.

From the models of GPR43 and GPR40, the TM2 positively charged residue that is conserved in the family was not predicted to act as a charge partner for the carboxylate containing ligands. Therefore, the function of the GPR41 and GPR43 mutants, where the Lys or Arg was replaced by Ala, was unexpected. In the single cell Ca²⁺ assay it was found that both GPR41 and GPR43 TM2 mutants were not as efficacious as the wild type receptors in the mobilization of [Ca²⁺]_i. In the FLIPR based Ca²⁺ mobilization assay, GPR43 Lys⁶⁵Ala was unable to generate a large enough rise in [Ca²⁺]_i for it to be measured by the FLIPR, therefore potencies against fatty acids could not be determined. The only potency data for this mutation in GPR41 or GPR43 was generated using the GPR41-Gα_{i3} Cys³⁵¹Ile fusion protein containing the Arg⁷¹Ala mutation. Using this fusion protein, the potency of propionate was shown to be reduced at this mutant and it appeared to be much less efficacious in its ability to increase [³⁵S]GTPγS binding, although the relative amounts of each receptor were not monitored. For GPR43 Lys⁶⁵Ala, the most striking difference from the wild type receptor was its inability to mediate a rise in [Ca²⁺]_i in response to butyrate. In the single cell Ca²⁺ experiments it was shown that the mutant receptor when challenged with butyrate was unable to generate a rise in [Ca²⁺]_i but the same cells still retained the ability to mediate a rise in [Ca²⁺]_i when challenged with acetate or propionate. This demonstrates that the Lys is not providing a charge partner for the carboxylic acid. It

is possible that butyrate may now act as an antagonist at GPR43 Lys⁶⁵Ala but as the mutant was unable to generate a signal in the FLIPR based assay this was difficult to assess. As shown in Figure 5.3, the Lys/Arg in TM2 was predicted on the basis of homology models to not be available to co-ordinate the carboxylate group of the fatty acids. It is possible that mutation of this residue affects the receptors trafficking to the cell surface but this is hard to determine from the visualisation of eYFP fluorescence. Further work would have to be carried out to determine their cell surface expression in comparison to the wild type receptor. The models of GPR41 and GPR43 are homology models based on the crystal structure of rhodopsin. It is possible that this is one of the regions of the receptors that may differ considerably between family A receptors and may be more exposed to the proposed binding site than predicted from the model.

GPR42 is a non-functional pseudo-gene which shares 98% homology with GPR41, and only differs by six residues. Brown et al., (2003) undertook a study to replace the residues in rat GPR41(rGPR41) with the corresponding residues in human GPR42. They found that mutation of Arg¹⁷⁰ in rGPR41 to Trp, which corresponds to position 174 in the human receptor, resulted in a receptor unable to respond to short chain fatty acids. They suggested that this residue may form a salt bridge with the carboxylate group of the fatty acids. This residue is found in extracellular loop 2 and is unlikely to form the binding site for the receptor as the majority of small molecule family A GPCRs have the binding site within the transmembrane regions of the receptor. Although it is thought that GPR40-43 act similarly to the small molecule GPCRs, other receptors within family A, such as opioid and chemokine receptors, have been shown to bind their ligands within their extracellular domains. In addition to this proposed role for residues in extracellular regions for ligand binding, the crystal structure of rhodopsin revealed that extracellular loops form a compact lid that enclose the covalently bound retinal and some of these residues, especially residues in extracellular loop 2, are in close contact with the retinal molecule (Palczewski et al., 2000). Further studies will need to be carried out to determine the role of this residue within GPR41. Figure 5.22 shows the positions of the residues that differ between GPR41 and GPR42 and none of the residues are found around the proposed ligand binding site of GPR41.

The mutation of the TM2 Lys in GPR40 also effected the receptor's function but not to as large an extent than in GPR41 and GPR43. Using the FLIPR based assay the potencies of a range of fatty acid and synthetic ligands were determined at GPR40 Lys⁶²Ala-YFP. Only two of the fatty acids were unable to activate this mutant although a reduction of potency was recorded for a large proportion of the fatty acids. Unlike the two other

GPR40 single mutants, GPR40 Lys⁶²Ala retained the ability to mediate a rise in $[Ca^{2+}]_i$ in response to two of the small molecule agonists. Using the [³⁵S]GTP γ S binding assay it was confirmed that the introduction of this mutation into the GPR40-G α_q fusion protein resulted in a receptor that was activated in a concentration dependent by GSK250089A albeit with a reduction in potency. It was also found that troglitazone was able to activate this mutant. The introduction of the Lys⁶²Ala into the GPR40 His¹³⁷Ala or GPR40 Arg¹⁸³Ala single mutants resulted in an apparent restoration of the some of the function of the single mutant receptors. The large effect observed upon the mutation of both His¹³⁷ and Arg¹⁸³ in GPR40 and the lesser effects seen upon the mutation of Lys⁶² along with either of these mutations supports the theory that His¹³⁷ and Arg¹⁸³ play a key role in the activation of the receptor. In the model for GPR40 Lys⁶² is not shown to form part of the ligand binding domain and the mutagenesis studies go some way in supporting this.

Considering all the data it appears that the residues important in activation of GPR41 and GPR43 by short chain fatty acids are similar, with the Arg in TM5 critical for activation of the receptors. It also shows that the Arg or Lys in TM2 plays a role in activation of the receptor but it does not provide a charge partner for the carboxylate group of the fatty acids. The data on GPR40 indicates a different model for ligand induced activation of the receptor. The receptor does not required the TM5 Arg for activation by fatty acids and it is likely that there will be a scaffold of important residues in the ligand binding pocket that allow fatty acids to bind. The His residue in TM4 appears to have a role within the binding pocket of the receptor and may affect the fatty acid chain length selectivity of the receptor. Unlike GPR41 and GPR43, the Lys in TM2 does not appear to play as large a role in GPR40. The data on the GPR40 mutants also suggests that a more rigid binding pocket is required for activation by the small molecule agonists or thiazolidinediones, as both the His¹³⁷Ala and Arg¹⁸³Ala mutants were unable to respond to any of the synthetic agonists.

The thiazolidinediones are established agonists of PPAR γ but as shown by Kotarsky et al., (2003) and in this study, certain members of the family can act as agonists at GPR40. PPAR γ can also be activated by fatty acids such as linoleic acid (Kliwer et al., 1997). The structure of the ligand binding domain (LBD) of PPAR γ has been extensively studied (Nolte et al., 1998, Uppenberg et al., 1998, Gamp et al., 2000, Lu et al., 2006). The ligand binding site contained within the LBD is mainly hydrophobic. X-ray crystallography studies on the LBD of PPAR γ with rosiglitazone docked has shown that the ligand makes several specific interactions, including hydrogen bonding with two His residues (Nolte et al., 1998). Tyr⁴⁷³ has also been shown to form hydrogen bonds with rosiglitazone (Lu et

al., 2006) and mutation of this residue results in the receptor being unable to respond to thiazolidinediones (Sarraf et al., 1999). The His residues have been predicted to make interactions with the carboxylic head group of fatty acids ligand of PPAR γ . The hydrophobic chain of the fatty acid is likely to interact in a non-specific manner with the rest of the binding pocket (Nolte et al., 1998). Tsukahara et al (2005) demonstrated that the residues important in binding of an analogue of lysophatidic acid (1-*O*-octadecenyl-2-hydroxy-*sn*-glycer-3-phosphate) differed from those important in the binding of rosiglitazone. The data on PPAR γ demonstrates that the binding of synthetic ligands, such as the thiazolidinediones, is more specific than the binding of fatty acids. This is similar to the finding with GPR40, as mutations that only slightly impair the receptors ability to respond to fatty acids (i.e. His¹³⁷Ala and Arg¹⁸³) render the receptor unable to respond to thiazolidinediones or small molecule agonists. Figure 5.23 shows the position of two further residues, Tyr⁹¹ and Phe¹⁹¹, which are found in close proximity to the small molecule agonist when docked into GPR40. They may play a role in stabilising the binding of an agonist into the receptor as they are close enough to interact with the small molecule agonist when co-ordinated by the Arg in TM5. If the ligand binding properties of GPR40 and PPAR γ are similar then they could act in a similar manner to Tyr⁴⁷³ of PPAR γ and be critical in binding of a ligand and the activation of GPR40.

The current study also aimed to address the possible determinants of fatty acid chain length selectivity of GPR40 and GPR43. A triplet of residues in TM3 of both receptors was predicted from modelling to only allow long chain fatty acids to activate GPR40 and short chain fatty acids to activate GPR43. Single cell Ca²⁺ mobilization experiment indicated that the GPR40 mutant in which its glycine triplet had been replaced by the equivalent region of GPR43 was now able to mediate a rise in [Ca²⁺]_i in response to acetate. It was found that the wild type receptor did possess some ability to mediate a rise in [Ca²⁺]_i when challenged with propionate. Stewart et al., (2006) showed that *Xenopus* oocytes expressing mouse GPR40 were able to generate a rise in [Ca²⁺]_i measured by voltage clamp recordings in response to the addition of 500 μ M butyrate. They also found that acetate or propionate were unable to generate a release of [Ca²⁺]_i. The increase in sensitivity of measuring [Ca²⁺]_i release by voltage clamping, as with the single cell [Ca²⁺]_i assay utilised in this study, may expose the very slight ability of GPR40 to respond to short chain fatty acid that can not be observed using a FLIPR based Ca²⁺ release method or in a [³⁵S]GTP γ S binding study. Butyrate was not tested in this study for its ability to mediate a rise in [Ca²⁺]_i in single cells. When attempting to confirm the change in fatty acid chain length selectivity in the FLIPR based Ca²⁺ release assay, no signal could be detected upon

the addition of any of the short chain fatty acids. It was therefore difficult to draw any conclusions about the change in fatty acid chain length selectivity of GPR40 GGG⁹³⁻⁹⁵STW. From the data on GPR40 GGG⁹³⁻⁹⁵STW from the single cell Ca²⁺ experiments, it is possible that acetate (or any of the other short chain fatty acids) may occupy the wild type receptor binding site but is unable to activate the receptor. The Gly triplet in GPR40 is found within the base of the proposed binding pocket so with the substitution with Ser, Thr, Trp allows the short chain fatty acids to now activate the receptor. This leads to the suggestion that short chain fatty acids may antagonise wild type GPR40 but this has not been examined. To support the theory that the synthetic ligands require a more conserved ligand binding pocket in GPR40, none of the synthetic agonists were able to activate GPR40 GGG⁹³⁻⁹⁵STW. The equivalent mutation in GPR43 gave some interesting results. Due to difficulties in mutating all three residues, three mutants were made and all were tested in their ability to mediate a rise in [Ca²⁺]_i in a FLIPR based assay system. The data was not very clear but suggested that this region may confer the fatty acid chain length selectivity of GPR43 but it is likely that other regions of the receptor are also important. Further experiments need to be carried out to determine the full pharmacology of these receptors as it is possible that the longer chain fatty acid can activate the receptor but the signal generated is too small to be detected by the FLIPR.

It is important to note that the inability of some of the fatty acids and synthetic ligands to activate the mutants in the FLIPR based assay system may reflect a reduction in efficacy of the ligands rather than a loss of potency. This is difficult to assess as the mutant receptors were transiently expressed therefore expression levels may vary greatly. This is demonstrated by the inability of troglitazone to mediate a rise in [Ca²⁺]_i in the FLIPR based assay at GPR40 Lys⁶²Ala but in the [³⁵S]GTPγS assay activation of the mutant receptor could be detected. As mentioned previously, the FLIPR assay system is not very sensitive and to fully assess the function of the mutant receptors a combination of techniques would have to be utilised.

Considering all the data, I would propose that short chain fatty acids bind in a similar fashion to GPR41 and GPR43, but this differs from the way fatty acids bind GPR40. The models of each of the receptor will have to be revised to take into account of the results of the mutagenesis studies. A fuller understanding of the particular residues that constitute the ligand-binding pocket will be useful in determining any unusual features the receptors may contain and assist in the development of receptor specific ligands.

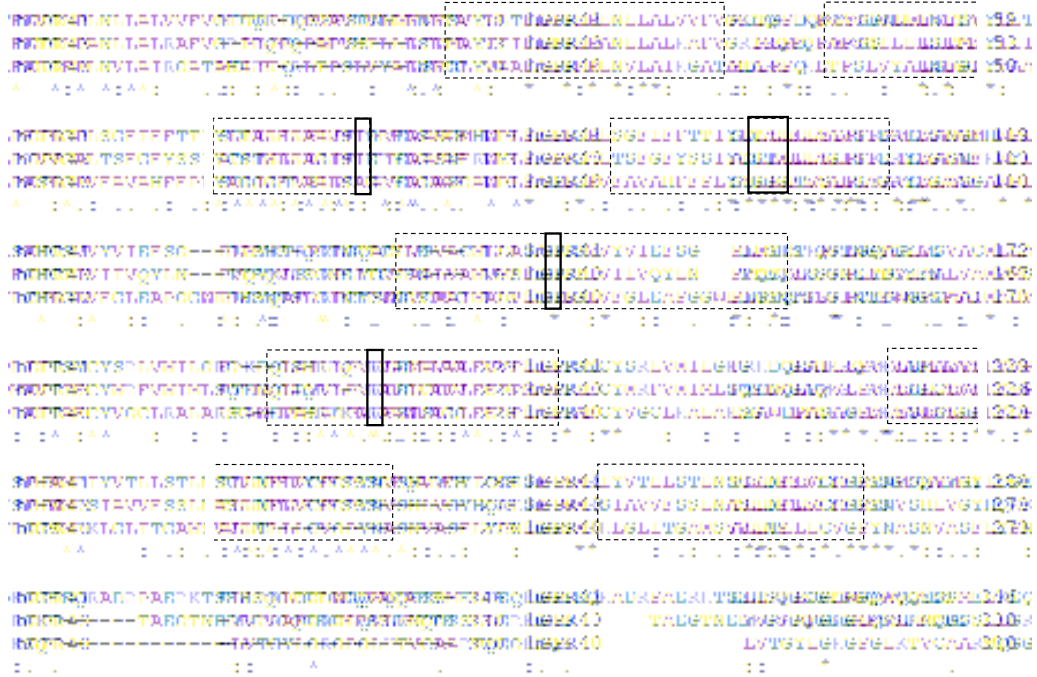
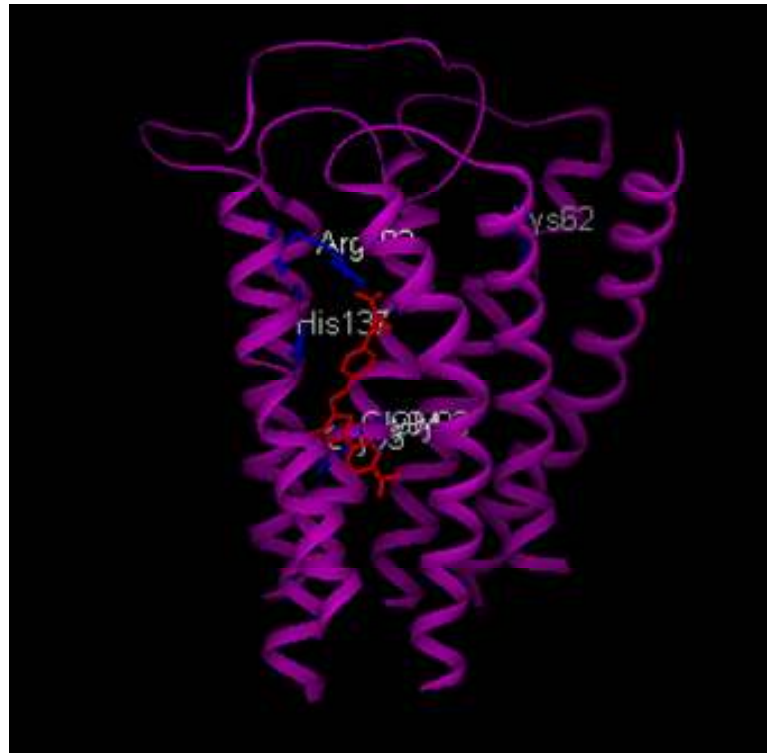


Figure 5.1 Amino acid sequence alignment of GPR40, GPR41 and GPR43

Amino acid sequences corresponding to human GPR40, GPR41 and GPR43 were aligned using the ClustalX algorithm. Residues are coloured as follows; small and hydrophobic residues are coloured red, acidic residues coloured blue, basic residues coloured magenta, hydroxyl and amine containing residues are coloured green. Transmembrane regions are boxed with a dashed line. Conserved basic transmembrane residues and an area within TM3 proposed to confer fatty acid chain length specificity are boxed with a continuous line. Accession numbers are as follows: human GPR40, NP005294; human GPR41, NP005295; human GPR43, NP005297.

(a)



(b)

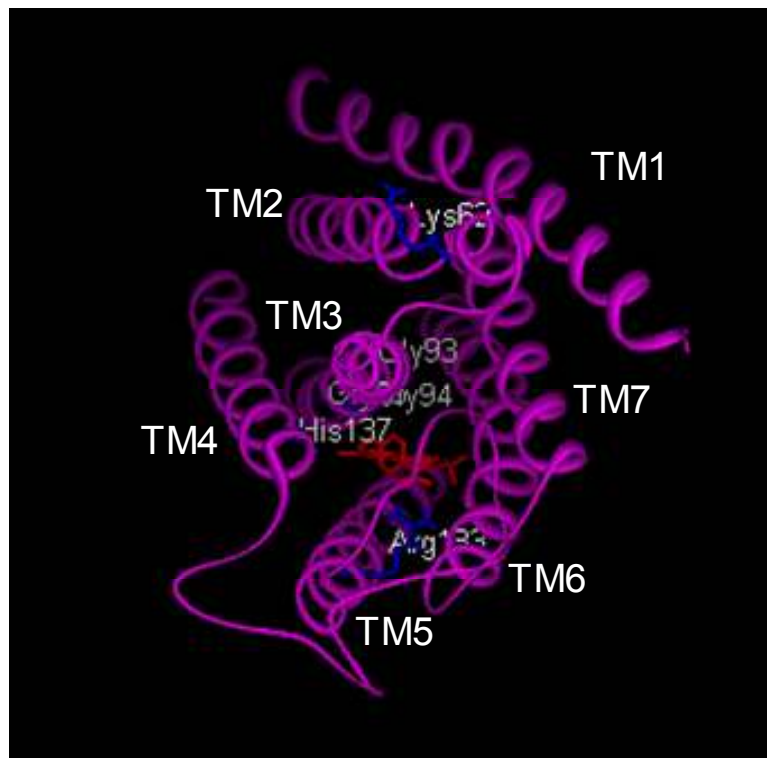
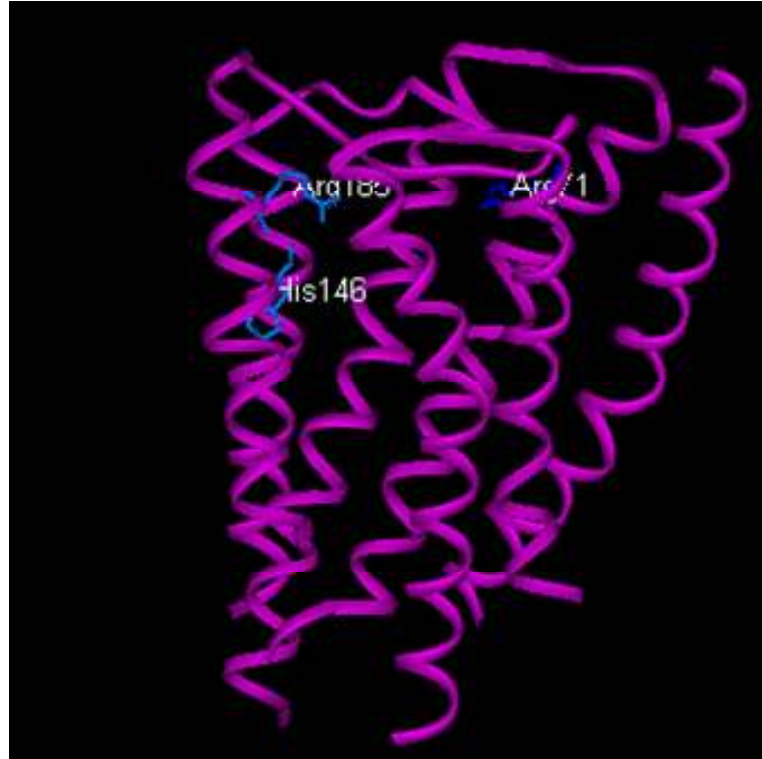


Figure 5.2 GPR40 homology model with a small molecule agonist docked in the proposed binding site

The homology model of GPR40 was generated by GlaxoSmithKline using the GPCR_Builder programme based on the crystal structure of rhodopsin. GPR40 was aligned with rhodopsin on the basis of highly conserved residues found in family A GPCRs. The model shows the residues that might be important in forming a salt bridge with fatty acid agonists; Lys⁶², His¹³⁷ and Arg¹⁸³ (coloured blue). It also shows a synthetic small molecule agonist (coloured red) co-ordinated by Arg¹⁸³ and a triplet of Gly residues in TM3. (a) view from the side of the membrane and (b) view from above the membrane with TM helices numbered 1-7.

(a)



(b)

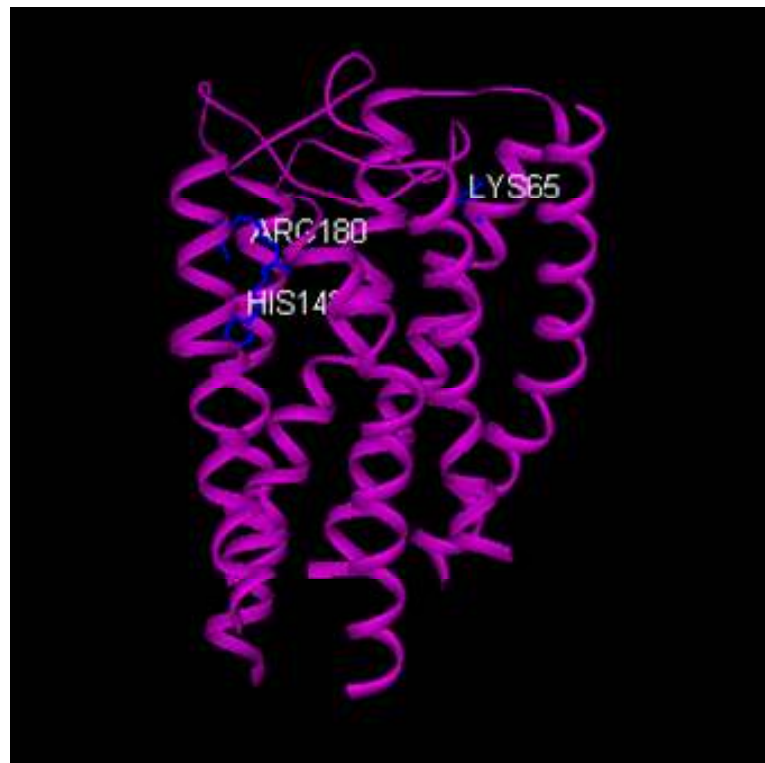
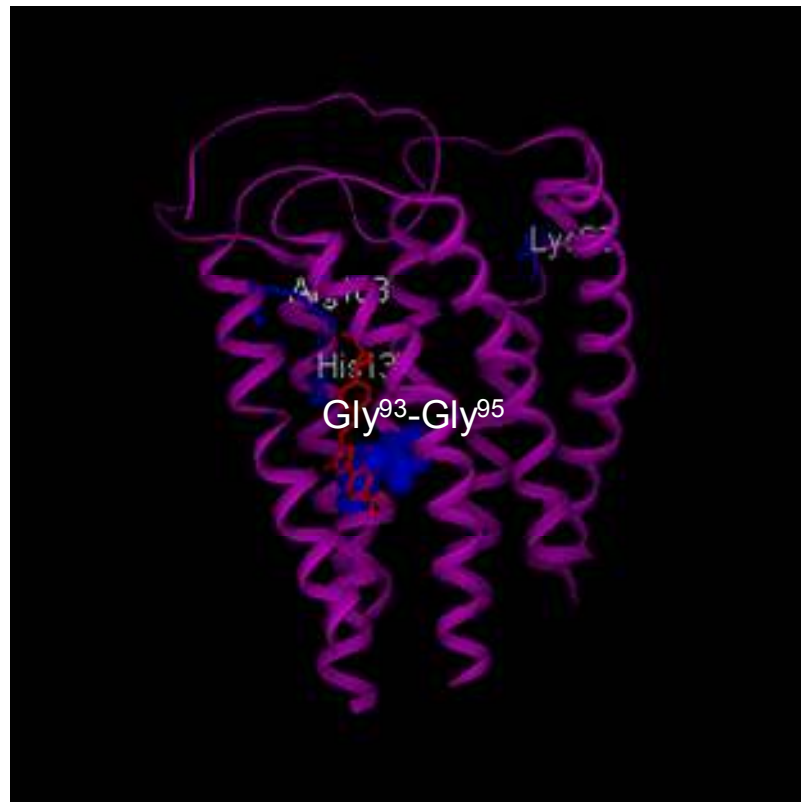


Figure 5.3 GPR41 and GPR43 homology models

The homology models of GPR41 (a) and GPR43 (b) were generated by GlaxoSmithKline using the GPCR_Builder programme based on the crystal structure of rhodopsin. GPR41 and GPR43 were aligned with rhodopsin on the basis of highly conserved residues found in family A GPCRs. (a) GPR41 viewed from the side of the membrane. The model shows the residues implicated in forming a salt bridge with the fatty acid agonists; Arg⁷¹, His¹⁴⁶ and Arg¹⁸⁵ (coloured blue). (b) GPR43 viewed from the side of the membrane. The model shows the residues implicated in forming a salt bridge with the fatty acid; Lys⁶⁵, His¹⁴⁰ and Arg¹⁸⁰

(a)



(b)

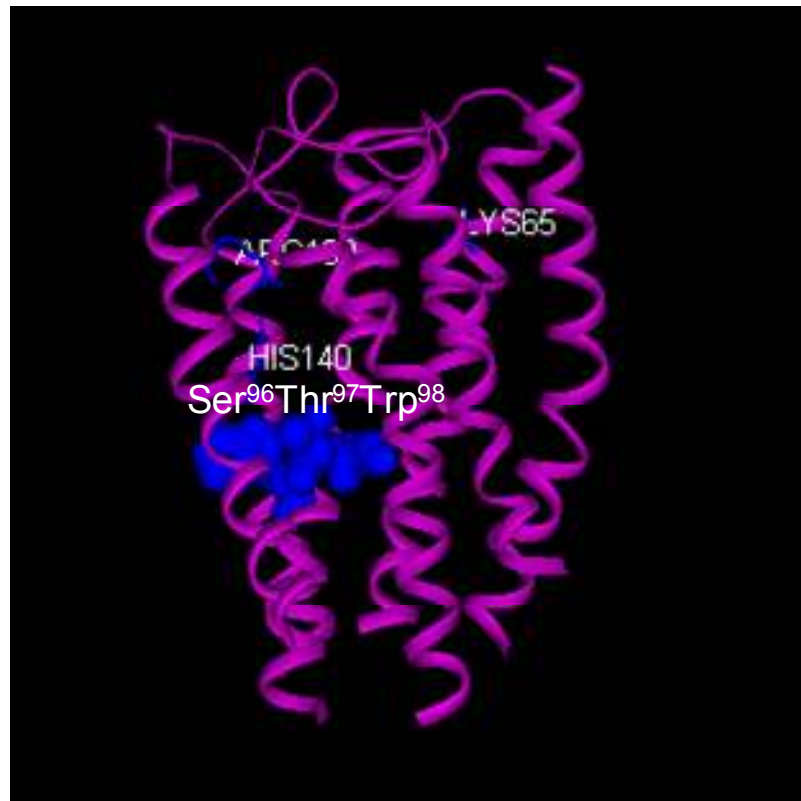


Figure 5.4 GPR40 and GPR43 homology models showing position of TM3 triplet implicated in fatty acid chain length selectivity

The homology models of GPR40 (a) and GPR43 (b) were generated by GlaxoSmithKline using the GPCR_Builder programme based on the crystal structure of rhodopsin. GPR40 and GPR43 were aligned with rhodopsin on the basis of highly conserved residues found in family A GPCRs. (a) GPR40 viewed from the side of the membrane. The model shows the residues implicated in forming a salt bridge with fatty acid agonists (blue sticks) as detailed in Figure 5.2 and Gly⁹³, Gly⁹⁴ and Gly⁹⁵ (blue space-filled residues). (b) GPR43 viewed from the side of the membrane. The model shows the residues implicated in forming a salt bridge with the fatty acid (blue sticks) as detailed in Figure 5.3 and Ser⁹⁶, Thr⁹⁷ and Trp⁹⁸ (blue space-filled residues).

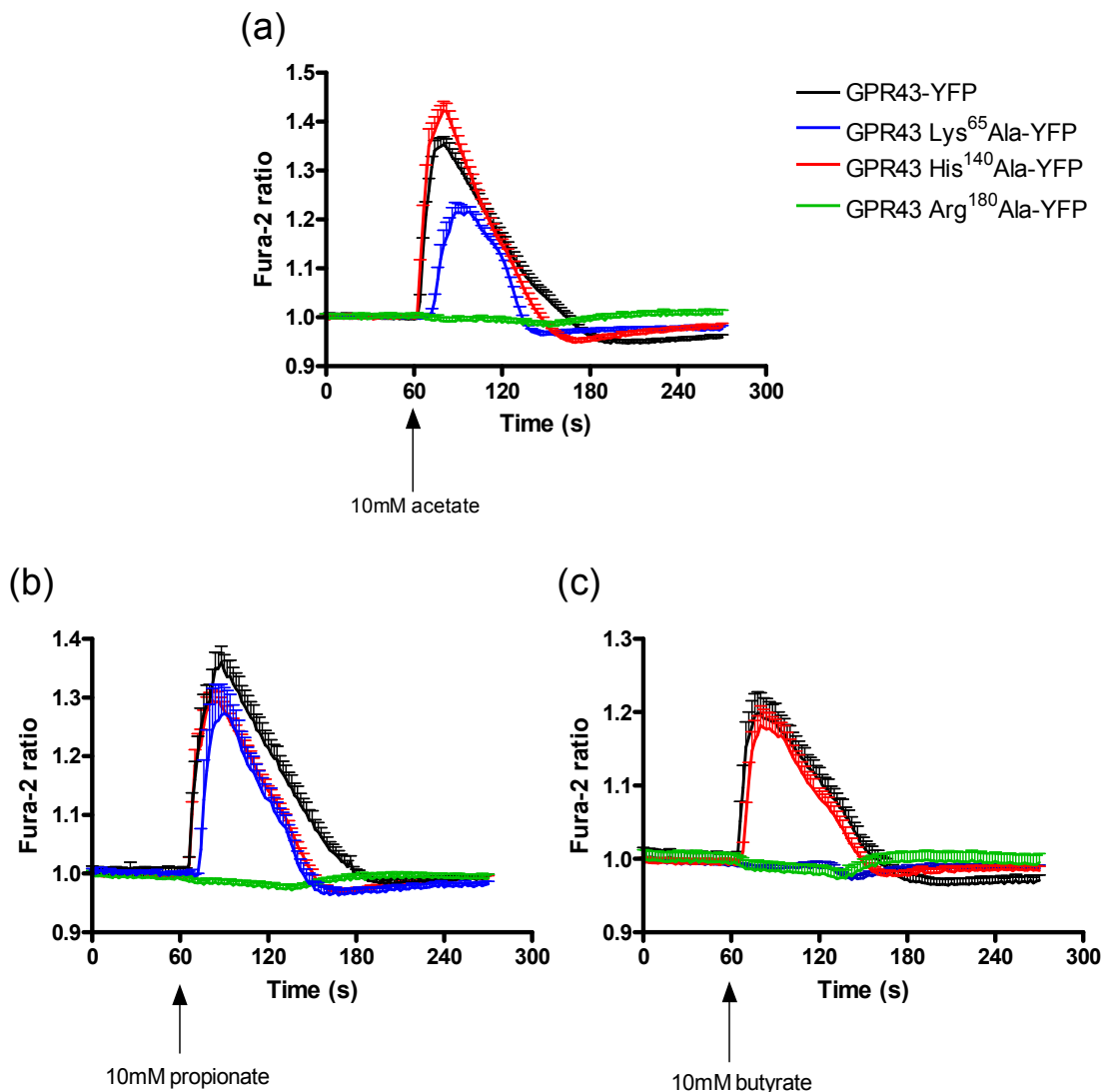


Figure 5.5 Effect of mutation of three conserved basic residues in GPR43 on the ability to mediate a rise in $[Ca^{2+}]_i$ in response to short chain fatty acids

Using the Stratagene Quikchange method of mutagenesis, three GPR43 mutants were generated. HEK293T cells were transiently transfected to express GPR43-eYFP (black line), GPR43 Lys⁶⁵Ala-eYFP (blue line), GPR43 His¹⁴⁰Ala-eYFP (red line) or GPR43 Arg¹⁸⁰Ala-eYFP (green line). Following loading with Fura-2, changes in fluorescence were measured upon the addition of 10mM (a) acetate, (b) propionate or (c) butyrate at the 60s time point. Images were collected every 2s for a total of 300s. Data represents means \pm SEM for at least 20 positively transfected cells selected on the basis of eYFP fluorescence.

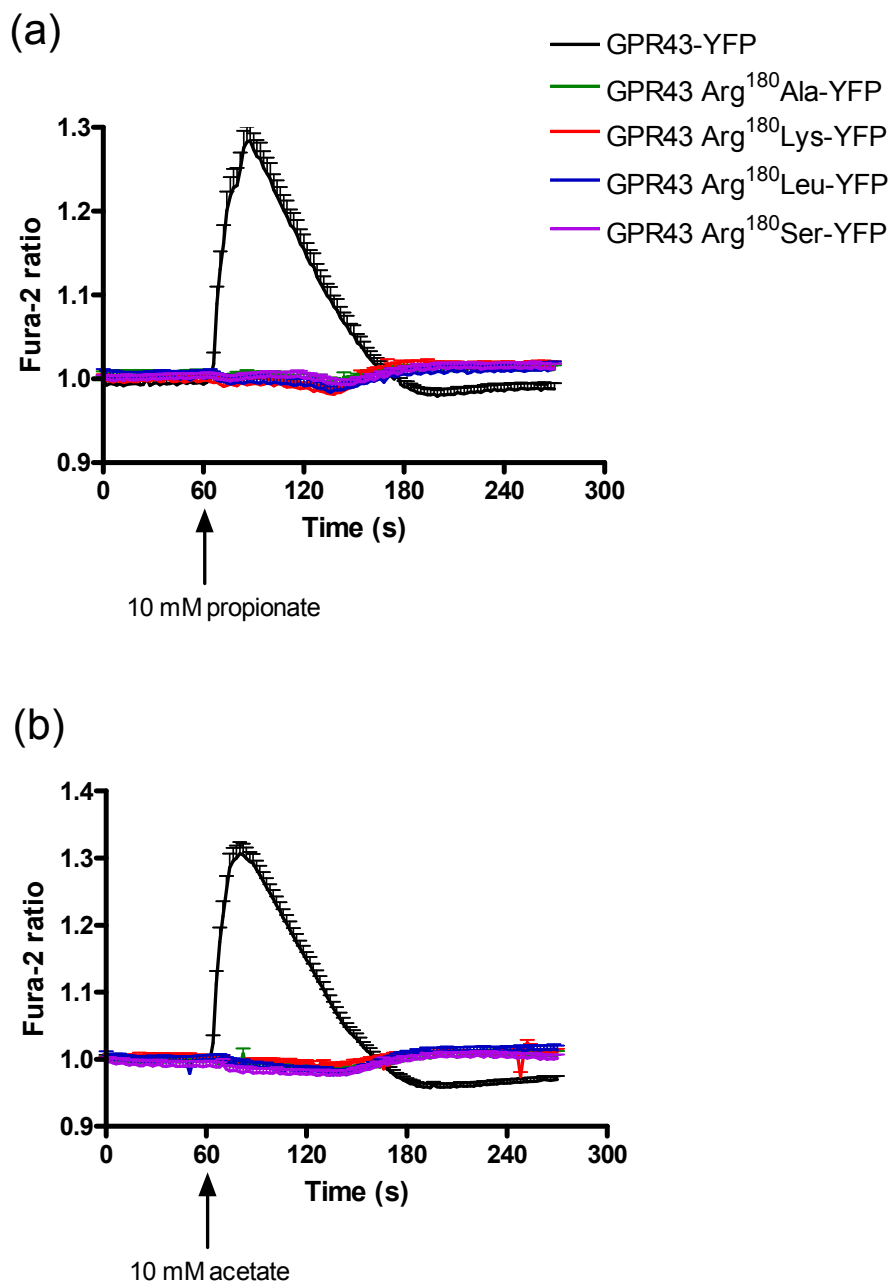


Figure 5.6 Arginine is required at position 180 in GPR43 to allow the receptor to respond to short chain fatty acids

HEK293T cells were transiently transfected to express GPR43-eYFP (black line), GPR43 Arg¹⁸⁰Ala-eYFP (green line), GPR43 Arg¹⁸⁰Lys-eYFP (red line), GPR43 Arg¹⁸⁰Leu-eYFP (blue line) or GPR43 Arg¹⁸⁰Ser-eYFP (purple line). Cells were loaded with the Ca²⁺ sensitive dye, Fura-2 and changes in fluorescence monitored in response to 10mM (a) propionate or (b) acetate added at the 60s time point. Images were collected every 2s for a total of 300s. Data represents means \pm SEM for at least 20 positively transfected cells selected on the basis of eYFP fluorescence.

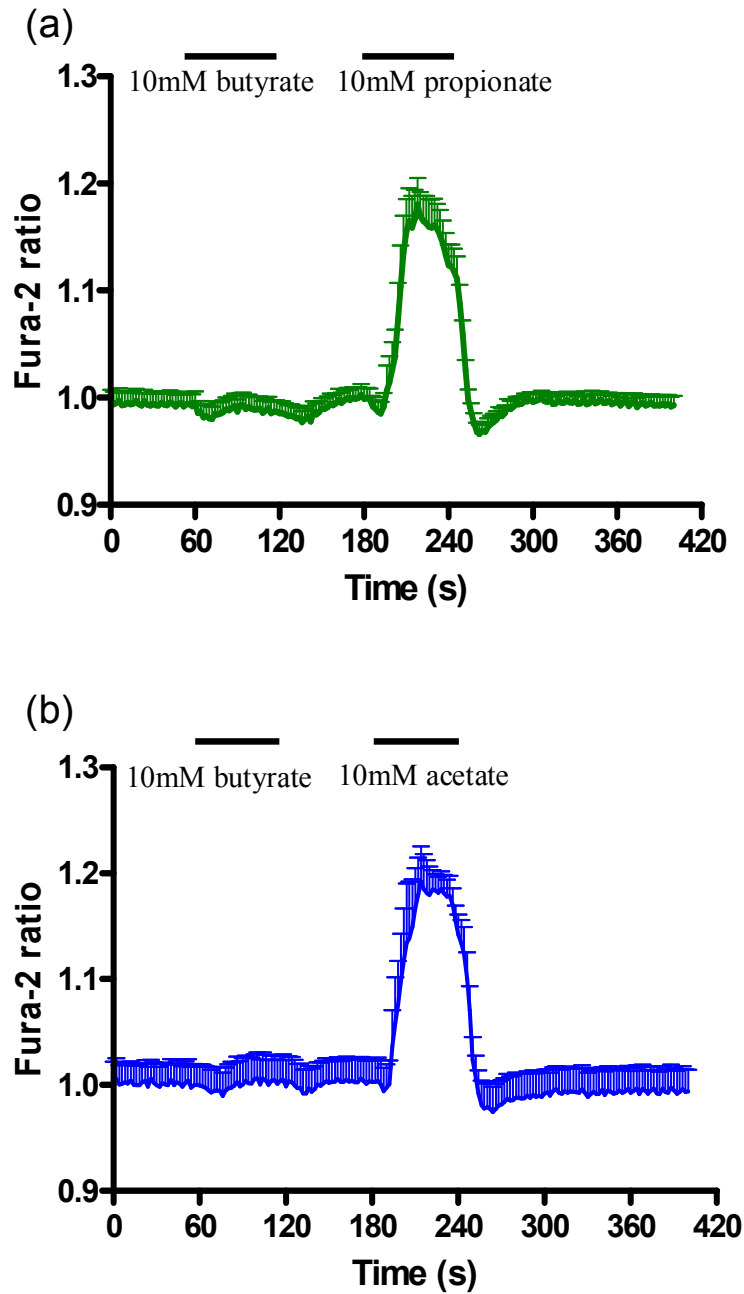


Figure 5.7 GPR43 Lys⁶⁵Ala has lost the ability to mediate a rise in $[Ca^{2+}]_i$ when challenged with butyrate but retains the ability to respond to acetate or propionate

GPR43 Lys⁶⁵Ala-eYFP was transiently transfected into HEK293T cells grown on coated coverslips. Cells were loaded with Fura-2 and changes in fluorescence measured. Cells were exposed to 10mM butyrate at the 60s time point for 60s and then to 10mM (a) propionate or (b) acetate at the 180s time point for 60s. Images were collected every 2s for a further 180s. Data represents means \pm SEM from at least 20 positively transfected cells selected on the basis of eYFP fluorescence.

	GPR43	GPR43 Lys⁶⁵Ala	GPR43 His¹⁴⁰Ala	GPR43 Arg¹⁸⁰Ala
Formate	2.8±1.0	inactive	inactive	inactive
Acetate	4.6±0.2	inactive	4.0±0.1 *	inactive
Propionate	4.9±0.2	inactive	4.2±0.7	inactive
Butyrate	4.4±0.5	inactive	3.6±1	inactive

	GPR43 Arg¹⁸⁰Lys	GPR43 Arg¹⁸⁰Leu	GPR43 Arg¹⁸⁰Ser
Formate	inactive	inactive	inactive
Acetate	inactive	inactive	inactive
Propionate	inactive	inactive	inactive
Butyrate	inactive	inactive	inactive

Table 5.1 Potency of various short chain fatty acids at GPR43 mutants

HEK293 MSRII cells were transiently transfected to express the GPR43-eYFP or the indicated GPR43 mutant. 24h post transfection cells were seeded at 15,000 cells per well into 384 well microtitre plates. Cells were loaded with the Ca²⁺ sensitive dye, Fluo-4. Changes in intracellular calcium levels were measured using the FLIPR apparatus following challenge with the required short chain fatty acid added at the 10 second time point and data was collected for a further 110 seconds. Data represent mean±SEM of pEC₅₀ values from three individual experiments performed in duplicate. Data was analysed using Students paired T-test (GraphPad Prism 4). Means were compared to wild type GPR43, * = p<0.05.

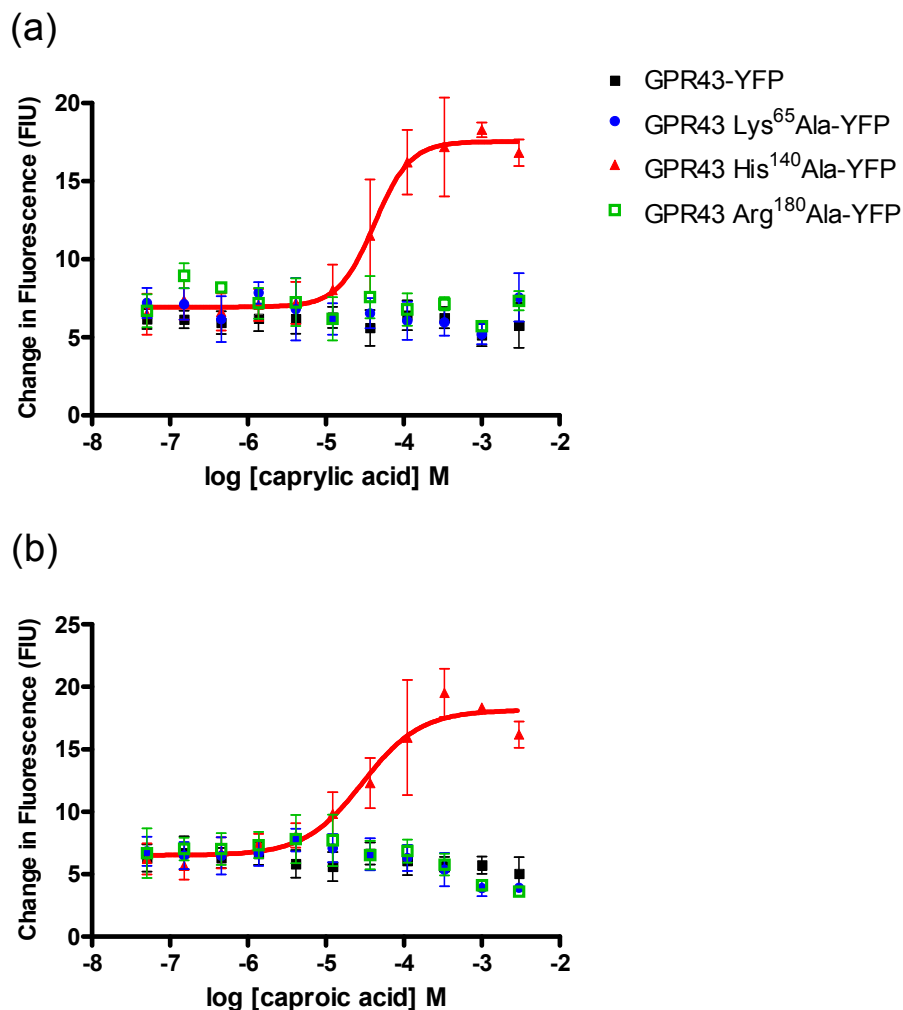
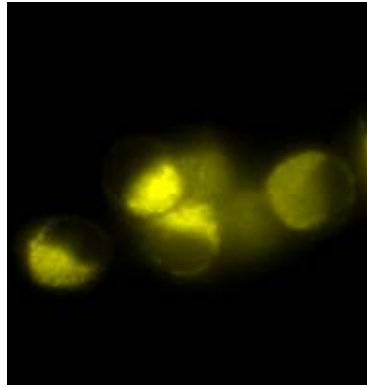


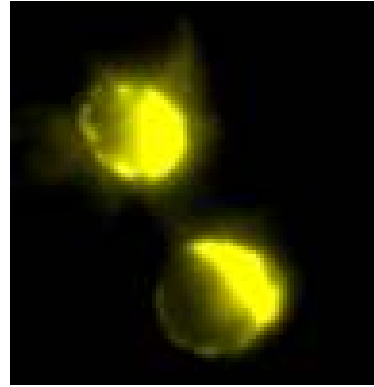
Figure 5.8 GPR43 His¹⁴⁰Ala has gained the ability to generate a rise in $[Ca^{2+}]_i$ in response to caproic acid and caprylic acid

HEK293 MSRII cells were transiently co-transfected to express GPR43-eYFP (black squares), GPR43 Lys⁶⁵Ala-eYFP (blue circles), GPR43 His¹⁴⁰Ala-eYFP (red triangles) or GPR43 Arg¹⁸⁰Ala-eYFP (green open squares) with a G protein cocktail. 24h post transfection cells were seeded at 15,000 cells per well into 384 well microtitre plates. Changes in intracellular calcium levels were measured using the FLIPR apparatus following challenge with increasing concentrations of (a) caprylic acid or (b) caproic acid added at the 10 second time point and data collected for a further 110 seconds. Graph shown are representative of data obtained from three individual experiments performed in duplicate. Data points represent means \pm SEM.

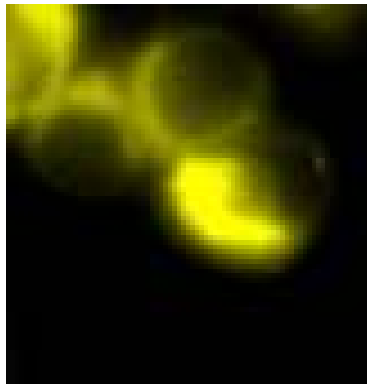
(a)



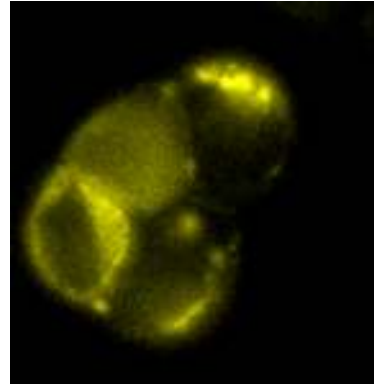
(b)



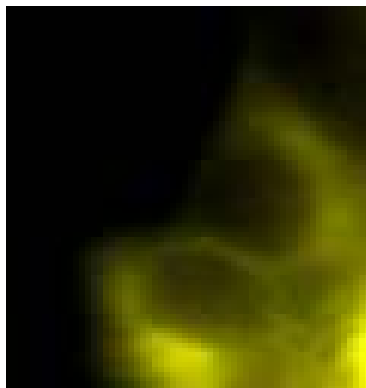
(c)



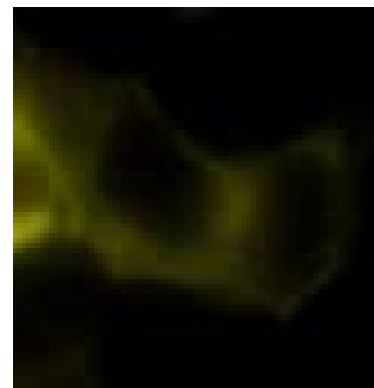
(d)



(e)



(f)



(g)



Figure 5.9 Localisation of GPR43 mutants visualised using eYFP fluorescence

HEK293T cells were transiently transfected to express (a) GPR43-eYFP, (b) GPR43 Lys⁶⁵Ala-eYFP, (c) GPR43 His¹⁴⁰Ala-eYFP, (d) GPR43 Arg¹⁸⁰Ala-eYFP, (e) GPR43 Arg¹⁸⁰Lys-eYFP, (f) GPR43 Arg¹⁸⁰Leu-eYFP or (g) GPR43 Arg¹⁸⁰Ser-eYFP. Cells were directly imaged using fluorescence microscopy. Results shown are of a single experiment, representative of three experiments performed.

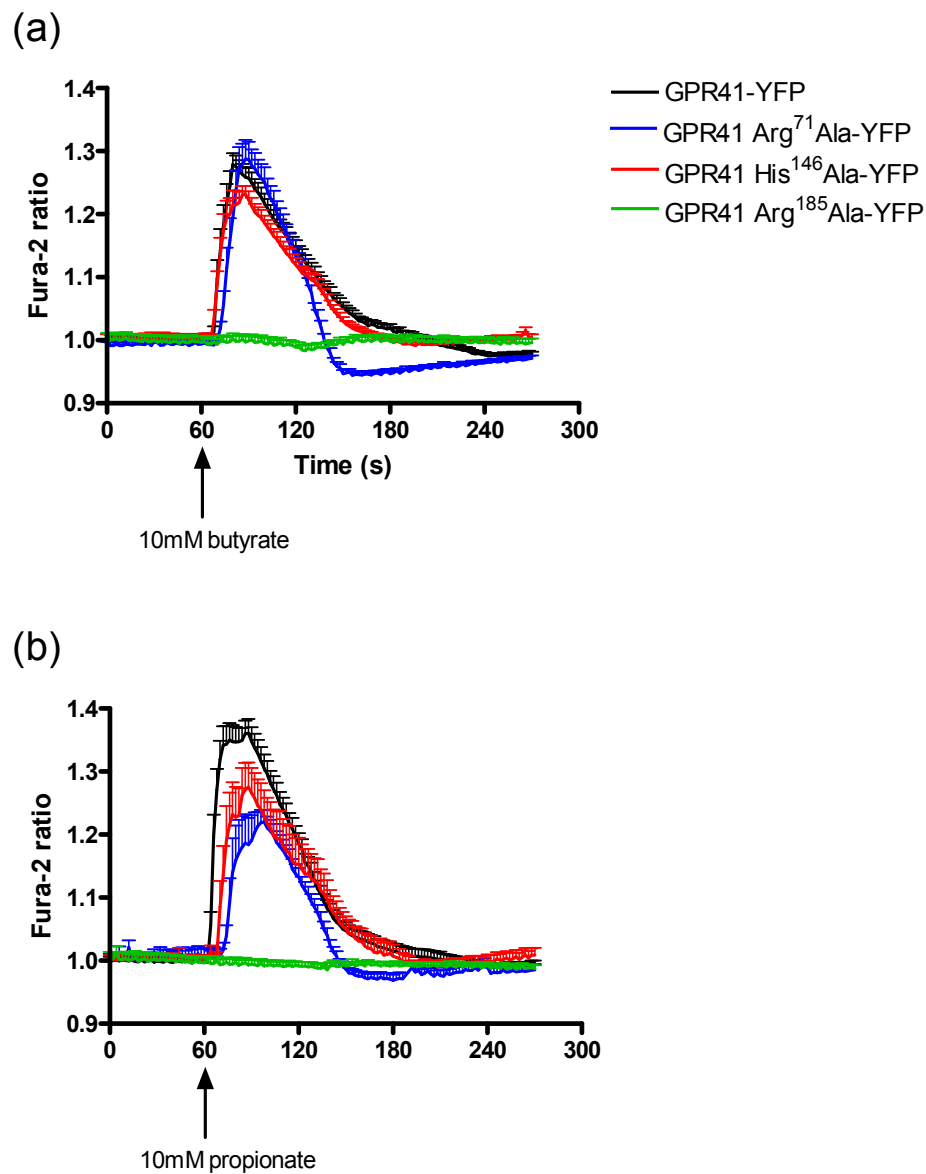


Figure 5.10 Ability of GPR41 basic mutants to mediate a rise in $[Ca^{2+}]_i$ when challenged with propionate or butyrate

HEK293T cells were transiently co-transfected to express GPR41-eYFP (black line), GPR41 Arg⁷¹Ala-eYFP (blue line), GPR41 His¹⁴⁶Ala-eYFP (red line) or GPR41 Arg¹⁸⁵Ala-eYFP (green line) with $G\alpha_{qG66Di5}$. Cells were loaded with the Ca^{2+} sensitive dye, Fura-2 and challenged with 10mM (a) butyrate or (b) propionate at the 60s time point. Images were collected every 2s and collected for a total of 300s. Data represents means \pm SEM from at least 20 positively transfected cells selected on the basis of eYFP fluorescence.

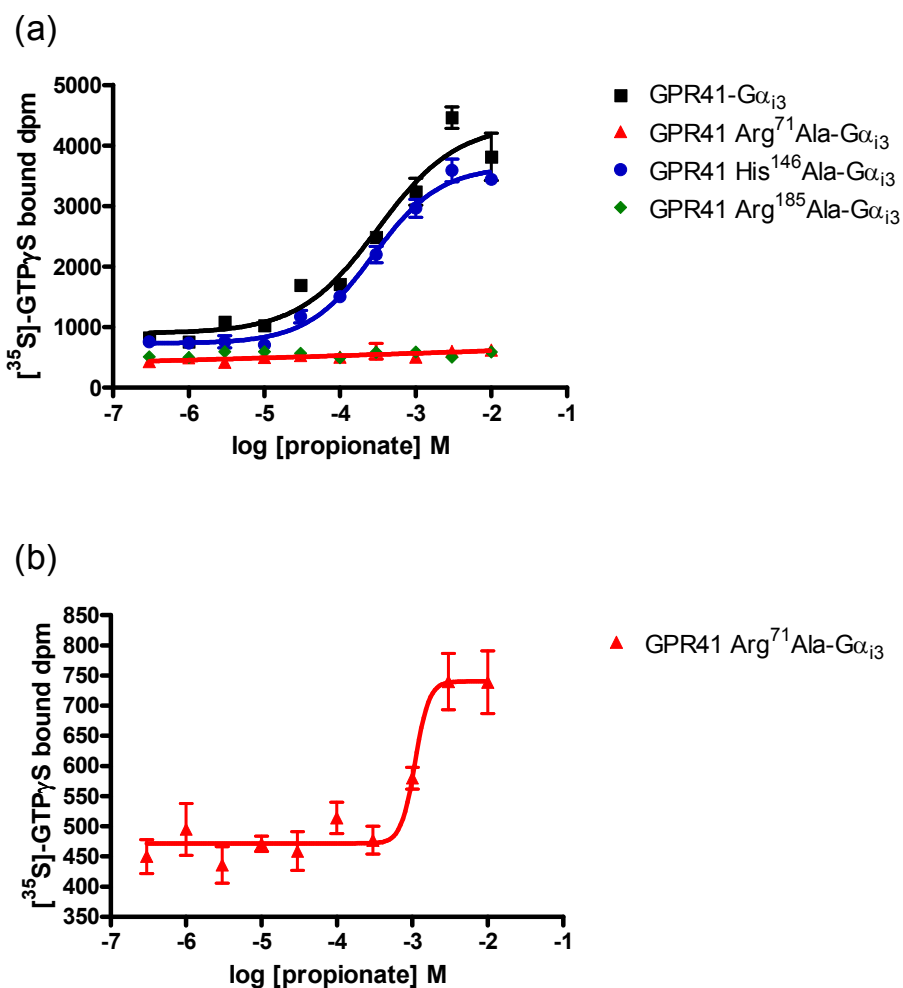


Figure 5.11 Ability of GPR41 mutants to mediate a concentration-dependent increase in [³⁵S]GTP γ S binding in response to propionate

(a) HEK293T cells were transiently transfected to express GPR41-G α_{i3} Cys³⁵¹Ile (black squares), GPR41 Arg⁷¹Ala-G α_{i3} Cys³⁵¹Ile (red triangles), GPR41 His¹⁴⁶Ala-G α_{i3} Cys³⁵¹Ile (blue circles) or GPR41 Arg¹⁸⁵Ala-G α_{i3} Cys³⁵¹Ile (green diamonds). [³⁵S]GTP γ S binding studies were performed on the resulting membranes in the presence of increasing concentrations of propionate. Assay samples were immunoprecipitated with the anti-G α_{i3} antiserum I3 before scintillation counting. (b) Data from GPR41 Arg⁷¹Ala-G α_{i3} Cys³⁵¹Ile [³⁵S]GTP γ S binding studies shown on a reduced scale. Graphs shown are representative of results obtained for three individual experiments performed in triplicate. Data points represent means \pm SEM.

	GPR41	GPR41 Arg ⁷¹ Ala	GPR41 His ¹⁴⁶ Ala	GPR41 Arg ¹⁸⁵ Ala
Propionate	3.66±0.1	2.3±0.3*	3.59±0.02	inactive

Table 5.2 Potency of propionate at GPR41 mutants measured by [³⁵S]GTPγS binding studies

[³⁵S]GTPγS binding studies were performed on membranes expressing GPR41-Gα_{i3} Cys³⁵¹Ile or the specified mutant in the presence of increasing concentrations of propionate. Data represent mean±SEM of pEC₅₀ from three individual experiments. Data was analysed using Students paired T-test (GraphPad Prism 4). Means were compared to wild type GPR41 * = p<0.05

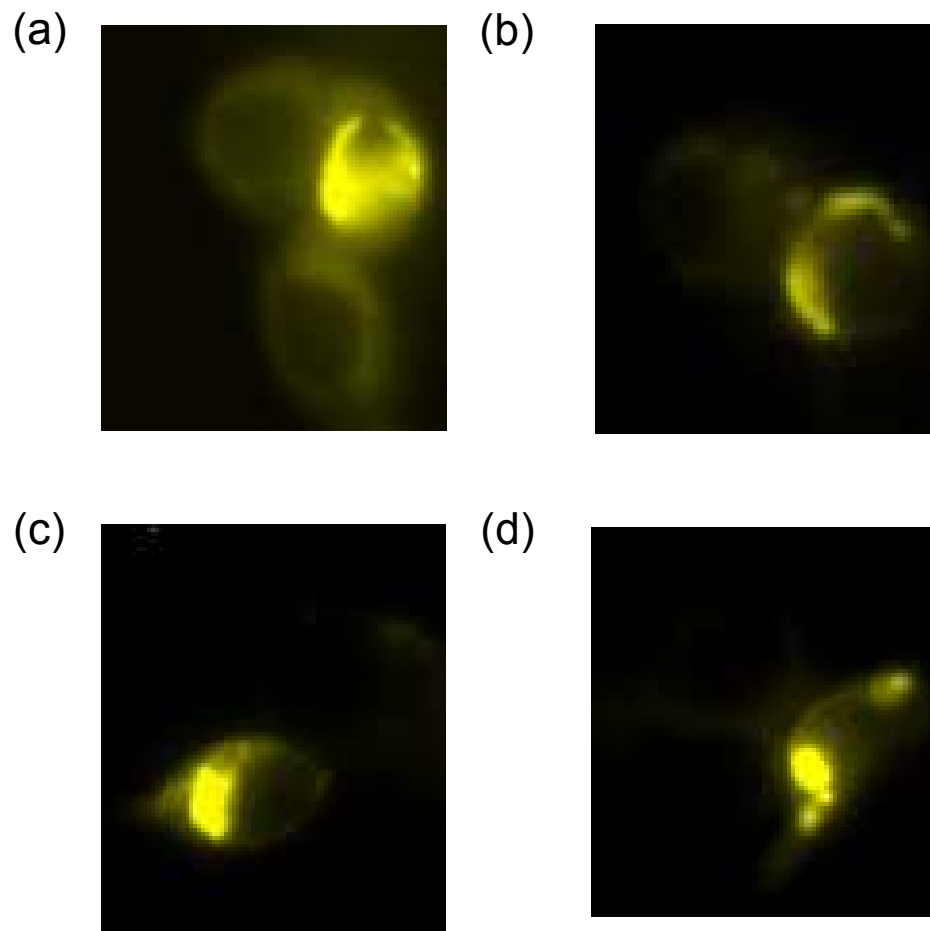


Figure 5.12 Localisation of GPR41 mutants visualised using eYFP fluorescence

HEK293T cells were transiently transfected to express (a) GPR41-eYFP, (b) GPR41 Arg⁷¹Ala-eYFP, (c) GPR41 His¹⁴⁶Ala-eYFP or (d) GPR41 Arg¹⁸⁵Ala-eYFP. Cells were directly imaged using fluorescence microscopy. Results shown are of a single experiment, representative of three experiments performed.

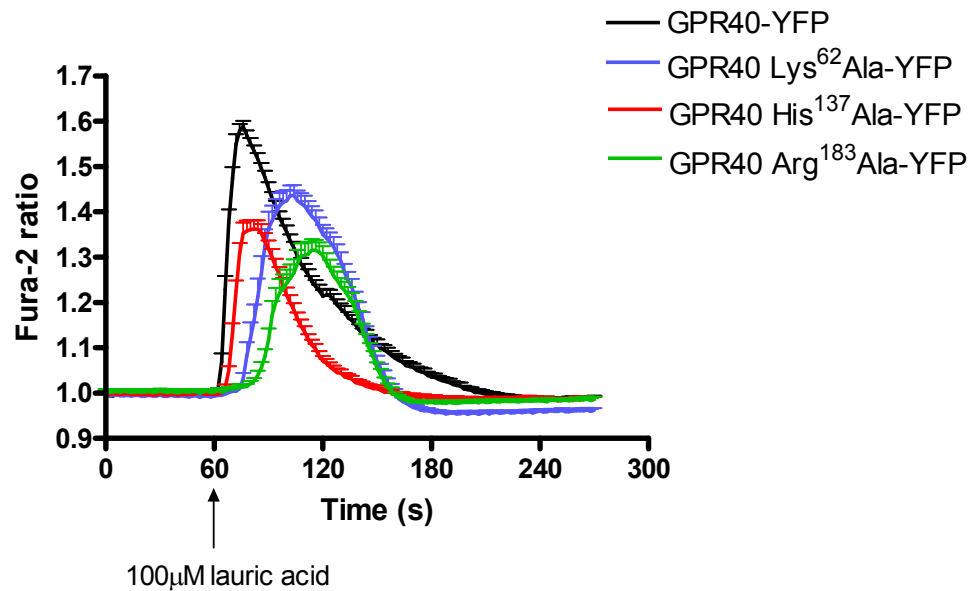


Figure 5.13 Activation of wild type and single point mutant GPR40 receptors by lauric acid in single cell $[Ca^{2+}]_i$ assays

Wild type and single point mutant GPR40 receptors were transiently transfected into HEK293T cells. Cells were loaded with Fura-2 and changes in fluorescence monitored upon the addition of 100 μ M lauric acid after 60s. Images were collected every 2s for a total of 300s. Data shown represents means \pm SEM from at least 20 cells positively transfected with GPR40-eYFP (black line), GPR40 Lys⁶²Ala-eYFP (blue line), GPR40 His¹³⁷Ala-eYFP (red line) or GPR40 Arg¹⁸³Ala-eYFP (green line) selected on the basis of eYFP fluorescence.

	GPR40-YFP	GPR40 Lys ⁶² Ala -YFP	GPR40 His ¹³⁷ Ala - YFP	GPR40 Arg ¹⁸³ Ala - YFP
Caproic Acid	4.0±0.1	inactive	inactive	inactive
Caprylic Acid	4.3±0.3	3.1±0.1*	inactive	3.8±1.0
Capric Acid	5.5±0.6	inactive	inactive	5.5±0.3
Lauric Acid	5.3±0.4	4.9±0.3	4.8±0.5	5.0±0.1
Myristic Acid	5.4±0.5	5.0±0.4	inactive	4.6±0.4
Palmitic Acid	5.5±0.8	4.7±0.7	5.4±0.7	inactive
Stearic Acid	4.9±0.7	6.3±0.1*	inactive	5.5±0.5
Palmitoleic Acid	5.3±0.3	4.9±0.3	4.9±0.1	5.2±0.4
Linolenic Acid	5.6±0.3	5.2±0.2 ***	4.8±1.0	5.3±0.1 *
γ-Linolenic Acid	5.5±0.2	5.3±0.2	5.2±0.3	5.4±0.2
Linoleic Acid	5.6±0.2	5.1±0.1 **	5.3±0.1	5.1±0.2 **
Elaidic Acid	5.2±0.2	4.9±0.1 *	inactive	inactive
Retinoic Acid	5.3±0.4	4.7±0.1 *	4.6±0.5 *	5.0±0.1 *
Arachidonic Acid	5.4±0.3	5.1±0.3	4.9±0.1 *	5.2±0.2
Docosapent - aenoic Acid	5.3±0.2	5.0±0.2	4.9±0.1	5.2±0.2

Table 5.3 Potency of fatty acids agonists at GPR40 single mutants

HEK293 MSRII cells were transiently transfected to express the GPR40-eYFP or the indicated GPR40 mutant. 24h post transfection cells were seeded at 15,000 cells per well into 384 well microtitre plates. Cells were loaded with the Ca²⁺ sensitive dye, Fluo-4. Changes in [Ca²⁺]_i levels were measured using the FLIPR apparatus following challenge with the indicated fatty acid added at the 10 second time point and data collected for a further 110 seconds. Data represents mean±SEM of pEC₅₀ from three individual experiments performed in duplicate. Data was analysed using Students paired T-test (GraphPad Prism 4). Means were compared to wild type GPR40, * = p<0.05, ** = p<0.01, ***=p<0.001.

	GPR40-YFP	GPR40 Lys ⁶² Ala -YFP	GPR40 His ¹³⁷ Ala - YFP	GPR40 Arg ¹⁸³ Ala - YFP
Rosiglitazone	5.7±0.3	inactive	inactive	inactive
Troglitazone	5.9±0.1	inactive	inactive	inactive
GW839508X	7.6±0.3	5.6±0.5 ***	inactive	inactive
GSK250089A	7.0±0.2	5.2±0.1 **	inactive	inactive
GSK223112A	5.7±0.7	inactive	inactive	inactive

Table 5.4 Potency of thiazolidinediones and small molecule agonists at GPR40 single mutants

HEK293 MSRII cells were transiently transfected to express the GPR40-eYFP or the indicated GPR40 mutant. 24h post transfection cells were seeded at 15,000 cells per well into 384 well microtitre plates. Cells were loaded with the Ca²⁺ sensitive dye, Fluo-4. Changes in intracellular calcium levels were measured using the FLIPR apparatus following challenge with the indicated test compound added at the 10 second time point and data collected for a further 110 seconds. Data represent mean±SEM of pEC₅₀ from three individual experiments performed in duplicate. Data was analysed using Students paired T-test (GraphPad Prism 4). Means were compared to wild type GPR40, ** = p<0.01, ***=p<0.001.

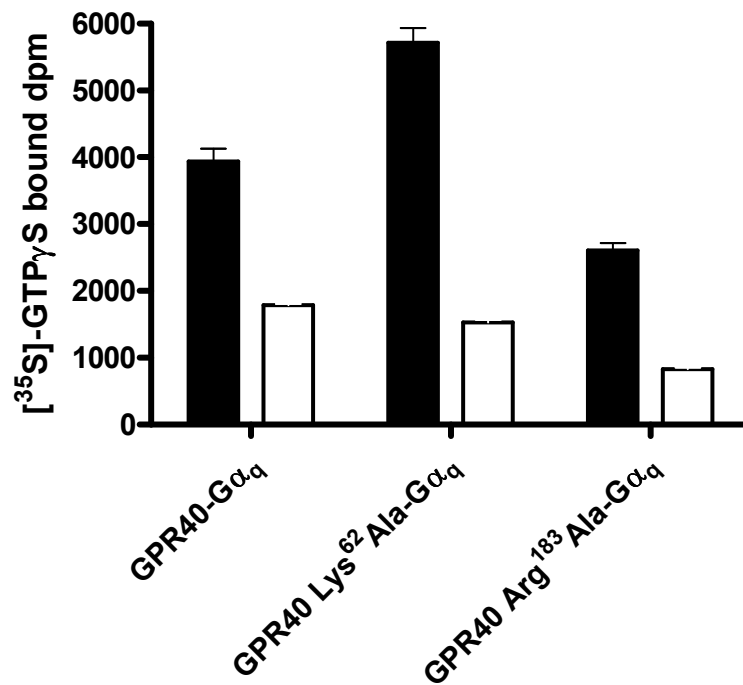
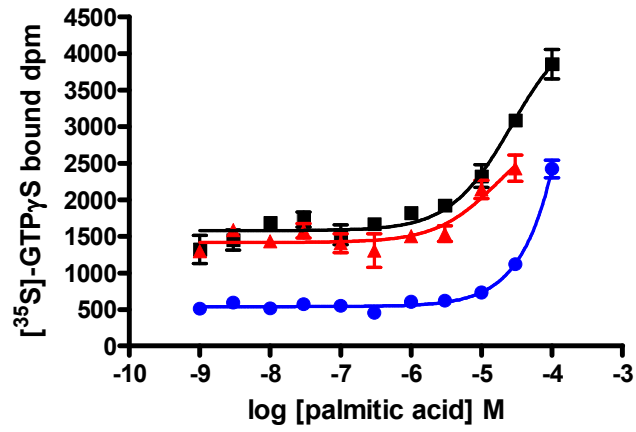


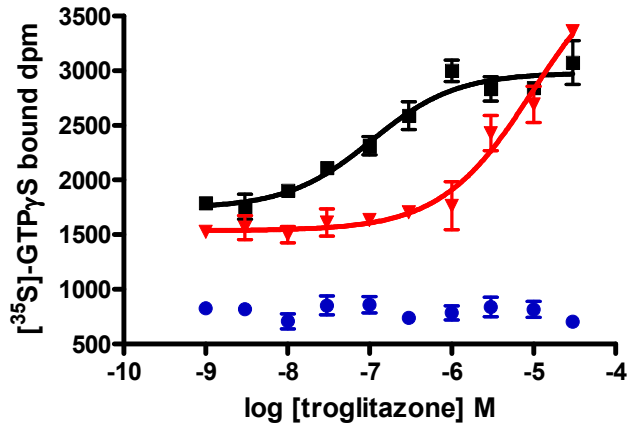
Figure 5.14 The addition of fatty acid free BSA can reduce the basal [³⁵S]GTPγS loading of GPR40 mutant-Gα_q fusion proteins

HEK293T cells were transiently transfected with GPR40-Gα_q, GPR40 Lys⁶²Ala-Gα_q or GPR40 Arg¹⁸³Ala-Gα_q and membranes prepared. [³⁵S]GTPγS binding studies were performed in the absence (black bars) or presence (white bars) of 10 μM fatty acid free BSA. All assay samples were immunoprecipitated with the Gα_{q/11} antiserum CQ before scintillation counting. Data shown is representative of results obtained for three individual experiments performed in triplicate. Data points represent means±SEM.

(a)



(b)



(c)

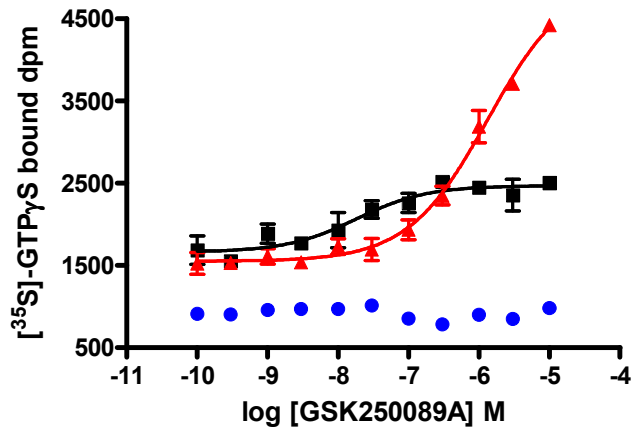


Figure 5.15 Comparison of [³⁵S]GTPγS concentration response curves to different ligands generated by wild type GPR40-Gα_q, GPR40 Lys⁶²Ala-Gα_q and GPR40 Arg¹⁸³Ala-Gα_q

HEK293T cells were transiently transfected to express GPR40-Gα_q (black squares), GPR40 Lys⁶²Ala-Gα_q (red triangles), or GPR40 Arg¹⁸³Ala-Gα_q (blue circles). [³⁵S]GTPγS binding studies were performed on the resulting membranes in the presence of 10 μM fatty acid free BSA and increasing concentrations of (a) palmitic acid, (b) troglitazone or (c) GSK250089A. Assay samples were immunoprecipitated with the anti-Gα_q antiserum CQ before scintillation counting. Graphs shown are representative of results obtained from three individual experiments performed in triplicate. Data points indicate means±SEM.

	GPR40-G α_q	GPR40 Lys ⁶² Ala-G α_q	GPR40 Arg ¹⁸³ Ala-G α_q
Palmitic Acid	4.6±0.1	4.9±0.1	3.5±0.4*
Troglitazone	6.5±0.3	5.3±0.1*	inactive
GSK250089A	7.6±0.2	5.4±0.2*	inactive

Table 5.5 Potency of palmitic acid, troglitazone and GSK250089A at GPR40 Lys⁶²Ala-G α_q and GPR40 Arg¹⁸³Ala-G α_q measured in a [³⁵S]GTP γ S binding assay

[³⁵S]GTP γ S binding studies were performed on membranes expressing GPR40-G α_q , GPR40 Lys⁶²Ala-G α_q or GPR40 Arg¹⁸³Ala-G α_q in the presence of increasing concentrations of the indicated test compound. Data represent mean±SEM of pEC₅₀ from three individual experiments. Data was analysed using Students paired T-test (GraphPad Prism 4). Means were compared to wild type GPR40, * = p<0.05

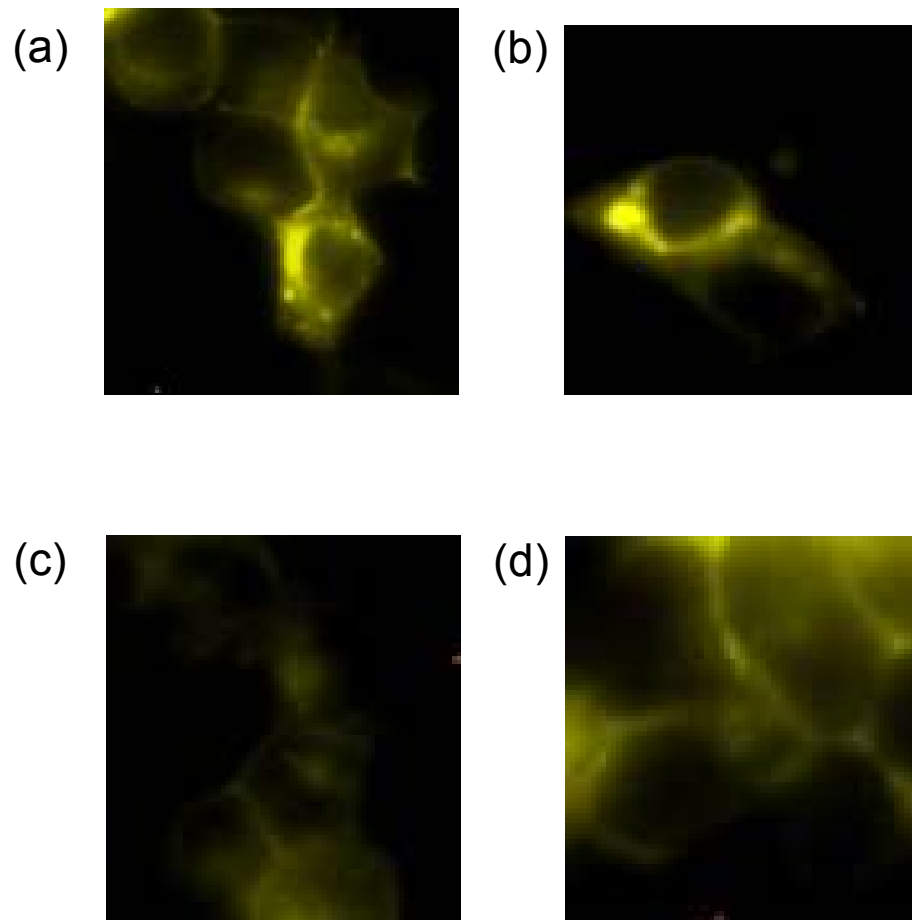


Figure 5.16 Localisation of GPR40 single mutants visualised by eYFP fluorescence

HEK293T cells were transiently transfected to express (a) GPR40-eYFP, (b) GPR40 Lys⁶²Ala-eYFP, (c) GPR40 His¹³⁷Ala-eYFP or (d) GPR40 Arg¹⁸³Ala-eYFP. Cells were directly imaged using fluorescence microscopy. Results shown are of a single experiment, representative of three experiments performed.

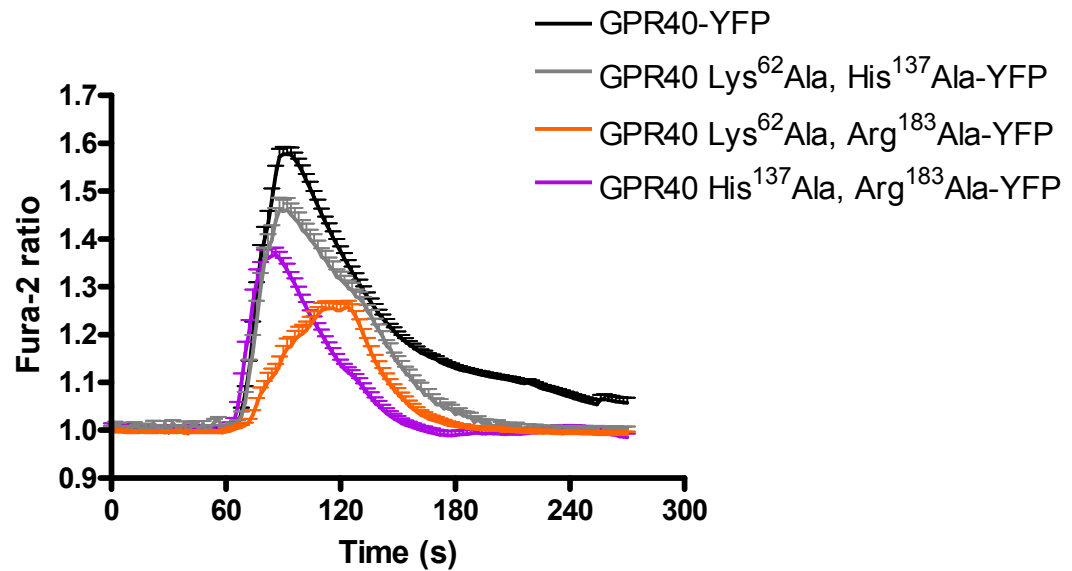


Figure 5.17 Lauric acid mediated rise in $[Ca^{2+}]_i$ via GPR40 double mutants

HEK293T cells were transiently transfected with GPR40-eYFP (black line), GPR40 Lys⁶²Ala, His¹³⁷Ala-eYFP (grey line), GPR40 Lys⁶²Ala, Arg¹⁸³Ala-eYFP (orange line) or GPR40 His¹³⁷Ala, Arg¹⁸³Ala-eYFP (purple line). Cells were loaded with Fura-2 and the change in fluorescence measured in response to the addition of 100 μ M lauric acid at the 60s time point. Images were collected every 2s for a total of 300s. Data represent means \pm SEM from at least 20 positively transfected cells selected on the basis of eYFP fluorescence.

	GPR40-YFP	GPR40 Lya ⁶² Ala, His ¹³⁷ Ala - YFP	GPR40 Lya ⁶² Ala, Arg ¹⁸³ Ala - YFP	GPR40 His137Ala, Arg ¹⁸³ Ala - YFP
Caproic Acid	4.0±0.1	inactive	inactive	inactive
Caprylic Acid	4.3±0.3	3.2±0.3	3.2±0.2 *	inactive
Capric Acid	5.5±0.6	5.4±0.2	inactive	inactive
Lauric Acid	5.3±0.4	4.9±0.1	5.0±0.2	inactive
Myristic Acid	5.4±0.5	5.3±0.3	4.9±0.3	inactive
Palmitic Acid	5.5±0.8	4.9±0.1	4.8±0.1	inactive
Stearic Acid	4.9±0.7	4.3±0.8	4.1±0.2	inactive
Palmitoleic Acid	5.3±0.3	inactive	5.0±0.1	inactive
Linolenic Acid	5.6±0.3	5.1±0.2 *	5.2±0.2***	5.1±0.9
γ-Linolenic Acid	5.5±0.2	5.3±0.4	5.3±0.2	5.3±0.1
Linoleic Acid	5.6±0.2	5.2±0.2 **	5.1±0.1 *	5.1±0.3
Elaidic Acid	5.2±0.2	inactive	4.9±0.2	inactive
Retinoic Acid	5.3±0.4	5.2±0.2	inactive	inactive
Arachidonic Acid	5.4±0.3	5.2±0.3 *	5.2±0.1	inactive
Docosapent - aenoic Acid	5.3±0.2	4.9±0.1	5.2±0.2	5.1±0.3

Table 5.6 Potency of fatty acids agonists at GPR40 double mutants

HEK293 MSRII cells were transiently transfected to express the GPR40-eYFP or the indicated GPR40 double mutant. 24h post transfected cells were seeded at 15,000 cells per well into 384 well microtitre plates. Cells were loaded with the Ca²⁺ sensitive dye, Fluo-4. Changes in intracellular calcium levels were measured using the FLIPR apparatus following challenge with the indicated fatty acid added at the 10 second time point and data collected for a further 110 seconds. Data represent mean±SEM of pEC₅₀ from three individual experiments performed in duplicate. Data was analysed using Students paired T-test (GraphPad Prism 4). Means were compared to wild type GPR40, * = p<0.05, ** = p<0.01, ***=p<0.001.

	GPR40-YFP	GPR40 Lys ⁶² Ala, His ¹³⁷ Ala - YFP	GPR40 Lys ⁶² Ala, Arg ¹⁸³ Ala - YFP	GPR40 His ¹³⁷ Ala, Arg ¹⁸³ Ala - YFP
Rosiglitazone	5.7±0.3	5.7±0.5	5.3±0.5	inactive
Troglitazone	5.9±0.1	inactive	inactive	inactive
GW839508X	7.6±0.3	6.3±0.1 ***	4.7±0.2 ***	inactive
GSK250089A	7.0±0.2	6.1±0.3 *	inactive	inactive
GSK223112A	5.7±0.7	inactive	inactive	inactive

Table 5.7 Potency of thiazolidinediones and small molecule agonists at GPR40 double mutants

HEK293 MSRII cells were transiently transfected to express the GPR40-eYFP or the indicated GPR40 double mutant. 24h post transfected cells were seeded at 15,000 cells per well into 384 well microtitre plates. Cells were loaded with the Ca²⁺ sensitive dye, Fluo-4. Changes in intracellular calcium levels were measured using the FLIPR apparatus following challenge with the indicated test compound added at the 10 second time point and data collected for a further 110 seconds. Data represent mean±SEM of three individual experiments performed in duplicate. Data was analysed using Students paired T-test (GraphPad Prism 4). Means were compared to wild type GPR40, ** = p<0.01, ***=p<0.001.

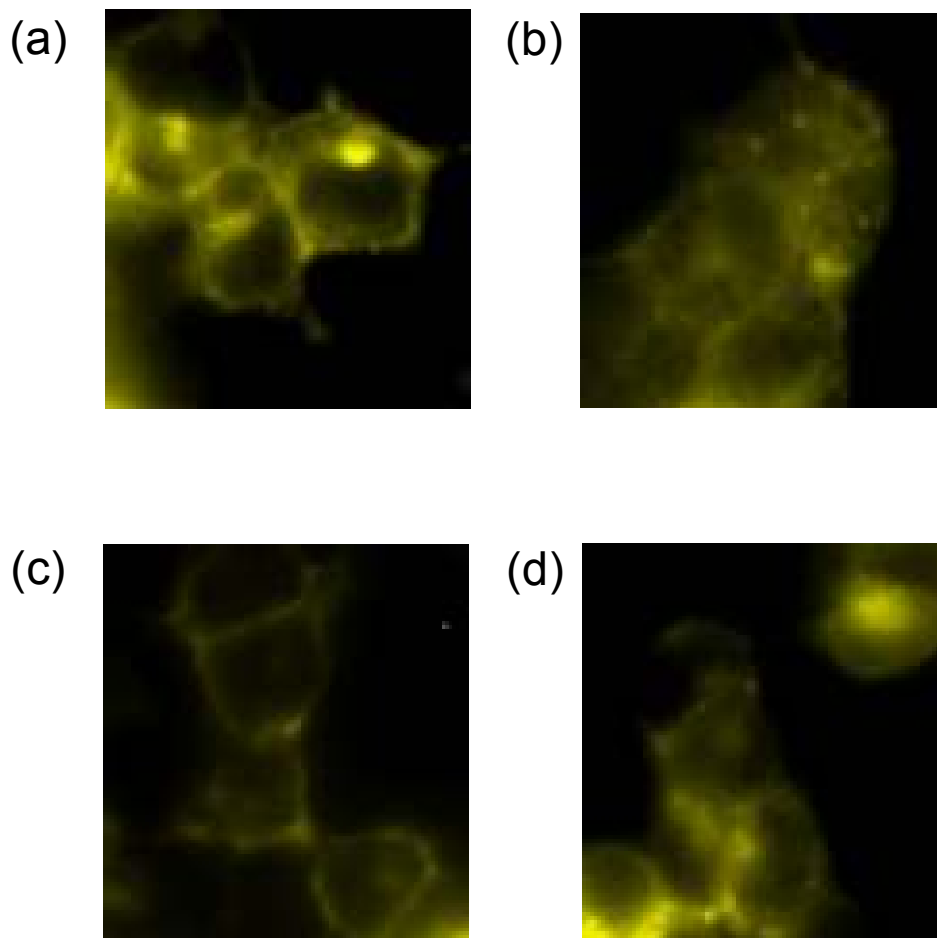
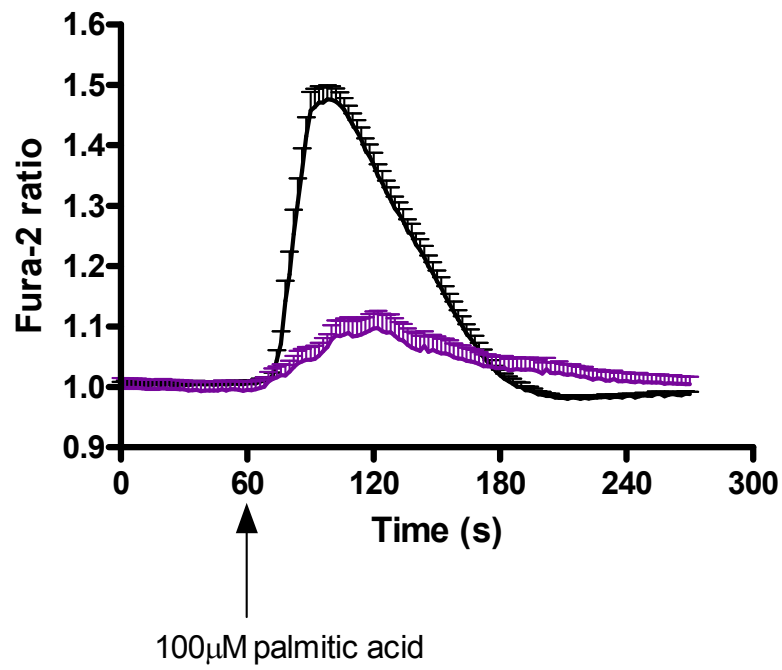


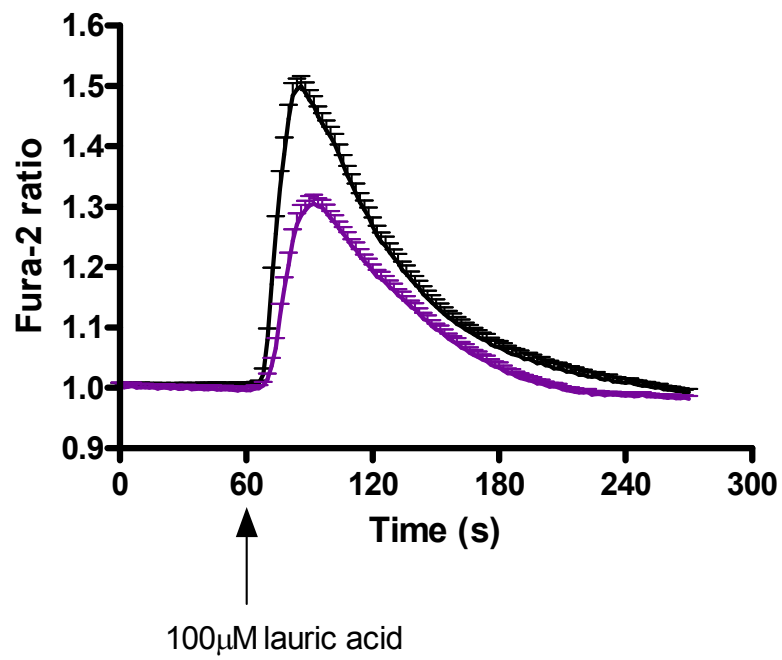
Figure 5.18 Cellular localisation of GPR40 double mutants visualised using eYFP fluorescence

HEK293T cells were transiently transfected to express (a) GPR40-eYFP, (b) GPR40 Lys⁶²Ala, His¹³⁷Ala-eYFP, (c) GPR40 Lys⁶²Ala, Arg¹⁸³Ala-eYFP or (d) GPR40 His¹³⁷Ala, Arg¹⁸³Ala-eYFP. Cells were directly imaged using fluorescence microscopy. Results shown are of a single experiment, representative of three experiments performed.

(a)



(b)



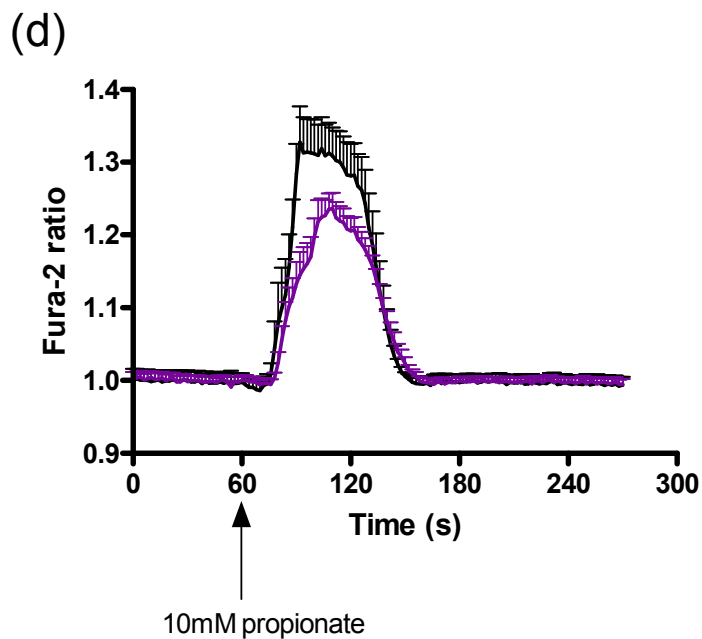
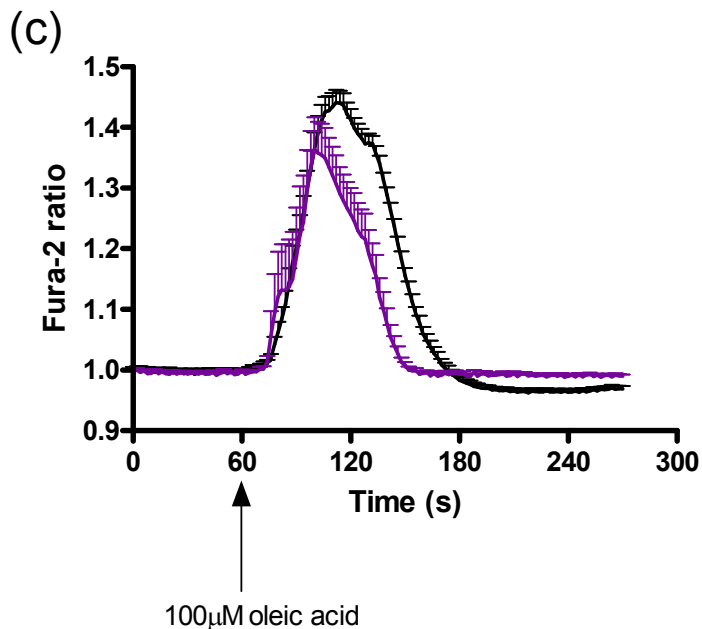


Figure 5.19 Responses to various chain length fatty acids by GPR40 GGG⁹³⁻⁹⁵STW

HEK293T cells were transiently transfected with GPR40-eYFP (black line) or GPR40 GGG⁹³⁻⁹⁵STW-eYFP (purple line). Cells were loaded with Fura-2 and exposed to 100 μ M (a) palmitic acid, (b) lauric acid, (c) oleic acid or (d) 10mM propionate after 60s of basal readings and alterations in fluorescence were monitored. Images were collected every 2s for a total of 300s. Data represents means \pm SEM from at least 20 positively transfected cells selected on the basis of eYFP fluorescence (GPR40-eYFP response to propionate represents means \pm SEM from 7 positively transfected cells).

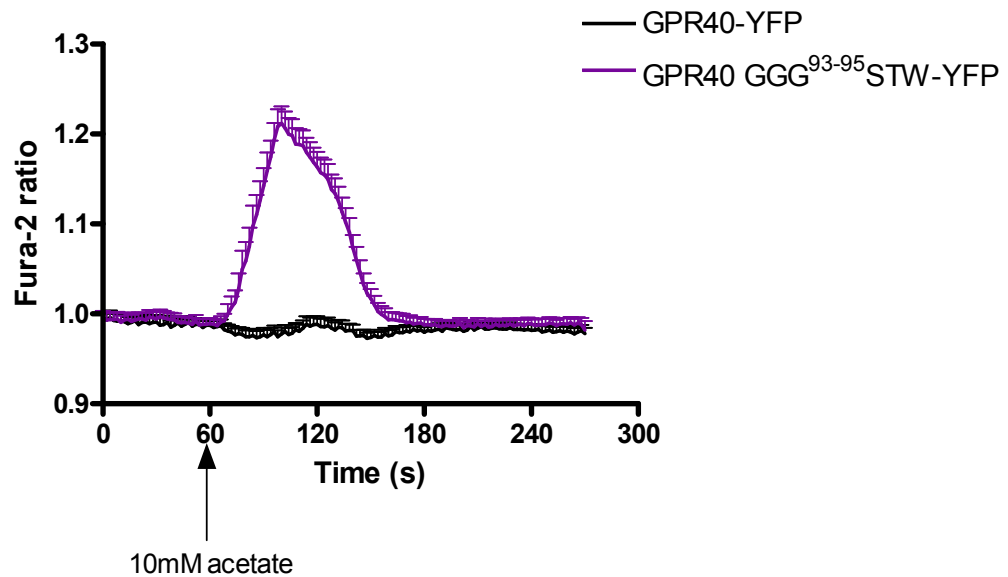


Figure 5.20 GPR40 GGG⁹³⁻⁹⁵STW can mediate a rise in $[Ca^{2+}]_i$ when challenged with acetate

HEK293T cells were transiently transfected with GPR40-eYFP (black line) or GPR40 GGG⁹³⁻⁹⁵STW-eYFP (purple line). Cells were loaded with Fura-2 and exposed to 10mM acetate after 60s of basal readings and alteration in Fura-2 fluorescence monitored. Images were collected every 2s for a total of 300s. Data represents means \pm SEM from at least 30 positively transfected cells selected on the basis of eYFP fluorescence.

	GPR40-YFP	GPR40 GGG ⁹³⁻ ₉₅ STW-YFP	GPR43-YFP	GPR43 Trp ⁹⁸ Gly-YFP	GPR43 Thr ⁹⁷ Gly, Trp ⁹⁸ Gly-YFP	GPR43 Ser, Thr, Trp ⁹⁶⁻ ₉₈ Gly, Gly, Gly-YFP
Formate	inactive	inactive	2.8±1.0	inactive	inactive	inactive
Acetate	inactive	inactive	4.6±0.2	4.4±0.9	inactive	inactive
Propionate	inactive	inactive	4.9±0.2	4.7±0.6	inactive	inactive
Butyrate	inactive	inactive	4.4±0.5	4	inactive	inactive
Caproic Acid	4.0±0.1	inactive	inactive	inactive	inactive	inactive
Caprylic Acid	3.9±0.9	3.9±0.4	inactive	inactive	inactive	inactive
Capric Acid	5.5±0.6	5.1±0.9	inactive	inactive	inactive	inactive
Lauric Acid	5.3±0.4	5.0±0.3	inactive	inactive	7	7.4
Myristic Acid	5.4±0.5	5.0±0.4	inactive	5.2	6.2±2.5	5
Palmitic Acid	5.5±0.8	inactive	inactive	inactive	inactive	inactive
Stearic Acid	4.9±0.7	5.1±0.4	inactive	inactive	inactive	inactive
Palmitoleic Acid	5.3±0.3	inactive	inactive	inactive	6.2±1.4	inactive
Linolenic Acid	5.6±0.2	5.1±0.2 *	inactive	5.1±0.9	inactive	inactive
γ-Linolenic Acid	5.4±0.1	5.1±0.2	inactive	5.3±0.1	inactive	inactive
Linoleic Acid	5.6±0.2	5.1±0.1 *	inactive	5.1±0.3	inactive	inactive
Elaidic Acid	5.0±0.1	inactive	inactive	inactive	6.2±2.4	4.5±0.2
Retinoic Acid	5.3±0.4	inactive	inactive	inactive	inactive	inactive
Arachidonic Acid	5.4±0.3	5.0±0.1	inactive	inactive	inactive	inactive
Docosapent - aenoic Acid	5.3±0.2	5.1±0.1 *	inactive	5.1±0.3	inactive	inactive

Table 5.8 Potency of a range of fatty acids at TM3 mutants of GPR40 and GPR43

HEK293 MSRII cells were transiently transfected to express the indicated wild type or mutant receptor. 24h post transfected cells were seeded at 15,000 cells per well into 384 well microtitre plates. Cells were loaded with the Ca²⁺ sensitive dye, Fluo-4. Changes in intracellular calcium levels were measured using the FLIPR apparatus following challenge with the indicated test compound added at the 10 second time point and data collected for a further 110 seconds. Data represent mean±SEM of three individual experiments performed in duplicate. Data was analysed using Students paired T-test (GraphPad Prism 4). * = p<0.05. Dashes indicate that no signal was observed when the test fatty acid was added.

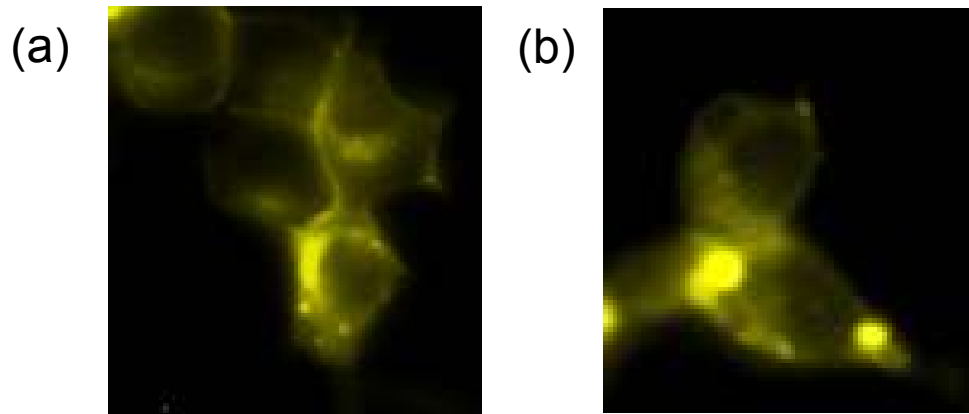


Figure 5.21 Cellular localisation of GPR40 GGG⁹³⁻⁹⁵STW visualised using eYFP fluorescence

HEK293T cells were transiently transfected to express (a) GPR40-eYFP or (b) GPR40 GGG⁹³⁻⁹⁵STW-eYFP. Cells were directly imaged using fluorescence microscopy. Results shown are of a single experiment, representative of three experiments performed.

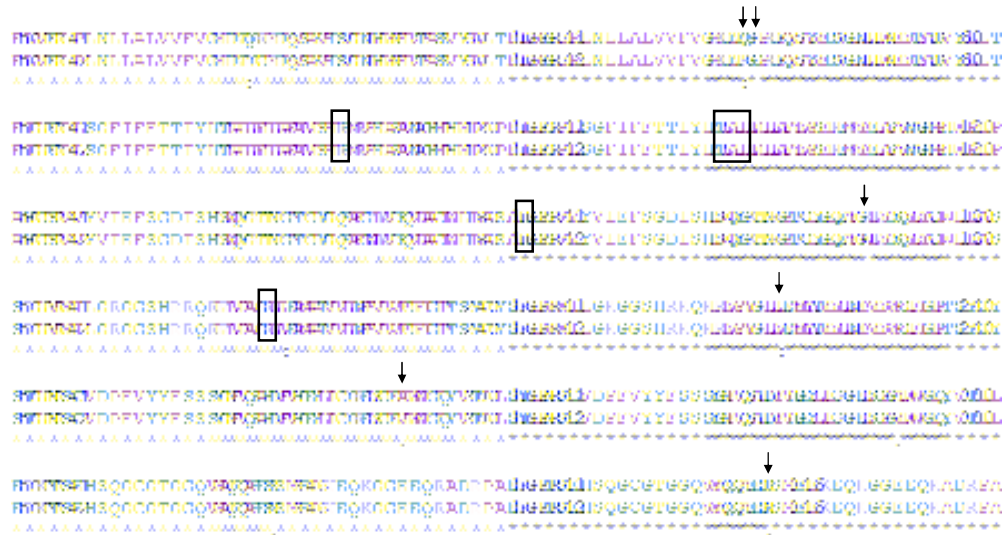


Figure 5.22 Amino acid positions differing between GPR41 and GPR42

Amino acid sequences corresponding to GPR41 and GPR42 were aligned using the ClustalX algorithm. Residues are coloured as follows; small and hydrophobic residues are coloured red, acidic residues coloured blue, basic residues coloured magenta, hydroxyl and amine containing residues are coloured green. Conserved basic transmembrane residues and area within TM3 proposed to confer fatty acid chain length specificity boxed with a continuous line. Residues that differ between GPR41 and GPR42 are indicated by arrows. Accession numbers are as follows: human GPR41, NP005295; human GPR42, NP005296.

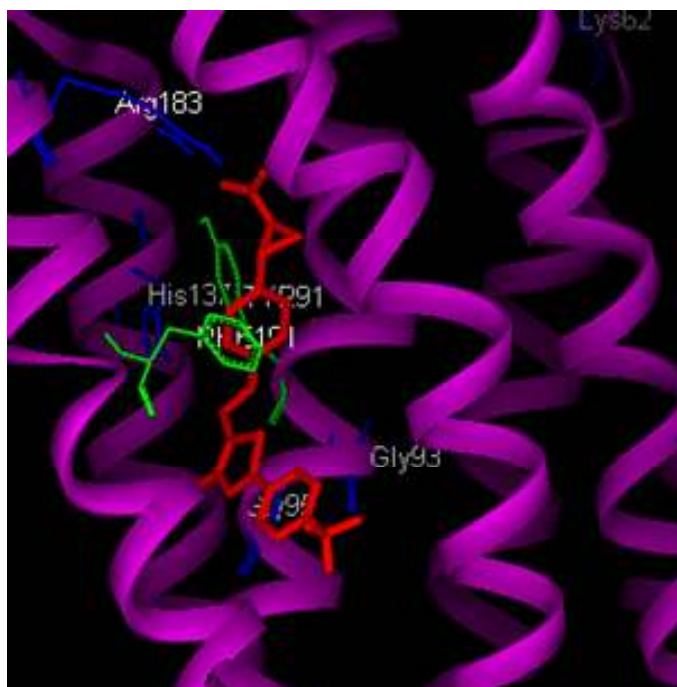


Figure 5.23 GPR40 homology model showing positions of Tyr⁹¹ and Phe¹⁹¹ in relation to proposed binding site of small molecule agonists

The homology model of GPR40 was generated by GlaxoSmithKline using the GPCR_Builder programme based on the crystal structure of rhodopsin. GPR40 was aligned with rhodopsin on the basis of highly conserved residues found in family A GPCRs. The model shows the residues implicated in forming a salt bridge with the fatty acid agonists; Lys⁶², Gly⁹³⁻⁹⁵, His¹³⁷ and Arg¹⁸³ (coloured blue). It also shows a synthetic small molecule agonist (coloured red) co-ordinated by Arg¹⁸³ and Tyr⁹¹ and Phe¹⁹¹ (coloured green).

6 Detection of GPR40 and GPR43 homo-oligomers using a variety of techniques

6.1 Introduction

The ability of family A GPCRs to form homo- and hetero-oligomers has become widely accepted (Bulenger et al., 2005; Milligan, 2006). The role of oligomerisation is unclear but it has been proposed to be involved in protein folding, correct membrane delivery and interaction with G proteins. There are a growing number of studies on the effects of hetero-oligomerisation on ligand pharmacology and function. Hetero-oligomerisation has been shown to switch the G protein coupling of MOP and DOP receptors when co-expressed (George et al., 2000; Fan et al., 2006) and to affect the potency of orexin A at the orexin-1 receptor when it is co-expressed with the CB1 receptor (Hilaireret et al., 2003).

An obvious requirement for hetero-oligomerisation is that both receptors are expressed in the same cell. Although GPR40, GPR41 and GPR43 have distinct expression patterns, they have been reported to be co-expressed in certain tissues. Xiong et al., (2004) were able to detect both GPR41 and GPR43 mRNA in adipocytes and all three receptors have been found to be expressed in immune cells (Briscoe et al., 2003; Brown et al., 2003; Le Poul et al., 2003). Examination of different immune cells suggests that there is a greater overlap of the expression of GPR40 and GPR43. Recent patents by Arena Pharmaceuticals indicated that expression of all three receptors could be detected in pancreatic islet cells. The overlap of expression suggests that interactions between these receptors may occur *in vivo*, and this may modulate their function and/or pharmacology.

To date, there have been no studies into the potential for the receptors to form homo- or hetero-oligomers. From expression studies, GPR40 and GPR43 have the most overlapping expression pattern. Before studies into their ability to form hetero-oligomers can be undertaken, their capacity to assemble into homo-oligomers had to be determined. This was achieved using three complementary techniques, co-immunoprecipitation, FRET and Tr-FRET.

6.2 Co-immunoprecipitation allows detection of GPR40 and GPR43 homo-oligomers

To investigate the potential homo-oligomerisation of GPR40, GPR40-Flag and GPR40-c-Myc were transiently expressed individually or co-expressed in HEK293T cells. Cells were harvested 24h post-transfection and solubilised by the addition of 1x RIPA buffer. Mock-transfected HEK293T cells were included as a control, as was a control composed of cells individually expressing the two constructs that were mixed prior to immunoprecipitation. Samples were incubated with anti-Flag antibody and immunoprecipitated material resolved by SDS-PAGE. Proteins were transferred onto nitrocellulose membrane and a western blot performed using anti-c-Myc antibody. Figure 6.1 demonstrates the co-immunoprecipitation of GPR40-Flag and GPR40-c-Myc only in the sample where the differentially tagged receptors were co-expressed. A band representing the 32kDa GPR40-c-Myc receptor can be observed in the co-expressed sample, which is consistent with an interaction between GPR40-Flag and GPR40-c-Myc. Higher molecular mass species were also detected and this suggested that a fraction of the immunoprecipitated oligomer was not efficiently separated by the SDS-PAGE conditions used. No immunoreactivity could be detected in samples where each of the constructs was expressed individually. Mixing of samples individually expressing GPR40-Flag and GPR40-c-Myc prior to immunoprecipitation did not result in co-immunoprecipitation, implying that expression of both epitope tagged receptors within the same cell was required to allow interaction. To confirm expression of the tagged receptors, lysates from each of the samples were also subjected to western blot analysis using both the anti-Flag and anti-c-Myc antibodies.

A similar experimental protocol was followed to investigate the formation of GPR43 homo-oligomers (Figure 6.2). Immunoreactivity at 33kDa corresponding to GPR43-c-Myc was observed in the lane where the differentially epitope tagged receptors were co-expressed. No immunoreactivity was observed in the sample in which the individually expressed receptors were mixed prior to immunoprecipitation or when each construct was expressed individually. A larger fraction of the co-immunoprecipitated anti-c-Myc immunoreactivity remained as a dimer and higher order oligomers.

6.3 Investigation of homo-oligomerisation of GPR40 and GPR43 using FRET imaging in living cells

As GPCR immunoprecipitation studies require solubilisation of the membrane surrounding the receptors, the formation of GPR40 and GPR43 homo-oligomers in living cells was investigated. This was achieved by the attachment of either eCFP or eYFP at the C-terminus of the receptor, expression of the modified receptors in HEK293T cells and the quantification of the resulting FRET signal as eCFP and eYFP are well established FRET partners. Expression of either GPR40-eYFP or GPR40-eCFP allowed selective imaging of each construct and quantification of the bleed-through values to be calculated due to the overlapping spectral properties of the two fluorescent proteins. Co-expression of GPR40-eCFP and GPR40-eYFP resulted in a $\text{FRET}_{\text{NORM}}$ signal of 0.82 ± 0.07 (Figure 6.3). Previous studies performed within the Milligan group have demonstrated that co-expression of the isolated forms of eCFP and eYFP did not result in significant levels of FRET (Carrillo et al., 2004), which suggest that the $\text{FRET}_{\text{NORM}}$ signal is from direct protein-protein interactions involving GPR40.

The specificity of the FRET signal was investigated using the histamine H_1 receptor. There is no overlap between the expression pattern of this receptor and GPR40 or GPR43. The interactions between GPR40 and histamine H_1 receptor were monitored by expression of GPR40-eCFP and H_1 -eYFP in HEK293T cells and quantification of the resulting FRET signal. The $\text{FRET}_{\text{NORM}}$ signal was 0.30 ± 0.02 , which demonstrated significantly lower levels of energy transfer between these two receptor than the GPR40 homo-oligomer. Imaging of individual cells confirmed their co-expression in the same cell (Figure 6.3 (d)).

Homo-oligomerisation of GPR43 was also investigated using this technique (Figure 6.4). GPR43-eCFP and GPR43-eYFP were co-expressed and resulted in a $\text{FRET}_{\text{NORM}}$ of 0.75 ± 0.04 . The specificity of the interaction was investigated by co-expression of GPR43-eCFP and H_1 -eYFP, which yielded a $\text{FRET}_{\text{NORM}}$ of 0.34 ± 0.03 . The $\text{FRET}_{\text{NORM}}$ value obtained upon co-expression of GPR43-eCFP and H_1 -eYFP is significantly less than that observed with the GPR43 homo-oligomer and imaging confirmed expression of both receptors in the same cell.

6.4 Demonstration of homo-oligomerisation of GPR40 and GPR43 using Tr-FRET

A further technique, Tr-FRET, was used to confirm the homo-oligomerisation of GPR40 and GPR43. GPR40-Flag and GPR40-c-Myc were expressed transiently in HEK293T cells. As a control, mixed cells expressing the differentially tagged constructs individually were also used. Membranes were prepared and incubated with an anti-c-Myc antibody conjugated to Europium (Eu^{3+}), which acts the energy donor, and an anti-Flag antibody conjugated to allophycocyanin (APC), which acts as the energy acceptor. The energy transfer signal obtained when GPR40-c-Myc and GPR40-Flag were co-expressed was 0.017 ± 0.003 . A low energy transfer signal of 0.004 ± 0.0008 was obtained for the mixed sample. The energy transfer observed using membranes expressing GPR43-c-Myc and GPR43-Flag was 0.012 ± 0.0005 (Figure 6.5). The mixed control of the GPR43 constructs also yielded a low energy transfer of 0.002 ± 0.0005 .

6.5 Discussion

Using a variety of techniques it was found that GPR40 and GPR43 could form homo-oligomers. The first technique used in this study to investigate the ability of GPR40 and GPR43 to homo-oligomerise was co-immunoprecipitation. This technique has been used as a starting point for many of the studies into the oligomerisation of GPCRs (Milligan and Bouvier, 2005). Despite its widespread use there have been questions raised about its validity due the requirement for cell lysis and solubilisation. It has been suggested that this may result in artefactual positive results due to the hydrophobic nature of GPCRs (Salim et al., 2002). To address this, a mixed cell control can be utilised, in which cells expressing each tagged receptor alone are mixed prior to immunoprecipitation (Wilson et al., 2005). This control was included in my studies and yielded no immunoreactivity, confirming that the positive results obtained were not an artefact of the experimental procedure. Another issue that may yield false positive results is if the membranes are not fully solubilised prior to immunoprecipitation (Milligan and Bouvier, 2005). In many studies, the samples are only subjected to a short period in a microcentrifuge, in which the force is not enough to ensure that the remaining membrane fragments are removed from the soluble fraction. This can be overcome by increasing the centrifuge duration and speed. In my study, samples were centrifuged for 60 mins at $100,000 \times g$, which should ensure the complete removal of any remaining membrane fragments.

Figures 6.1 and 6.2 demonstrate that a portion of the immunoprecipitated oligomer was not fully separated by the SDS-PAGE conditions used. Immunoreactivity corresponding to the predicted weight for the homo-dimer of GPR40 and GPR43, along with higher order oligomers was observed. This indicates that a fraction of both the GPR40 and GPR43 homo-oligomers exist through non-covalent interactions. The occurrence of SDS-resistant oligomers has been observed for a variety of other receptors including the α_{1b} receptor (Carrillo et al., 2004), CXCR1 and CXCR2 chemokine receptors (Wilson et al., 2005), and MOR and DOR opioid receptors (George et al., 2000). The formation of SDS-resistant oligomers may be due to over-expression of the receptors. Using the oxytocin receptor, Devost and Zingg (2004) demonstrated that at low levels of receptor expression the formation of SDS-resistant oligomer is favoured while at high levels of receptor expression (400 fmol/mg) the formation of SDS-sensitive oligomers was observed.

The use of single cell FRET allows protein-protein interactions to be measured in living cells. Using this technique confirmed the ability of GPR40 and GPR43 to form constitutive homo-oligomers (Figures 6.3, 6.4). It has been found that some wild type GFPs have the tendency to oligomerise, which may cause aggregation of receptors they are fused to. The use of eCFP and eYFP reduces the possibility of artefactual results as they have less affinity for one another than wild type GFP. A study carried out by Carrillo et al., (2004) in which they co-expressed isolated forms of eCFP and eYFP did not result in a significant amount of FRET. This confirms that the FRET observed in the present study is not due to the properties of the fluorescent proteins.

The specificity of the homo-oligomers was investigated by measuring the amount of FRET upon co-expression with the histamine H₁ receptor. For both GPR40 and GPR43, co-expression with this distantly related receptor resulted in significantly less FRET than that observed with the homo-oligomer. Although this suggests that the GPR40/H₁ and GPR43/H₁ oligomers have less affinity to form it may be due to conformation of the hetero-oligomer being such that there is a large distance between the donor and acceptor fluorescent moieties that prevents energy transfer from taking place. Although the FRET values obtained with the H₁ receptor was reduced compared to the homo-oligomer, it does indicate that the receptors can form hetero-oligomers. To gain a greater understanding of the relative affinity of the homo-oligomer versus a hetero-oligomer, saturation BRET experiments could be employed. Saturation BRET studies have been used to determine the relative affinity a variety of homo- and hetero-oligomers including, CXCR1/CXCR2 homo- and hetero-oligomers (Wilson et al., 2005), the adenosine A_{2A} receptor (Canals et

al., 2004), adenosine A_{2A}-dopamine D₂ hetero-oligomers (Canals et al., 2003) and β_2 - β_3 adrenergic receptor hetero-oligomers (Breit et al., 2004).

Using Tr-FRET confirmed the observations from the co-immunoprecipitation and FRET studies that GPR40 and GPR43 could form homo-oligomers. Tr-FRET utilises antibodies that recognise specific epitope tags and are conjugated to energy transfer donor and acceptor moieties. It has been suggested that the binding of antibodies may cause receptor aggregation that would give a false positive result (McVey et al., 2001). Although the antibodies used are bivalent, any antibody mediated aggregation would only occur between receptors expressing the same epitope tag. As the technique relies on the energy transfer between two different moieties conjugated to the antibodies, any clustering is unlikely to have any effect on the energy transfer. This is confirmed by the inclusion of a control in which cells individually expressing the different epitope tagged receptors were mixed prior to membrane preparation and very low levels of energy transfer were observed, ruling out the possibility of antibody mediated aggregation.

Tr-FRET is normally utilised to demonstrate the formation of GPCR oligomers at the cell surface. This is achieved by attaching the epitope tag to the N-terminus of the receptor; therefore only receptors at the cell surface are available for the antibodies to bind to. Unfortunately, I found that GPR43 did not tolerate the attachment of the c-Myc epitope tag to its N-terminus (see Figure 3.5). This may have been due to low levels of receptor expression or that the attachment of the epitope sequence prevents the receptor from expressing. It was concluded that the N-terminally epitope tagged versions of GPR43 were not suitable to be used in these experiments. The attachment of an epitope tag to the N-terminus of GPR40 was not attempted. Therefore, the Tr-FRET experiments in this study were carried out on membranes rather than whole cells. As the receptors cannot be N-terminally tagged this makes the detection of oligomers at the cell surface difficult. The attachment of the Flag epitope did not appear to have as large effect on the function of GPR43 but further experiments would need to be carried out to confirm this. This suggests that different epitope tags have different effects on the function and expression of GPR43. The attachment of other epitope such as VSV or HA at the N-terminus may not affect the function of the receptors and could be used to assess their ability to form cell surface delivered oligomers.

Time constraints prevented the investigation into the ability of GPR40 and GPR43 to form a hetero-oligomer. The data obtained with the histamine H₁ receptor suggests that the receptors are able to form a hetero-oligomer with a distantly related receptor; therefore it is

likely that they will be able to form hetero-oligomers with each other as they are more closely related. These studies show that GPR40 and GPR43 homo-oligomers exist and can be monitored easily using a variety of techniques. The construction of epitope tagged receptors and receptor-fluorescent protein fusions will make the investigation of hetero-oligomers a relatively simple process.

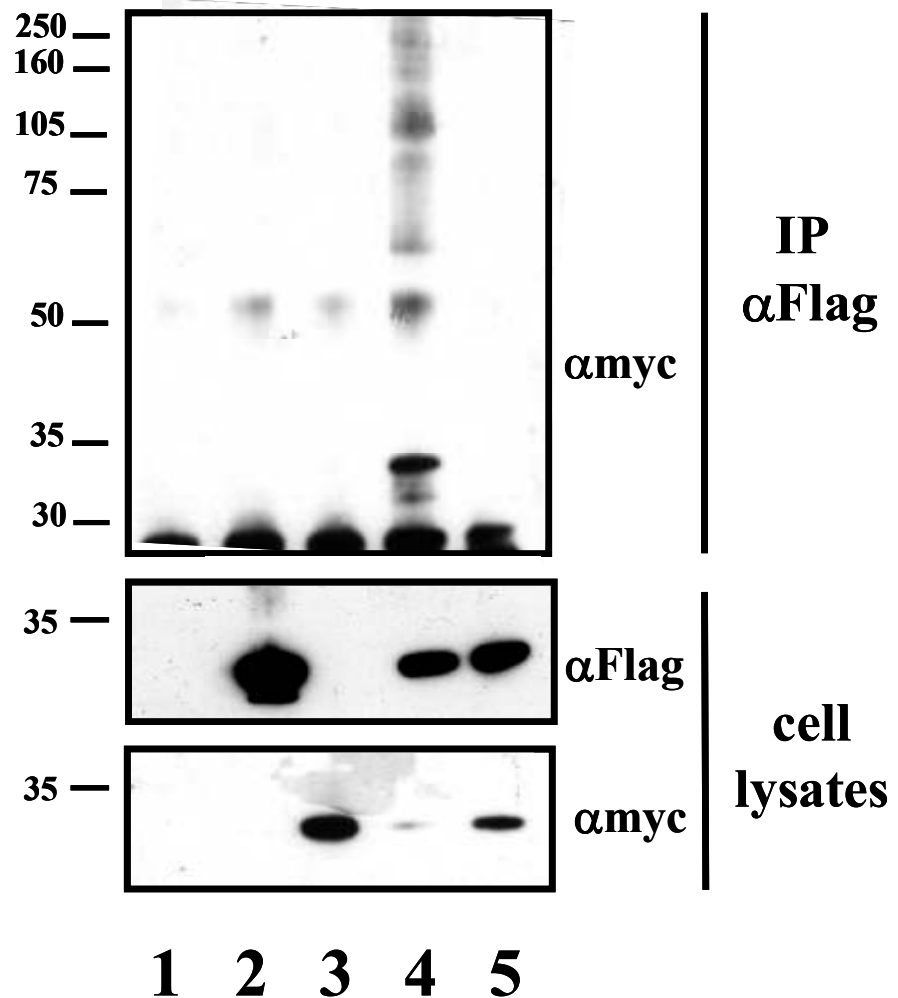
Mr ($\times 10^{-3}$)

Figure 6.1 Co-immunoprecipitation of differentially epitope-tagged forms of the human GPR40 receptor

HEK293T cells were transiently transfected to express GPR40-Flag (lane 2), GPR40-c-Myc (lane 3) or co-transfected to transiently express GPR40-Flag and GPR40-c-Myc (lane 4). Lane 1 represents non-transfected HEK293T cells. Lane 5 represents a mixed cell control in which cells individually expressing the constructs were mixed prior to immunoprecipitation. Cell lysates were prepared and immunoprecipitated with anti-Flag antibody. The resulting immunoprecipitates were resolved by SDS-PAGE and immunoblotted with anti-c-Myc antibody (upper panel). Immunoblot analysis of original cell lysates using anti-Flag and anti-c-Myc antibodies was also performed to ensure correct protein expression (lower panels). One experiment representative of three experiments is shown.

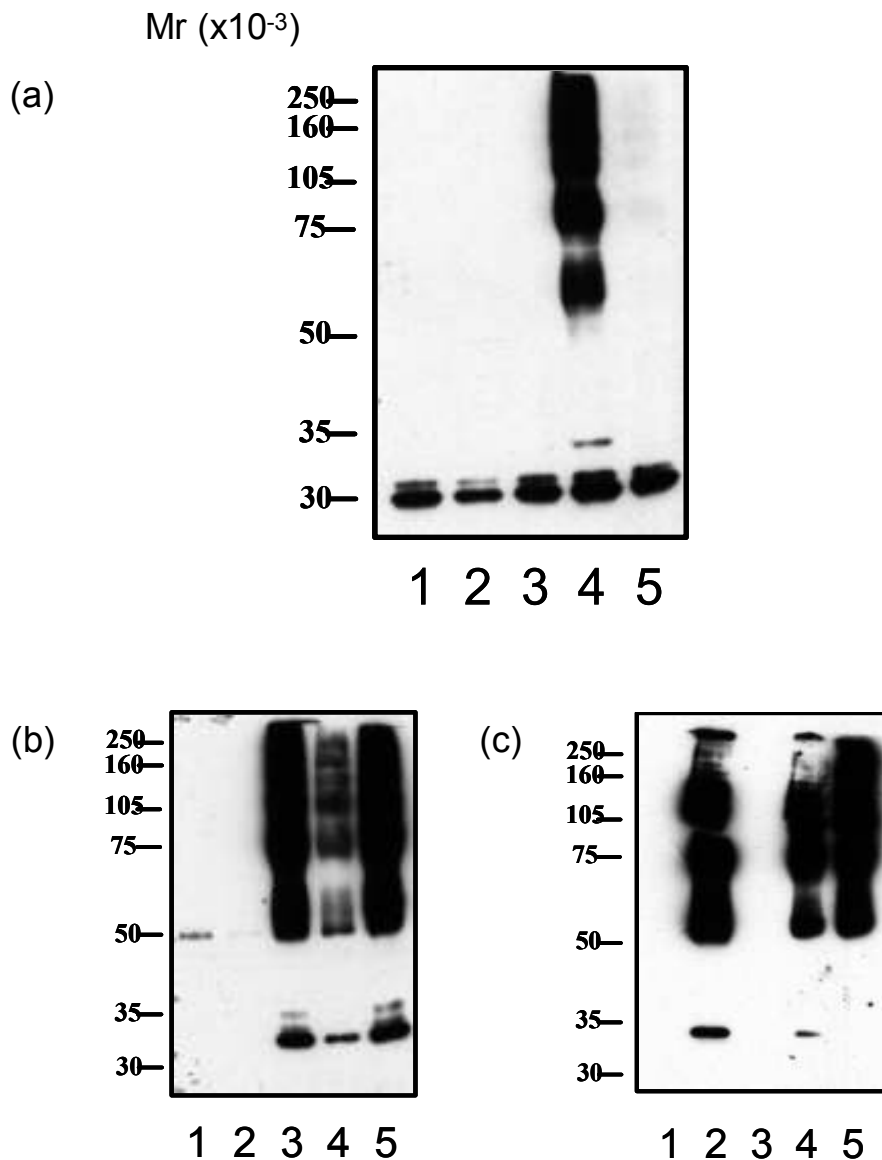
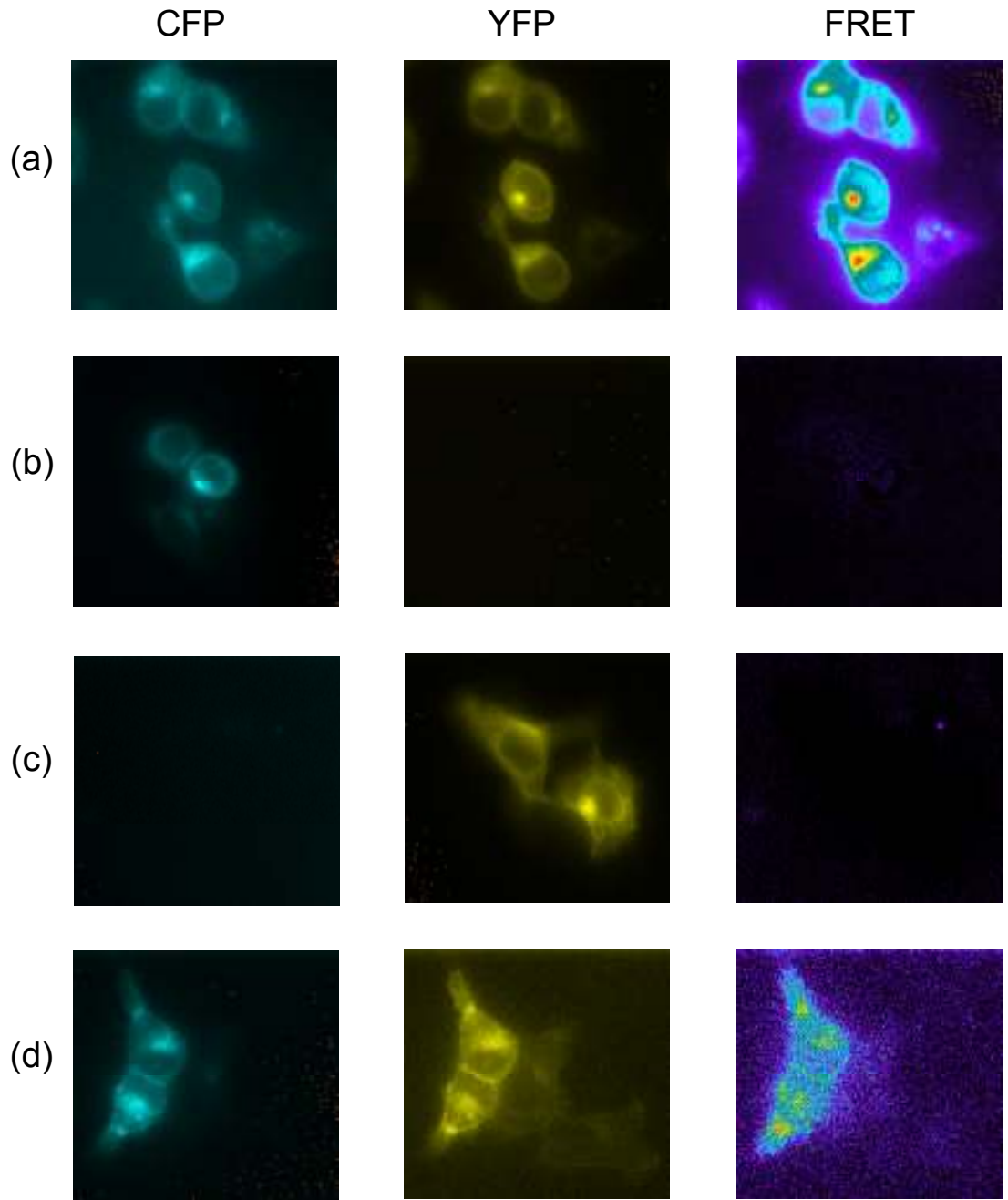


Figure 6.2 Co-immunoprecipitation of differentially epitope-tagged forms of the human GPR43 receptor

HEK293T cells were transiently transfected to express GPR43-c-Myc (lane 2), GPR43-Flag (lane 3) or co-transfected to transiently express GPR43-Flag and GPR43-c-Myc (lane 4). Lane 1 represents non-transfected HEK293T cells. Lane 5 represents a mixed cell control in which cells individually expressing the constructs were mixed prior to immunoprecipitation. Cell lysates were prepared and immunoprecipitated with anti-Flag antibody. The resulting immunoprecipitates were resolved by SDS-PAGE and immunoblotted with anti-c-Myc antibody (a). Immunoblot analysis of original cell lysates using anti-Flag (b) and anti-c-Myc (c) antibodies was also performed to ensure correct protein expression. One experiment representative of three experiments is shown.



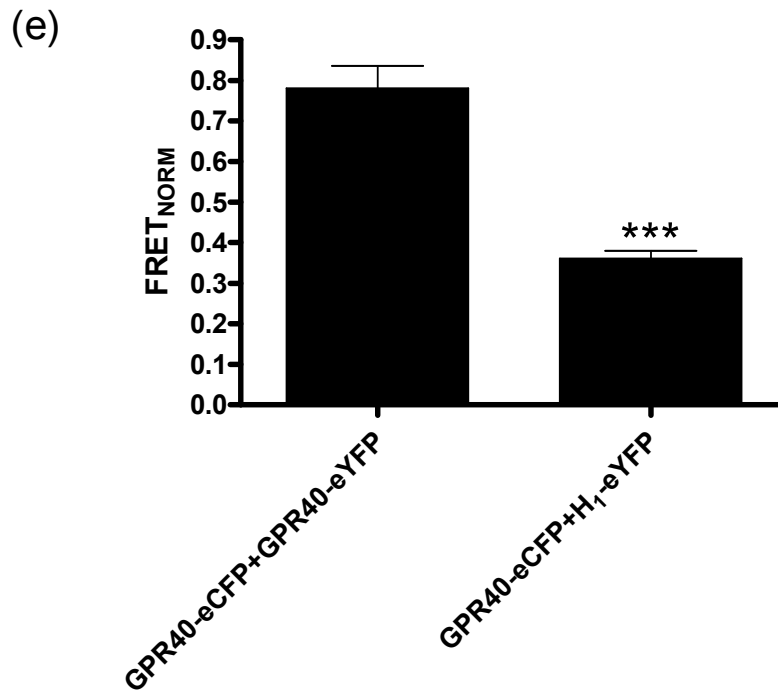
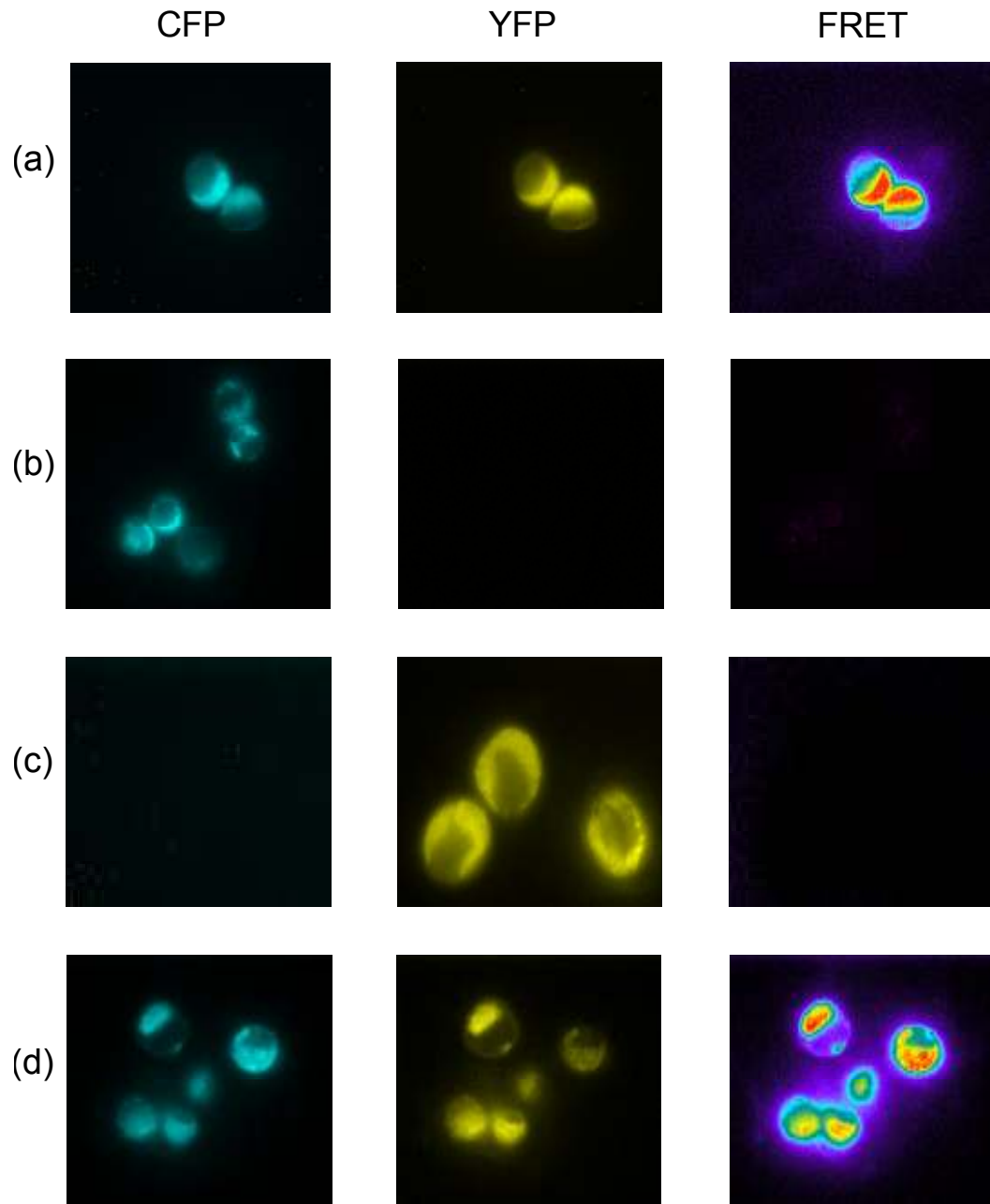


Figure 6.3 FRET imaging of GPR40 homo-oligomerisation in single cells

HEK293T cells were transiently transfected to co-express GPR40-eCFP and GPR40-eYFP (a) or to express either GPR40-eCFP (b) or GPR40-eYFP (c) individually. Control interactions with the histamine H₁ receptor were recorded. H₁-eYFP was co-expressed with GPR40-eCFP (d). Images were obtained individually for eYFP, eCFP and FRET filter channels using an Optoscan monochromator and a dichroic mirror 86002v2bs. Left hand panels represent eCFP images, centre panels represent eYFP images and right hand panels represent FRET. MetaMorph imaging software was used to quantify the FRET images as described in section 2.8.7 and are shown in (e). Data shown are means±SEM from three experiments. *** = $p < 0.005$ versus homo-oligomer FRET.



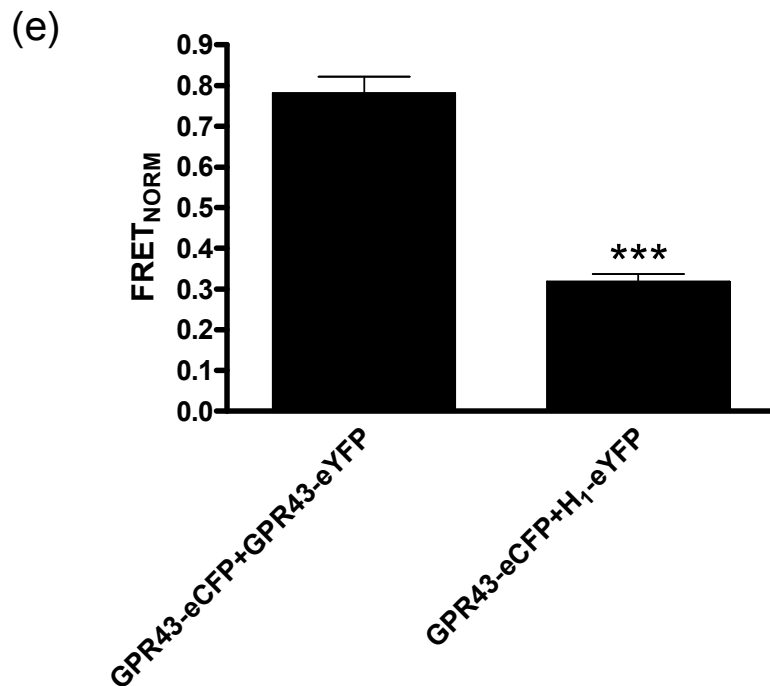


Figure 6.4 FRET imaging of GPR43 homo-oligomerisation in single cells

HEK293T cells were transiently transfected to co-express GPR43-eCFP and GPR43-eYFP (a) or to express either GPR43-eCFP (b) or GPR43-eYFP (c) individually. Control interactions with the histamine H₁ receptor were recorded. H₁-eYFP was co-expressed with GPR43-eCFP (d). Images were obtained individually for eYFP, eCFP and FRET filter channels using an Optoscan monochromator and a dichroic mirror 86002v2bs. Left hand panels represent eCFP images, centre panels represent eYFP images and right hand panels represent FRET. MetaMorph imaging software was used to quantify the FRET images as described in section 2.8.7, and are shown in (e). Data shown are means \pm SEM from three experiments. *** = $p < 0.005$ versus homo-oligomer FRET.

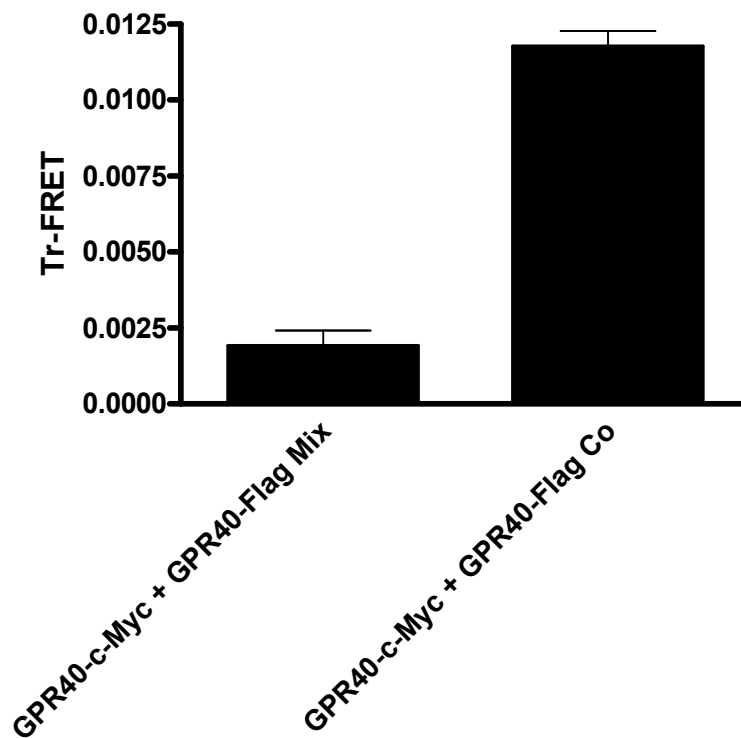


Figure 6.5 GPR40 homo-oligomer detected using Tr-FRET

HEK293T cells were transiently transfected to express GPR40-Flag or GPR40-c-Myc individually and were mixed prior to membrane preparation (mix). Cells were also transiently transfected to co-express both GPR40-Flag and GPR40-c-Myc and membranes prepared (co). The resulting membranes were incubated with anti-c-Myc-Eu³⁺ antibody alone or both anti-c-Myc-Eu³⁺ and anti-Flag-APC antibodies. Tr-FRET was measured and calculated as detailed in section 2.8.6. Data shown are representative of three individual experiments.

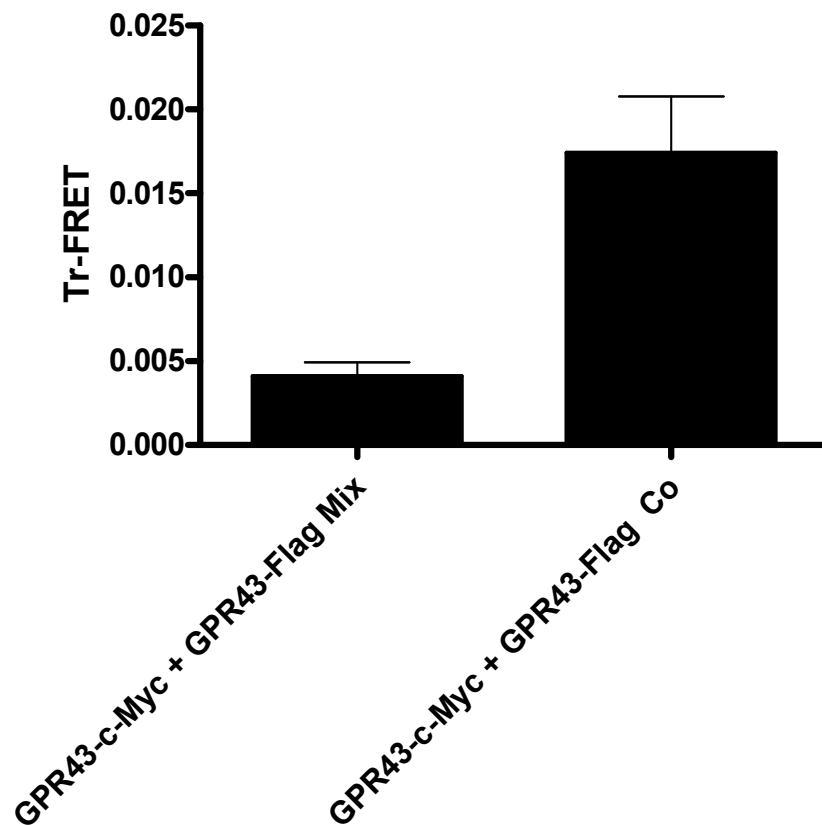


Figure 6.6 GPR43 homo-oligomer detected using Tr-FRET

HEK293T cells were transiently transfected to express GPR43-Flag or GPR43-c-Myc individually and were mixed prior to membrane preparation. Cells were also transiently transfected to co-express both GPR43-Flag and GPR43-c-Myc (co) and membranes prepared. The resulting membranes were incubated with anti-c-Myc-Eu³⁺ antibody alone or both anti-c-Myc-Eu³⁺ and anti-Flag-APC antibodies. Tr-FRET was measured and calculated as detailed in section 2.8.6. Data shown are representative of three individual experiments.

7 Final Discussion

GPR40, GPR41 and GPR43 are a small family of GPCRs that are able to respond to fatty acids (Covenington et al., 2006; Milligan et al., 2006). GPR40 responds to long chain fatty acids (Briscoe et al., 2003; Itoh et al., 2003; Kotarsky et al., 2003) whereas GPR41 and GPR43 are activated by short chain fatty acids (Brown et al., 2003; Le Poul et al., 2003; Nilsson et al., 2003). Their expression pattern, along with the plethora of disease states in which fatty acids have been shown to play an important role, has led to a requirement for a fuller understanding of their function and pharmacology.

Due to the recent identification of fatty acids as the ligands for GPR40-43, assays to monitor activation of the receptors are poorly developed. When GPR41 was expressed with $G\alpha_{i3}$ only a small concentration-dependent increase of [35 S]GTP γ S binding could be observed in response to the short chain fatty acid propionate. The signal to background ratio was greatly increased when a GPR41- $G\alpha_{i3}$ fusion protein was used. A GPR40- $G\alpha_q$ fusion protein was also utilised but it was found that the addition of long chain fatty acids were unable to generate a significant increase of [35 S]GTP γ S binding. The high basal [35 S]GTP γ S binding at GPR40 could be reduced, in a concentration-dependent manner, by the addition of fatty acid free BSA. Using fatty acid free BSA to reduce the basal [35 S]GTP γ S binding at GPR40- $G\alpha_q$ allowed the pharmacology of a variety of fatty acids to be determined and the potencies obtained were in agreement with potencies measured in different assay systems (Briscoe et al., 2003; Itoh et al., 2003; Nilsson et al., 2003). Briscoe et al., (2003) and Itoh et al., (2003) found that GPR40 could respond to a wide range of fatty acids, with varying chain lengths and degrees of saturation. Both studies measured the potencies of the fatty acids in Ca^{2+} based assay systems. The development of a [35 S]GTP γ S binding assay with this receptor could be used to confirm the potencies of a wide range of fatty acids as time constraints only allowed the potency of four fatty acids to be determined. There appears to be no relationship between chain length and degree of saturation to the ability of a fatty acid to activate GPR40. Subtle difference may be more apparent in the [35 S]GTP γ S binding assay and may allow full and partial agonists to be defined.

One of the original reports on GPR40 found that the thiazolidinedione, rosiglitazone, acted as an agonist at GPR40 (Kotarsky et al., 2003). I found that rosiglitazone and the related compound, troglitazone, both acted as agonists at GPR40 in the [35 S]GTP γ S binding assay and in a FLIPR based Ca^{2+} mobilisation assay. The thiazolidinediones are known agonists

of PPAR γ and are currently used clinically in the treatment of NIDDM. There is a growing body of evidence showing that not all of the effects of thiazolidinediones can be explained through action on PPAR γ . The finding that some of these compounds can act as agonists at GPR40 may provide an explanation to some of their PPAR γ independent effects. Further use of the GPR40-eYFP inducible cell line generated in my work will help define the action of thiazolidinediones at GPR40, as expression of the receptor can be controlled. I found that troglitazone was able to mediate a rise in $[Ca^{2+}]_i$ in the β cell line, INS-1E, that expresses GPR40 endogenously. It has been found that β cells also express PPAR γ (Braissant et al., 1996) and this complicates interpretation of the results. Both Shapiro et al., (2005) and Schnell et al., (2006) were able to reduce the expression of GPR40 significantly in INS-1E cells by siRNA treatment. Reducing the expression of GPR40 will allow the effects of the thiazolidinediones in these cells to be uncovered.

Small molecule agonists (Garrido et al., 2006; Briscoe et al., 2006) and an antagonist (Briscoe et al., 2006) of GPR40 have recently been described. I was able to test six of the small molecule agonists (Figure 1.2) in the $[^{35}S]GTP\gamma S$ binding assay and in the FLIPR based Ca^{2+} mobilisation assay. Garrido et al., (2006) reported that a carboxylate group was not required for agonist activation of GPR40. In the $[^{35}S]GTP\gamma S$ assay, the non-carboxyl containing agonists were found to be essentially inactive. This may be due to problems with compound solubility and needs to be examined further. The GPR40 antagonist, GW1100 is useful tool in studying the receptor. It was able to block troglitazone and GSK250089A mediated activation of GPR40 and to reduce the high basal $[^{35}S]GTP\gamma S$ binding in a concentration-dependent manner. Time constraints prevented its ability to block fatty acid mediated activation of the receptor to be investigated. Briscoe et al., (2006) found that in MIN-6 cells it was unable to fully block linolenic acid potentiation of glucose stimulated insulin secretion but could fully block the effects of GW839508X. Although attributed to non-GPR40 pathways it may also indicate that the antagonist, and small molecule agonists, may bind and activate the receptor slightly differently than fatty acids.

Homology modelling and sequence alignment of GPR40, GPR41 and GPR43 indicated that an Arg residue in TM domain 5 could be important in co-ordinating the carboxylate group of the fatty acids. Mutagenesis studies confirmed that the Arg in TM5 was critical for activation of GPR41 and GPR43 by fatty acids. In GPR40, neutralisation of the charge in TM5 did not abolish the receptors ability to respond to fatty acids although the mutant receptor was unable to be activated by the small molecule agonists or thiazolidinediones.

Further mutants were generated which suggested a His in TM4 also plays a role in the binding of ligands to GPR40. The data suggests that the His in TM4 can compensate for the loss of the charge in TM5 and vice versa. It should be noted that the models are static images of the initial binding of the ligand to the receptor. Activation of a receptor is a dynamic process and causes significant changes in receptor conformation. In rhodopsin, the covalently bound ligand, 11-*cis*-retinal, interacts with a range of residues within the TM regions. These interactions are thought to be disrupted due to the conformational changes that occur with the isomerisation of 11-*cis*-retinal to all-*trans*-retinal. The disruption of these interactions is a prerequisite to receptor activation (Meng and Bourne, 2001). Further mutagenesis studies need to be undertaken to gain a fuller understanding of the residues important in ligand binding and activation of GPR40.

It is important to consider the apparent difference between rat and human GPR40. Using membranes prepared from INS-1E cells, it was found that GSK250089A was unable to increase [³⁵S]GTPγS binding in the presence of fatty acid free BSA. Briscoe et al., (2003) also found that the related compound GW839508X was unable to potentiate glucose stimulated insulin release in isolated rat or mouse islets. Figure 7.1 shows the sequence alignment of rat and human GPR40. Rat and human GPR40 share 82% homology and none of the residues mutated in this study differ between the species. When placed onto the homology model of GPR40 (Figure 7.2), it can be seen that the majority of the residues that appear on the model are concentrated at the top of the TM helices and the extracellular loops. Three residues, Val¹⁴¹, Leu¹⁸⁶ and Val²³⁷, which in rat GPR40 are Ala, Ile and Leu respectively, occur close to the proposed binding site. The difference in the binding sites may prevent the synthetic ligands from binding and activating the receptors. These residues could also be mutated in human GPR40 to further characterise the binding site of the receptor. The differences between rat and human GPR40 needs to be examined further, with the pharmacology of the small molecule human GPR40 agonists at rat GPR40 determined. If these compounds display very different characteristics at the different species it will impede the study of the receptor in animal models and the development of clinically relevant compounds.

In light of the findings from the mutagenesis studies it is also important to examine the position of the polymorphisms found in GPR40. There have been two polymorphisms recorded within the open reading frame of GPR40, Arg²¹¹His (Hamid et al., 2005; Ogawa et al., 2005) and Asp¹⁷⁵Asn (Hamid et al., 2005). It is unclear what effect these polymorphisms have on the function of GPR40. Hamid et al., (2005) reported a reduction in efficacy towards eicosatriynoic acid for GPR40 Asp¹⁷⁵Asn but no change in potency.

They found no change in potency or efficacy for this fatty acid at GPR40 Arg²¹¹His. However, studies on Japanese men have indicated that the Arg²¹¹His polymorphism is linked to insulin secretory capacity (Ogawa et al., 2005). Asp¹⁷⁵ occurs at the very top of TM5, which is close to the proposed binding site but is not expected to make any contacts with the agonists. Arg²¹¹His is found within intracellular loop 3, which therefore may affect the receptors ability to activate G proteins or other effectors. Although Hamid et al., (2005) studied the effects of the polymorphisms in a recombinant system; it would be interesting to carry out a more detailed examination of their effects. The polymorphisms could be incorporated into the GPR40-G α_q fusion protein to allow [³⁵S]GTP γ S binding studies to be performed. This may uncover more subtle changes in the potency or efficacy of a variety of ligands. Wenzel-Seifert and Seifert (2003) used a receptor-G protein fusion to study the consequence of the Arg³⁸⁹Gly polymorphism of the β_1 -adrenoceptor. This polymorphism has been linked to heart function and to the therapeutic effects of β -blocker treatment (Liggett et al., 2006). Using a β_1 -adrenoceptor-G α_s fusion protein they could not detect any difference between the two receptor variants (Wenzel-Seifert and Seifert, 2003).

Due to time constraints, I was unable to test the GPR40 antagonist, GW1100, at the GPR40 mutants. Antagonists do not always share the same binding site as agonists. In the case of α_{1b} adrenergic receptor antagonists, such as pentolamine and WB4101, they do not make the same interactions as agonists (Zhao et al., 1996). Agonists of this receptor bind within a crevice formed by the transmembrane helices, whereas these antagonists are thought to interact with residues in extracellular loop 2. In the case of the β_2 adrenergic receptor antagonists, alprenolol and propranolol, they have been shown to interact with the aspartic acid residue in TM3 (Asp¹¹³), which is conserved in the biogenic amine receptors, but other key interactions differ (Suryanarayana et al., 1991). The two GPR40-G α_q mutants displayed high basal [³⁵S]GTP γ S binding which could be reduced by treatment with fatty acid free BSA. GW1100 was able to reduce the basal [³⁵S]GTP γ S binding in the wild type GPR40-G α_q fusion protein in a concentration dependent manner. Therefore, testing the ability of GW1100 to reduce the basal [³⁵S]GTP γ S at the GPR40 mutants would give an indication if it could still act as an antagonist.

The models of GPR40, GPR41 and GPR43 were built based on homology of the receptors to bovine rhodopsin. The mutagenesis studies on the receptors have demonstrated some of the shortcomings with drawing conclusions only from homology modelling. In the case of GPR41 and GPR43 the models predicted that the Arg in TM5 was in a position to co-ordinate the carboxylate group of the fatty acid and this was supported by the mutagenesis

studies. A similar mechanism was suggested from the model of GPR40 but this was not confirmed by the data generated from the mutant receptors. The receptors share low sequence homology with bovine rhodopsin therefore a model based on the structure of rhodopsin may not be entirely accurate. Unfortunately, bovine rhodopsin is the only GPCR for which high-resolution structural data exists. The models of GPR40, GPR41 and GPR43 now need to be refined to take into account the finding of the mutagenesis studies.

The small size of the ligands of GPR41 and GPR43 make their positioning into the models difficult as they can be accommodated in a variety of ways. It is possible that more than one fatty acid needs to be bound for activation of the receptor. This will be a hard question to answer as no small molecule agonists exist for either GPR41 or GPR43, and as seen with GPR40, they may not even bind in a similar manner to the fatty acids. There is a range of radioactively labelled fatty acids i.e. ^3H -palmitic acid, and fluorescent labelled fatty acids available commercially i.e. BODIPY labelled fatty acids (Molecular Probes). In the case of fluorescent fatty acids, the fluorescent moiety is attached to the end of the carbon chain that leaves the carboxyl group intact. Fluorescent probes have been used to investigate the BLT₁ receptor whose ligands also contain a carboxyl group. In this case, the fluorescent moiety was attached to the carboxyl end, which helped show that a carboxyl group was not essential for activation of the receptor and provided clues to the binding of the ligand to the receptor (Sabrish et al., 2005; Sabrish et al., 2006). The possible problem with fluorescent and radioactive fatty acids is that they may become incorporated into the membrane and render any specific binding impossible to detect. Fatty acids are not very potent ligands and this would impact on the level of specific binding, which in turn makes the fluorescent or radioactive fatty acids unsuitable to monitor ligand binding at these receptors.

The limitations of studying the pharmacology of GPR40, GPR41 and GPR43 are wide ranging, especially for GPR41 and GPR43 as there has been no small molecule agonists or antagonists described for either receptor. With the mutagenesis studies it is impossible to determine if the fatty acids or other ligands are actually binding the receptor. As discussed above, it is unlikely that a modified fatty acid would be of use in a ligand-binding assay. In this study I have shown that rosiglitazone and troglitazone act as agonists of GPR40 and troglitazone was more potent than any of the fatty acids tested. Radiolabelled rosiglitazone (^3H -rosiglitazone – American Radiolabeled Chemicals) is available commercially and may prove to be a useful compound to investigate the ligand binding properties of wild type GPR40 and the GPR40 mutants.

The majority of studies into GPR40, GPR41 and GPR43 have used one fatty acid to activate the receptor. A recent study by Dass et al., (2007) examined the effects of short chain fatty acids on intestinal motility and the possible contribution of GPR43. Although they showed that fatty acid mediated intestinal contraction was unlikely to be due to activation of GPR43, they did test *in vivo* concentrations of fatty acids. They determined the concentrations of short chain fatty acids in rat intestine and found acetate to be the most predominant fatty acid, followed by propionate then butyrate, with a molar ratio of 59:7:34 and a maximum concentration of 115mmol L^{-1} . When testing a combination of fatty acids at *in vivo* concentrations they found they exerted highly significant effects on intestinal motility compared to the individual fatty acids (Dass et al., 2007). It would be of interest to test a combination of fatty acids at *in vivo* concentrations in a recombinant system and the [^{35}S]GTP γ S binding assay developed for GPR41 would be a obvious starting point.

As shown in chapter 6, GPR40 and GPR43 were able to form homo-oligomers. They were also able to form hetero-oligomers with the histamine H₁ receptor, albeit with apparent lower affinity than the homo-oligomers. The potential for the receptors to form hetero-oligomers with a receptor that they share little homology with, makes the probability of them forming hetero-oligomers with each other high. There is a growing amount of interest into the functional significance of hetero-oligomers and how it may alter the pharmacology of receptors. It would be interesting to determine the ability of GPR40, GPR41 and GPR43 to form hetero-oligomers and how this may alter their pharmacology.

In conclusion, this study has led to a fuller understanding of the pharmacology, function and oligomerisation of GPR40, GPR41 and GPR43 and uncovered some unusual properties of GPR40 in particular. This study will provide a good basis for further investigations into the function and physiological relevance of these receptors.

```

hGPR40      MDLPPQLSFGLYVAAFALGFPLNVLAIRGATAHARLRLTPSLVYALNLGCSDLLLTVSLP 60
rGPR40      MDLPPQLSFALYVSAAFALGFPLNLLAIRGAVSHAKLRLTPSLVYTLHLACSDLLLAIITLP 60
*****:***:*****:*****:***:*****:***:*****:***

hGPR40      I[RA]VEALASGAWPLPASLCPVFAVAHFFPLYA[GGG]FLAALSAGRYLGAAPPLGYQAFRRP 120
rGPR40      I[RA]VEALASGVWPLPLPFCPVFALAHFAPLYA[GGG]FLAALSAGRYLGAAPFPGYQAIIRP 120
*****:***:*****:*** *****:*****:*****:***

hGPR40      CYSWGVCAAIWALVLC[HL]GLVFGLEAPGGWLDHSNTSLGINTPVNGSPVCLEAWDPASAG 180
rGPR40      CYSWGVCAAIWALVLC[HL]GLLALGLEAPRGWVDNTTSSLGINIPVNGSPVCLEAWDPDSAR 180
*****:*****:*****:***:***:***** *****

hGPR40      P[RF]PSLSLLLFFLPLAITAFCYVGCLRALARSGLTHRRKLRAAWVAGGALLLLLLCVGPY 240
rGPR40      P[RF]PSFSILLFFLPLVITAFICYVGCLRALVHSGLSHKRKLRAAWVAGGALLLLLLCLGPY 240
***:***:*****:*****:***:***:*****:*****:***

hGPR40      NASNVASFLYPNLGGSWRKLG[LITG]AMSVVLNPLVTGYLGRGPKLTVCAARTQGGKSQK 300
rGPR40      NASNVASFIMPDL[EG]SWRKLG[LITG]AMSVVLNPLVTGYLGTGPGQGTICVTRTPRGTIQK 300
*****:***:*****:*****:***:***:***** *****

```

Figure 7.1 Amino acid sequence alignment of human and rat GPR40

Amino acid sequences corresponding to human GPR40 and rat GPR40 were aligned using the ClustalX algorithm. Residues are coloured as follow; small and hydrophobic residues are coloured red, acidic residues coloured blue, basic residues coloured magenta, hydroxyl and amine containing residues are coloured green. The residues mutated in human GPR40 during the mutagenesis studies are boxed. Accession numbers of the sequences used are as follows: human GPR40, NP005294; rat GPR40, NP695216.

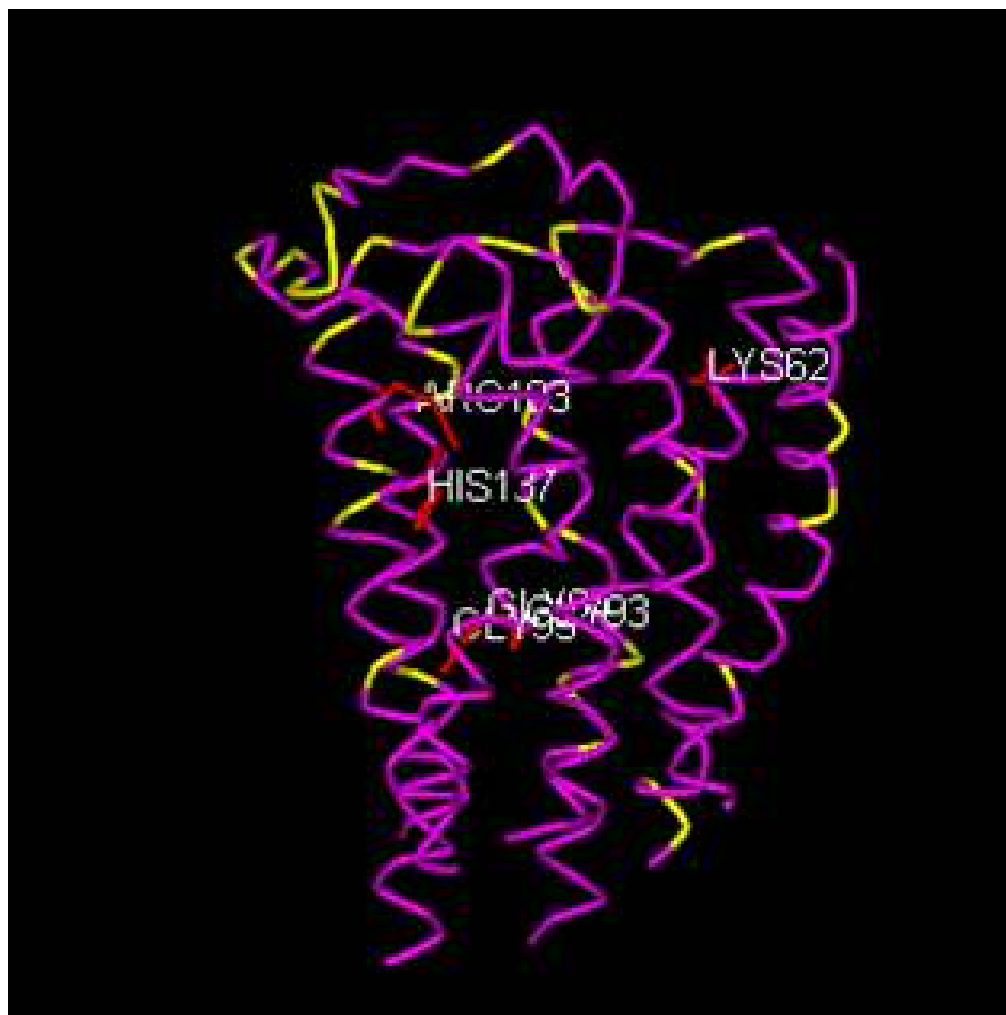


Figure 7.2 Position of residues that differ between human and rat GPR40

The homology model of GPR40 was generated by GlaxoSmithKline using the GPCR_Builder programme based on the structure of rhodopsin. GPR40 was aligned with rhodopsin on the basis of highly conserved residues found in family A GPCRs. The model shows the residues mutated in human GPR40 during the mutagenesis studies, which are coloured red, and the residues that differ in rat GPR40, which are coloured yellow.

8 References

- Arnis S, Fahmy K, Hofmann K P and Sakmar T P (1994) A Conserved Carboxylic Acid Group Mediates Light-Dependent Proton Uptake and Signaling by Rhodopsin. *J Biol Chem* **269**: pp 23879-23881.
- Ashcroft FM and Rorsman P (1990) ATP-Sensitive K⁺ Channels: a Link Between B-Cell Metabolism and Insulin Secretion. *Biochem Soc Trans* **18**: pp 109-111.
- Ayoub MA, Couturier C, Lucas-Meunier E, Angers S, Fossier P, Bouvier M and Jockers R (2002) Monitoring of Ligand-Independent Dimerization and Ligand-Induced Conformational Changes of Melatonin Receptors in Living Cells by Bioluminescence Resonance Energy Transfer. *J Biol Chem* **277**: pp 21522-21528.
- Bahia DS, Wise A, Fanelli F, Lee M, Rees S and Milligan G (1998) Hydrophobicity of Residue 351 of the G Protein Gi1 Alpha Determines the Extent of Activation by the Alpha 2A-Adrenoceptor. *Biochemistry* **37**: pp 11555-11562.
- Ballesteros JA, Weinstein H (1995) Integrated Methods for the Construction of Three-dimensional Models and Computational Probing of Structure-function relations in G Protein Coupled Receptors. *Methods Neurosci* **25**: pp 366-428.
- Ballesteros JA, Jensen A D, Liapakis G, Rasmussen S G, Shi L, Gether U and Javitch J A (2001) Activation of the Beta 2-Adrenergic Receptor Involves Disruption of an Ionic Lock Between the Cytoplasmic Ends of Transmembrane Segments 3 and 6. *J Biol Chem* **276**: pp 29171-29177.
- Baneres JL and Parelo J (2003) Structure-Based Analysis of GPCR Function: Evidence for a Novel Pentameric Assembly Between the Dimeric Leukotriene B4 Receptor BLT1 and the G-Protein. *J Mol Biol* **329**: pp 815-829.
- Bautista AP (2002) Neutrophilic Infiltration in Alcoholic Hepatitis. *Alcohol* **27**: pp 17-21.
- Bayewitch ML, Avidor-Reiss T, Levy R, Pfeuffer T, Nevo I, Simonds W F and Vogel Z (1998) Differential Modulation of Adenylyl Cyclases I and II by Various G Beta Subunits. *J Biol Chem* **273**: pp 2273-2276.
- Bazin H, Trinquet E and Mathis G (2002) Time Resolved Amplification of Cryptate Emission: a Versatile Technology to Trace Biomolecular Interactions. *J Biotechnol* **82**: pp 233-250.

Berkhout TA, Blaney F E, Bridges A M, Cooper D G, Forbes I T, Gribble A D, Groot P H, Hardy A, Ife R J, Kaur R, Moores K E, Shillito H, Willetts J and Witherington J (2003) CCR2: Characterization of the Antagonist Binding Site From a Combined Receptor Modeling/Mutagenesis Approach. *J Med Chem* **46**: pp 4070-4086.

Blin N, Yun J and Wess J (1995) Mapping of Single Amino Acid Residues Required for Selective Activation of Gq/11 by the M3 Muscarinic Acetylcholine Receptor. *J Biol Chem* **270**: pp 17741-17748.

Bluml K, Mutschler E and Wess J (1994) Functional Role of a Cytoplasmic Aromatic Amino Acid in Muscarinic Receptor-Mediated Activation of Phospholipase C. *J Biol Chem* **269**: pp 11537-11541.

Bokoch GM, Katada T, Northup J K, Ui M and Gilman A G (1984) Purification and Properties of the Inhibitory Guanine Nucleotide-Binding Regulatory Component of Adenylate Cyclase. *J Biol Chem* **259**: pp 3560-3567.

Bollheimer LC, Landauer H C, Troll S, Schweimer J, Wrede C E, Scholmerich J and Buettner R (2004) Stimulatory Short-Term Effects of Free Fatty Acids on Glucagon Secretion at Low to Normal Glucose Concentrations. *Metabolism* **53**: pp 1443-1448.

Bond RA and Ijzerman A P (2006) Recent Developments in Constitutive Receptor Activity and Inverse Agonism, and Their Potential for GPCR Drug Discovery. *Trends Pharmacol Sci* **27**: pp 92-96.

Bonini JA, Anderson S M and Steiner D F (1997) Molecular Cloning and Tissue Expression of a Novel Orphan G Protein-Coupled Receptor From Rat Lung. *Biochem Biophys Res Commun* **234**: pp 190-193.

Braissant O, Fougelle F, Scotto C, Dauca M and Wahli W (1996) Differential Expression of Peroxisome Proliferator-Activated Receptors (PPARs): Tissue Distribution of PPAR-Alpha, -Beta, and -Gamma in the Adult Rat. *Endocrinology* **137**: pp 354-366.

Breit A, Lagace M and Bouvier M (2004) Hetero-Oligomerization Between Beta2- and Beta3-Adrenergic Receptors Generates a Beta-Adrenergic Signaling Unit With Distinct Functional Properties. *J Biol Chem* **279**: pp 28756-28765.

Breuer RI, Soergel K H, Lashner B A, Christ M L, Hanauer S B, Vanagunas A, Harig J M, Keshavarzian A, Robinson M, Sellin J H, Weinberg D, Vidican D E, Flemal K L and

Rademaker A W (1997) Short Chain Fatty Acid Rectal Irrigation for Left-Sided Ulcerative Colitis: a Randomised, Placebo Controlled Trial. *Gut* **40**: pp 485-491.

Briscoe CP, Tadayyon M, Andrews J L, Benson W G, Chambers J K, Eilert M M, Ellis C, Elshourbagy N A, Goetz A S, Minnick D T, Murdock P R, Sauls H R, Jr., Shabon U, Spinage L D, Strum J C, Szekeres P G, Tan K B, Way J M, Ignar D M, Wilson S and Muir A I (2003) The Orphan G Protein-Coupled Receptor GPR40 Is Activated by Medium and Long Chain Fatty Acids. *J Biol Chem* **278**: pp 11303-11311.

Briscoe CP, Peat A J, McKeown S C, Corbett D F, Goetz A S, Littleton T R, McCoy D C, Kenakin T P, Andrews J L, Ammala C, Fornwald J A, Ignar D M and Jenkinson S (2006) Pharmacological Regulation of Insulin Secretion in MIN6 Cells Through the Fatty Acid Receptor GPR40: Identification of Agonist and Antagonist Small Molecules. *Br J Pharmacol* **148**: pp 619-628.

Brown AJ, Goldsworthy S M, Barnes A A, Eilert M M, Tcheang L, Daniels D, Muir A I, Wigglesworth M J, Kinghorn I, Fraser N J, Pike N B, Strum J C, Steplewski K M, Murdock P R, Holder J C, Marshall F H, Szekeres P G, Wilson S, Ignar D M, Foord S M, Wise A and Dowell S J (2003) The Orphan G Protein-Coupled Receptors GPR41 and GPR43 Are Activated by Propionate and Other Short Chain Carboxylic Acids. *J Biol Chem* **278**: pp 11312-11319.

Brown AJ, Jupe S and Briscoe C P (2005) A Family of Fatty Acid Binding Receptors. *DNA Cell Biol* **24** : pp 54-61.

Bulenger S, Marullo S and Bouvier M (2005) Emerging Role of Homo- and Heterodimerization in G-Protein-Coupled Receptor Biosynthesis and Maturation. *Trends Pharmacol Sci* **26**: pp 131-137.

Burant CF, Sreenan S, Hirano K, Tai T A, Lohmiller J, Lukens J, Davidson N O, Ross S and Graves R A (1997) Troglitazone Action Is Independent of Adipose Tissue. *J Clin Invest* **100** : pp 2900-2908.

Burstein ES, Spalding T A, Hill-Eubanks D and Brann M R (1995) Structure-Function of Muscarinic Receptor Coupling to G Proteins. Random Saturation Mutagenesis Identifies a Critical Determinant of Receptor Affinity for G Proteins. *J Biol Chem* **270**: pp 3141-3146.

Cabrera-Vera TM, Vanhauwe J, Thomas T O, Medkova M, Preininger A, Mazzoni M R and Hamm H E (2003) Insights into G Protein Structure, Function, and Regulation. *Endocr Rev* **24**: pp 765-781.

Canals M, Marcellino D, Fanelli F, Ciruela F, de Benedetti P, Goldberg S R, Neve K, Fuxe K, Agnati L F, Woods A S, Ferre S, Lluís C, Bouvier M and Franco R (2003) Adenosine A2A-Dopamine D2 Receptor-Receptor Heteromerization: Qualitative and Quantitative Assessment by Fluorescence and Bioluminescence Energy Transfer. *J Biol Chem* **278**: pp 46741-46749.

Canals M, Burgueno J, Marcellino D, Cabello N, Canela E I, Mallol J, Agnati L, Ferre S, Bouvier M, Fuxe K, Ciruela F, Lluís C and Franco R (2004) Homodimerization of Adenosine A2A Receptors: Qualitative and Quantitative Assessment by Fluorescence and Bioluminescence Energy Transfer. *J Neurochem* **88**: pp 726-734.

Canals M, Jenkins L, Kellett E and Milligan G (2006) Up-Regulation of the Angiotensin II Type 1 Receptor by the MAS Proto-Oncogene Is Due to Constitutive Activation of Gq/G11 by MAS. *J Biol Chem* **281**: pp 16757-16767.

Cantello BC, Cawthorne M A, Cottam G P, Duff P T, Haigh D, Hindley R M, Lister C A, Smith S A and Thurlby P L (1994) [[Omega-(Heterocyclamino)Alkoxy]Benzyl]-2,4-Thiazolidinediones As Potent Antihyperglycemic Agents. *J Med Chem* **37**: pp 3977-3985.

Carrillo JJ, Stevens P A and Milligan G (2002) Measurement of Agonist-Dependent and -Independent Signal Initiation of Alpha(1b)-Adrenoceptor Mutants by Direct Analysis of Guanine Nucleotide Exchange on the G Protein G α (11). *J Pharmacol Exp Ther* **302**: pp 1080-1088.

Carrillo JJ, Pediani J and Milligan G (2003) Dimers of Class A G Protein-Coupled Receptors Function Via Agonist-Mediated Trans-Activation of Associated G Proteins. *J Biol Chem* **278**: pp 42578-42587.

Carrillo JJ, Lopez-Gimenez J F and Milligan G (2004) Multiple Interactions Between Transmembrane Helices Generate the Oligomeric Alpha1b-Adrenoceptor. *Mol Pharmacol* **66**: pp 1123-1137.

Cavaglieri CR, Nishiyama A, Fernandes L C, Curi R, Miles E A and Calder P C (2003) Differential Effects of Short-Chain Fatty Acids on Proliferation and Production of Pro- and Anti-Inflammatory Cytokines by Cultured Lymphocytes. *Life Sci* **73**: pp 1683-1690.

Chawla A, Barak Y, Nagy L, Liao D, Tontonoz P and Evans R M (2001) PPAR-Gamma Dependent and Independent Effects on Macrophage-Gene Expression in Lipid Metabolism and Inflammation. *Nat Med* **7**: pp 48-52.

Chen Z, Singer W D, Sternweis P C and Sprang S R (2005) Structure of the P115RhoGEF RgRGS Domain-Galpha13/I1 Chimera Complex Suggests Convergent Evolution of a GTPase Activator. *Nat Struct Mol Biol* **12**: pp 191-197.

Christopoulos A, Parsons A M, Lew M J and El Fakahany E E (1999) The Assessment of Antagonist Potency Under Conditions of Transient Response Kinetics. *Eur J Pharmacol* **382**: pp 217-227.

Chubet RG and Brizzard B L (1996) Vectors for Expression and Secretion of FLAG Epitope-Tagged Proteins in Mammalian Cells. *Biotechniques* **20**: pp 136-141.

Clapham DE and Neer E J (1997) G Protein Beta Gamma Subunits. *Annu Rev Pharmacol Toxicol* **37**: pp 167-203.

Cohen GB, Yang T, Robinson P R and Oprian D D (1993) Constitutive Activation of Opsin: Influence of Charge at Position 134 and Size at Position 296. *Biochemistry* **32**: pp 6111-6115.

Cohen LA, Rose D P and Wynder E L (1993) A Rationale for Dietary Intervention in Postmenopausal Breast Cancer Patients: an Update. *Nutr Cancer* **19**: pp 1-10.

Cohen P, Zhao C, Cai X, Montez J M, Rohani S C, Feinstein P, Mombaerts P and Friedman J M (2001) Selective Deletion of Leptin Receptor in Neurons Leads to Obesity. *J Clin Invest* **108**: pp 1113-1121.

Coleman DE, Berghuis A M, Lee E, Linder M E, Gilman A G and Sprang S R (1994) Structures of Active Conformations of Gi Alpha 1 and the Mechanism of GTP Hydrolysis. *Science* **265**: pp 1405-1412.

Conn PJ and Pin J P (1997) Pharmacology and Functions of Metabotropic Glutamate Receptors. *Annu Rev Pharmacol Toxicol* **37**: pp 205-237.

Corberand JX, Laharrague P F and Fillola G (1989) Human Neutrophils Are Not Severely Injured in Conditions Mimicking Social Drinking. *Alcohol Clin Exp Res* **13**: pp 542-546.

Costa T and Herz A (1989) Antagonists With Negative Intrinsic Activity at Delta Opioid Receptors Coupled to GTP-Binding Proteins. *Proc Natl Acad Sci U S A* **86**: pp 7321-7325.

Covington DK, Briscoe C A, Brown A J and Jayawickreme C K (2006) The G-Protein-Coupled Receptor 40 Family (GPR40-GPR43) and Its Role in Nutrient Sensing. *Biochem Soc Trans* **34**: pp 770-773.

- Cubitt AB, Woollenweber L A and Heim R (1999) Understanding Structure-Function Relationships in the Aequorea Victoria Green Fluorescent Protein. *Methods Cell Biol* **58**: pp 19-30.
- Cummings JH, Pomare E W, Branch W J, Naylor C P and Macfarlane G T (1987) Short Chain Fatty Acids in Human Large Intestine, Portal, Hepatic and Venous Blood. *Gut* **28**: pp 1221-1227.
- Dandona P, Aljada A and Bandyopadhyay A (2004) Inflammation: the Link Between Insulin Resistance, Obesity and Diabetes. *Trends Immunol* **25**: pp 4-7.
- Dass NB, John A K, Bassil A K, Crumbley C W, Shehee W R, Maurio F P, Moore G B, Taylor C M and Sanger G J (2007) The Relationship Between the Effects of Short-Chain Fatty Acids on Intestinal Motility in Vitro and GPR43 Receptor Activation. *Neurogastroenterol Motil* **19**: pp 66-74.
- Davidson JS, Flanagan C A, Zhou W, Becker I I, Elario R, Emeran W, Sealfon S C and Millar R P (1995) Identification of N-Glycosylation Sites in the Gonadotropin-Releasing Hormone Receptor: Role in Receptor Expression but Not Ligand Binding. *Mol Cell Endocrinol* **107**: pp 241-245.
- Davies A, Gowen B E, Krebs A M, Schertler G F and Saibil H R (2001) Three-Dimensional Structure of an Invertebrate Rhodopsin and Basis for Ordered Alignment in the Photoreceptor Membrane. *J Mol Biol* **314**: pp 455-463.
- De Vries L and Gist F M (1999) RGS Proteins: More Than Just GAPs for Heterotrimeric G Proteins. *Trends Cell Biol* **9**: pp 138-144.
- DeFronzo RA (1997) Insulin Resistance: a Multifaceted Syndrome Responsible for NIDDM, Obesity, Hypertension, Dyslipidaemia and Atherosclerosis. *Neth J Med* **50**: pp 191-197.
- Devost D and Zingg H H (2004) Homo- and Hetero-Dimeric Complex Formations of the Human Oxytocin Receptor. *J Neuroendocrinol* **16**: pp 372-377.
- Dinger MC, Bader J E, Kobor A D, Kretschmar A K and Beck-Sickinger A G (2003) Homodimerization of Neuropeptide y Receptors Investigated by Fluorescence Resonance Energy Transfer in Living Cells. *J Biol Chem* **278**: pp 10562-10571.

Drinnan, S. L. Golf in the basal ganglia. Hope, B. T., Snutch, T. P., and Vincet, S. R. *Mol Cell Neurosci* **2**, 66-70.

Ref Type: Generic

Dulac C and Axel R (1995) A Novel Family of Genes Encoding Putative Pheromone Receptors in Mammals. *Cell* **83**: pp 195-206.

El Assaad W, Buteau J, Peyot M L, Nolan C, Roduit R, Hardy S, Joly E, Dbaibo G, Rosenberg L and Prentki M (2003) Saturated Fatty Acids Synergize With Elevated Glucose to Cause Pancreatic Beta-Cell Death. *Endocrinology* **144**: pp 4154-4163.

Evan GI, Lewis G K, Ramsay G and Bishop J M (1985) Isolation of Monoclonal Antibodies Specific for Human C-Myc Proto-Oncogene Product. *Mol Cell Biol* **5**: pp 3610-3616.

Evans RM, Barish G D and Wang Y X (2004) PPARs and the Complex Journey to Obesity. *Nat Med* **10**: pp 355-361.

Fajas L, Auboeuf D, Raspe E, Schoonjans K, Lefebvre A M, Saladin R, Najib J, Laville M, Fruchart J C, Deeb S, Vidal-Puig A, Flier J, Briggs M R, Staels B, Vidal H and Auwerx J (1997) The Organization, Promoter Analysis, and Expression of the Human PPARgamma Gene. *J Biol Chem* **272**: pp 18779-18789.

Fan T, Varghese G, Nguyen T, Tse R, O'Dowd B F and George S R (2005) A Role for the Distal Carboxyl Tails in Generating the Novel Pharmacology and G Protein Activation Profile of Mu and Delta Opioid Receptor Hetero-Oligomers. *J Biol Chem* **280**: pp 38478-38488.

Farningham DA and Whyte C C (1993) The Role of Propionate and Acetate in the Control of Food Intake in Sheep. *Br J Nutr* **70**: pp 37-46.

Farrell RJ and Peppercorn M A (2002) Ulcerative Colitis. *Lancet* **359**: pp 331-340.

Feinstein DL, Spagnolo A, Akar C, Weinberg G, Murphy P, Gavriluk V and Dello R C (2005) Receptor-Independent Actions of PPAR Thiazolidinedione Agonists: Is Mitochondrial Function the Key? *Biochem Pharmacol* **70**: pp 177-188.

Feliz B, Witt D R and Harris B T (2003) Propionic Acidemia: a Neuropathology Case Report and Review of Prior Cases. *Arch Pathol Lab Med* **127**: pp e325-e328.

Feng DD, Luo Z, Roh S G, Hernandez M, Tawadros N, Keating D J and Chen C (2006) Reduction in Voltage-Gated K⁺ Currents in Primary Cultured Rat Pancreatic Beta-Cells by Linoleic Acids. *Endocrinology* **147**: pp 674-682.

Ferguson SS (2001) Evolving Concepts in G Protein-Coupled Receptor Endocytosis: the Role in Receptor Desensitization and Signaling. *Pharmacol Rev* **53**: pp 1-24.

Fiocchi C (1998) Inflammatory Bowel Disease: Etiology and Pathogenesis. *Gastroenterology* **115**: pp 182-205.

Flanagan CA (2005) A GPCR That Is Not "DRY". *Mol Pharmacol* **68**: pp 1-3.

Flodgren E, Olde B, Meidute-Abaraviciene S, Sorhede-Winzell M, Ahren B and Salehi A (2007) GPR40 Is Expressed in Glucagon Producing Cells and Affects Glucagon Secretion. *Biochem Biophys Res Commun*.

Foord SM, Jupe S and Holbrook J (2002) Bioinformatics and Type II G-Protein-Coupled Receptors. *Biochem Soc Trans* **30**: pp 473-479.

Forster T (1948) Zwischenmolekulare Energiewanderung Und Fluoreszenz. *Annu Phys* **2**: pp 54-75.

Fotiadis D, Liang Y, Filipek S, Saperstein D A, Engel A and Palczewski K (2003) Atomic-Force Microscopy: Rhodopsin Dimers in Native Disc Membranes. *Nature* **421**: pp 127-128.

Fotiadis D, Liang Y, Filipek S, Saperstein D A, Engel A and Palczewski K (2004) The G Protein-Coupled Receptor Rhodopsin in the Native Membrane. *FEBS Lett* **564**: pp 281-288.

Fotiadis D, Jastrzebska B, Philippsen A, Muller D J, Palczewski K and Engel A (2006) Structure of the Rhodopsin Dimer: a Working Model for G-Protein-Coupled Receptors. *Curr Opin Struct Biol* **16**: pp 252-259.

Fujiwara K, Maekawa F and Yada T (2005) Oleic Acid Interacts With GPR40 to Induce Ca²⁺ Signaling in Rat Islet Beta-Cells: Mediation by PLC and L-Type Ca²⁺ Channel and Link to Insulin Release. *Am J Physiol Endocrinol Metab* **289**: pp E670-E677.

Funk CD, Furci L, Moran N and Fitzgerald G A (1993) Point Mutation in the Seventh Hydrophobic Domain of the Human Thromboxane A₂ Receptor Allows Discrimination Between Agonist and Antagonist Binding Sites. *Mol Pharmacol* **44**: pp 934-939.

Galvez J, Rodriguez-Cabezas M E and Zarzuelo A (2005) Effects of Dietary Fiber on Inflammatory Bowel Disease. *Mol Nutr Food Res* **49**: pp 601-608.

Gampe RT, Jr., Montana V G, Lambert M H, Miller A B, Bledsoe R K, Milburn M V, Kliewer S A, Willson T M and Xu H E (2000) Asymmetry in the PPARgamma/RXRalpha Crystal Structure Reveals the Molecular Basis of Heterodimerization Among Nuclear Receptors. *Mol Cell* **5**: pp 545-555.

Gantz I, DelValle J, Wang L D, Tashiro T, Munzert G, Guo Y J, Konda Y and Yamada T (1992) Molecular Basis for the Interaction of Histamine With the Histamine H2 Receptor. *J Biol Chem* **267**: pp 20840-20843.

Gardner A and Mallet P E (2006) Suppression of Feeding, Drinking, and Locomotion by a Putative Cannabinoid Receptor 'Silent Antagonist'. *Eur J Pharmacol* **530**: pp 103-106.

Gardner OS, Dewar B J and Graves L M (2005) Activation of Mitogen-Activated Protein Kinases by Peroxisome Proliferator-Activated Receptor Ligands: an Example of Nongenomic Signaling. *Mol Pharmacol* **68**: pp 933-941.

Garrido DM, Corbett D F, Dwornik K A, Goetz A S, Littleton T R, McKeown S C, Mills W Y, Smalley T L, Jr., Briscoe C P and Peat A J (2006) Synthesis and Activity of Small Molecule GPR40 Agonists. *Bioorg Med Chem Lett* **16**: pp 1840-1845.

Gee KR, Brown K A, Chen W N, Bishop-Stewart J, Gray D and Johnson I (2000) Chemical and Physiological Characterization of Fluo-4 Ca(2+)-Indicator Dyes. *Cell Calcium* **27**: pp 97-106.

Genolet R, Wahli W and Michalik L (2004) PPARs As Drug Targets to Modulate Inflammatory Responses? *Curr Drug Targets Inflamm Allergy* **3**: pp 361-375.

George SR, Lee S P, Varghese G, Zeman P R, Seeman P, Ng G Y and O'Dowd B F (1998) A Transmembrane Domain-Derived Peptide Inhibits D1 Dopamine Receptor Function Without Affecting Receptor Oligomerization. *J Biol Chem* **273**: pp 30244-30248.

George SR, Fan T, Xie Z, Tse R, Tam V, Varghese G and O'Dowd B F (2000) Oligomerization of Mu- and Delta-Opioid Receptors. Generation of Novel Functional Properties. *J Biol Chem* **275**: pp 26128-26135.

Gether U, Lin S, Ghanouni P, Ballesteros J A, Weinstein H and Kobilka B K (1997) Agonists Induce Conformational Changes in Transmembrane Domains III and VI of the Beta2 Adrenoceptor. *EMBO J* **16**: pp 6737-6747.

- Gether U (2000) Uncovering Molecular Mechanisms Involved in Activation of G Protein-Coupled Receptors. *Endocr Rev* **21**: pp 90-113.
- Giepmans BN, Adams S R, Ellisman M H and Tsien R Y (2006) The Fluorescent Toolbox for Assessing Protein Location and Function. *Science* **312**: pp 217-224.
- Gillies PS and Dunn C J (2000) Pioglitazone. *Drugs* **60**: pp 333-343.
- Graham DJ, Green L, Senior J R and Nourjah P (2003) Troglitazone-Induced Liver Failure: a Case Study. *Am J Med* **114**: pp 299-306.
- Granovsky AE and Artemyev N O (2001) Partial Reconstitution of Photoreceptor CGMP Phosphodiesterase Characteristics in CGMP Phosphodiesterase-5. *J Biol Chem* **276**: pp 21698-21703.
- Grommes C, Landreth G E and Heneka M T (2004) Antineoplastic Effects of Peroxisome Proliferator-Activated Receptor Gamma Agonists. *Lancet Oncol* **5**: pp 419-429.
- Guo W, Shi L and Javitch J A (2003) The Fourth Transmembrane Segment Forms the Interface of the Dopamine D2 Receptor Homodimer. *J Biol Chem* **278**: pp 4385-4388.
- Guo W, Shi L, Filizola M, Weinstein H and Javitch J A (2005) Crosstalk in G Protein-Coupled Receptors: Changes at the Transmembrane Homodimer Interface Determine Activation. *Proc Natl Acad Sci U S A* **102**: pp 17495-17500.
- Haber EP, Ximenes H M, Procopio J, Carvalho C R, Curi R and Carpinelli A R (2003) Pleiotropic Effects of Fatty Acids on Pancreatic Beta-Cells. *J Cell Physiol* **194**: pp 1-12.
- Hamid YH, Vissing H, Holst B, Urhammer S A, Pyke C, Hansen S K, Glumer C, Borch-Johnsen K, Jorgensen T, Schwartz T W, Pedersen O and Hansen T (2005) Studies of Relationships Between Variation of the Human G Protein-Coupled Receptor 40 Gene and Type 2 Diabetes and Insulin Release. *Diabet Med* **22**: pp 74-80.
- Hamm HE (1998) The Many Faces of G Protein Signaling. *J Biol Chem* **273**: pp 669-672.
- Han M, Groesbeek M, Sakmar T P and Smith S O (1997) The C9 Methyl Group of Retinal Interacts With Glycine-121 in Rhodopsin. *Proc Natl Acad Sci U S A* **94**: pp 13442-13447.
- Hardy S, Langelier Y and Prentki M (2000) Oleate Activates Phosphatidylinositol 3-Kinase and Promotes Proliferation and Reduces Apoptosis of MDA-MB-231 Breast Cancer Cells, Whereas Palmitate Has Opposite Effects. *Cancer Res* **60**: pp 6353-6358.

Hardy S, El Assaad W, Przybytkowski E, Joly E, Prentki M and Langelier Y (2003) Saturated Fatty Acid-Induced Apoptosis in MDA-MB-231 Breast Cancer Cells. A Role for Cardiolipin. *J Biol Chem* **278**: pp 31861-31870.

Hardy S, St Onge G G, Joly E, Langelier Y and Prentki M (2005) Oleate Promotes the Proliferation of Breast Cancer Cells Via the G Protein-Coupled Receptor GPR40. *J Biol Chem* **280**: pp 13285-13291.

He L, Grammer A C, Wu X and Lipsky P E (2004) TRAF3 Forms Heterotrimers With TRAF2 and Modulates Its Ability to Mediate NF- κ B Activation. *J Biol Chem* **279**: pp 55855-55865.

He W, Miao F J, Lin D C, Schwandner R T, Wang Z, Gao J, Chen J L, Tian H and Ling L (2004) Citric Acid Cycle Intermediates As Ligands for Orphan G-Protein-Coupled Receptors. *Nature* **429**: pp 188-193.

Hebert TE, Moffett S, Morello J P, Loisel T P, Bichet D G, Barret C and Bouvier M (1996) A Peptide Derived From a Beta2-Adrenergic Receptor Transmembrane Domain Inhibits Both Receptor Dimerization and Activation. *J Biol Chem* **271**: pp 16384-16392.

Heim R and Tsien R Y (1996) Engineering Green Fluorescent Protein for Improved Brightness, Longer Wavelengths and Fluorescence Resonance Energy Transfer. *Curr Biol* **6**: pp 178-182.

Hepler JR and Gilman A G (1992) G Proteins. *Trends Biochem Sci* **17**: pp 383-387.

Hereld D and Devreotes P N (1992) The CAMP Receptor Family of Dictyostelium. *Int Rev Cytol* **137B**: pp 35-47.

Herve D, Levi-Strauss M, Marey-Semper I, Verney C, Tassin J P, Glowinski J and Girault J A (1993) G(Olf) and Gs in Rat Basal Ganglia: Possible Involvement of G(Olf) in the Coupling of Dopamine D1 Receptor With Adenylyl Cyclase. *J Neurosci* **13**: pp 2237-2248.

Higashijima T, Burnier J and Ross E M (1990) Regulation of Gi and Go by Mastoparan, Related Amphiphilic Peptides, and Hydrophobic Amines. Mechanism and Structural Determinants of Activity. *J Biol Chem* **265**: pp 14176-14186.

Hilairret S, Bouaboula M, Carriere D, Le Fur G and Casellas P (2003) Hypersensitization of the Orexin 1 Receptor by the CB1 Receptor: Evidence for Cross-Talk Blocked by the Specific CB1 Antagonist, SR141716. *J Biol Chem* **278**: pp 23731-23737.

Hill SJ (2006) G-Protein-Coupled Receptors: Past, Present and Future. *Br J Pharmacol* **147 Suppl 1**: pp S27-S37.

Hirasawa A, Tsumaya K, Awaji T, Katsuma S, Adachi T, Yamada M, Sugimoto Y, Miyazaki S and Tsujimoto G (2005) Free Fatty Acids Regulate Gut Incretin Glucagon-Like Peptide-1 Secretion Through GPR120. *Nat Med* **11**: pp 90-94.

Holst B and Schwartz T W (2004) Constitutive Ghrelin Receptor Activity As a Signaling Set-Point in Appetite Regulation. *Trends Pharmacol Sci* **25**: pp 113-117.

Holst B, Holliday N D, Bach A, Elling C E, Cox H M and Schwartz T W (2004) Common Structural Basis for Constitutive Activity of the Ghrelin Receptor Family. *J Biol Chem* **279**: pp 53806-53817.

Hong J, Abudula R, Chen J, Jeppesen P B, Dyrskog S E, Xiao J, Colombo M and Hermansen K (2005) The Short-Term Effect of Fatty Acids on Glucagon Secretion Is Influenced by Their Chain Length, Spatial Configuration, and Degree of Unsaturation: Studies in Vitro. *Metabolism* **54**: pp 1329-1336.

Hong YH, Nishimura Y, Hishikawa D, Tsuzuki H, Miyahara H, Gotoh C, Choi K C, Feng D D, Chen C, Lee H G, Katoh K, Roh S G and Sasaki S (2005) Acetate and Propionate Short Chain Fatty Acids Stimulate Adipogenesis Via GPCR43. *Endocrinology* **146**: pp 5092-5099.

Hsieh CS, Macatonia S E, Tripp C S, Wolf S F, O'Garra A and Murphy K M (1993) Development of TH1 CD4+ T Cells Through IL-12 Produced by Listeria-Induced Macrophages. *Science* **260**: pp 547-549.

Huang JW, Shiao C W, Yang Y T, Kulp S K, Chen K F, Brueggemeier R W, Shapiro C L and Chen C S (2005) Peroxisome Proliferator-Activated Receptor Gamma-Independent Ablation of Cyclin D1 by Thiazolidinediones and Their Derivatives in Breast Cancer Cells. *Mol Pharmacol* **67**: pp 1342-1348.

Hwa J, Graham R M and Perez D M (1996) Chimeras of Alpha1-Adrenergic Receptor Subtypes Identify Critical Residues That Modulate Active State Isomerization. *J Biol Chem* **271**: pp 7956-7964.

Hwa J and Perez D M (1996) The Unique Nature of the Serine Interactions for Alpha 1-Adrenergic Receptor Agonist Binding and Activation. *J Biol Chem* **271**: pp 6322-6327.

- Hwang D (2000) Fatty Acids and Immune Responses--a New Perspective in Searching for Clues to Mechanism. *Annu Rev Nutr* **20**: pp 431-456.
- Iakoubov R, Izzo A, Yeung A, Whiteside C I and Brubaker P L (2006) Protein Kinase C{Zeta} Is Required for Oleic Acid-Induced Secretion of Glucagon-Like Peptide-1 by Intestinal Endocrine L Cells. *Endocrinology*.
- Itoh Y, Kawamata Y, Harada M, Kobayashi M, Fujii R, Fukusumi S, Ogi K, Hosoya M, Tanaka Y, Uejima H, Tanaka H, Maruyama M, Satoh R, Okubo S, Kizawa H, Komatsu H, Matsumura F, Noguchi Y, Shinohara T, Hinuma S, Fujisawa Y and Fujino M (2003) Free Fatty Acids Regulate Insulin Secretion From Pancreatic Beta Cells Through GPR40. *Nature* **422**: pp 173-176.
- Ji TH, Grossmann M and Ji I (1998) G Protein-Coupled Receptors. I. Diversity of Receptor-Ligand Interactions. *J Biol Chem* **273**: pp 17299-17302.
- Jiang C, Ting A T and Seed B (1998) PPAR-Gamma Agonists Inhibit Production of Monocyte Inflammatory Cytokines. *Nature* **391**: pp 82-86.
- Jones KA, Borowsky B, Tamm J A, Craig D A, Durkin M M, Dai M, Yao W J, Johnson M, Gunwaldsen C, Huang L Y, Tang C, Shen Q, Salon J A, Morse K, Laz T, Smith K E, Nagarathnam D, Noble S A, Branchek T A and Gerald C (1998) GABA(B) Receptors Function As a Heteromeric Assembly of the Subunits GABA(B)R1 and GABA(B)R2. *Nature* **396**: pp 674-679.
- Jordan BA and Devi L A (1999) G-Protein-Coupled Receptor Heterodimerization Modulates Receptor Function. *Nature* **399**: pp 697-700.
- Karaki S, Mitsui R, Hayashi H, Kato I, Sugiya H, Iwanaga T, Furness J B and Kuwahara A (2006) Short-Chain Fatty Acid Receptor, GPR43, Is Expressed by Enteroendocrine Cells and Mucosal Mast Cells in Rat Intestine. *Cell Tissue Res* **324**: pp 353-360.
- Katsuma S, Hatae N, Yano T, Ruike Y, Kimura M, Hirasawa A and Tsujimoto G (2005) Free Fatty Acids Inhibit Serum Deprivation-Induced Apoptosis Through GPR120 in a Murine Enteroendocrine Cell Line STC-1. *J Biol Chem* **280**: pp 19507-19515.
- Kaupmann K, Malitschek B, Schuler V, Heid J, Froestl W, Beck P, Mosbacher J, Bischoff S, Kulik A, Shigemoto R, Karschin A and Bettler B (1998) GABA(B)-Receptor Subtypes Assemble into Functional Heteromeric Complexes. *Nature* **396**: pp 683-687.

Kliwer SA, Umesono K, Noonan D J, Heyman R A and Evans R M (1992) Convergence of 9-Cis Retinoic Acid and Peroxisome Proliferator Signalling Pathways Through Heterodimer Formation of Their Receptors. *Nature* **358**: pp 771-774.

Kliwer SA, Forman B M, Blumberg B, Ong E S, Borgmeyer U, Mangelsdorf D J, Umesono K and Evans R M (1994) Differential Expression and Activation of a Family of Murine Peroxisome Proliferator-Activated Receptors. *Proc Natl Acad Sci U S A* **91**: pp 7355-7359.

Kliwer SA, Lenhard J M, Willson T M, Patel I, Morris D C and Lehmann J M (1995) A Prostaglandin J2 Metabolite Binds Peroxisome Proliferator-Activated Receptor Gamma and Promotes Adipocyte Differentiation. *Cell* **83**: pp 813-819.

Kliwer SA, Sundseth S S, Jones S A, Brown P J, Wisely G B, Koble C S, Devchand P, Wahli W, Willson T M, Lenhard J M and Lehmann J M (1997) Fatty Acids and Eicosanoids Regulate Gene Expression Through Direct Interactions With Peroxisome Proliferator-Activated Receptors Alpha and Gamma. *Proc Natl Acad Sci U S A* **94**: pp 4318-4323.

Knudsen LB, Kiel D, Teng M, Behrens C, Bhumralkar D, Kodra J T, Holst J J, Jeppesen C B, Johnson M D, de Jong J C, Jorgensen A S, Kercher T, Kostrowicki J, Madsen P, Olesen P H, Petersen J S, Poulsen F, Sidelmann U G, Sturis J, Truesdale L, May J and Lau J (2007) Small-Molecule Agonists for the Glucagon-Like Peptide 1 Receptor. *Proc Natl Acad Sci U S A* **104**: pp 937-942.

Kostenis E (2001) Is Galpha16 the Optimal Tool for Fishing Ligands of Orphan G-Protein-Coupled Receptors? *Trends Pharmacol Sci* **22**: pp 560-564.

Kostenis E, Waelbroeck M and Milligan G (2005) Techniques: Promiscuous Galpha Proteins in Basic Research and Drug Discovery. *Trends Pharmacol Sci* **26**: pp 595-602.

Kostenis E, Martini L, Ellis J, Waldhoer M, Heydorn A, Rosenkilde M M, Norregaard P K, Jorgensen R, Whistler J L and Milligan G (2005) A Highly Conserved Glycine Within Linker I and the Extreme C Terminus of G Protein Alpha Subunits Interact Cooperatively in Switching G Protein-Coupled Receptor-to-Effector Specificity. *J Pharmacol Exp Ther* **313**: pp 78-87.

Kota P, Reeves P J, Rajbhandary U L and Khorana H G (2006) Opsin Is Present As Dimers in COS1 Cells: Identification of Amino Acids at the Dimeric Interface. *Proc Natl Acad Sci U S A* **103**: pp 3054-3059.

Kotarsky K, Nilsson N E, Flodgren E, Owman C and Olde B (2003) A Human Cell Surface Receptor Activated by Free Fatty Acids and Thiazolidinedione Drugs. *Biochem Biophys Res Commun* **301**: pp 406-410.

Kristiansen K (2004) Molecular Mechanisms of Ligand Binding, Signaling, and Regulation Within the Superfamily of G-Protein-Coupled Receptors: Molecular Modeling and Mutagenesis Approaches to Receptor Structure and Function. *Pharmacol Ther* **103**: pp 21-80.

Krupnick JG and Benovic J L (1998) The Role of Receptor Kinases and Arrestins in G Protein-Coupled Receptor Regulation. *Annu Rev Pharmacol Toxicol* **38**: pp 289-319.

Kunishima N, Shimada Y, Tsuji Y, Sato T, Yamamoto M, Kumasaka T, Nakanishi S, Jingami H and Morikawa K (2000) Structural Basis of Glutamate Recognition by a Dimeric Metabotropic Glutamate Receptor. *Nature* **407**: pp 971-977.

Lambright DG, Sondek J, Bohm A, Skiba N P, Hamm H E and Sigler P B (1996) The 2.0 Å Crystal Structure of a Heterotrimeric G Protein. *Nature* **379**: pp 311-319.

Le Poul E, Loison C, Struyf S, Springael J Y, Lannoy V, Decobecq M E, Brezillon S, Dupriez V, Vassart G, Van Damme J, Parmentier M and Detheux M (2003) Functional Characterization of Human Receptors for Short Chain Fatty Acids and Their Role in Polymorphonuclear Cell Activation. *J Biol Chem* **278**: pp 25481-25489.

Lee SP, So C H, Rashid A J, Varghese G, Cheng R, Lanca A J, O'Dowd B F and George S R (2004) Dopamine D1 and D2 Receptor Co-Activation Generates a Novel Phospholipase C-Mediated Calcium Signal. *J Biol Chem* **279**: pp 35671-35678.

Lee Y, Hirose H, Ohneda M, Johnson J H, McGarry J D and Unger R H (1994) Beta-Cell Lipotoxicity in the Pathogenesis of Non-Insulin-Dependent Diabetes Mellitus of Obese Rats: Impairment in Adipocyte-Beta-Cell Relationships. *Proc Natl Acad Sci U S A* **91**: pp 10878-10882.

Lehmann JM, Moore L B, Smith-Oliver T A, Wilkison W O, Willson T M and Kliewer S A (1995) An Antidiabetic Thiazolidinedione Is a High Affinity Ligand for Peroxisome Proliferator-Activated Receptor Gamma (PPAR Gamma). *J Biol Chem* **270**: pp 12953-12956.

- Lerea CL, Somers D E, Hurley J B, Klock I B and Bunt-Milam A H (1986) Identification of Specific Transducin Alpha Subunits in Retinal Rod and Cone Photoreceptors. *Science* **234**: pp 77-80.
- Levay K, Cabrera J L, Satpaev D K and Slepak V Z (1999) Gbeta5 Prevents the RGS7-Galphao Interaction Through Binding to a Distinct Ggamma-Like Domain Found in RGS7 and Other RGS Proteins. *Proc Natl Acad Sci U S A* **96**: pp 2503-2507.
- Liang Y, Fotiadis D, Filipek S, Saperstein D A, Palczewski K and Engel A (2003) Organization of the G Protein-Coupled Receptors Rhodopsin and Opsin in Native Membranes. *J Biol Chem* **278**: pp 21655-21662.
- Liggett SB, Mialet-Perez J, Thaneemit-Chen S, Weber S A, Greene S M, Hodne D, Nelson B, Morrison J, Domanski M J, Wagoner L E, Abraham W T, Anderson J L, Carlquist J F, Krause-Steinrauf H J, Lazzeroni L C, Port J D, Lavori P W and Bristow M R (2006) A Polymorphism Within a Conserved Beta(1)-Adrenergic Receptor Motif Alters Cardiac Function and Beta-Blocker Response in Human Heart Failure. *Proc Natl Acad Sci U S A* **103**: pp 11288-11293.
- Linder ME, Pang I H, Duronio R J, Gordon J I, Sternweis P C and Gilman A G (1991) Lipid Modifications of G Protein Subunits. Myristoylation of Go Alpha Increases Its Affinity for Beta Gamma. *J Biol Chem* **266**: pp 4654-4659.
- Liu S, Carrillo J J, Padiani J D and Milligan G (2002) Effective Information Transfer From the Alpha 1b-Adrenoceptor to Galpha 11 Requires Both Beta/Gamma Interactions and an Aromatic Group Four Amino Acids From the C Terminus of the G Protein. *J Biol Chem* **277**: pp 25707-25714.
- Lohse MJ, Benovic J L, Codina J, Caron M G and Lefkowitz R J (1990) Beta-Arrestin: a Protein That Regulates Beta-Adrenergic Receptor Function. *Science* **248**: pp 1547-1550.
- Lohse MJ, Andexinger S, Pitcher J, Trukawinski S, Codina J, Faure J P, Caron M G and Lefkowitz R J (1992) Receptor-Specific Desensitization With Purified Proteins. Kinase Dependence and Receptor Specificity of Beta-Arrestin and Arrestin in the Beta 2-Adrenergic Receptor and Rhodopsin Systems. *J Biol Chem* **267**: pp 8558-8564.
- Lopez-Gimenez JF, Canals M, Padiani J D and Milligan G (2007) The {Alpha}1b-Adrenoceptor Exists As a Higher-Order Oligomer: Effective Oligomerization Is Required for Receptor Maturation, Surface Delivery and Function. *Mol Pharmacol* **71**: pp 994-1005

Lu IL, Huang C F, Peng Y H, Lin Y T, Hsieh H P, Chen C T, Lien T W, Lee H J, Mahindroo N, Prakash E, Yueh A, Chen H Y, Goparaju C M, Chen X, Liao C C, Chao Y S, Hsu J T and Wu S Y (2006) Structure-Based Drug Design of a Novel Family of PPARgamma Partial Agonists: Virtual Screening, X-Ray Crystallography, and in Vitro/in Vivo Biological Activities. *J Med Chem* **49**: pp 2703-2712.

Lu ZL, Curtis C A, Jones P G, Pavia J and Hulme E C (1997) The Role of the Aspartate-Arginine-Tyrosine Triad in the M1 Muscarinic Receptor: Mutations of Aspartate 122 and Tyrosine 124 Decrease Receptor Expression but Do Not Abolish Signaling. *Mol Pharmacol* **51**: pp 234-241.

Luttrell LM and Lefkowitz R J (2002) The Role of Beta-Arrestins in the Termination and Transduction of G-Protein-Coupled Receptor Signals. *J Cell Sci* **115**: pp 455-465.

Margolskee RF (2002) Molecular Mechanisms of Bitter and Sweet Taste Transduction. *J Biol Chem* **277**: pp 1-4.

McLaughlin SK, McKinnon P J, Spickofsky N, Danho W and Margolskee R F (1994) Molecular Cloning of G Proteins and Phosphodiesterases From Rat Taste Cells. *Physiol Behav* **56**: pp 1157-1164.

McVey M, Ramsay D, Kellett E, Rees S, Wilson S, Pope A J and Milligan G (2001) Monitoring Receptor Oligomerization Using Time-Resolved Fluorescence Resonance Energy Transfer and Bioluminescence Resonance Energy Transfer. The Human Delta - Opioid Receptor Displays Constitutive Oligomerization at the Cell Surface, Which Is Not Regulated by Receptor Occupancy. *J Biol Chem* **276**: pp 14092-14099.

Meng EC and Bourne H R (2001) Receptor Activation: What Does the Rhodopsin Structure Tell Us? *Trends Pharmacol Sci* **22**: pp 587-593.

Meng EC and Bourne H R (2001) Receptor Activation: What Does the Rhodopsin Structure Tell Us? *Trends Pharmacol Sci* **22**: pp 587-593.

Mercier JF, Salahpour A, Angers S, Breit A and Bouvier M (2002) Quantitative Assessment of Beta 1- and Beta 2-Adrenergic Receptor Homo- and Heterodimerization by Bioluminescence Resonance Energy Transfer. *J Biol Chem* **277**: pp 44925-44931.

Milligan G, Parenti M and Magee A I (1995) The Dynamic Role of Palmitoylation in Signal Transduction. *Trends Biochem Sci* **20**: pp 181-187.

- Milligan G (2003) Constitutive Activity and Inverse Agonists of G Protein-Coupled Receptors: a Current Perspective. *Mol Pharmacol* **64**: pp 1271-1276.
- Milligan G (2003) Principles: Extending the Utility of [³⁵S]GTP Gamma S Binding Assays. *Trends Pharmacol Sci* **24**: pp 87-90.
- Milligan G, Feng G J, Ward R J, Sartania N, Ramsay D, McLean A J and Carrillo J J (2004) G Protein-Coupled Receptor Fusion Proteins in Drug Discovery. *Curr Pharm Des* **10**: pp 1989-2001.
- Milligan G and Bouvier M (2005) Methods to Monitor the Quaternary Structure of G Protein-Coupled Receptors. *FEBS J* **272**: pp 2914-2925.
- Milligan G, Stoddart L A and Brown A J (2006) G Protein-Coupled Receptors for Free Fatty Acids. *Cell Signal* **18**: pp 1360-1365.
- Milligan G (2006) G Protein-Coupled Receptor Dimerisation: Molecular Basis and Relevance to Function. *Biochim Biophys Acta* **1768**: pp 825-835.
- Milligan G (2006) G-Protein-Coupled Receptor Heterodimers: Pharmacology, Function and Relevance to Drug Discovery. *Drug Discov Today* **11**: pp 541-549.
- Milligan G and Kostenis E (2006) Heterotrimeric G-Proteins: a Short History. *Br J Pharmacol* **147 Suppl 1**: pp S46-S55.
- Mitchell FM, Mullaney I, Godfrey P P, Arkinstall S J, Wakelam M J and Milligan G (1991) Widespread Distribution of Gq Alpha/G11 Alpha Detected Immunologically by an Antipeptide Antiserum Directed Against the Predicted C-Terminal Decapeptide. *FEBS Lett* **287**: pp 171-174.
- Mochizuki N, Ohba Y, Kiyokawa E, Kurata T, Murakami T, Ozaki T, Kitabatake A, Nagashima K and Matsuda M (1999) Activation of the ERK/MAPK Pathway by an Isoform of Rap1GAP Associated With G Alpha(i). *Nature* **400**: pp 891-894.
- Monnot C, Bihoreau C, Conchon S, Curnow K M, Corvol P and Clauser E (1996) Polar Residues in the Transmembrane Domains of the Type 1 Angiotensin II Receptor Are Required for Binding and Coupling. Reconstitution of the Binding Site by Co-Expression of Two Deficient Mutants. *J Biol Chem* **271**: pp 1507-1513.
- Montanelli L, Delbaere A, Di Carlo C, Nappi C, Smits G, Vassart G and Costagliola S (2004) A Mutation in the Follicle-Stimulating Hormone Receptor As a Cause of Familial

- Spontaneous Ovarian Hyperstimulation Syndrome. *J Clin Endocrinol Metab* **89**: pp 1255-1258.
- Naccache PH, Faucher N, Caon A C and McColl S R (1988) Propionic Acid-Induced Calcium Mobilization in Human Neutrophils. *J Cell Physiol* **136**: pp 118-124.
- Nakajima T, Iikura M, Okayama Y, Matsumoto K, Uchiyama C, Shirakawa T, Yang X, Adra C N, Hirai K and Saito H (2004) Identification of Granulocyte Subtype-Selective Receptors and Ion Channels by Using a High-Density Oligonucleotide Probe Array. *J Allergy Clin Immunol* **113**: pp 528-535.
- Nakao S, Fujii A and Niederman R (1992) Alteration of Cytoplasmic Ca²⁺ in Resting and Stimulated Human Neutrophils by Short-Chain Carboxylic Acids at Neutral PH. *Infect Immun* **60**: pp 5307-5311.
- Nakayama TA and Khorana H G (1991) Mapping of the Amino Acids in Membrane-Embedded Helices That Interact With the Retinal Chromophore in Bovine Rhodopsin. *J Biol Chem* **266**: pp 4269-4275.
- Nanevicz T, Wang L, Chen M, Ishii M and Coughlin S R (1996) Thrombin Receptor Activating Mutations. Alteration of an Extracellular Agonist Recognition Domain Causes Constitutive Signaling. *J Biol Chem* **271**: pp 702-706.
- Negus SS (2006) Some Implications of Receptor Theory for in Vivo Assessment of Agonists, Antagonists and Inverse Agonists. *Biochem Pharmacol* **71**: pp 1663-1670.
- Nilsson NE, Kotarsky K, Owman C and Olde B (2003) Identification of a Free Fatty Acid Receptor, FFA2R, Expressed on Leukocytes and Activated by Short-Chain Fatty Acids. *Biochem Biophys Res Commun* **303**: pp 1047-1052.
- Noel JP, Hamm H E and Sigler P B (1993) The 2.2 Å Crystal Structure of Transducin-Alpha Complexed With GTP Gamma S. *Nature* **366**: pp 654-663.
- Nolan CJ, Madiraju M S, Delghingaro-Augusto V, Peyot M L and Prentki M (2006) Fatty Acid Signaling in the β -Cell and Insulin Secretion. *Diabetes* **55 Suppl 2**: pp S16-S23.
- Nolte RT, Wisely G B, Westin S, Cobb J E, Lambert M H, Kurokawa R, Rosenfeld M G, Willson T M, Glass C K and Milburn M V (1998) Ligand Binding and Co-Activator Assembly of the Peroxisome Proliferator-Activated Receptor-Gamma. *Nature* **395**: pp 137-143.

- Novotny J and Svoboda P (1998) The Long (Gs(Alpha)-L) and Short (Gs(Alpha)-S) Variants of the Stimulatory Guanine Nucleotide-Binding Protein. Do They Behave in an Identical Way? *J Mol Endocrinol* **20**: pp 163-173.
- Ogawa T, Hirose H, Miyashita K, Saito I and Saruta T (2005) GPR40 Gene Arg211His Polymorphism May Contribute to the Variation of Insulin Secretory Capacity in Japanese Men. *Metabolism* **54**: pp 296-299.
- Olofsson CS, Salehi A, Gopel S O, Holm C and Rorsman P (2004) Palmitate Stimulation of Glucagon Secretion in Mouse Pancreatic Alpha-Cells Results From Activation of L-Type Calcium Channels and Elevation of Cytoplasmic Calcium. *Diabetes* **53**: pp 2836-2843.
- Palakurthi SS, Aktas H, Grubissich L M, Mortensen R M and Halperin J A (2001) Anticancer Effects of Thiazolidinediones Are Independent of Peroxisome Proliferator-Activated Receptor Gamma and Mediated by Inhibition of Translation Initiation. *Cancer Res* **61**: pp 6213-6218.
- Palczewski K, Kumasaka T, Hori T, Behnke C A, Motoshima H, Fox B A, Le T, I, Teller D C, Okada T, Stenkamp R E, Yamamoto M and Miyano M (2000) Crystal Structure of Rhodopsin: A G Protein-Coupled Receptor. *Science* **289**: pp 739-745.
- Parnot C, Miserey-Lenkei S, Bardin S, Corvol P and Clauser E (2002) Lessons From Constitutively Active Mutants of G Protein-Coupled Receptors. *Trends Endocrinol Metab* **13**: pp 336-343.
- Pascal G and Milligan G (2005) Functional Complementation and the Analysis of Opioid Receptor Homodimerization. *Mol Pharmacol* **68**: pp 905-915.
- Patz J, Jacobsohn W Z, Gottschalk-Sabag S, Zeides S and Braverman D Z (1996) Treatment of Refractory Distal Ulcerative Colitis With Short Chain Fatty Acid Enemas. *Am J Gastroenterol* **91**: pp 731-734.
- Pauwels PJ and Wurch T (1998) Review: Amino Acid Domains Involved in Constitutive Activation of G-Protein-Coupled Receptors. *Mol Neurobiol* **17**: pp 109-135.
- Perez DM and Karnik S S (2005) Multiple Signaling States of G-Protein-Coupled Receptors. *Pharmacol Rev* **57**: pp 147-161.

- Pershadsingh HA (2004) Peroxisome Proliferator-Activated Receptor-Gamma: Therapeutic Target for Diseases Beyond Diabetes: Quo Vadis? *Expert Opin Investig Drugs* **13**: pp 215-228.
- Pfleger KD and Eidne K A (2005) Monitoring the Formation of Dynamic G-Protein-Coupled Receptor-Protein Complexes in Living Cells. *Biochem J* **385**: pp 625-637.
- Pinchasov Y and Elmaliah S (1995) Broiler Chick Responses to Anorectic Agents: Dietary Acetic and Propionic Acids and the Blood Metabolites. *Ann Nutr Metab* **39**: pp 107-116.
- Plosker GL and Faulds D (1999) Troglitazone: a Review of Its Use in the Management of Type 2 Diabetes Mellitus. *Drugs* **57**: pp 409-438.
- Popova JS, Johnson G L and Rasenick M M (1994) Chimeric G Alpha S/G Alpha I2 Proteins Define Domains on G Alpha s That Interact With Tubulin for Beta-Adrenergic Activation of Adenylyl Cyclase. *J Biol Chem* **269**: pp 21748-21754.
- Prentki M, Vischer S, Glennon M C, Regazzi R, Deeney J T and Corkey B E (1992) Malonyl-CoA and Long Chain Acyl-CoA Esters As Metabolic Coupling Factors in Nutrient-Induced Insulin Secretion. *J Biol Chem* **267**: pp 5802-5810.
- Prentki M (1996) New Insights into Pancreatic Beta-Cell Metabolic Signaling in Insulin Secretion. *Eur J Endocrinol* **134**: pp 272-286.
- Prentki M, Joly E, El Assaad W and Roduit R (2002) Malonyl-CoA Signaling, Lipid Partitioning, and Glucolipotoxicity: Role in Beta-Cell Adaptation and Failure in the Etiology of Diabetes. *Diabetes* **51 Suppl 3**: pp S405-S413.
- Probst WC, Snyder L A, Schuster D I, Brosius J and Sealfon S C (1992) Sequence Alignment of the G-Protein Coupled Receptor Superfamily. *DNA Cell Biol* **11**: pp 1-20.
- Ramsay D, Carr I C, Padiani J, Lopez-Gimenez J F, Thurlow R, Fidock M and Milligan G (2004) High-Affinity Interactions Between Human Alpha1A-Adrenoceptor C-Terminal Splice Variants Produce Homo- and Heterodimers but Do Not Generate the Alpha1L-Adrenoceptor. *Mol Pharmacol* **66**: pp 228-239.
- Rang HP (2006) The Receptor Concept: Pharmacology's Big Idea. *Br J Pharmacol* **147 Suppl 1**: pp S9-16.
- Rangwala SM and Lazar M A (2004) Peroxisome Proliferator-Activated Receptor Gamma in Diabetes and Metabolism. *Trends Pharmacol Sci* **25**: pp 331-336.

- Rasmussen SG, Jensen A D, Liapakis G, Ghanouni P, Javitch J A and Gether U (1999) Mutation of a Highly Conserved Aspartic Acid in the Beta2 Adrenergic Receptor: Constitutive Activation, Structural Instability, and Conformational Rearrangement of Transmembrane Segment 6. *Mol Pharmacol* **56**: pp 175-184.
- Ray K, Clapp P, Goldsmith P K and Spiegel A M (1998) Identification of the Sites of N-Linked Glycosylation on the Human Calcium Receptor and Assessment of Their Role in Cell Surface Expression and Signal Transduction. *J Biol Chem* **273**: pp 34558-34567.
- Rice AM, Fain J N and Rivkees S A (2000) A1 Adenosine Receptor Activation Increases Adipocyte Leptin Secretion. *Endocrinology* **141**: pp 1442-1445.
- Ricote M, Li A C, Willson T M, Kelly C J and Glass C K (1998) The Peroxisome Proliferator-Activated Receptor-Gamma Is a Negative Regulator of Macrophage Activation. *Nature* **391**: pp 79-82.
- Riobo NA and Manning D R (2005) Receptors Coupled to Heterotrimeric G Proteins of the G12 Family. *Trends Pharmacol Sci* **26**: pp 146-154.
- Roe MW, Lemasters J J and Herman B (1990) Assessment of Fura-2 for Measurements of Cytosolic Free Calcium. *Cell Calcium* **11**: pp 63-73.
- Rose DP (1997) Effects of Dietary Fatty Acids on Breast and Prostate Cancers: Evidence From in Vitro Experiments and Animal Studies. *Am J Clin Nutr* **66**: pp 1513S-1522S.
- Rotella CM, Pala L and Mannucci E (2005) Glucagon-Like Peptide 1 (GLP-1) and Metabolic Diseases. *J Endocrinol Invest* **28**: pp 746-758.
- Rumi MA, Ishihara S, Kazumori H, Kadowaki Y and Kinoshita Y (2004) Can PPAR Gamma Ligands Be Used in Cancer Therapy? *Curr Med Chem Anticancer Agents* **4**: pp 465-477.
- Sabirsh A, Wetterholm A, Bristulf J, Leffler H, Haeggstrom J Z and Owman C (2005) Fluorescent Leukotriene B4: Potential Applications. *J Lipid Res* **46**: pp 1339-1346.
- Sabirsh A, Bywater R P, Bristulf J, Owman C and Haeggstrom J Z (2006) Residues From Transmembrane Helices 3 and 5 Participate in Leukotriene B4 Binding to BLT1. *Biochemistry* **45**: pp 5733-5744.
- Sakmar TP (1998) Rhodopsin: a Prototypical G Protein-Coupled Receptor. *Prog Nucleic Acid Res Mol Biol* **59**: pp 1-34.

- Salahpour A, Angers S, Mercier J F, Lagace M, Marullo S and Bouvier M (2004) Homodimerization of the Beta2-Adrenergic Receptor As a Prerequisite for Cell Surface Targeting. *J Biol Chem* **279**: pp 33390-33397.
- Salehi A, Flodgren E, Nilsson N E, Jimenez-Feltstrom J, Miyazaki J, Owman C and Olde B (2005) Free Fatty Acid Receptor 1 (FFA(1)R/GPR40) and Its Involvement in Fatty-Acid-Stimulated Insulin Secretion. *Cell Tissue Res* **322**: pp 207-215.
- Salim K, Fenton T, Bacha J, Urien-Rodriguez H, Bonnert T, Skynner H A, Watts E, Kerby J, Heald A, Beer M, McAllister G and Guest P C (2002) Oligomerization of G-Protein-Coupled Receptors Shown by Selective Co-Immunoprecipitation. *J Biol Chem* **277**: pp 15482-15485.
- Sarraf P, Mueller E, Smith W M, Wright H M, Kum J B, Aaltonen L A, de la C A, Spiegelman B M and Eng C (1999) Loss-of-Function Mutations in PPAR Gamma Associated With Human Colon Cancer. *Mol Cell* **3**: pp 799-804.
- Sawzdargo M, George S R, Nguyen T, Xu S, Kolakowski L F and O'Dowd B F (1997) A Cluster of Four Novel Human G Protein-Coupled Receptor Genes Occurring in Close Proximity to CD22 Gene on Chromosome 19q13.1. *Biochem Biophys Res Commun* **239**: pp 543-547.
- Scheer A, Fanelli F, Costa T, De Benedetti P G and Cotecchia S (1996) Constitutively Active Mutants of the Alpha 1B-Adrenergic Receptor: Role of Highly Conserved Polar Amino Acids in Receptor Activation. *EMBO J* **15**: pp 3566-3578.
- Schnell S, Schaefer M and Schofl C (2007) Free Fatty Acids Increase Cytosolic Free Calcium and Stimulate Insulin Secretion From Beta-Cells Through Activation of GPR40. *Mol Cell Endocrinol* **263**: pp 173-180.
- Seifert R and Wenzel-Seifert K (2002) Constitutive Activity of G-Protein-Coupled Receptors: Cause of Disease and Common Property of Wild-Type Receptors. *Naunyn Schmiedebergs Arch Pharmacol* **366**: pp 381-416.
- Senga T, Iwamoto S, Yoshida T, Yokota T, Adachi K, Azuma E, Hamaguchi M and Iwamoto T (2003) LSSIG Is a Novel Murine Leukocyte-Specific GPCR That Is Induced by the Activation of STAT3. *Blood* **101**: pp 1185-1187.
- Seyffert WA, Jr. and Madison L L (1967) Physiologic Effects of Metabolic Fuels on Carbohydrate Metabolism. I. Acute Effect of Elevation of Plasma Free Fatty Acids on

Hepatic Glucose Output, Peripheral Glucose Utilization, Serum Insulin, and Plasma Glucagon Levels. *Diabetes* **16**: pp 765-776.

Shapiro H, Shachar S, Sekler I, Hershfinkel M and Walker M D (2005) Role of GPR40 in Fatty Acid Action on the Beta Cell Line INS-1E. *Biochem Biophys Res Commun* **335**: pp 97-104.

Shi L and Javitch J A (2002) The Binding Site of Aminergic G Protein-Coupled Receptors: the Transmembrane Segments and Second Extracellular Loop. *Annu Rev Pharmacol Toxicol* **42**: pp 437-467.

Shiau CW, Yang C C, Kulp S K, Chen K F, Chen C S, Huang J W and Chen C S (2005) Thiazolidenediones Mediate Apoptosis in Prostate Cancer Cells in Part Through Inhibition of Bcl-XL/Bcl-2 Functions Independently of PPARgamma. *Cancer Res* **65**: pp 1561-1569.

Siler SQ, Neese R A and Hellerstein M K (1999) De Novo Lipogenesis, Lipid Kinetics, and Whole-Body Lipid Balances in Humans After Acute Alcohol Consumption. *Am J Clin Nutr* **70**: pp 928-936.

Sondek J, Bohm A, Lambright D G, Hamm H E and Sigler P B (1996) Crystal Structure of a G-Protein Beta Gamma Dimer at 2.1A Resolution. *Nature* **379**: pp 369-374.

Sondek J, Bohm A, Lambright D G, Hamm H E and Sigler P B (1996) Crystal Structure of a G-Protein Beta Gamma Dimer at 2.1A Resolution. *Nature* **379**: pp 369-374.

Spalding TA, Birdsall N J, Curtis C A and Hulme E C (1994) Acetylcholine Mustard Labels the Binding Site Aspartate in Muscarinic Acetylcholine Receptors. *J Biol Chem* **269**: pp 4092-4097.

Spring DJ and Neer E J (1994) A 14-Amino Acid Region of the G Protein Gamma Subunit Is Sufficient to Confer Selectivity of Gamma Binding to the Beta Subunit. *J Biol Chem* **269**: pp 22882-22886.

Stanasila L, Perez J B, Vogel H and Cotecchia S (2003) Oligomerization of the Alpha 1a- and Alpha 1b-Adrenergic Receptor Subtypes. Potential Implications in Receptor Internalization. *J Biol Chem* **278**: pp 40239-40251.

Stein DT, Esser V, Stevenson B E, Lane K E, Whiteside J H, Daniels M B, Chen S and McGarry J D (1996) Essentiality of Circulating Fatty Acids for Glucose-Stimulated Insulin Secretion in the Fasted Rat. *J Clin Invest* **97**: pp 2728-2735.

Stein DT, Stevenson B E, Chester M W, Basit M, Daniels M B, Turley S D and McGarry J D (1997) The Insulinotropic Potency of Fatty Acids Is Influenced Profoundly by Their Chain Length and Degree of Saturation. *J Clin Invest* **100**: pp 398-403.

Steinhart AH, Brzezinski A and Baker J P (1994) Treatment of Refractory Ulcerative Proctosigmoiditis With Butyrate Enemas. *Am J Gastroenterol* **89**: pp 179-183.

Steneberg P, Rubins N, Bartoov-Shifman R, Walker M D and Edlund H (2005) The FFA Receptor GPR40 Links Hyperinsulinemia, Hepatic Steatosis, and Impaired Glucose Homeostasis in Mouse. *Cell Metab* **1**: pp 245-258.

Stenkamp RE, Filipek S, Driessen C A, Teller D C and Palczewski K (2002) Crystal Structure of Rhodopsin: a Template for Cone Visual Pigments and Other G Protein-Coupled Receptors. *Biochim Biophys Acta* **1565**: pp 168-182.

Stewart G, Hira T, Higgins A, Smith C P and McLaughlin J T (2006) Mouse GPR40 Heterologously Expressed in *Xenopus* Oocytes Is Activated by Short-, Medium-, and Long-Chain Fatty Acids. *Am J Physiol Cell Physiol* **290**: pp C785-C792.

Stitham J, Stojanovic A, Merenick B L, O'Hara K A and Hwa J (2003) The Unique Ligand-Binding Pocket for the Human Prostacyclin Receptor. Site-Directed Mutagenesis and Molecular Modeling. *J Biol Chem* **278**: pp 4250-4257.

Strader CD, Gaffney T, Sugg E E, Candelore M R, Keys R, Patchett A A and Dixon R A (1991) Allele-Specific Activation of Genetically Engineered Receptors. *J Biol Chem* **266**: pp 5-8.

Sullivan R, Chateauneuf A, Coulombe N, Kolakowski L F, Jr., Johnson M P, Hebert T E, Ethier N, Belley M, Metters K, Abramovitz M, O'Neill G P and Ng G Y (2000) Coexpression of Full-Length Gamma-Aminobutyric Acid(B) (GABA(B)) Receptors With Truncated Receptors and Metabotropic Glutamate Receptor 4 Supports the GABA(B) Heterodimer As the Functional Receptor. *J Pharmacol Exp Ther* **293**: pp 460-467.

Suryanarayana S, Daunt D A, Von Zastrow M and Kobilka B K (1991) A Point Mutation in the Seventh Hydrophobic Domain of the Alpha 2 Adrenergic Receptor Increases Its Affinity for a Family of Beta Receptor Antagonists. *J Biol Chem* **266**: pp 15488-15492.

Takasaki J, Saito T, Taniguchi M, Kawasaki T, Moritani Y, Hayashi K and Kobori M (2004) A Novel Galphaq/11-Selective Inhibitor. *J Biol Chem* **279**: pp 47438-47445.

- Takeda S, Yamamoto A, Okada T, Matsumura E, Nose E, Kogure K, Kojima S and Haga T (2003) Identification of Surrogate Ligands for Orphan G Protein-Coupled Receptors. *Life Sci* **74**: pp 367-377.
- Teller DC, Okada T, Behnke C A, Palczewski K and Stenkamp R E (2001) Advances in Determination of a High-Resolution Three-Dimensional Structure of Rhodopsin, a Model of G-Protein-Coupled Receptors (GPCRs). *Biochemistry* **40**: pp 7761-7772.
- Tesmer JJ, Sunahara R K, Gilman A G and Sprang S R (1997) Crystal Structure of the Catalytic Domains of Adenylyl Cyclase in a Complex With G α .GTP γ S. *Science* **278**: pp 1907-1916.
- Theocharis S, Margeli A, Vielh P and Kouraklis G (2004) Peroxisome Proliferator-Activated Receptor-Gamma Ligands As Cell-Cycle Modulators. *Cancer Treat Rev* **30**: pp 545-554.
- Tolman KG and Chandramouli J (2003) Hepatotoxicity of the Thiazolidinediones. *Clin Liver Dis* **7**: pp 369-79, vi.
- Tomita T, Masuzaki H, Noguchi M, Iwakura H, Fujikura J, Tanaka T, Ebihara K, Kawamura J, Komoto I, Kawaguchi Y, Fujimoto K, Doi R, Shimada Y, Hosoda K, Imamura M and Nakao K (2005) GPR40 Gene Expression in Human Pancreas and Insulinoma. *Biochem Biophys Res Commun* **338**: pp 1788-1790.
- Tomita T, Masuzaki H, Iwakura H, Fujikura J, Noguchi M, Tanaka T, Ebihara K, Kawamura J, Komoto I, Kawaguchi Y, Fujimoto K, Doi R, Shimada Y, Hosoda K, Imamura M and Nakao K (2006) Expression of the Gene for a Membrane-Bound Fatty Acid Receptor in the Pancreas and Islet Cell Tumours in Humans: Evidence for GPR40 Expression in Pancreatic Beta Cells and Implications for Insulin Secretion. *Diabetologia* **49**: pp 962-968.
- Tota MR, Candelore M R, Dixon R A and Strader C D (1991) Biophysical and Genetic Analysis of the Ligand-Binding Site of the Beta-Adrenoceptor. *Trends Pharmacol Sci* **12**: pp 4-6.
- Tsien RY (1998) The Green Fluorescent Protein. *Annu Rev Biochem* **67**: pp 509-544.
- Tsuchiya D, Kunishima N, Kamiya N, Jingami H and Morikawa K (2002) Structural Views of the Ligand-Binding Cores of a Metabotropic Glutamate Receptor Complexed

- With an Antagonist and Both Glutamate and Gd³⁺. *Proc Natl Acad Sci U S A* **99**: pp 2660-2665.
- Tsukahara T, Tsukahara R, Yasuda S, Makarova N, Valentine W J, Allison P, Yuan H, Baker D L, Li Z, Bittman R, Parrill A and Tigyi G (2006) Different Residues Mediate Recognition of 1-O-Oleyllysophosphatidic Acid and Rosiglitazone in the Ligand Binding Domain of Peroxisome Proliferator-Activated Receptor Gamma. *J Biol Chem* **281**: pp 3398-3407.
- Tugwood JD, Issemann I, Anderson R G, Bundell K R, McPheat W L and Green S (1992) The Mouse Peroxisome Proliferator Activated Receptor Recognizes a Response Element in the 5' Flanking Sequence of the Rat Acyl CoA Oxidase Gene. *EMBO J* **11**: pp 433-439.
- Tunaru S, Lattig J, Kero J, Krause G and Offermanns S (2005) Characterization of Determinants of Ligand Binding to the Nicotinic Acid Receptor GPR109A (HM74A/PUMA-G). *Mol Pharmacol* **68**: pp 1271-1280.
- Unger VM, Hargrave P A, Baldwin J M and Schertler G F (1997) Arrangement of Rhodopsin Transmembrane Alpha-Helices. *Nature* **389**: pp 203-206.
- Uppenberg J, Svensson C, Jaki M, Bertilsson G, Jendeberg L and Berkenstam A (1998) Crystal Structure of the Ligand Binding Domain of the Human Nuclear Receptor PPARgamma. *J Biol Chem* **273**: pp 31108-31112.
- Urizar E, Claeysen S, Deupi X, Govaerts C, Costagliola S, Vassart G and Pardo L (2005) An Activation Switch in the Rhodopsin Family of G Protein-Coupled Receptors: the Thyrotropin Receptor. *J Biol Chem* **280**: pp 17135-17141.
- Venkataraman C and Kuo F (2005) The G-Protein Coupled Receptor, GPR84 Regulates IL-4 Production by T Lymphocytes in Response to CD3 Crosslinking. *Immunol Lett* **101**: pp 144-153.
- Vernia P, Caprilli R, Latella G, Barbetti F, Magliocca F M and Cittadini M (1988) Fecal Lactate and Ulcerative Colitis. *Gastroenterology* **95**: pp 1564-1568.
- Waldhoer M, Fong J, Jones R M, Lunzer M M, Sharma S K, Kostenis E, Portoghese P S and Whistler J L (2005) A Heterodimer-Selective Agonist Shows in Vivo Relevance of G Protein-Coupled Receptor Dimers. *Proc Natl Acad Sci U S A* **102**: pp 9050-9055.

Wall MA, Coleman D E, Lee E, Iniguez-Lluhi J A, Posner B A, Gilman A G and Sprang S R (1995) The Structure of the G Protein Heterotrimer Gi Alpha 1 Beta 1 Gamma 2. *Cell* **83**: pp 1047-1058.

Wang J, Wu X, Simonavicius N, Tian H and Ling L (2006) Medium-Chain Fatty Acids As Ligands for Orphan G Protein-Coupled Receptor GPR84. *J Biol Chem* **281**: pp 34457-34464.

Wedegaertner PB, Wilson P T and Bourne H R (1995) Lipid Modifications of Trimeric G Proteins. *J Biol Chem* **270**: pp 503-506.

Weng JR, Chen C Y, Pinzone J J, Ringel M D and Chen C S (2006) Beyond Peroxisome Proliferator-Activated Receptor Gamma Signaling: the Multi-Facets of the Antitumor Effect of Thiazolidinediones. *Endocr Relat Cancer* **13**: pp 401-413.

Wenzel-Seifert K and Seifert R (2003) Properties of Arg389-Beta1-Adrenoceptor-Gsalpha Fusion Proteins: Comparison With Gly389-Beta1-Adrenoceptor-Gsalpha Fusion Proteins. *Receptors Channels* **9**: pp 315-323.

Wess J, Bonner T I, Dorje F and Brann M R (1990) Delineation of Muscarinic Receptor Domains Conferring Selectivity of Coupling to Guanine Nucleotide-Binding Proteins and Second Messengers. *Mol Pharmacol* **38**: pp 517-523.

Wess J (1998) Molecular Basis of Receptor/G-Protein-Coupling Selectivity. *Pharmacol Ther* **80**: pp 231-264.

White JH, Wise A, Main M J, Green A, Fraser N J, Disney G H, Barnes A A, Emson P, Foord S M and Marshall F H (1998) Heterodimerization Is Required for the Formation of a Functional GABA(B) Receptor. *Nature* **396**: pp 679-682.

Wieland K, Zuurmond H M, Krasel C, Ijzerman A P and Lohse M J (1996) Involvement of Asn-293 in Stereospecific Agonist Recognition and in Activation of the Beta 2-Adrenergic Receptor. *Proc Natl Acad Sci U S A* **93**: pp 9276-9281.

Willson TM, Cobb J E, Cowan D J, Wiethe R W, Correa I D, Prakash S R, Beck K D, Moore L B, Kliewer S A and Lehmann J M (1996) The Structure-Activity Relationship Between Peroxisome Proliferator-Activated Receptor Gamma Agonism and the Antihyperglycemic Activity of Thiazolidinediones. *J Med Chem* **39**: pp 665-668.

Wilson S, Bergsma D J, Chambers J K, Muir A I, Fantom K G, Ellis C, Murdock P R, Herrity N C and Stadel J M (1998) Orphan G-Protein-Coupled Receptors: the Next Generation of Drug Targets? *Br J Pharmacol* **125**: pp 1387-1392.

Wilson S, Wilkinson G and Milligan G (2005) The CXCR1 and CXCR2 Receptors Form Constitutive Homo- and Heterodimers Selectively and With Equal Apparent Affinities. *J Biol Chem* **280** : pp 28663-28674.

Wing MR, Snyder J T, Sondek J and Harden T K (2003) Direct Activation of Phospholipase C-Epsilon by Rho. *J Biol Chem* **278**: pp 41253-41258.

Wise A, Jupe S C and Rees S (2004) The Identification of Ligands at Orphan G-Protein Coupled Receptors. *Annu Rev Pharmacol Toxicol* **44**: pp 43-66.

Wong JM, de Souza R, Kendall C W, Emam A and Jenkins D J (2006) Colonic Health: Fermentation and Short Chain Fatty Acids. *J Clin Gastroenterol* **40**: pp 235-243.

Wu P and Brand L (1994) Resonance Energy Transfer: Methods and Applications. *Anal Biochem* **218**: pp 1-13.

Xiong Y, Miyamoto N, Shibata K, Valasek M A, Motoike T, Kedzierski R M and Yanagisawa M (2004) Short-Chain Fatty Acids Stimulate Leptin Production in Adipocytes Through the G Protein-Coupled Receptor GPR41. *Proc Natl Acad Sci U S A* **101**: pp 1045-1050.

Xu Y, Piston D W and Johnson C H (1999) A Bioluminescence Resonance Energy Transfer (BRET) System: Application to Interacting Circadian Clock Proteins. *Proc Natl Acad Sci U S A* **96**: pp 151-156.

Yonezawa T, Katoh K and Obara Y (2004) Existence of GPR40 Functioning in a Human Breast Cancer Cell Line, MCF-7. *Biochem Biophys Res Commun* **314**: pp 805-809.

Yonezawa T, Kobayashi Y and Obara Y (2007) Short-Chain Fatty Acids Induce Acute Phosphorylation of the P38 Mitogen-Activated Protein Kinase/Heat Shock Protein 27 Pathway Via GPR43 in the MCF-7 Human Breast Cancer Cell Line. *Cell Signal* **19**: pp 185-193.

Yousefi S, Cooper P R, Potter S L, Mueck B and Jarai G (2001) Cloning and Expression Analysis of a Novel G-Protein-Coupled Receptor Selectively Expressed on Granulocytes. *J Leukoc Biol* **69**: pp 1045-1052.

Youssef J and Badr M (2004) Role of Peroxisome Proliferator-Activated Receptors in Inflammation Control. *J Biomed Biotechnol* **2004**: pp 156-166.

Yu K, Bayona W, Kallen C B, Harding H P, Ravera C P, McMahon G, Brown M and Lazar M A (1995) Differential Activation of Peroxisome Proliferator-Activated Receptors by Eicosanoids. *J Biol Chem* **270**: pp 23975-23983.

Zhao MM, Hwa J and Perez D M (1996) Identification of Critical Extracellular Loop Residues Involved in Alpha 1-Adrenergic Receptor Subtype-Selective Antagonist Binding. *Mol Pharmacol* **50**: pp 1118-1126.

Zhou JY, Toth P T and Miller R J (2003) Direct Interactions Between the Heterotrimeric G Protein Subunit G Beta 5 and the G Protein Gamma Subunit-Like Domain-Containing Regulator of G Protein Signaling 11: Gain of Function of Cyan Fluorescent Protein-Tagged G Gamma 3. *J Pharmacol Exp T*

9 Additional Material

The following paper was published as a result of the studies carried out for this thesis.